

Some pages of this thesis may have been removed for copyright restrictions.

If you have discovered material in Aston Research Explorer which is unlawful e.g. breaches copyright, (either yours or that of a third party) or any other law, including but not limited to those relating to patent, trademark, confidentiality, data protection, obscenity, defamation, libel, then please read our [Takedown policy](#) and contact the service immediately (openaccess@aston.ac.uk)

TRIASSIC STRATIGRAPHY AND SEDIMENTOLOGY IN
CENTRAL ENGLAND

BY

ALI DAUD ALI

THESIS SUBMITTED FOR THE DEGREE OF
DOCTOR OF PHILOSOPHY

AT THE

UNIVERSITY OF ASTON IN BIRMINGHAM

MAY 1982

Dedication

To my parents

ACKNOWLEDGEMENTS

The author is greatly indebted to his supervisor Dr. P. Turner of the Department of Geological Sciences for his encouragement and guidance especially in reading the manuscript and providing invaluable comments and discussions. He also extends his thanks to Professor D.D.Hawkes, the head of department, for providing the facilities, and acknowledges the help given to him by Dr. R.A. Ixer, Dr. J.R. Ashworth, and Dr. D.J. Vaughan of the Department of Geological Sciences for providing fruitful discussions and suggestions. Special thanks to the technical staff of the department and to Mr. R.J. Howell of the Department of Metallurgy for his technical assistance.

The author would also like to extend his thanks to the Ministry of Higher Education and Scientific Research for their financial support.

UNIVERSITY OF ASTON IN BIRMINGHAM
TRIASSIC STRATIGRAPHY AND SEDIMENTOLOGY IN
CENTRAL ENGLAND

A.D. ALI

SUMMARY

The Triassic rocks of Central England consist of three major stratigraphic units: Sherwood Sandstone Group, Mercia Mudstone Group, and Penarth Group. The lower part of the Sherwood Sandstone Group represented by the Kidderminster, Cannock Chase, and Polesworth Formations represents pebbly braided river deposits carried by a major fluvial system flowing to the North-Northwest. The upper part of the Sherwood Sandstone Group includes the Wildmoor and Bromsgrove Sandstone Formations, the deposits of a sandy alluvial system. The Mercia Mudstone Group represents quiet-water deposits of marginal palya type which were subjected to occasional marine flooding. The overlying Penarth Group represent shallow marine and lagoonal environment associated with the Rhaetian marine transgression.

The mineralogy of the Triassic sandstones indicates that the main source was from medium to low rank metamorphic rocks with additional supplies from igneous and metamorphic rocks. The study of size-composition trends shows that the climate was semiarid in early Triassic time and became more humid later.

The Triassic sandstones show a variety of diagenetic features typical of continental red beds; these include:

1. the dissolution of unstable ferromagnesian silicates,
2. the replacement of detrital grains by clay,
3. the pseudomorphism of biotite by haematite, and
4. the formation of a suite of authigenic minerals including quartz, illite, mixed-layer illite-montmorillonite, kaolinite, K-feldspar, haematite, titanium oxide and later carbonate cement.

Palaeomagnetic studies of selected samples show that the magnetization is multicomponent with the various components being carried by different textural phases of haematite.

Key Words: RED BEDS, TRIASSIC, STRATIGRAPHY, DIAGENESIS, PALAEOMAGNETISM.

LIST OF CONTENTS

	<u>Page No.</u>
CHAPTER 1 - INTRODUCTION	1
1.1 TRIASSIC DEPOSITS OF CENTRAL ENGLAND	1
1.2 STRATIGRAPHICAL DIVISIONS	7
1.3 PREVIOUS WORK	12
1.4 METHODS	14
 CHAPTER 2 - TRIASSIC SEDIMENTOLOGY OF CENTRAL ENGLAND	 17
2.1 INTRODUCTION	17
2.2 KIDDERMINSTER, CANNOCK CHASE, AND POLESWORTH FORMATIONS	18
2.2.1 Braid Bar Deposits	27
2.2.2 Sheet Flood Deposits	32
2.2.3 Progradational Alluvial Fanglomerates (Coarsening Upward)	32
2.2.4 Channel Deposits	34
2.3 PALAEOCURRENTS	37
2.4 WILDMOOR SANDSTONE FORMATION	43
2.5 BROMSGROVE SANDSTONE FORMATION	51
2.6 BIVARIATE PLOTS OF SIZE PARAMETERS AS ENVIRONMENTAL INDICATORS	58
2.7 MERCIA MUDSTONE GROUP	64
2.8 CONCLUSIONS	69

	<u>Page No.</u>
CHAPTER 3 - PETROLOGY AND PROVENANCE	71
3.1 MINERALOGY OF THE TRIASSIC SANDSTONES	71
3.2 QUARTZ	71
3.2.1 Igneous Quartz	73
3.2.2 Metamorphic Quartz	75
3.2.3 Sedimentary Quartz	76
3.3 UNDULATORY EXTINCTION AND POLYCRYSTALLINITY AS PROVENANCE INDICATORS	76
3.4 CATHODOLUMINESCENCE	79
3.5 FELDSPARS	80
3.6 ROCK FRAGMENTS	84
3.7 PHYLLOSILICATES	85
3.8 HEAVY MINERALS	86
3.8.1 Non-opaque Minerals	87
3.8.2 Opaque Minerals	91
3.9 PROVENANCE	93
3.10 SIZE-COMPOSITION TRENDS	94
3.11 CONCLUSIONS	97
 CHAPTER 4 - DIAGENESIS	 101
4.1 DIAGENESIS OF THE TRIASSIC SANDSTONES IN CENTRAL ENGLAND	101
4.2 MECHANICAL INFILTRATION OF CLAY	102
4.3 DISSOLUTION OF FRAMEWORK SILICATES	104
4.4 CLAY REPLACEMENT	105
4.5 AUTHIGENIC MINERALS	105

	<u>Page No.</u>
4.5.1 Clay Minerals	106
4.5.2 Quartz	108
4.5.3 K-feldspar	110
4.5.4 Haematite	118
4.5.5 Titanium Oxides	119
4.6 PSEUDOMORPHISM OF BIOTITE BY HAEMATITE	121
4.7 MARTITIZATION	125
4.8 CEMENTATION	126
4.9 DISCUSSION	128
 CHAPTER 5 - PALAEOMAGNETISM OF THE TRIASSIC RED BEDS	 135
5.1 ROCK MINERALS	135
5.2 RED BED MAGNETISM	137
5.3 PALEOMAGNETISM OF THE BRITISH TRIASSIC RED BEDS	138
5.4 INITIAL MEASUREMENTS	140
5.5 THERMAL DEMAGNETIZATION-PILOT SPECIMENS	140
5.5.1 Specularite Dominant Magnetization	143
5.5.2 Mixed Specularite-pigment Magnetization	149
5.6 BULK DEMAGNETIZATION	153
5.7 CONCLUSIONS	154
REFERENCES	159

LIST OF FIGURES

- Fig. 1.1 General geology of Central England.
- Fig. 1.2 Triassic palaeogeography (after Ziegler, 1978)
- Fig. 2.1 Pressure solution impressions on pebble surfaces. Some are surrounded by cemented sandy matrix.
- Fig. 2.2 Frequency distribution of grain size parameters in the sandstone units of the Kidderminster, Cannock Chase, and Polesworth Formations.
- Fig. 2.3 Vertical variations in grain size parameters in the Kidderminster Formation. Section at High Habberly (SO 803 765).
- Fig. 2.4 Section in the Polesworth Formation showing vertical variations in grain size and palaeo-current direction depicted from pebble imbrication, Weeford (SP 134 031).
- Fig. 2.5 a. Braid bar model after Eynon and Walker (1974).
 b. Section in the Cannock Chase Formation showing braid bar deposits, Huntington (SO 967 124).
- Fig. 2.6 Clast supported bimodal conglomerate showing crude horizontal stratification, Polesworth Formation, Weeford (SP 134 031).
- Fig. 2.7 Flat bottomed sandstone units overlying bar core facies, Cannock Chase Formation, Brownhills (SK 063 042).
- Fig. 2.8 Sand wedge resting abruptly on the bar core facies, Polesworth Formation, Weeford (SP 134 031).
- Fig. 2.9 Sand drapes along reactivation surfaces on the bar front facies, Cannock Chase Formation, Brownhills (SK 063 042).
- Fig. 2.10 Mud clast preserved within sheet flood deposits, Cannock Chase Formation, Huntington (SJ 965 124).
- Fig. 2.11 A coarsening-upward sequence in the Polesworth Formation, Weeford (SO 134 031).

- Fig. 2.12 Channel deposit consisting of flat-topped sandstone capped by thin laminae of silt and clay, Cannock Chase Formation, Huntington (SJ 965 124).
- Fig. 2.13 Enlargement of 2.12 showing fining-upward sequence underlying the channel sand.
- Fig. 2.14 Stream channel deposits represented by concave-based lenticular, cross-stratified pebbly sandstone, Kidderminster Formation, High Habberly (SO 803 765).
- Fig. 2.15 Pebble imbrication with the longest axis (a) transverse to the flow direction and the ab plane dipping upstream.
- Fig. 2.16 Preferred oreintation of pebble imbrication (intermediate axis) in the Kidderminster, Cannock Chase, and Polesworth Fm.
- Fig. 2.17 Rose diagrams of pebble imbrication (intermediate axis) and inferred palaeocurrent directions in the Kidderminster, Cannock Chase, and Polesworth Formations in Central England.
- Fig. 2.18 Facies model showing the drainage being axial in the central part of the basin whereas on the basin margins alluvial fans drain laterally into the basin area.
- Fig. 2.19 Frequency distribution of grain size parameters in the Wildmoor Sandstone Formation.
- Fig. 2.20 Vertical variations in grain size parameters in the Wildmoor Sandstone Formation, Section at Claverly (SJ 784 939).
- Fig. 2.21 Large scale trough cross-stratification in the Wildmoor sandstone, Claverly (SJ 784 939).
- Fig. 2.22 Isolated unit of tabular cross-stratification in the Wildmoor sandstones, Claverly (SJ 784 939).
- Fig. 2.23 Large scale tabular cross-stratification in the Wildmoor sandstones, Worfield (SJ 757 956).
- Fig. 2.24 Frequency distribution of grain size parameters in the Bromsgrove Sandstone Formation.

- Fig. 2.25 Vertical variations in grain size parameters in the Bromsgrove Sandstone Formation, Rudge Heath (SO 804 957).
- Fig. 2.26 Poorly defined tabular cross-stratification in the Bromsgrove sandstones, Stone (SO 859 752).
- Fig. 2.27 Bromsgrove sandstones with abundant clay lenses, Stone (SO 859 752).
- Fig. 2.28 a. Section in the Bromsgrove Sandstone Formation showing five fining-upward cycles, Stone (SO 859 752).
b. Part of the type section at Suquerbrook borehold showing three micocycles (after Wills, 1976).
- Fig. 2.29 Green reduction horizons in the Bromsgrove sandstones, Rudge Heath (SJ 804 957).
- Fig. 2.30 Trough cross-stratification and water escape structures in the Bromsgrove sandstones, Rudge Heath (SJ 804 957).
- Fig. 2.31 Meandered channel deposits represented by lenticular sandstone unit pinching out laterally, Bromsgrove Sandstone Formation, Rudge Heath (SJ 804 957).
- Fig. 2.32 Erosional lower contact of the channel deposits, Bromsgrove Sandstone Formation, Rudge Heath (SJ 804 957).
- Fig. 2.33 Bivariate plot of C (first percentile) vs M (median) after Passega (1957).
- Fig. 2.34 Bivariate plot of standard deviation vs median after Stewart (1958).
- Fig. 2.35 Bivariate plot of skewness vs standard deviation (after Friedman, 1967).
- Fig. 2.36 Bivariate plot of mean vs standard deviation (after Moiola and Wieser, 1968).
- Fig. 2.37 Section in the lower part of the Mercia Mudstone Group at Bickenhill (SP 205 829) where the sandstones and mudstones are with abundant green reduction spots).
- Fig. 2.28 a. Section in the Arden Sandstone Member. Henley in Arden (SP 167 654).
b. Ripple cross-lamination.

- Fig. 3.1 Classification of the Triassic sandstones (after Folk, 1968).
- Fig. 3.2 Four variable plot of detrital quartz in the Triassic sandstones. Dashed lined boundaries between source rock areas are taken from Basu et al. (1976, Fig. 6).
- Fig. 3.3 Vertical variations in the mineralogical composition of the Triassic sandstones.
- Fig. 3.4 Vertical variations in heavy mineral content in the Triassic sandstones.
- Fig. 3.5 Variations in composition with size in the Triassic sandstones.
- Fig. 3.6 Variations in composition as a function of stratigraphic position in the Sherwood Sandstone Group.
- Fig. 4.1 X-ray diffraction patterns of clay fraction in the Triassic sandstones showing the presence of illite, kaolinite, mixed-layer illite-montmorillonite, and a small amount of chlorite. Each one represents diffraction patterns of untreated, glycolated, and heated (550°C) samples.
- Fig. 4.2 Electron probe traverse across a zoned K-feldspar overgrowth and the host detrital grain showing fluctuations in K_2O , BaO , and Na_2O .
- Fig. 4.3 EDAX spot analysis of A. hexagonal haematite flake, and B. the surface of a biotite grain in the background.
- Fig. 4.4 Combination diagram showing the relationships between K-mica, K-feldspar, and kaolinite in terms of K^+/H^+ ratio and H_4SiO_4 activity (after Helgeson et al. 1969).⁴
- Fig. 4.5 Eh-pH diagram for the system $Fe-H_2O-O_2-CO_2$ (after Whittemore and Langmuir, 1975).²
- Fig. 5.1 Stereographic projection showing site mean directions of the Triassic sandstones. Initial measurements at 20°C.
- Fig. 5.2 Partial thermal demagnetization of sample T_9 from the Kidderminster Fm.
a. Normalized intensity changes.
b. Stereographic projection showing directional changes.
c. Zijderveld diagram.

- Fig. 5.3 Partial thermal demagnetixation of sample T_2 from the Mercia Mudstone Group.
- Normalized intensity changes.
 - Stereographic projection showing directional changes.
 - Zijderveld diagram.
- Fig. 5.4 Partial thermal demagnetization of sample T_{13} from the Wildmoor Sandstone Fm.
- Normalized intensity changes.
 - Stereographic projection showing directional changes.
 - Zijderveld diagram.
- Fig. 5.5 Partial thermal demagnetization of sample T_{10} from the Bromsgrove Sandstone Fm.
- Normalized intensity changes.
 - Stereographic projection showing directional changes.
 - Zijderveld diagram.
- Fig. 5.6 Stereographic projection showing site mean directions of the Triassic sandstones after thermal cleaning at 300°C .

LIST OF TABLES

- Table 2.1 Facies characteristics of the Kidderminster, Cannock Chase, and Polesworth Formations in Central England.
- Table 4.1 Composition of cores and corresponding overgrowths of K-feldspar grains in the Triassic sandstones. The molecular compositions are calculated by normalizing the oxide totals. (1 - 4 Cannock Chase Formation, 5 - 8 Wildmoor Sandstone Formation, 9 - 21 Bromsgrove Sandstone Formation).
- Table 4.2 Electron probe microanalysis of detrital and authigenic haematites in the Triassic sandstones. (1 - 4 Wildmoor Sandstone Formation, 5 - 13 Bromsgrove Sandstone Formation).
- Table 4.3 Electron probe microanalyses of authigenic and detrital titanium oxides in the Bromsgrove Sandstone Formation.
- Table 5.1 Site mean directions - initial measurements at 20°C.
- Table 5.2 Site mean directions after thermal cleaning at 300°C.

LIST OF PLATES

CHAPTER THREE

- | | |
|----------------|---|
| 1. Plate 3.1 | Detrital quartz types |
| 2. Plate 3.2 | Detrital quartz types |
| 3. Plate 3.3 | Detrital quartz types (Cathodoluminescence) |
| 4. Plate 3.4 | Detrital feldspar types |
| 5. Plate 3.5 | Rock fragments |
| 6. Plate 3.6 | Rock fragments |
| 7. Plate 3.7 | Heavy minerals |
| 8. Plate 3.8 | Heavy minerals |
| 9. Plate 3.9 | Heavy minerals |
| 10. Plate 3.10 | Heavy minerals |

CHAPTER FOUR

- | | |
|----------------|--|
| 1. Plate 4.1 | Mechanically infiltrated clay and dissolved ferromagnesian silicates |
| 2. Plate 4.2 | Clay replacement of detrital grains and authigenic clays |
| 3. Plate 4.3 | Authigenic clays |
| 4. Plate 4.4 | Authigenic quartz |
| 5. Plate 4.5 | Authigenic K-feldspar |
| 6. Plate 4.6 | Authigenic K-feldspar |
| 7. Plate 4.7 | Authigenic K-feldspar |
| 8. Plate 4.8 | Authigenic haematite |
| 9. Plate 4.9 | Authigenic haematite |
| 10. Plate 4.10 | Authigenic titanium oxide |
| 11. Plate 4.11 | Biotite haematization |
| 12. Plate 4.12 | Martites |
| 13. Plate 4.13 | Calcite cement |
| 14. Plate 4.14 | Dolomite and calcite cements |
| 15. Plate 4.15 | Calcite and iron oxide cements |
| 16. Plate 4.16 | Cathodoluminescence of authigenic minerals and cementing materials. |

CHAPTER 1

INTRODUCTION

1.1 TRIASSIC DEPOSITS OF CENTRAL ENGLAND

Triassic rocks are exposed over a wide area in Central England. They include representatives of formations assigned to the Sherwood Sandstone, Mercia Mudstone, and Penarth Groups (Fig. 1.1). The Sherwood Sandstone Group (named after the ancient Sherwood Forest in Nottinghamshire) includes formations previously assigned to the "Bunter" and the arenaceous (Lower) part of the "Keuper" in Britain (Warrington et al. 1980). The conglomeratic Kidderminster, Cannock Chase, and Polesworth Formations (formerly the Bunter Pebble Beds) represent the lowest part of the Sherwood Sandstone Group and are arbitrarily recognized as the oldest Triassic Deposits in Central England. They consist of conglomerates interbedded with coarse-grained red, cross-bedded, pebbly sandstones. They are usually represented by poorly cemented conglomerates with abundant sandstone lenses, but in the Cannock Chase area these conglomerates and sandstones are cemented by calcium carbonate. The Wildmoor Sandstone Formation (formerly the Bunter Upper Mottled Sandstone) overlies the Pebble beds and consists of bright red medium to fine grained, cross-bedded sandstones. The highest unit of the Sherwood Sandstone Group is the Bromsgrove Sandstone Formation (formerly the Lower Keuper Sandstone) which is locally seen to rest unconformably on the

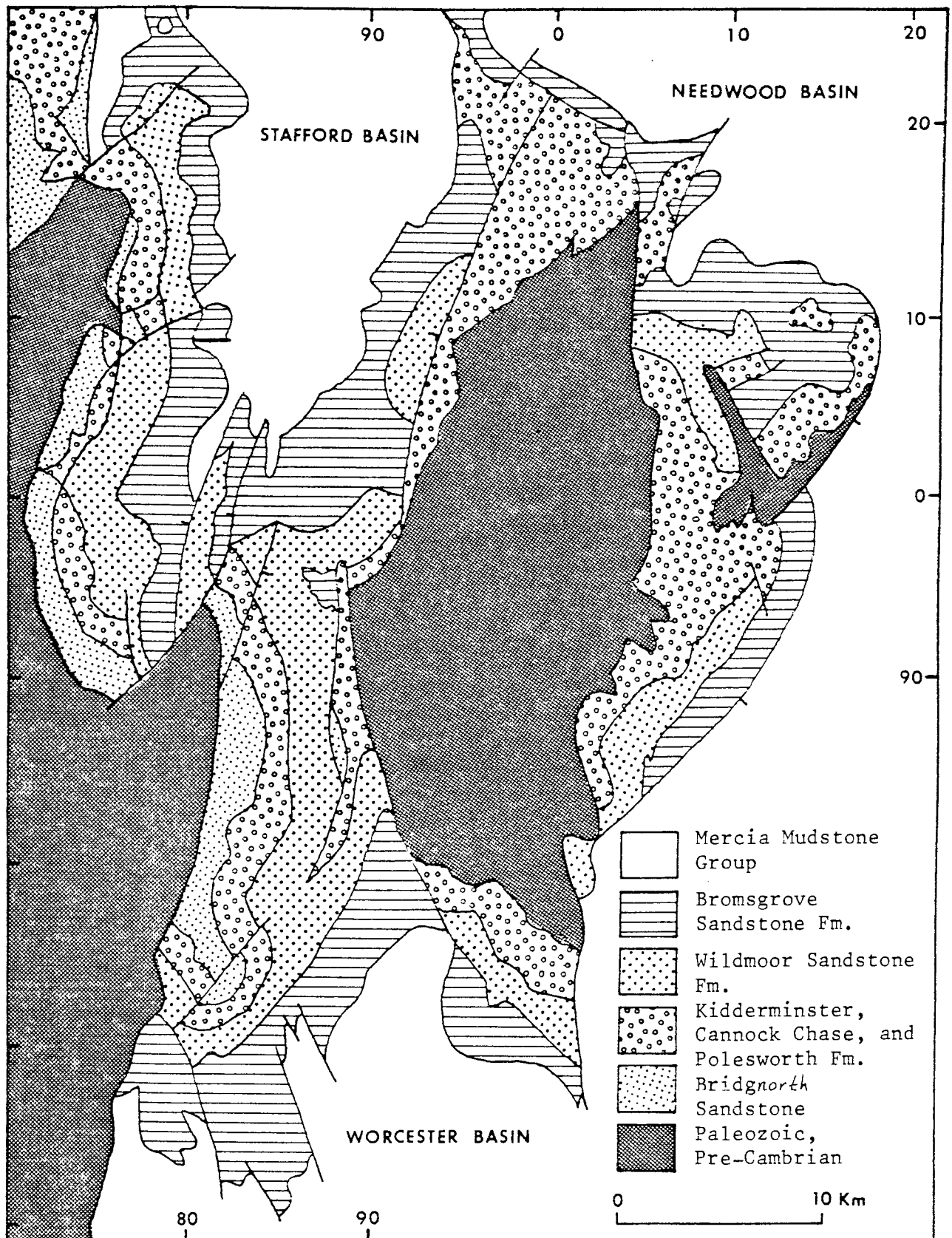


Fig.1.1 General geology of Central England.

Wildmoor Sandstone Formation. It consists of dark red medium grained, cross-bedded sandstones interbedded with reddish-brown and green mudstone units and abundant clay lenses. Green reduction spots and zones are abundant in the Bromsgrove Sandstone Formation.

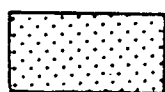
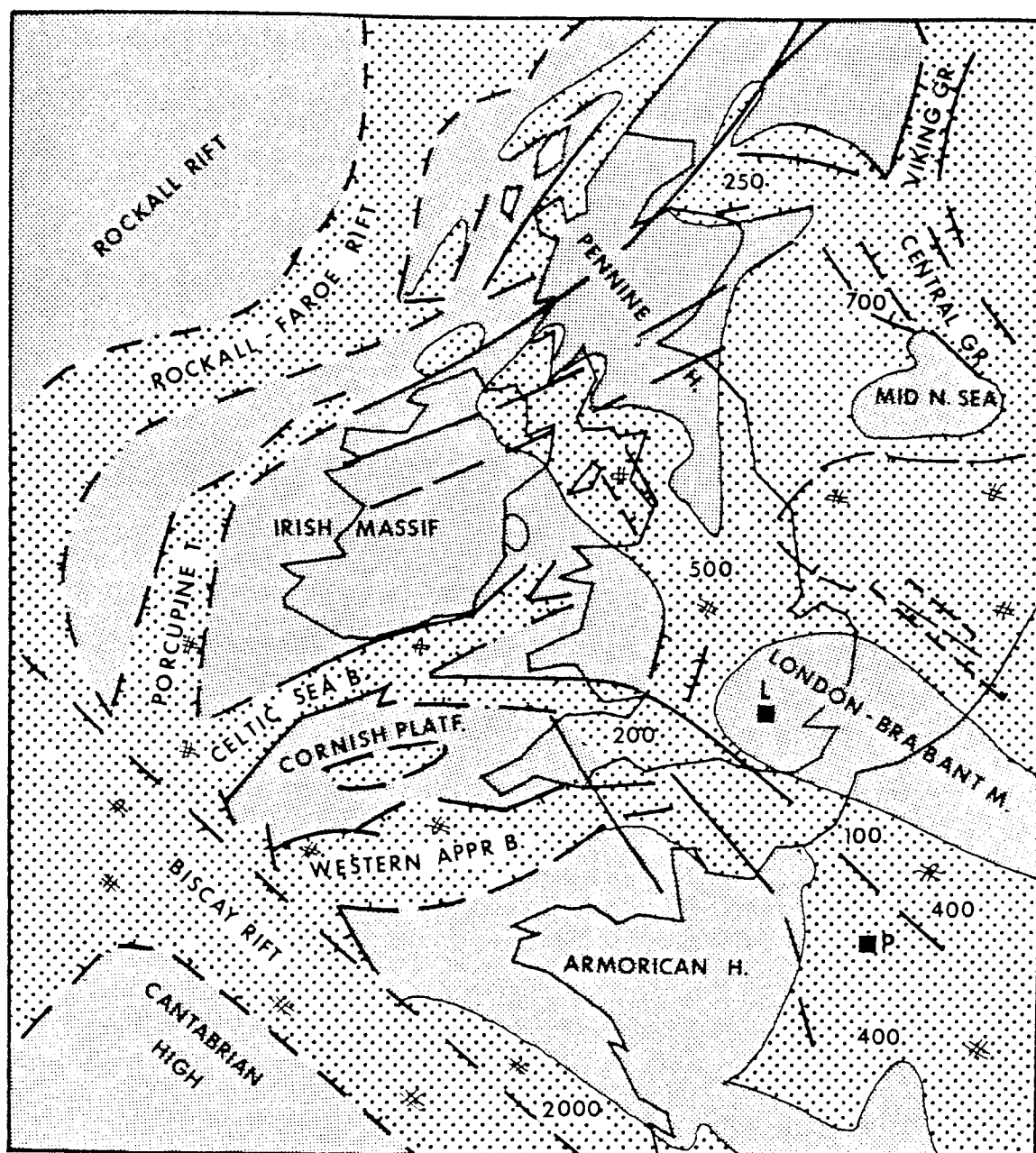
The Mercia Mudstone Group comprises the units of the former "Keuper Marl" and overlies the Sherwood Sandstone Group. Its base was taken at the base of the sandstone which underlies the argillaceous "Passage Beds" in the higher part of the former "Waterstone" unit (Warrington et al. 1980). It consists of red, green, and grey mudstones and siltstones, interbedded with red and green sandstone horizons. Some of the red sandstone horizons have abundant green reduction spots. Halite bearing units, gypsum, and anhydrite are present, especially in the basinal areas. The Arden Sandstone Member is the only widespread distinctive unit in the upper part of the Mercia Mudstone Group and is present throughout the region. It is represented by greenish-grey massive sandstones. The Blue Anchor Formation (formerly the Tea Green Marl) is present throughout the region below the Penarth Group.

The Penarth Group (formerly the Rhaetic) consist of dark grey shales and mudstones of predominantly marine origin. The Blue Anchor Formation and the Penarth Group are poorly exposed in the studied area and the previously described exposures are now much overgrown.

The structural pattern of Central England was mainly

developed during the Hercynian orogeny when faulting formed horst and graben structures which affected the pre-existing Caledonian tectonic elements. The main movements took place at the end of the Carboniferous Period and caused the transformation of the deltaic environment of the Coal Measures into the continental environment of the New Red Sandstones (the general term used to describe the Permo-Triassic red beds (Hains and Horton, 1969). Triassic sedimentary basins developed in association with the opening of the North Atlantic in a tensional regime (Ziegler, 1978) and are characterized by fault-bounded margins and great thickness (Audley-Charles, 1970a, b).

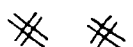
At the beginning of the Triassic time fast moving braided rivers flowing in a north-northwesterly direction (Audley-Charles, 1970b, Thompson, 1970) through the Worcester graben carried the earliest Triassic deposits in Central England. These deposits consist of conglomerates and pebbly sandstones. The source of these deposits lay in the south and southeast where the highlands are represented by the London-Brabant Massif and the Armorican Heights in Northern France (Fig. 1.2) (Brennand, 1975, Ziegler, 1975, 1978). These earliest Triassic deposits are represented in Central England by the Kidderminster, Cannock Chase, and Polesworth Formations. They were followed by the deposition of the Wildmoor Sandstone Formation after which the Hardeggen movement rejuvenated the Triassic morphology causing widespread erosion



Maximum distribution of Triassic deposits.



Edge Röt salt.



Areas with Keuper salt.

500

Total Triassic Thickness.

Fig.1.2 Triassic palaeogeography (after Ziegler, 1978).

(Zeigler, 1975). The deposition of the Bromsgrove Sandstone Formation followed, which caused the development of localized evaporite and salt pans. By this time the relief of the Triassic source areas had become lower and the rivers more sinuous. Deposition of the mudstones and sandstones of the Mercia Mudstone Group followed and represent quiet water deposits, probably of lacustrine or marginal marine origin. This was interrupted by a period of marine transgression causing the deposition of the Arden Sandstone Member. Just before the deposition of the Rhaetic which is represented by the Penarth Group the early Kimmerian movement started as a minor tectonic movement and continued intermittently throughout the Jurassic.

The Triassic rocks of Central England represent continental red beds deposited in an arid to semi-arid climate as indicated by the mineralogy and the presence of evaporites (Audley-Charles, 1970b, Jeans, 1978, Arthurton, 1980). The climate may have been relatively humid towards the end of the Sherwood Sandstone Group times as indicated by the size-composition trends utilized in this work, and became more arid in later Triassic times (Benton and Tucker, 1980). The conglomerates and sandstones of the Sherwood Sandstone Group were reddened post-depositionally through complex diagenetic processes similar to those described by Walker (1967, 1976) and Walker et al. (1978). The reddening of the Mercia

Mudstone Group may also have taken place post-depositionally through the ageing of clay-grade ferric hydroxide into haematite producing the red pigment in the mudstones. Some of the mudstones and associated thin sandstones may have not been completely oxidized as indicated by the presence of green reduction horizons and spots.

1.2 STRATIGRAPHICAL DIVISIONS

Triassic rocks are exposed over a wide area of England, and much of the previous work concerning their stratigraphical division and correlation was concentrated on the position of the base of the Triassic and on correlation with the European Triassic in Germany and Holland. The correlation was based mainly on lithostratigraphical evidence (Audley-Charles, 1970a).

Sherlock (1926, 1947) recommended the correlation of the Triassic as follows:

<u>System</u>	<u>Series</u>	<u>Approximate continental equivalent</u>
Epiric	Upper Triassic	Keuper
	Middle Triassic	Muschelkalk
	Lower Triassic	Bunter
	Eo-Epiric	Zechstein and Upper Rotliegende

and considered that the Muschelkalk sea never extended to England and was probably equivalent to the Keuper Sandstone. The Zechstein and Upper Rotliegende are now universally considered to be Permian.

Richardson (1929) classified the Triassic in the Midlands as follows:

	Tee Green Marl
Upper Keuper	Keuper Marl
	Arden Sandstone
	Waterstones
Lower Keuper	Building Stone Group
	Basement Beds
Upper Bunter	Upper Mottled Sandstone
Middle Bunter	Bunter Pebble Beds
Lower Bunter	Lower Mottled Sandstone

Wills (1948) divided the Triassic rocks as follows:

Keuper Marl Group
Keuper Sandstone Group
Upper Mottled Sandstone
Pebble Bed Group

and also regarded the Bunter Pebble Beds as the base of the Triassic and suggested that the lower Mottled Sandstone or so-called Bridgnorth Sandstone was Permian, a view which is now generally accepted. Wills (1976) regarded the shingle beds of the Bunter Pebble Beds as a marker bed defining the base of the Triassic in the Midlands.

Audley-Charles (1970a) suggested the following divisions of the Triassic rocks for Britain as a whole, considering the Bunter Pebble Beds as the base:

- Division 6: Limestones and shales with marine fossils and well-defined boundaries. The upper part represents the Rhaetic which is considered to be the top of the Triassic.
- Division 5: Mudstones and evaporites with thin sandstones and siltstones. The base is defined as the top of the Arden sandstones. This division is not present in the West Midlands and believed to have been removed by erosion.
- Division 4: Mudstones, evaporites, and saliferous beds, becoming mainly sandstones and siltstones towards the basic margins.
- Division 3: Represented by the Waterstones, and consists of interbedded sandstones, siltstones, and mudstones.
- Division 2: Represented by the Lower Keuper Sandstone.
- Division 1B: Represented by the Upper Mottled Sandstone.
- Division 1A: Represented by the Bunter Pebble Beds.

The present nomenclature of the Triassic rocks was introduced by Warrington et al. (1980) in which the major units were terms in ascending order, the Sherwood Sandstone Group, the Mercia Mudstone Group, and the Penarth Group.

The Sherwood Sandstone Group reached its maximum thickness in northern Worcestershire and southern Staffordshire and thins eastwards into Warwickshire where

it is overstepped by the Mercia Mudstone Group. The conglomeratic Kidderminster, Cannock Chase, and Polesworth Formations are arbitrarily considered the oldest Triassic deposits in Central England and are present only in the Western and Northern parts of the region with no lateral continuity. Later deposits spread progressively over a wide area and younger units overstepped older ones south-eastward towards the basin margin. The Wildmoor Sandstone Formation succeeds the pebble beds and has no well-defined base. The Bromsgrove Sandstone Formation is the highest unit of the Sherwood Sandstone Group and rests unconformably on the Wildmoor Sandstone Formation. The unconformable contact between the two formations is recognized by the reappearance of breccia and perthite feldspar. The lithology of the Bromsgrove Sandstone Formation is more variable and displays a clear cyclic sedimentation which was recognized by Wills (1970, 1976) in the Sherwood Sandstone Group as a whole.

The boundary between the Mercia Mudstone Group and the Sherwood Sandstone Group varies from sharp to gradational. In the latter case the contact is through a sandstone unit with a variable thickness (formerly called the Waterstones). Wills (1970) considered the base of the sandstone which underlies the argillaceous passage beds in the higher parts of the Waterstones as the boundary between the Bromsgrove and Droitwich stages which correspond to the Bromsgrove Sandstone Formation and the Mercia Mudstone

Group in this case. Halite units appear slightly below that boundary in Worcestershire and become more abundant above (Warrington, 1967, Wills, 1970).

The only widespread distinctive unit in the Mercia Mudstone Group in Central England is the Arden Sandstone Member. This unit separates a thick mudstone sequence with sulphate and halite units, which are represented by the Stafford and Droitwich Halite Formations in the Stafford, Needwood, and Worcester basins, from the overlying thinner mudstone sequence which lacks halite but contains some sulphate deposits (Warrington, 1974).

The highest unit in the Mercia Mudstone Group is the Blue Anchor Formation which is represented by the Tea Green Marl and present throughout the region. This is succeeded by the Penarth Group whose outcrop in Central England trends northeast to southwest and subcrop southeastward towards the flank of the London Platform. It is represented by the Westbury and the Lilstock Formations. The latter consists of the Cotham and the Langport Beds. The dark mudstones of the Westbury Formation rest non-sequentially upon the Blue Anchor Formation and are overlain by the grey-green calcareous mudstones of the Cotham Member which is succeeded by the limestones of the Langport Member. Alternating limestones and fissile shales of the "Ostrea Beds" of the Lias (Richardson, 1905) occur above the Langport Member and continue upwards into the basal Jurassic.

1.3 PREVIOUS WORK

The Triassic deposits of the North Sea area and Britain have received considerable attention in the past decade because of their hydrocarbon potential (Brennand, 1975, Colter and Barr, 1975, Colter and Ebbern, 1978) and in connection with underground exploration for water. The increasing availability of information from boreholes (especially in the off-shore region) and the continuing palynological studies have greatly improved the stratigraphical correlation and interpretation.

Many studies on the Triassic deposits of Central England were made with emphasis on the depositional environment and the nature of the source area. These include studies by Bonney (1900), Jeavons (1947), Fitch et al. (1966), Audley-Charles (1970b), and Wills (1976). As a result the early Triassic deposits were suggested to be fluviatile deposits transported by fast braided rivers which later became more sinuous by the time the Bromsgrove sandstones were deposited. Deposition of the Mercia Mudstone Group is believed to have taken place in a quiet water, probably lacustrine environment, interrupted by periods of marine transgression during which the main halites were formed (Arthurton, 1980). At the end of the Triassic the sediments were deposited in a shallow marine environment represented by the black shales, mudstones, and limestone of the Rhaetic.

Paleogeographic studies by Fitch et al.(1966), Audley-

Charles (1970b), Brennand (1975), and Ziegler (1975, 1978) suggested a north-northwest dispersal of detritus deposited in fault-bounded tensional basins with the main source area from the Variscan Mountains in N W Europe.

The mineralogy of the Triassic sandstones was previously studied by Bosworth (1912), Fleet (1923, 1925), Richardson and Fleet (1926), Dumbleton and West (1966), and Fitch et al. (1966). The emphasis in most of these previous mineralogical studies was on the relationship between heavy minerals and provenance. Other aspects of mineralogy have not been studied in detail.

Macrofossils occur sporadically in the Triassic sequence of Central England. They include vertebrate and invertebrate fossils especially fragmentary fish scales in the Kidderminster and Wildmoor Sandstone Formations. In the Bromsgrove Sandstone Formation different types of fauna, flora, and microflora are recorded (Warrington et al. 1980). The fauna includes annelids, brachiopods, bivalves, ostracods, fish, amphibia, and reptilia. The macrofossils include sphenopsids coniferopsids whereas the microflora is represented by various miospores.

Previous studies showed that the microfossils are of little stratigraphic value. However detailed palynological studies especially in the Mercia Mudstone Group (Warrington, 1970, 1976) have proved to be useful in stratigraphic correlation and environmental interpretations.

In Central England the work by Eastwood et al. (1925), Whitehead et al. (1928), Whitehead and Pocock (1947), and Mitchell et al. (1961), in the memoirs of the Geological Survey of Great Britain was based on old borehole data and surface exposures (although many are much overgrown now), and offered valuable information on the distribution of the Triassic rocks in the region.

1.4 METHODS

This thesis records the study of the Triassic red bed succession in Central England. Particular attention has been paid to the sedimentology, mineralogy, and diagenetic history of the rocks with the aim of providing a comprehensive analysis of the sequence. Samples were collected from quarries and road cuts which provided good sections for the different parts of the Sherwood Sandstone Group and the Mercia Mudstone Group throughout the studied area. The field work included logging of the different sections, sample collection, and the measurement of imbricated pebble orientation from different exposures of the Kidderminster, Cannock Chase, and Polesworth Formations. Between 30 to 150 measurements were taken from each locality and rose diagrams and stereographic projections constructed. The amount, declination, and inclination of the vector mean were calculated for each site.

Thin sections were prepared for each sandstone sample

and those containing carbonate cement were stained using the combined stain of potassium ferricyanide and Alizarin Red "S". Petrographic studies included routine investigation of thin sections and modal analysis using conventional techniques (Carver, 1967).

Heavy mineral separation was carried out using a heavy liquid (Bromoform, S.G. = 2.9), in which the disaggregated sandstone samples were immersed in a high intensity ultrasonic bath in order to clean the individual grain surfaces of clay. Grain mounts on glass slides and polished grain mounts were prepared and studied using both transmitted and reflected light microscopy.

The scanning electron microscope (SEM) with the energy dispersive analyser of X-rays (EDAX) was used to study most of the sandstone samples, both as small chips and individual grains of the heavy mineral separates. The specimens were prepared by mounting the chips or grains onto aluminium stubs, then coated under vacuum by carbon or gold palladium.

The electron probe microanalyser (EPMA) was also used to study quantitatively the authigenic and detrital K-feldspars and the iron and titanium oxides. The analysis was carried out on carbon coated polished thin sections and grain mounts using 15 KV voltage. The current was varied, depending on the mineral being analysed. In the case of the K-feldspar the current used was 0.25×10^{-7} Amp. because higher current causes the disintegration of

potassium giving lower counts, whereas in the case of the iron and titanium oxides the usual current of 0.5×10^{-7} Amp. was used.

The EPMA was also used for cathodoluminescence studies, and found to be especially useful for distinguishing detrital quartz of different origins and also authigenic quartz and K-feldspar.

X-ray diffraction was used to study the clay mineralogy. Oriented clay samples were prepared by suction onto ceramic tiles or sedimentation on glass slides and diffraction patterns of untreated, glycolated, and heated (550°C) samples were produced.

Grain size analysis was carried out on selected sandstone samples from different parts of the Sherwood Sandstone Group. These samples were disaggregated by crushing and wet sieving for the friable ones, by treatment with cold diluted hydrochloric acid for the carbonate cemented samples, and by heating with 50% hydrochloric acid for those containing a high proportion of iron oxide cement. After washing and drying, sieving at $\frac{1}{4}\phi$ intervals was carried out. Cumulative curves were plotted on a probability paper and the different statistical parameters according to Folk and Ward (1957) calculated.

CHAPTER 2

TRIASSIC SEDIMENTOLOGY IN CENTRAL ENGLAND

2.1 INTRODUCTION

The Triassic sequence in Central England illustrates an upward transition from fluvial to lacustrine and shallow marine environments as demonstrated by the previous studies of Audley-Charles (1970b), Warrington (1970), and Wills (1970). The main source area is represented by the uplands of northern France and the London Brabant Massif (Brennand, 1975, Wills, 1970, Ziegler, 1975, 1978). Central England is considered to be part of the main British Triassic basin. This basin is represented by a depression in the nature of a composite rift-valley extending from the Worcester Graben through Staffordshire and Cheshire into the northern part of the Irish Sea and Northern Ireland and separated from the North Sea Basin by an isthmus extending from Scotland via the Pennines, Charnwood and London Platform to Brabant (Wills, 1970).

The earliest Triassic deposits represented by the conglomeratic Kidderminster, Cannock Chase, and Polesworth Formations were transported by a major braided river system flowing in a north-northwesterly direction (Fitch et al. 1966, Audley-Charles, 1970b, Thompson, 1970a, Wills, 1970). The overlying sand-dominated Wildmoor Sandstone Formation was deposited in similar conditions. The relief in the

source area was initially high, but decreased gradually and the rivers became more sinuous during the deposition of the Bromsgrove Sandstone Formation (Warrington, 1970) which took place after the Hardegsen disconformity and was confined to the graben area of Worcester and a possible extension to the north (Wills, 1970).

During the deposition of the Mercia Mudstone Group the whole of northern and western Europe was a very flat peneplain and deposition took place in a quiet water environment probably lacustrine with periods of flooding by shallow seas and/or rivers and storm water (Arthurton, 1980). This caused cyclic changes in which sedimentation and evaporite precipitation were controlled by changing geographical settings (Wills, 1970). In this chapter the study of sedimentary structures, grain size, palaeocurrents, and facies relationships, together with information from subsurface data in the studied area is aimed at providing better understanding of the mechanism and environment of deposition of the Triassic rocks in Central England.

2.2 KIDDERMINSTER, CANNOCK CHASE, AND POLESWORTH FORMATIONS

These formations represent the lowest part of the Sherwood Sandstone Group in Central England and are present only in the western and northern part of the region with no lateral continuity. They reach a maximum thickness of about 200m east of Kidderminster recorded in the Billington No. 1 borehole (SO 876 766) in the Worcester Graben area as described by Wills (1976). The sequence thins eastward in

the horst area where it becomes discontinuous with a thickness of 0-50m and overstepped by younger formations in the sequence. The variations in original thickness is due to original topographic relief followed by irregular subsidence of the basin. The base of the Kidderminster, Cannock Chase, and Polesworth Formations (formerly the Bunter Pebble Beds) is considered to be at the base of the Shingle Beds which are confined to the graben area and rest unconformably on the Permian rocks (Wills, 1976). They consist mainly of quartzite and quartz (about 90%) conglomerates with a few rhyolites, porphyrites (some with tourmaline), and metamorphic clasts. This distinctive petrographic suite is different from any other conglomerates in the sequence (Wills, 1976). The Shingle Beds are overlain by a thick development of coarse, sometimes cross-stratified, pebbly sandstones and conglomerates. The conglomerates are usually polymodal, clast supported with poorly-sorted sandy matrix and a maximum clast size of up to 30 cm. Some are found to be locally cemented by calcium carbonate. The pebbles are well rounded and mainly oblate and equant in shape, few are bladed and prolate. They are composed mainly of quartzite, quartz, vein quartz, and occasional volcanic and sandstone pebbles. The pebbles are generally smooth surfaced except for concave impressions caused by pressure solution (Fig. 2.1) where the dissolved silica released cemented the sandy matrix around these impressions.

Mechanical analysis was carried out with $\frac{1}{4}\phi$ interval



Fig.2.1 Pressure solution impressions on pebble surfaces,
Some are surrounded by cemented sandy matrix.

on selected sandstone samples from the Kidderminster, Cannock Chase, and Polesworth Formations. The mean value ranged from 1.4ϕ to 2.62ϕ (medium to fine) showing a bimodal distribution (Fig. 2.2a). Standard deviation values range from 0.46ϕ to 0.66ϕ (well sorted to moderately well sorted) with a unimodal distribution (Fig. 2.2b). The skewness values range from -0.06 to 0.22 (near symmetrical to fine-skewed) showing a unimodal distribution (Fig. 2.2c). Kurtosis values range from 0.95 to 1.7 (mesokurtic to very leptokurtic) with a polymodal distribution (Fig. 2.2d).

Vertical variations in size parameters as observed in the road cut at High Habblerly near Kidderminster (SO 803 765) (Fig. 2.3) shows that the mean size fluctuates around 1.5ϕ with the finest grain size at the base of the section. The standard deviation value decreases upward indicating better sorting toward the top. The skewness values fluctuate at first between near symmetrical and fine-skewed then become more symmetrical upwards where the sandstones are better sorted. The kurtosis values fluctuate from meso to leptokurtic becoming very leptokurtic towards the top.

The Kidderminster, Cannock Chase, and Poleworth Formations were considered to be fluvial deposits (Bonney, 1900, Jeavons, 1947, Laming, 1966) transported by a major braided river system flowing in a north-northwesterly direction (Fitch et al. 1966, Audley-Charles, 1970b, Thompson, 1970a, Wills, 1970). Wills (1976) concluded that the deposition of the Pebble Beds took place in a basin with internal

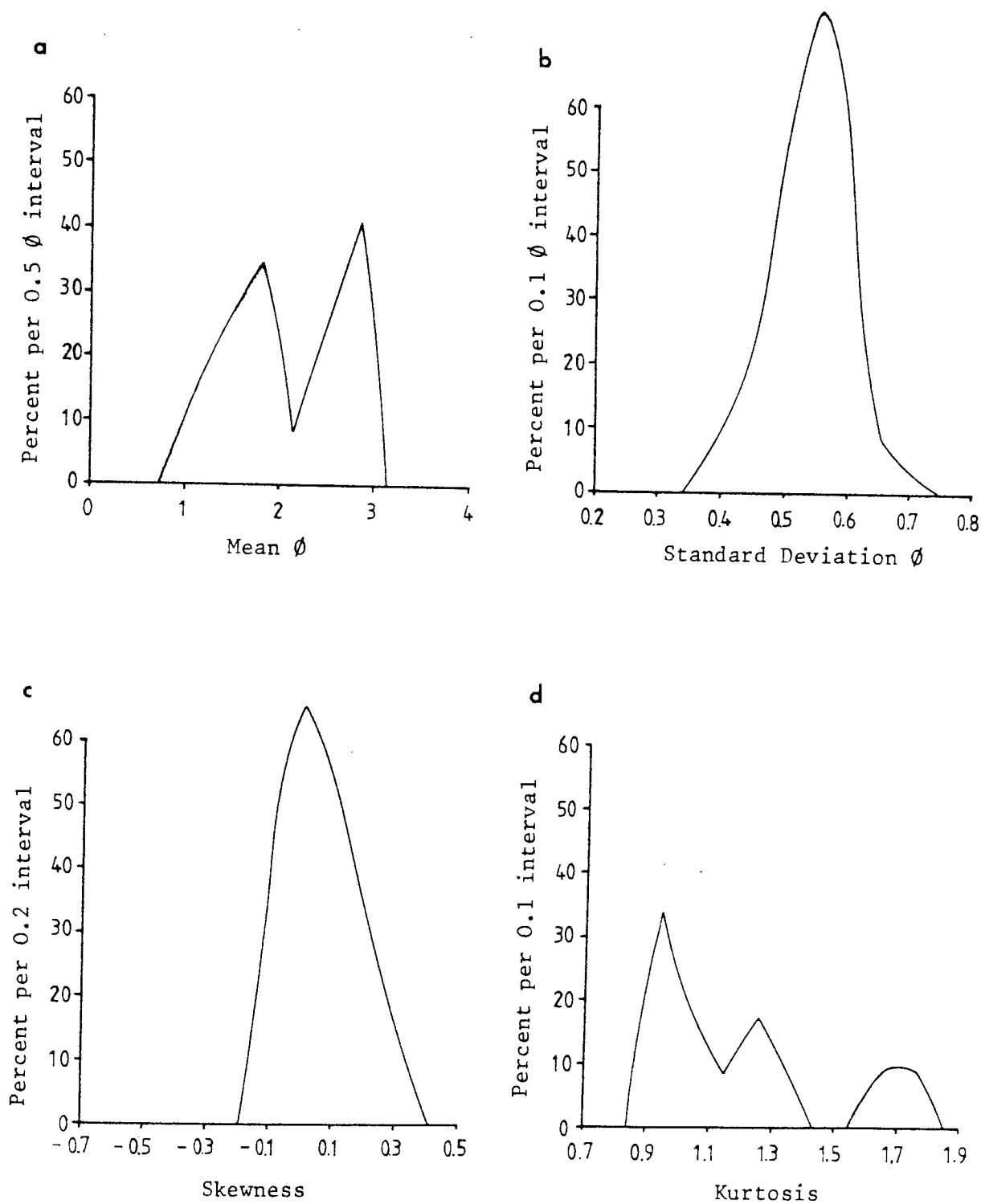


Fig.2.2 Frequency distribution of grain size parameters in the sandstone units of the Kidderminster, Cannock Chase, and Polesworth Formations.

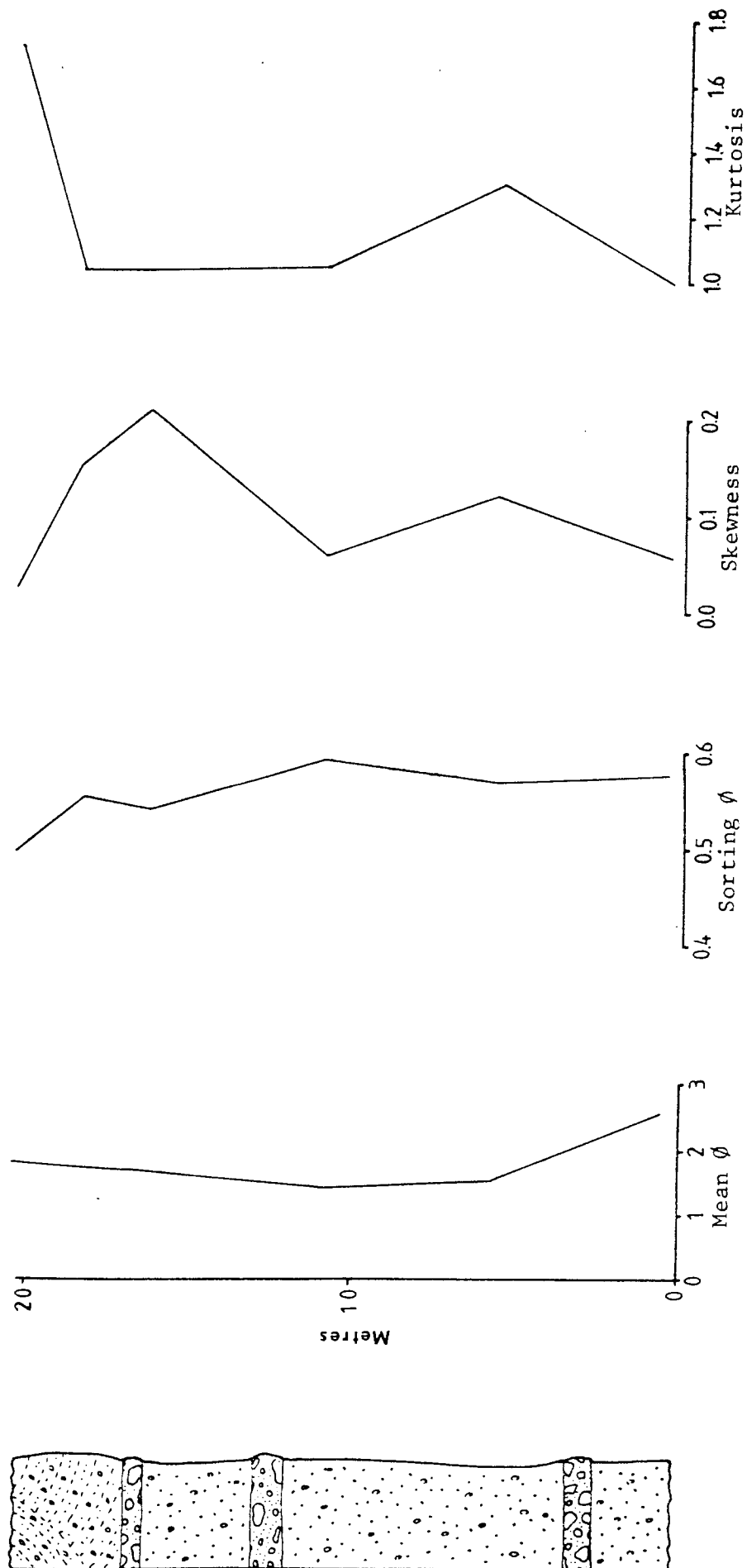


Fig.2.3 Vertical variations in grain size parameters in the Kidderminster Formation. Section at High Habberly (SO 803 765).

drainage where they represent alluvial fan and flood plain deposits. Wills (1970, 1976) described the cyclicity of the sequence and distinguished between drought and flood sequences. The drought sequences are generally composed of fine grained sandstones, siltstones, sometimes with mud pellets, and mudstones. The flood sequences, on the other hand, consist of pebbly sandstones and conglomerates with an upward decrease in the maximum clast size of pebbles. Surface exposures in the studied area shows that the sequence is characterised by both coarsening-upward and fining-upward cycles. A good example is the section at Weeford (SP 134 031) where each coarsening or fining upward sequence consists of 2-5m thick clast supported conglomerates with crude horizontal stratification (Fig. 2.4). At the basin margins these interfinger with coarser unstratified conglomerates which may represent alluvial fan deposits.

The main facies recognized in the Pebble Beds of Central England include:

- (1) Fining-upwards conglomerates.
- (2) Poorly sorted polymodal conglomerates.
- (3) Coarsening upward conglomerates.
- (4) Sandstones with thin siltstones.

The main characteristics of these facies are summarized in Table 2.1. They are considered to represent respectively the deposits of:

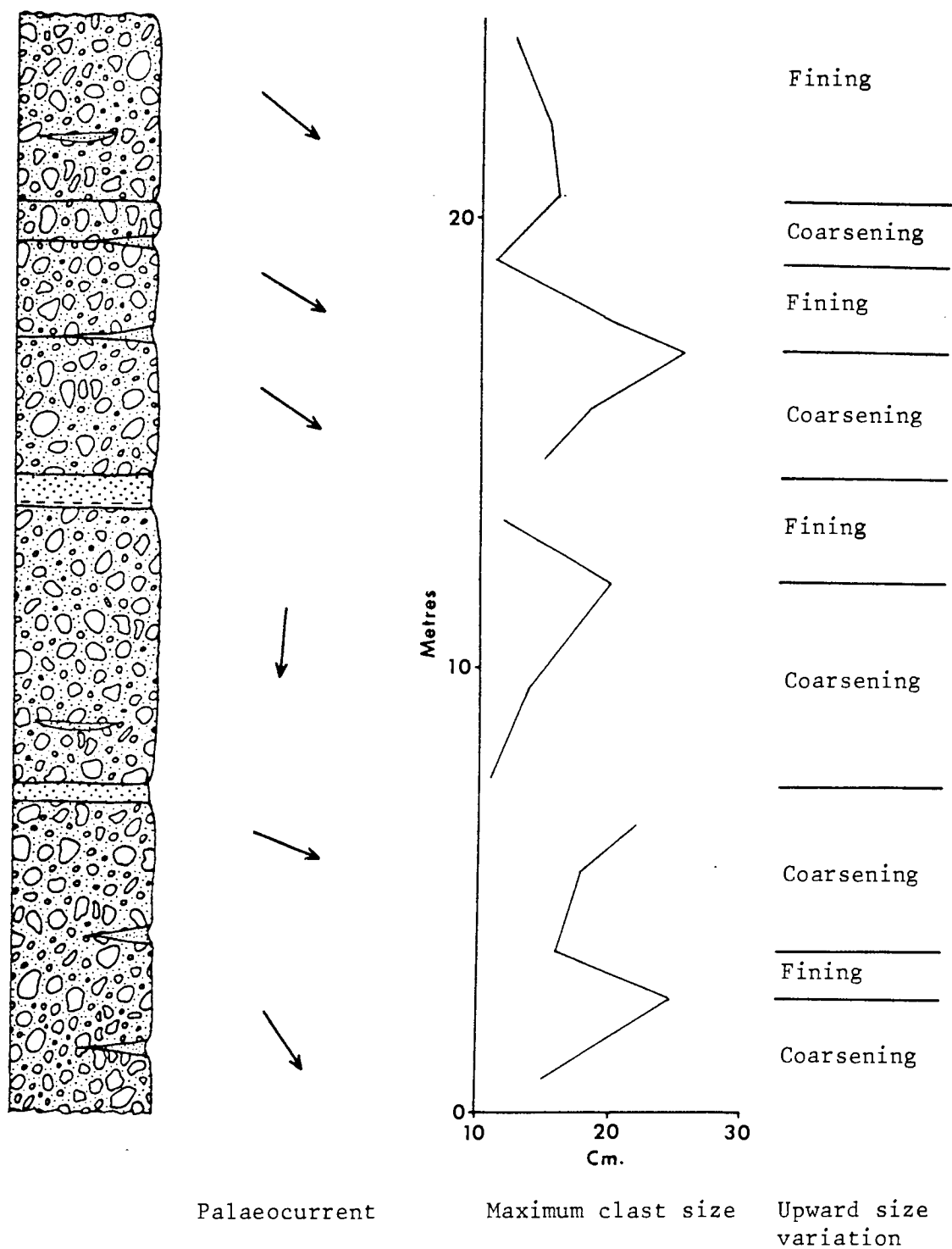


Fig.2.4 Section in the Polesworth Formation showing vertical variations in grain size and palaeocurrent direction depicted from pebble imbrication, Weeford (SP 134 031).

TABLE 2.1 FACIES CHARACTERISTICS OF THE KIDDERMINSTER,
CANNOCK CHASE, AND POLESWORTH FORMATIONS IN
CENTRAL ENGLAND

FACIES	MAIN CHARACTERISTICS
1. Braid bar deposits	Clast supported bidmodal conglomerates with crude horizontal stratification, abundant sandstone lenses, downstream decrease in grain size, tabular cross-stratification at the downstream end of the bar, and generally displaying a fining-upward sequence
2. Sheet flood deposits	Unstratified coarser, poly-modal clast supported conglomerates with abundant sandstone lenses, preservation of mud clasts, and non-erosive bases.
3. Progradational alluvial fan conglomerates	Unstratified conglomerates displaying a coarsening-upward sequence and occurring in the marginal areas of the basin.
4. Channel deposits	<p>a. Flat topped sandstone lenses 0.3 to 1m thick and 2 to 5m wide capped by thin laminae of siltstone and mudstone overlying fining-upward conglomerates.</p> <p>b. Concave-based lenticular cross-stratified pebbly sandstones up to 2m thick and 3 - 5m wide.</p>

- (1) Coarse-grained braid bars.
- (2) Sheet flood deposits.
- (3) Progradational alluvial fan conglomerates.
- (4) Sandy channel-fill deposits.

2.2.1 Braid Bar Deposits

Coarse grained braid bar deposits are characterized by crude horizontal stratification, downstream decrease in clast size, and more rarely, cross-stratification at the downstream end of the bar. In general they display a fining-upward sequence. These generalizations are based on the work of Williams and Rust (1969), Rust (1972), and Smith (1970, 1974). Eynon and Walker (1974) described in detail a model for bar growth in braided rivers based on the facies relationships in the Pleistocene outwash gravels of Southern Ontario. In this model (Fig. 2.5a) a bar about 400m long is described and a section parallel to the current direction is divided into a bar core, bar top, bar front, and stoss side. This passes laterally into channel deposits. The bar core is about 9m thick consisting of horizontally stratified, imbricated gravels with abundant sandstone lenses. The bar front consists of tabular cross-stratified gravels extending up to 150m downstream. Laterally the bar deposits interfinger with a trough cross-stratified sandstones representing side channel deposits; however in most modern braided rivers a coarser than sand fraction, i.e. pebbles are deposited in the channels (Reading, 1978).

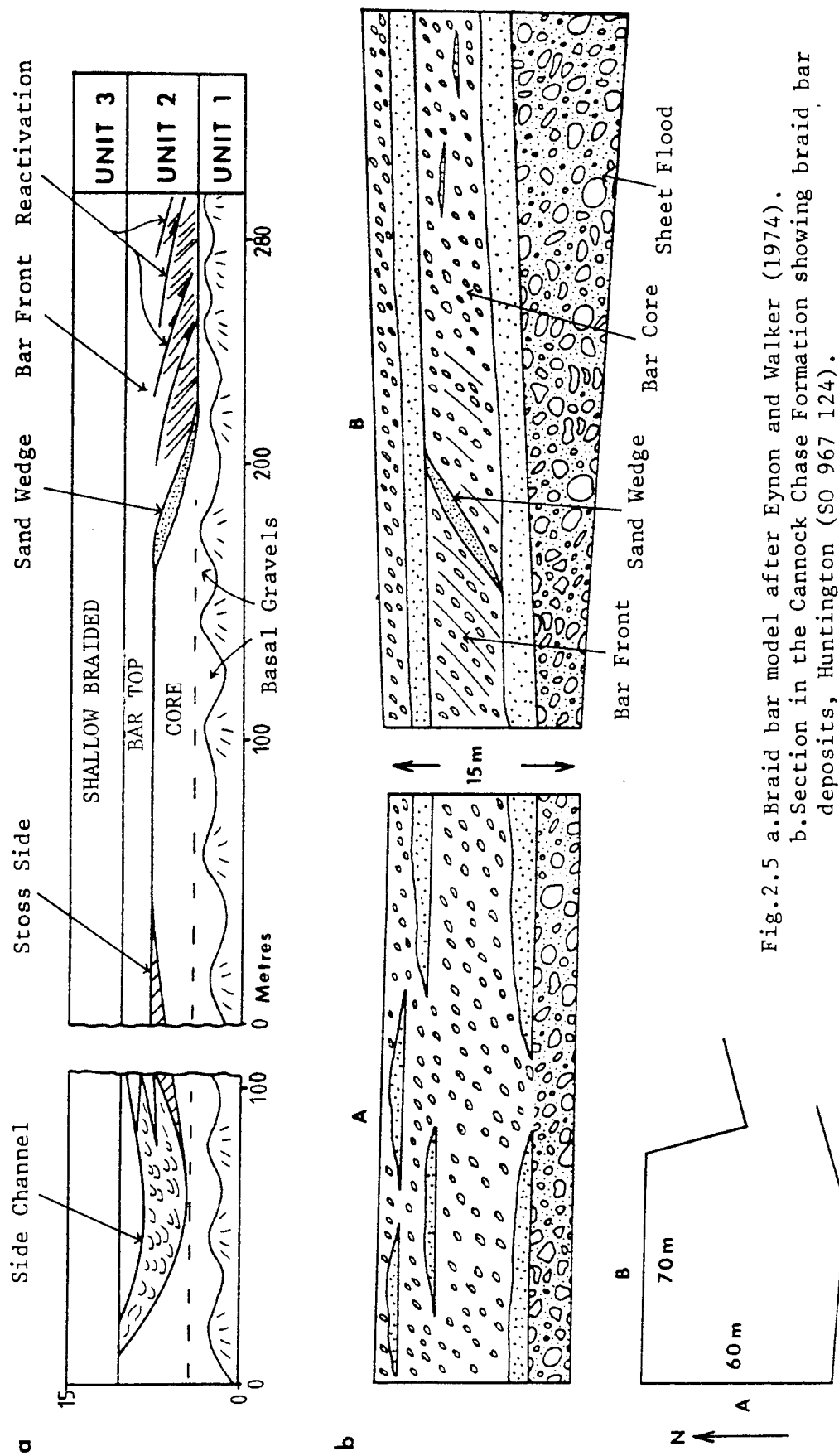


Fig.2.5 a.Braid bar model after Eynon and Walker (1974).
 b.Section in the Cannock Chase Formation showing braid bar
 deposits, Huntington (SO 967 124).

In the present study the section in the Cannock Chase Formation near Huntington (SJ 967 124) (Fig. 2.5b) shows the different facies of a braid bar. Bar core facies is usually represented by clast supported bimodal conglomerates with crude horizontal stratification and imbrication (Fig. 2.6). It shows a fining-upward sequence and usually topped by flat bottomed sandstone unit (Fig. 2.7). Sandstones lenses 0.2 to 0.5m thick and 1 to 3m wide are abundant as well as thin discontinuous horizontal finer pebble ^{beds} up to 0.3m thick and 1m wide. The sand wedge represents materials deposited from a current flowing obliquely alongside and across the bar (Eynon and Walker, 1974) and consists of cross-stratified, pebbly sandstones which rest abruptly on the bar core (Fig. 2.8). It also represents the initial stage of bar front development. The second stage of bar front development is the deposition of large scale tabular cross-stratified gravels. These tabular cross-stratified gravels are cut by reactivation surfaces which represent falling stages in the outwash system (Collinson, 1970). On these reactivation surfaces there are thin sand drapes up to 15 cm thick (Fig. 2.9) resting on a fining upward gravel. These sandy layers on the reactivation surfaces represent deposition during low flow stages (Eynon and Walker, 1974). The relatively thick sandstone horizons (3-6m thick) above and below the braid river bar may represent lower flow stages of the river or the draught sequences of Wills (1976); whereas the conglomerates represent flood sequences.



Fig.2.6 Clast supported bimodal conglomerate showing crude horizontal stratification, Polesworth Formation, Weeford (SP 134 031).



Fig.2.7 Flat bottomed sandstone units overlying bar core facies, Cannock Chase Formation, Brownhills (SK 063 042).



Fig.2.8 Sand wedge resting abruptly on the bar core facies, Pollesworth Formation, Weeford (SP 134 031).



Fig.2.9 Sand drapes along reactivation surfaces on the bar front facies, Cannock Chase Formation, Brownhills (SP 063 042).

2.2.2 Sheet Flood Deposits

Laterally persistent units of unstratified coarser, polymodal clast-supported conglomerates with abundant sandstone lenses, imbrication, and non-erosive bases were observed at Huntington (SJ 965 124), Weeford (SP 134 027), and Queslet (SP 065 945) in basin margin settings, and can be traced up to 100m with a thickness between 3-10m. Such units fall into the paraconglomerate type of Pettijohn (1957) and may represent sheet flood deposits of an alluvial fan as described by Bluck (1967). A good example is found at Huntington in the Cannock Chase Formation (Fig. 2.5b) where up to 8 metres of such coarse unstratified conglomerates, which is also characterized by the preservation of mud clasts (Fig. 2.10), underlie the braid bar deposits. Heward (1978) also described similar conglomerates in which sandstone lenses separate coarsening and fining upward sequences and considered them to be mid-fan deposits. The presence of conglomerates with the above mentioned characteristics may indicate the presence of alluvial fan deposits interfingering with braided river deposits at the basin margins.

2.2.3 Progradational Alluvial Fan conglomerates (Coarsening Upward)

A coarsening-upward sequence indicates an increase in fluid and sediment discharge caused by increasing flow power, possibly as a result of progradation. Progradation of alluvial fans is known to produce coarsening-upward



Fig.2.10 Mud clast preserved within sheet flood deposits,
Cannock Chase Formation, Huntington (SJ 965 124).

sequences (Reading, 1978). Coarsening-upward sequences may also represent aggrading base-level conditions which is the basic sedimentary response to basin floor subsidence (Steel, 1976, Steel et al. 1977).

In the present study coarsening-upward sequences 2-5m thick are abundant in the Kidderminster, Cannock Chase, and Polesworth Formations. An example is shown in Fig. 2.11. This may indicate the continuing of subsidence in the Triassic basin as the massive amounts of conglomeratic sediments were deposited in the early Triassic time and/or renewed uplift and accelerated erosion of the source area. In this case, coarsening-upward sequences occurring within unstratified conglomerates are considered to be alluvial fan deposits which prograded into basin areas in response to basin subsidence brought about by movement along marginal faults.

2.2.4 Channel Deposits

Channel deposits are abundant in the Kidderminster, Cannock Chase, and Polesworth Formations. They are represented by flat topped sandstone lenses 0.3 to 1m thick 2 to 5m wide, capped by horizontal laminae of siltstone and mudstone a few centimetres thick (Fig. 2.12). This sequence is similar to the fining-upward sequence of a channel fill described by Williams and Rust (1969). These channel deposits usually succeed a fining-upward sequence of conglomerates (Fig. 2.13). Another example of channel deposits is represented by concave-based lenticular cross-



Fig.2.11 A coarsening-upward sequence in the Polesworth Formation, Weeford (SO 134 031).



Fig.2.12 Channel deposits consisting of flat-topped sandstone capped by thin laminae of silt and clay, Cannock Chase Formation, Huntington (SJ 965 124).



Fig.2.13 Enlargement of Fig.2.12 showing fining-upward sequence underlying the channel sand.

stratified pebbly sandstone bodies up to 2m thick and 3-5m wide (Fig. 2.14). They are abundant in the predominantly sandy lower part of the Kidderminster Formation. They may represent the restoration of flow in a temporarily abandoned channel during rising water stages, causing the deposition of coarser pebbly sand. It may also be the result of cut and fill by migrating channels of low sinuosity rivers (Moody-Stuart, 1966, Thompson, 1970a).

2.3 PALAEOCURRENTS

The main directional structure in the Kidderminster Cannock Chase, and Polesworth Formations is pebble imbrication which form in response to a high flow stage (Bluck, 1974). Pebbles transported in contact with a frictional substratum tend to rest transverse to the current flow (Johanson, 1965, in Pettijohn, 1975). It has also been noted that elongate pebbles tend to be arranged transverse to current direction on the topset and bottom set units with extremely low dips and longitudinally on the foreset units having greater initial dips (Sengupta, 1966). Elongate pebbles larger than 2-3 cm have a strongly preferred orientation with their long axis perpendicular to the flow direction (Mc Donald and Banerjee, 1971, Rust, 1972), where the intermediate axis dipping upstream (Fig. 2.15), and transverse orientation is more pronounced when the pebbles are isolated, in which case a few large pebbles



Fig.2.14 Stream channel deposits represented by concave-based lenticular, cross-stratified pebbly sandstone, Kidderminster Formation, High Habberly (SO 803 765).

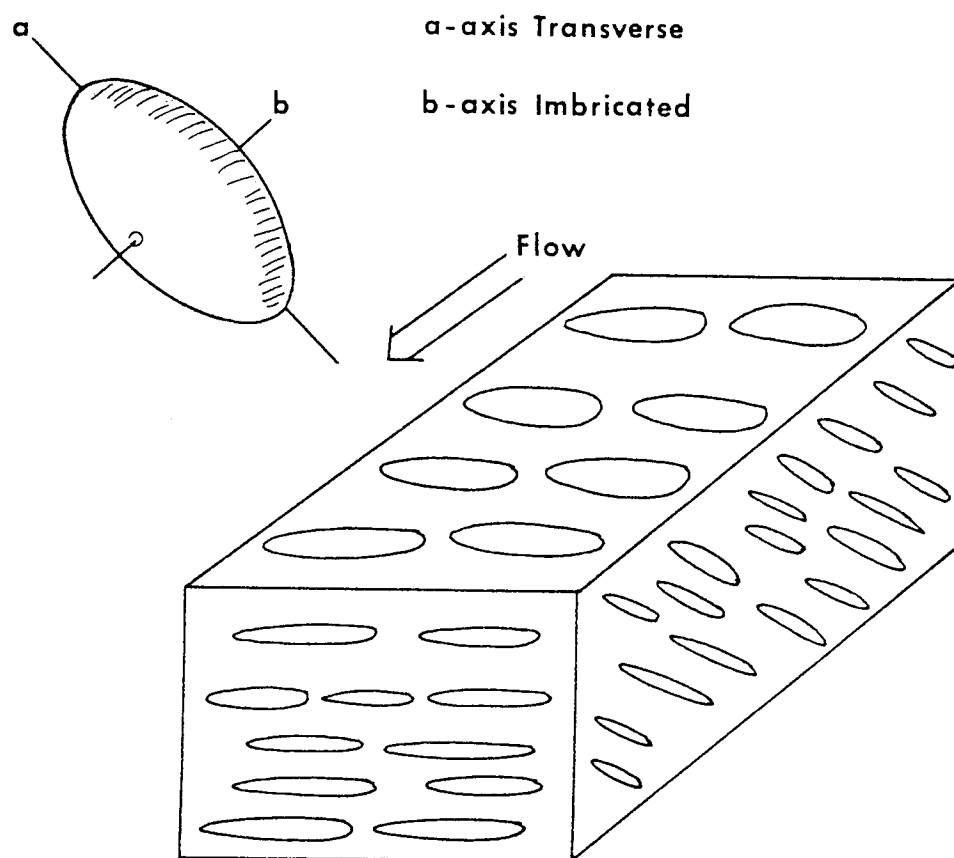


Fig.2.15 Pebble imbrication with the longest axis (a) transverse to the flow direction and the ab plane dipping upstream.

can give a high degree of orientation (Rust, 1972). However, other studies have showed that torrential flow tends to align the pebbles with their longest axis parallel to the flow direction (Pettijohn, 1975).

In the present study, most of the pebbles are oblate and equant in shape being slightly elongated and in almost all cases the long axis is transverse to the flow direction. In a few cases of large prolate pebbles located within the tabular cross-stratified gravels of the bar front facies the long axis was found to be parallel to the flow direction. Measurements of imbricated pebble orientations were taken throughout the studied area in different parts of the Triassic basins in Central England. Between 30 to 150 measurements were taken at each locality and from these the inclination and declination of the vector mean were calculated. The data were also plotted as poles on a Lambert equal area stereonet and the clustering of the points coincides with the direction of the vector mean (Fig. 2.16). The mean direction of pebble orientations shows that the palaeocurrent direction is generally towards the Northwest in the Wildmoor, Bridgnorth, and Brownhills areas, indicating that the main detritus movement is towards the Stafford Basin (Fig. 2.17). The palaeocurrent direction at Huntingdon near Cannock is northeastward towards the Needwood Basin; whereas at Weeford and Queslet the direction is to the South and Southeast, towards the Knowle Basin. At Kidderminster on the other hand, the palaeocurrent direction is to the

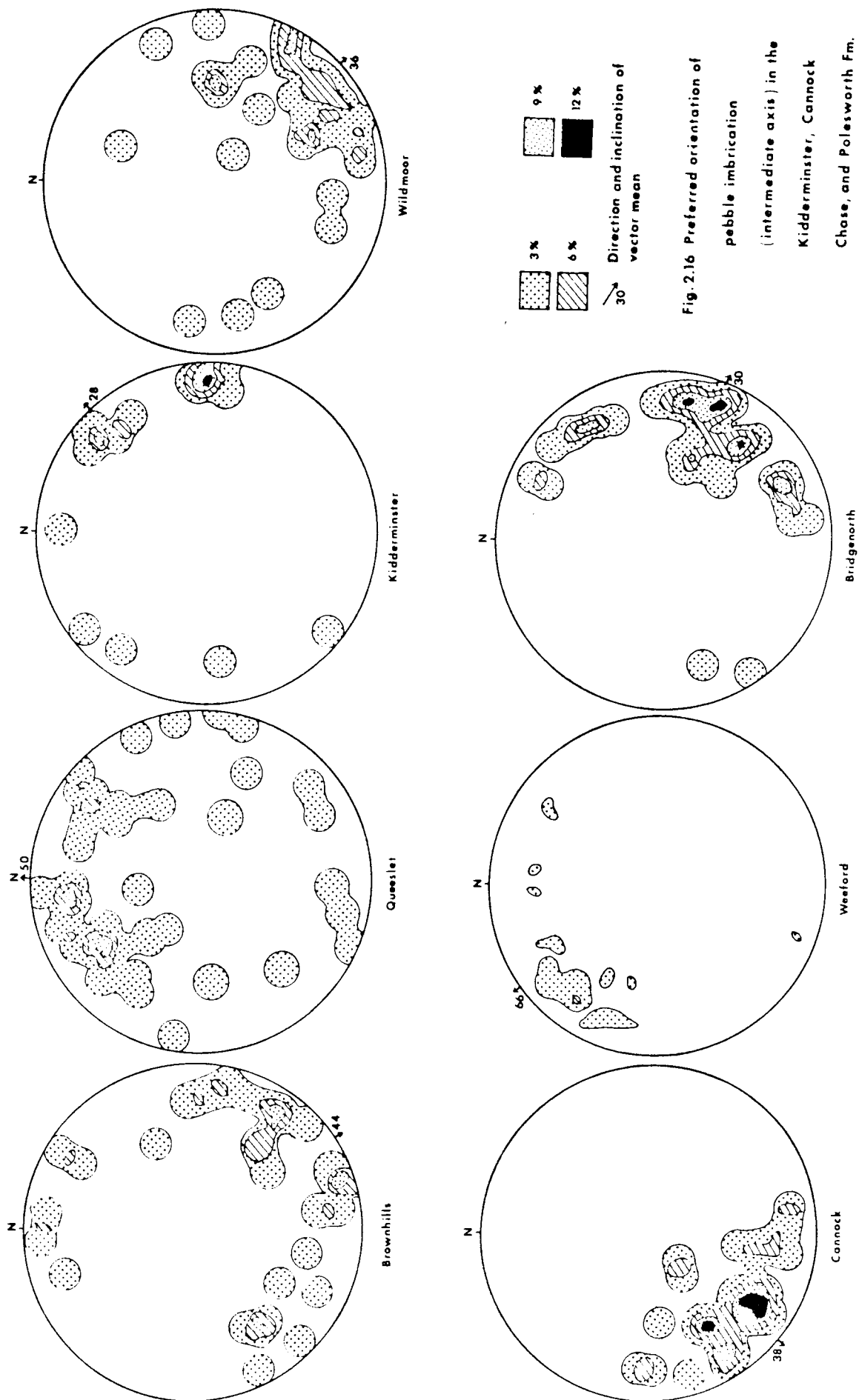


Fig. 2.16 Preferred orientation of pebble imbrication (intermediate axis) in the Kidderminster, Cannock, Chose, and Polesworth Fm.

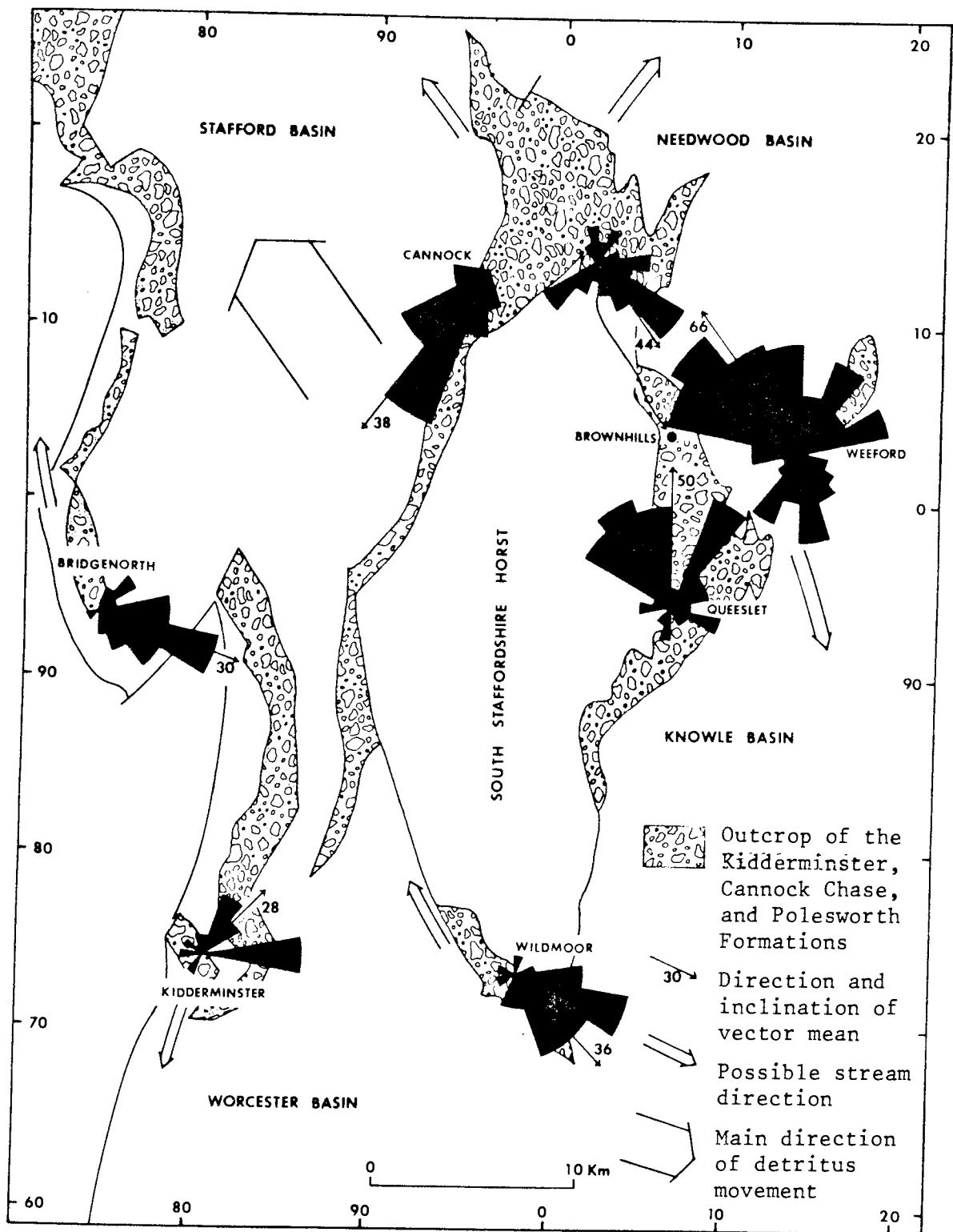


Fig.2.17 Rose diagrams of pebble imbrication (intermediate axis) and inferred palaeocurrent directions in the Kidderminster, Cannock Chase, and Polesworth Formations in Central England.

Southwest (Fig. 2.17). These palaeocurrent directions deduced from imbricated pebble orientations coincide with downstream decrease in grain size and the dip direction of cross-stratification. The deviation of palaeocurrent directions from the general north-northwesterly palaeoslope is due to the presence of marginal alluvial fans which drained laterally into the basin areas. Marginal areas nearer to high relief are represented by the Queeslet and Weeford sections located at the edge of the South Staffordshire Coalfield Horst. This is also supported by the fact that the inclination of the vector mean is very steep (Fig. 2.17). In the central parts of the basins drainage was predominantly axial along the northwesterly palaeoslope. A facies model depicting this interpretation is shown in Fig. 2.18.

2.4 WILDMOOR SANDSTONE FORMATION

The Wildmoor Sandstone Formation consists of soft friable bright red sandstones and brown mudstones. The sandstones are sometimes cross-bedded with occasional greenish bands and scattered pebbles. It reaches a thickness of up to 150m as recorded in the graben sequence east of Kidderminster at the Bellington No.1 borehole (SO 876 766) described by Wills (1976). Grain size analysis of selected samples from the exposed sections of the Wildmoor Sandstone Formation was carried out with $\frac{1}{4}\phi$ interval. The mean size ranges from 2.1ϕ to 3.27ϕ (fine to very fine) with a unimodal distribution (Fig. 2.19a).

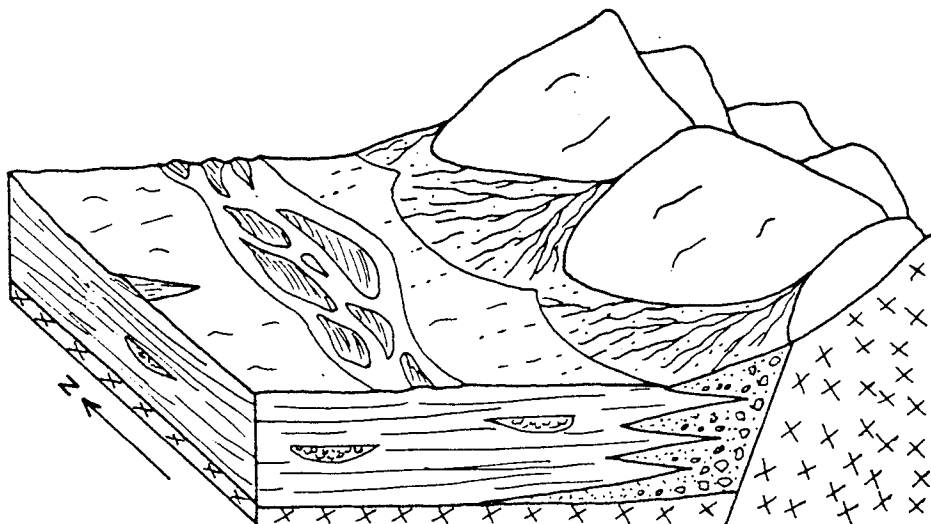


Fig.2.18 Facies model showing the drainage being axial in the central part of the basin whereas on the basin margins alluvial fans drain laterally into the basin area.

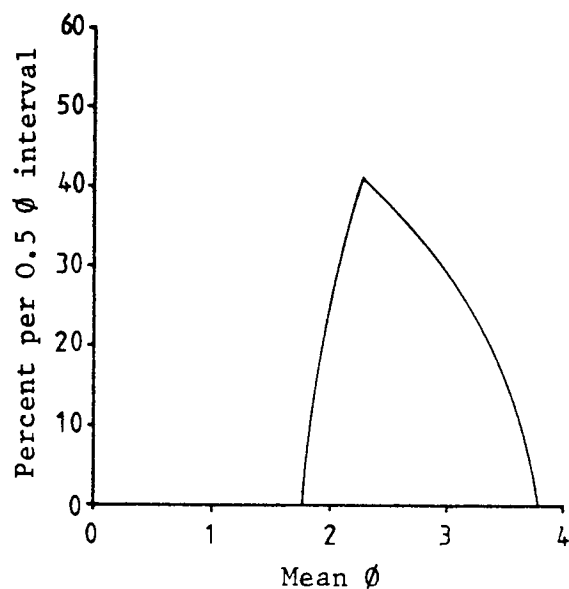
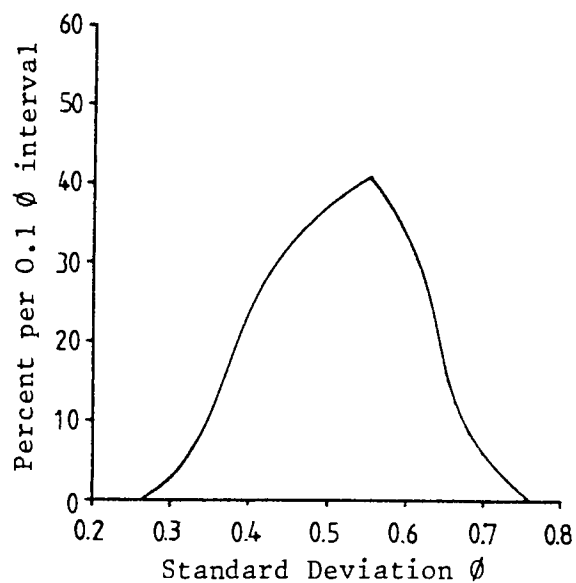
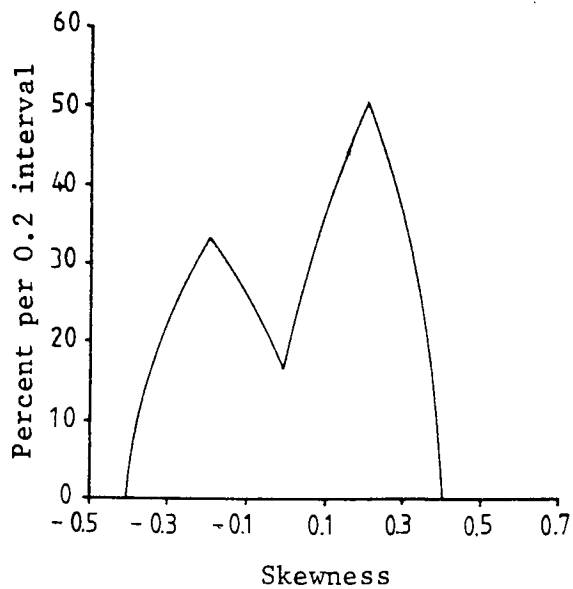
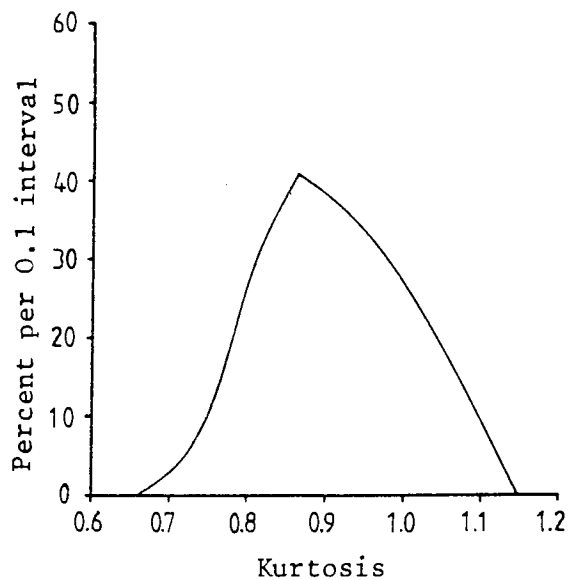
a**b****c****d**

Fig.2.19 Frequency distribution of grain size parameters in the Wildmoor Sandstone Formation.

The standard deviation ranges from -0.43ϕ to 0.62ϕ (well sorted to moderately well sorted) also showing a unimodal distribution (Fig. 2.19b). The skewness values range from -0.18 to 0.37 (coarse-skewed to fine skewed) with a bimodal distribution (Fig. 2.19c). The kurtosis values range from 0.75 to 1.1 (platykurtic to mesokurtic) showing a unimodal distribution (Fig. 2.19d).

Vertical variations in size parameters is best demonstrated by the section near Claverley (SJ 784 939) (Fig. 2.20). The mean size shows a slightly coarsening-upward pattern from very fine to fine. The standard deviation on the other hand shows a general upward increase i.e. the degree of sorting decreases upward. This variation in size and sorting may indicate a gradual rise in flow power. The skewness values show an upward decrease from near symmetrical to coarse-skewed indicating the presence of excess coarse materials. The kurtosis on the other hand, fluctuates between meso and leptokurtic.

It was suggested that the Wildmoor Sandstone Formation (formerly the Bunter Upper Mottled Sandstone) was deposited from slow rivers or lakes (Fleet, 1923, 1925, Wills, 1948). Fitch et al. (1966) suggested the same conditions for the deposition of the St. Bees Sandstone in Cumbria which is equivalent to the Wildmoor Sandstone Formation in Central England. Audley-Charles (1970b) considered the Wildmoor sandstones to be generally braided river deposits. Scottish rocks correlated with the Wildmoor sandstones were considered

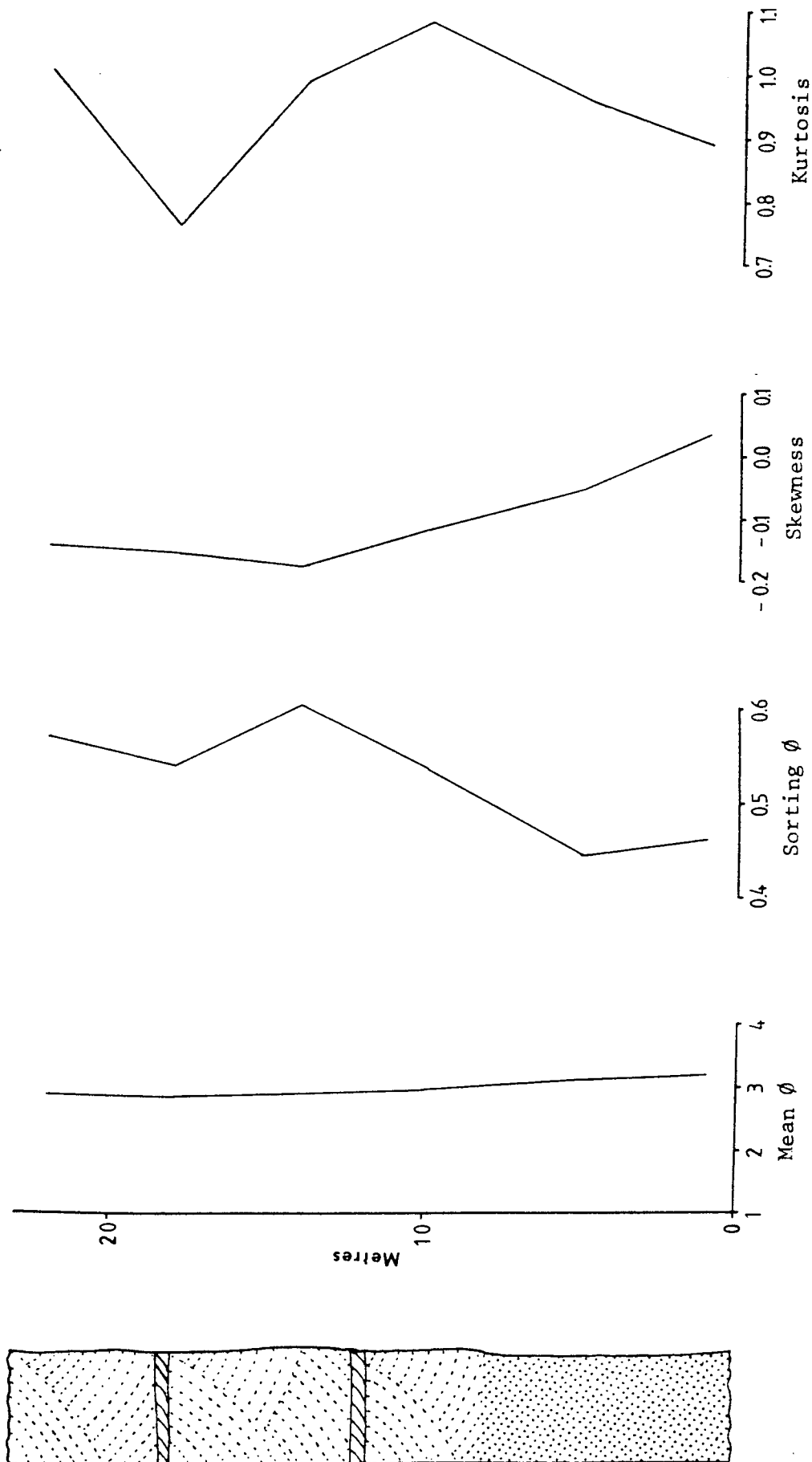


Fig.2.20 Vertical variations in grain size parameters in the Wildmoor Sandstone Formation, Section at Claverly (SJ 784 939).

by Craig (1965) as fluviatile and lacustrine deposits. Wills (1976) regarded the sequence to represent sheet flood deposits laid down by brief floods on a desert plain.

The Wildmoor Sandstone Formation in Central England is considered to be the deposits of low-sinuosity rivers with a sandy bed load representing an intermediate stage between pebbly braided rivers and meander rivers. A good example is the road cut near Claverley (SJ 784 939). The basal part of this section shows about 8 metres of bright red very fine grained sandstone with thin greenish bands near the top. It lacks any sedimentary organization with respect to sedimentary structures or grain size variation. This is succeeded by 15 metres of fine grained sandstones with large scale trough cross-stratification (Fig. 2.20, 2.21) and occasional units of planar-tabular cross-stratification (Fig. 2.22). Such a sequence may represent sandy braided river channel deposits. It is similar to the in-channel deposits of the braided-fluviatile facies model described by Cant and Walker (1976).

In other sections of the formation only thin horizons of small scale poorly defined trough cross-stratified sandstones are present. Large scale tabular cross-stratified sets (Fig. 2.23) are also common and may represent transverse or linguoid bars which have developed at high-intermediate water stages with well developed flow separation eddy in the lee of the bar producing asymptotic foresets (Collinson, 1970). In general, the cross-stratified sets dip towards



Fig.2.21 Large scale trough cross-stratification in the Wildmoor sandstones, Claverly (SJ 784 939).

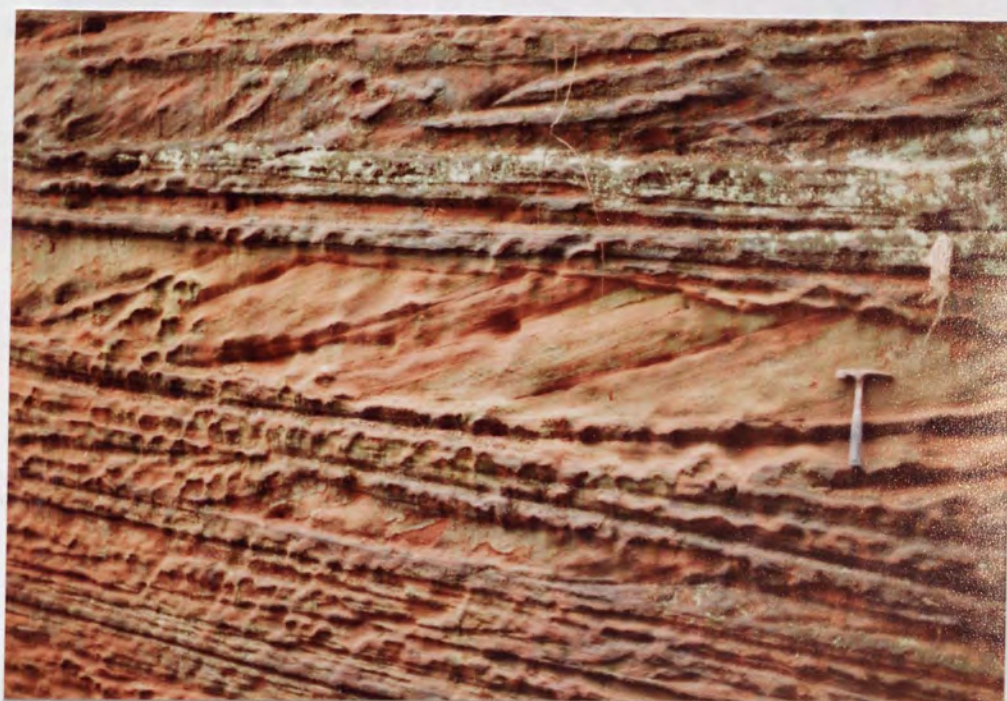


Fig.2.22 Isolated unit of tabular cross-stratification in the Wildmoor sandstones, Claverly (SJ 784 939).

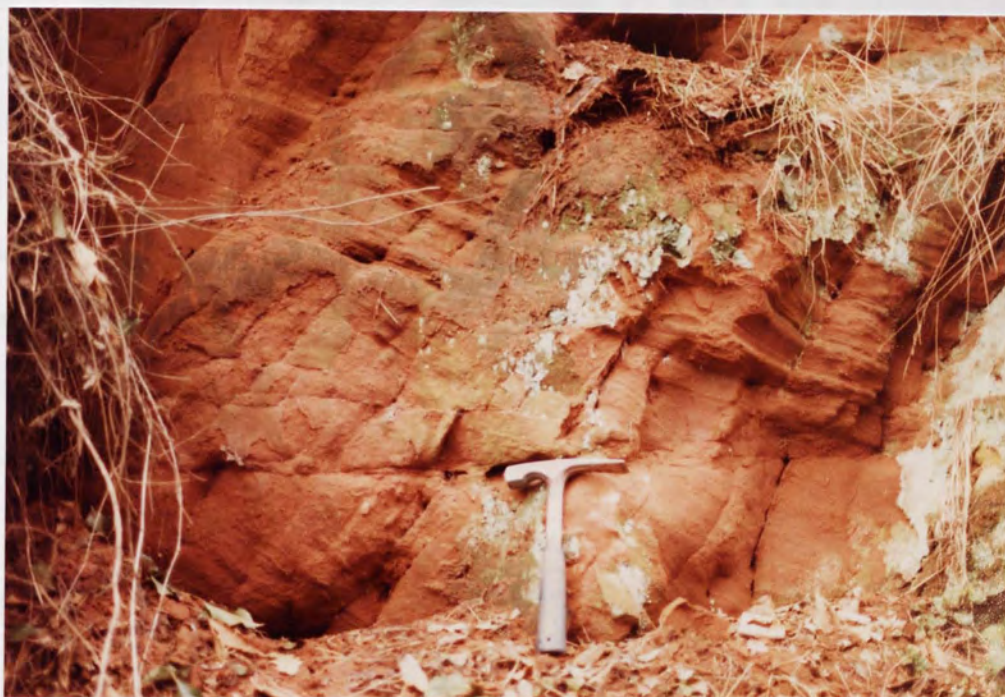


Fig.2.23 Large scale tabular cross-stratification in the Wildmoor sandstones, Worfield (SJ 757 956).

the northwest which coincides with the general north-north-westerly paleoslope of the Triassic basin in Central England.

2.5 BROMSGROVE SANDSTONE FORMATION

The Bromsgrove Sandstone Formation (formerly the Lower Keuper Sandstone) consists of dark red sandstones inter-bedded with red and green mudstones and abundant clay lenses. Green reduction horizons are common and are usually chlorite rich. The base has been recognized by coarse sandstone with fine breccia up to $\frac{3}{4}$ inch of unweathered feldspar, marking the Hardeggen disconformity (Warrington, 1970). The formation reaches a maximum thickness of 500m in the Worcester Graben area.

Grain size analysis of the Bromsgrove sandstones shows a mean size ranging from 1.61ϕ to 3.68ϕ (medium to very fine) with a bimodal distribution (Fig. 2.24a). The standard deviation values range from 0.18ϕ to 0.71ϕ (very well sorted to moderately sorted) with unimodal distribution (Fig. 2.24b). The skewness ranges from -0.38 to 0.28 (strongly coarse-skewed to fine-skewed) and also shows a unimodal distribution (Fig. 2.24c). The kurtosis values range from 0.86 to 1.45 (platykurtic to leptokurtic) with a bimodal distribution (Fig. 2.24d).

A good example of the vertical variation in size parameters is shown in the section at Rudge Heath (SJ 804 957) (Fig. 2.25) where the mean size fluctuates between 2ϕ to 3ϕ

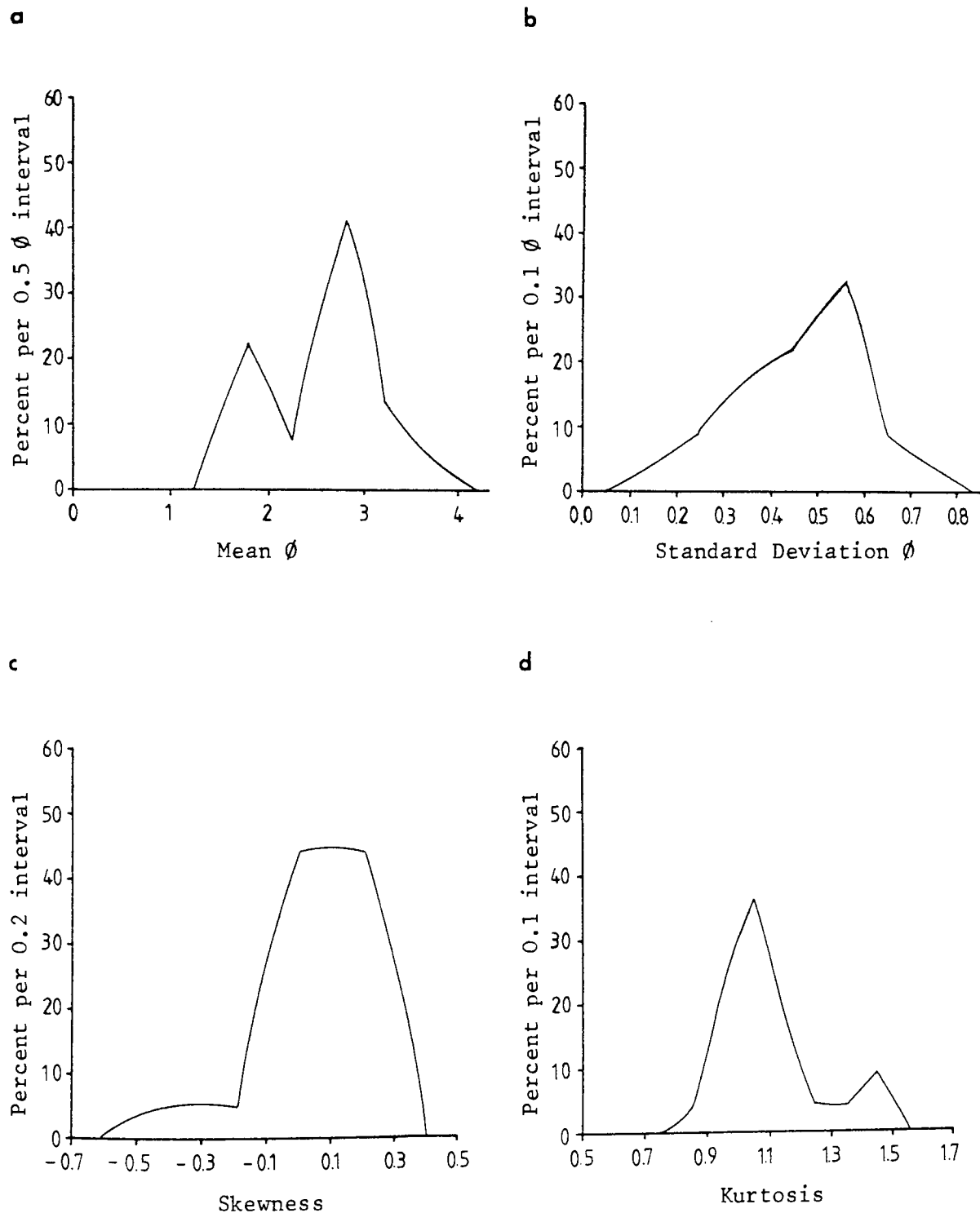


Fig.2.24 Frequency distribution of grain size parameters in the Bromsgrove Sandstone Formation.

with exceptional very fine grained horizons. The standard deviation fluctuates between the very well sorted and moderately well sorted extremes at the bottom then passes upwards to be moderately well sorted. The skewness values decreases progressively upward from fine-skewed to near symmetrical. The kurtosis values on the other hand fluctuates erratically between maso and leptokurtic.

Audley-Charles (1970b) suggested a meandering river and lake environment for the deposition of the Bromsgrove sandstones. Thompson (1970b) studied the Lower Keuper Sandstone in the Triassic Cheshire Basin and recognised different facies with varying fluvial, fluvial lacustrine, aeolian, and possible intertidal lagoonal origins. Intertidal sediments have been described in detail from the Waterstone horizon in the Cheshire basin (Ireland et al. 1978). The increased marine influence at the top of the "Lower Keuper Sandstone" marks the change to more persistent marine conditions during the deposition of the Mercia Mudstone Group. Warrington (1970) suggested fluvial deposition by rivers flowing in a northwesterly direction. These deposits have well-defined fining-upward cycles and contain a variety of macrofossils which include amphibia, lungfish, scorpions, and a variety of plants, indicating a fresh water fluviatile environment.

The deposition of the Bromsgrove Sandstone Formation represent a stage when the relief of the Triassic source area became lower and the rivers more sinuous. The road

section near Stone (SO 859 752) shows about 30 metres of dark red medium to fine grained sandstones, some with poorly defined tabular cross-stratification (Fig. 2.26). These sandstones are interbedded with red and green mudstones. Most of the sandstone units are rich with clay lenses (Fig. 2.27). In this section which represents the lower part of the Formation five fining-upward cycles can be recognized (Fig. 2.28a). These cycles usually consist of horizontal or cross-stratified medium to fine grained sandstones grading into finer or silty sandstones followed by a mudstone unit. Wills (1976) described 38 micocycles in the Sugerbrook borehole (SO 961 682) near Bromsgrove where the type section of the formation was described. These fining-upward cycles generally consist of massive brown, reddish brown, or grey sandstone with or without pebbles and/or mud flake breccia representing channel deposits (flood deposits of Wills, 1976) followed by chocolate marly sandstones, mudstones, and siltstone (Fig. 2.28b) representing floodplain deposits (drought deposits of Wills, 1976).

The fining-upward sandstone sequences in the Bromsgrove Sandstone Formation may represent point bar deposits of a meandering stream channel. Such a sequence reflects a decreasing flow regime as the river channel migrates laterally and deposition of fine grained material on the inner bank accumulates. This is also similar to the fining-upward sequence of the idealized point bar model



Fig.2.26 Poorly defined tabular cross-stratification in the Bromsgrove sandstones, Stone (SO 859 752).



Fig.2.27 Bromsgrove sandstones with abundant clay lenses, Stone (SO 859 752).

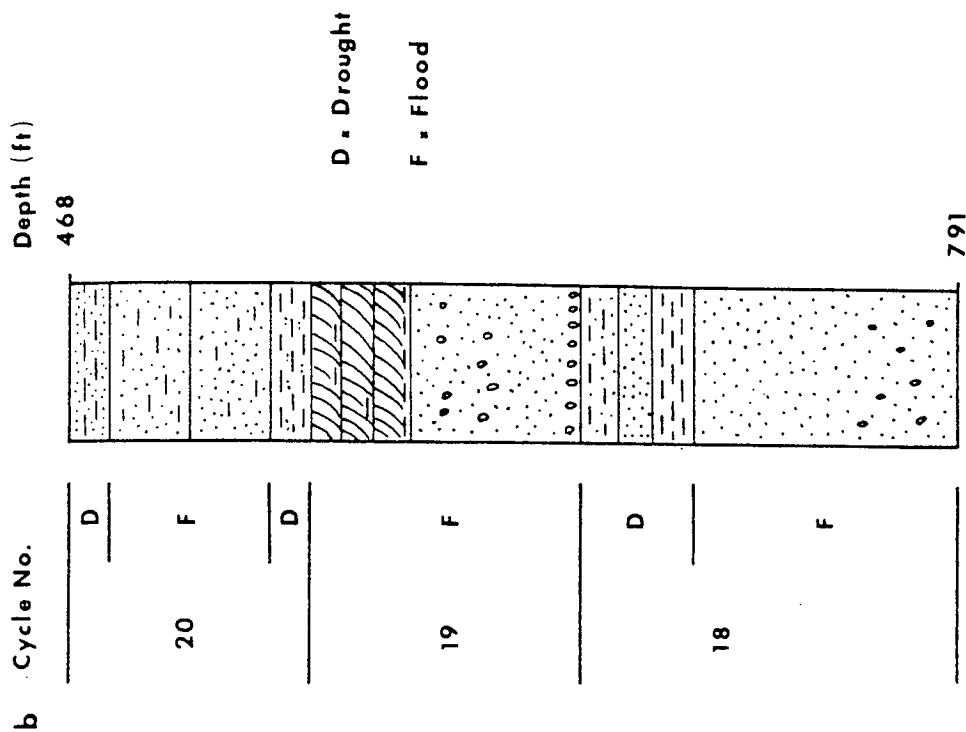
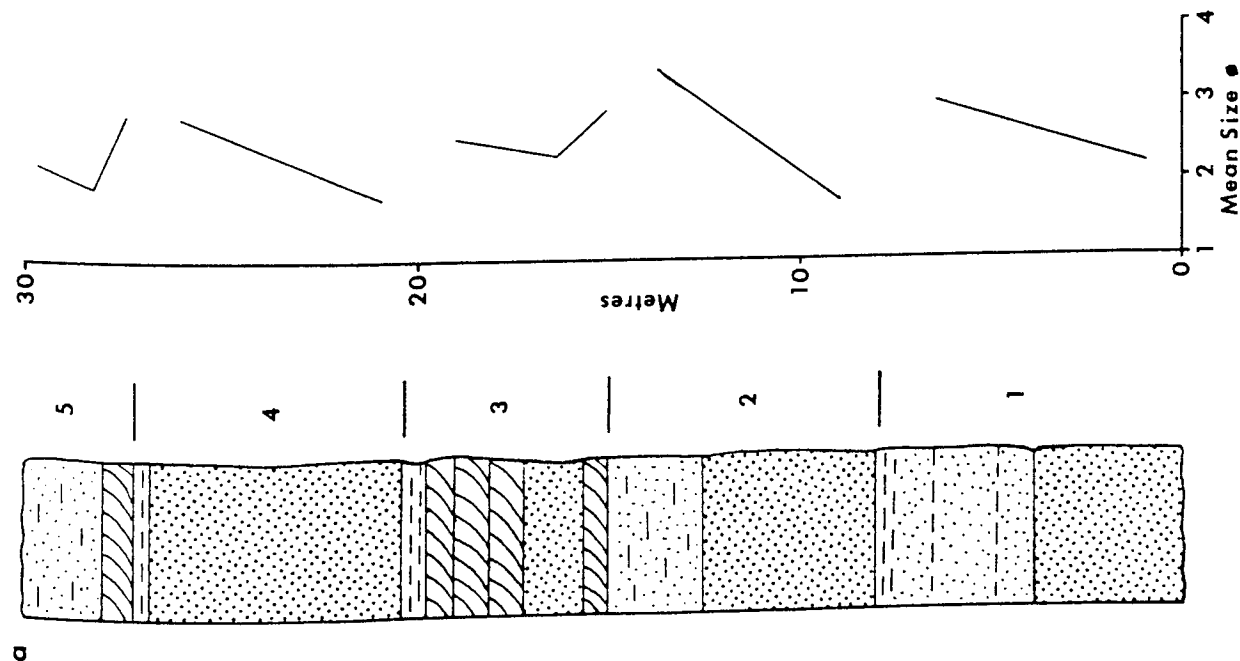


Fig.2.28 a. Section in the Bromsgrove Sandstone Formation showing five fining-upward cycles, Stone (SO 859 752).
 b. Part of the type section at Sugerbrook borehole showing three micocycles (after Wills, 1976).

described by Allen (1965, 1970).

The road section at Rudge Heath (SJ 804 957) consists of reddish brown sandstones and mudstones with abundant green reduction horizons (Fig. 2.29). Occasional small scale poorly defined trough cross-stratified units are present, some show water escape structures (Fig. 2.30). The lower contact of the sandstone units with the mudstones is usually green in colour and grades upwards into red (Fig. 2.31). Meandering channel deposits are represented by lenticular concave bottomed sandstones pinching out laterally (Fig. 2.31). These sandstones are usually resting with an erosional lower contact (Fig. 2.32). The cross-stratified sets generally dip in a north-north-westerly direction.

2.6 BIVARIATE PLOTS OF SIZE PARAMETERS AS ENVIRONMENTAL INDICATORS

Bivariate plots of the different size parameters are used in an attempt to interpret the depositional environment of the Triassic sandstones. They include: the first phi percentile (C) versus median, standard deviation versus median, skewness versus standard deviation, and mean size versus standard deviation.

The bivariate plot of the first phi percentile (C) versus the median used by Passega (1957) shows distinctive patterns for river, beach, quiet water, and turbidity current deposits. The sample distribution for the Triassic sandstones is scattered between the beach and tractive



Fig.2.29 Green reduction horizons in the Bromsgrove sandstones, Rudge Heath (SJ 804 957).



Fig.2.30 Trough cross-stratification and water escape structures in the Bromsgrove sandstones, Rudge Heath (SJ 804 957).



Fig.2.31 Meandering channel deposits represented by lenticular sandstone unit pinching out laterally, Bromsgrove Sandstone Formation, Rudge Heath (SJ 804 957).



Fig.2.32 Erosional lower contact of the channel deposits, Bromsgrove Sandstone Formation, Rudge Heath (SJ 804 957).

sediments (Fig. 2.33). The sample distribution on the plot of standard deviation versus median used by Stewart (1958) shows that most of the Bromsgrove sandstones and all the Wildmoor sandstones lie within the wave processes field, whereas most of the Kidderminster and Cannock Chase sandstones lie within the river processes field (Fig. 2.34). The distribution on Friedman's (1967) diagram which discriminates between beach and river sands by using the skewness versus standard deviation shows that the studied samples are almost equally distributed between the two fields (Fig. 2.35). The distribution on Miola and Weiser's (1968) diagram which discriminates between coastal dunes and river sands shows that all the samples are within the field of river processes (Fig. 2.36).

The fluviatile origin of the Kidderminster, Cannock Chase, Wildmoor Sandstone, and Bromsgrove Sandstone Formations is well known and proven through different studies of sedimentary structures and facies relationships associated with each formation, but three of the four bivariate plots show that many of the studied sandstones are not of fluviatile origin. This is due to many factors which affect the validity of these bivariate plots. They include in this case:

- (1) In many of the studied sandstone authigenic overgrowths of quartz and K-feldspar of various sizes have altered the grain-size parameters.

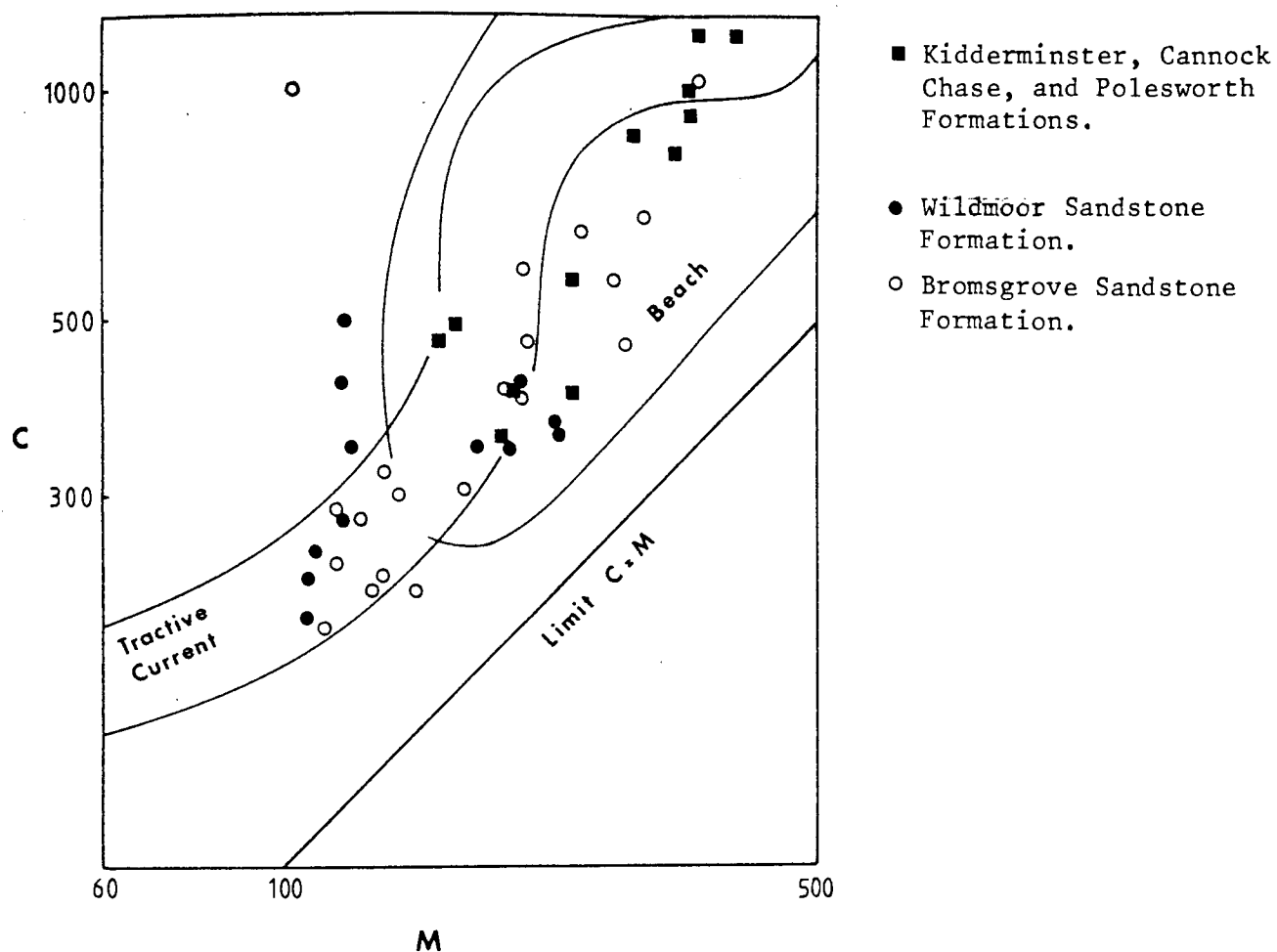


Fig.2.33 Bivariate plot of C (first percentile) vs M (median) after Passega (1957).

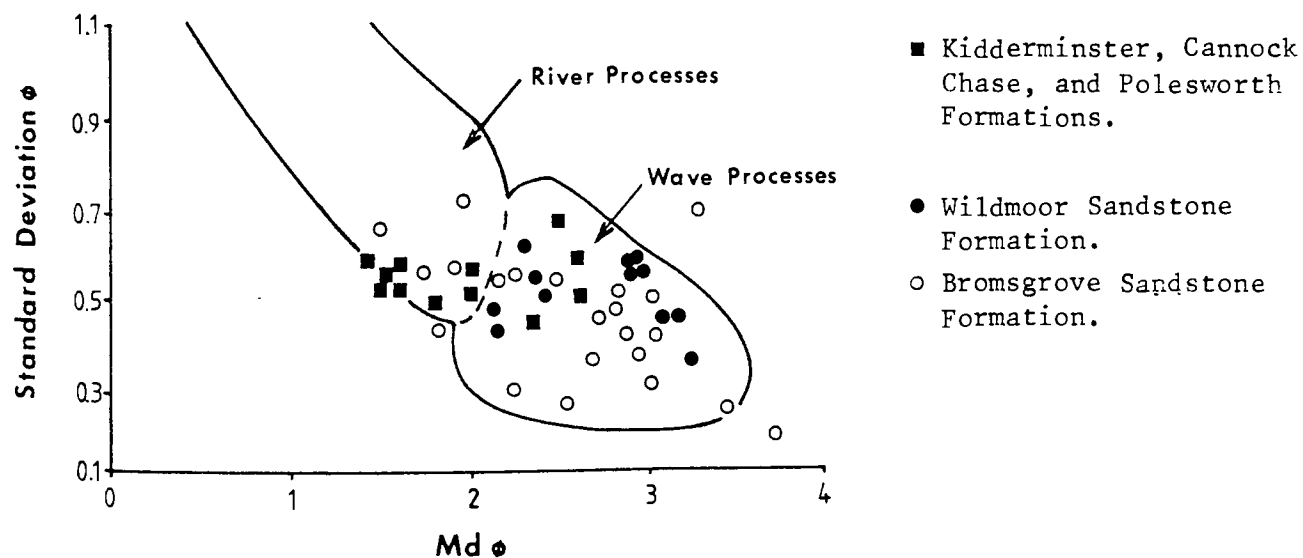


Fig.2.34 Bivariate plot of standard deviation vs median after Stewart (1958).

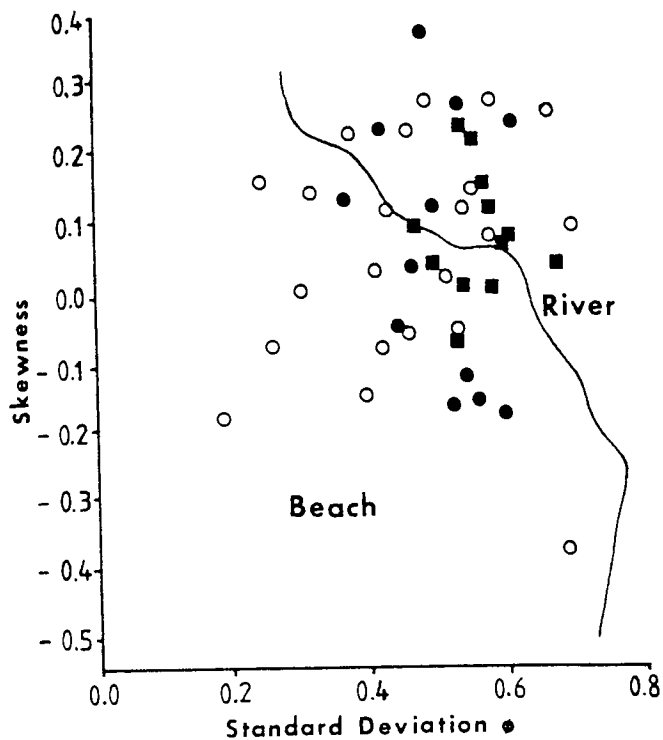


Fig.2.35 Bivariate plot of skewness vs standard deviation (after Friedman, 1967).

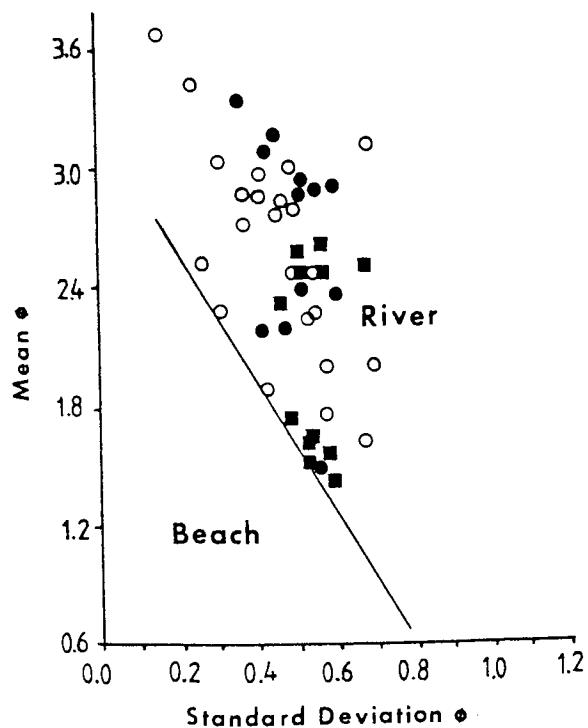


Fig.2.36 Bivariate plot of mean vs standard deviation (after Moiola and Wieser, 1968).

- (2) The possibility of mixing of grain populations from different laminae especially in the Wildmoor sandstones where distinctive lamination of fine and medium sand is present.
- (3) Error arising from disaggregating the samples where breakage may reduce large grains into smaller sizes.

Furthermore, such bivariate plots do not take into account the effect of regional variation in grain size, the effect of climate, diagenetic changes, the relative energy level within the same environment, and the possibility of mixing sediments from two different environments producing parameters characteristic of another. All these factors affect the reliability of these bivariate plots for predicting ancient depositional environments.

2.7 MERCIA MUDSTONE GROUP

The Mercia Mudstone Group covers most of the eastern and southern parts of the region. It consists predominantly of reddish brown blocky mudstones interbedded with subordinate green mudstones. Red and green sandstone and siltstone horizons are abundant throughout the sequence. Many of the red mudstones and sandstones are mottled with green reduction spots or green fisheye spots with a black speck in the middle. The mudstones are usually dolomitic (up to 30% dolomite) and dolomite is the main cementing material in the sandstones and siltstones. Halite, gypsum and saliferous deposits are present locally within the

sequence. The cyclicity of the sequence is distinctive and represented by variations in the proportions of evaporite to clastic materials (Wills, 1970, 1976). Bosworth (1912) suggested that the Mercia Mudstone Group was deposited in an inland, partly dried, quiet water basin. Lomas (1907), Matley (1912), Klein (1962), Elliott (1961), and Fitch et al (1966), suggested a lacustrine environment. Mineralogical studies by Dumbleton and West (1966) suggested that the Mercia Mudstone Group was deposited in a basin with an internal drainage and a hot climate with alternating wet and dry periods. Palynological studies by Warrington (1970) and the study of clay mineralogy by Jeans (1978) suggested deposition in a hypersaline environment interrupted by periods of marine transgression. Wills (1976) suggested deposition in numerous shallow water playa or lakes intermittently flooded by river water and/or seawater in a hot climate and that the halite and evaporite deposits were formed during periods of marine transgression. Arthurton (1980) suggested the same conditions for the deposition of the Mercia Mudstone Group in Northwest England where tectonic movements influenced the rate of basin subsidence and consequently the periods of emergence and submergence producing the cyclicity throughout the sequence.

The section at Bickenhill (SP 205 829) represents the lower part of the sequence. It consists of interbedded reddish brown blocky mudstones with gypsum veins,

reddish brown mudstones with fisheye green reduction spots, and alternatively mottled greenish grey and light reddish brown sandstones (Fig. 2.37). Sandstone and siltstone horizons of up to 0.5m thick are present throughout the section. Some of the sandstone horizons are light red with green reduction spots. Hard laminated mudstone horizons are also abundant. These mudstones are dolomitic with up to 30% dolomite and consist mainly of illite, chlorite, montmorillonite, and kaolinite. This section represents sediments deposited in a land locked basin probably lake environment in a hot climate. This was interrupted by periods of marine transgression represented by the halite and evaporite deposits.

The only widespread distinctive unit in the Mercia Mudstone Group is the Arden Sandstone Member. It broadly separates a thick mudstone sequence with local evaporite and halite deposits from thinner mudstone sequence which lacks halite. It is represented by fine to medium grained green sandstones and represents deposition in a shallow marine environment during a period of marine transgression (Matly, 1912). This is supported by the fact that the Arden Sandstone Member was found to be the only unit in the Mercia Mudstone Group with marine fossils (Wills, 1970, 1976). The section at the road cut near Henley in Arden (SP 167 654) shows 4 metres of greenish grey wave rippled sandstones with thin green mudstone bands (Fig. 2.38a). It overlies 4 metres of green and red mudstones with abundant sandstone lenses. The wave ripple cross-lamination

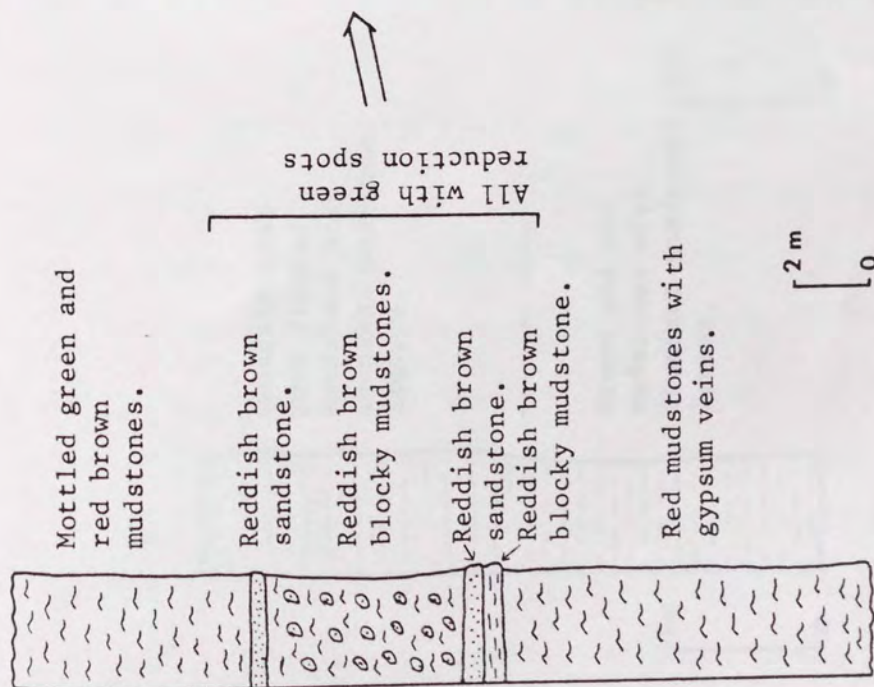


Fig.2.37 Section in the lower part of the Mercia Mudstone Group at Bickenhill (SP 205 829) where the sandstones and mudstones are with abundant green reduction spots.

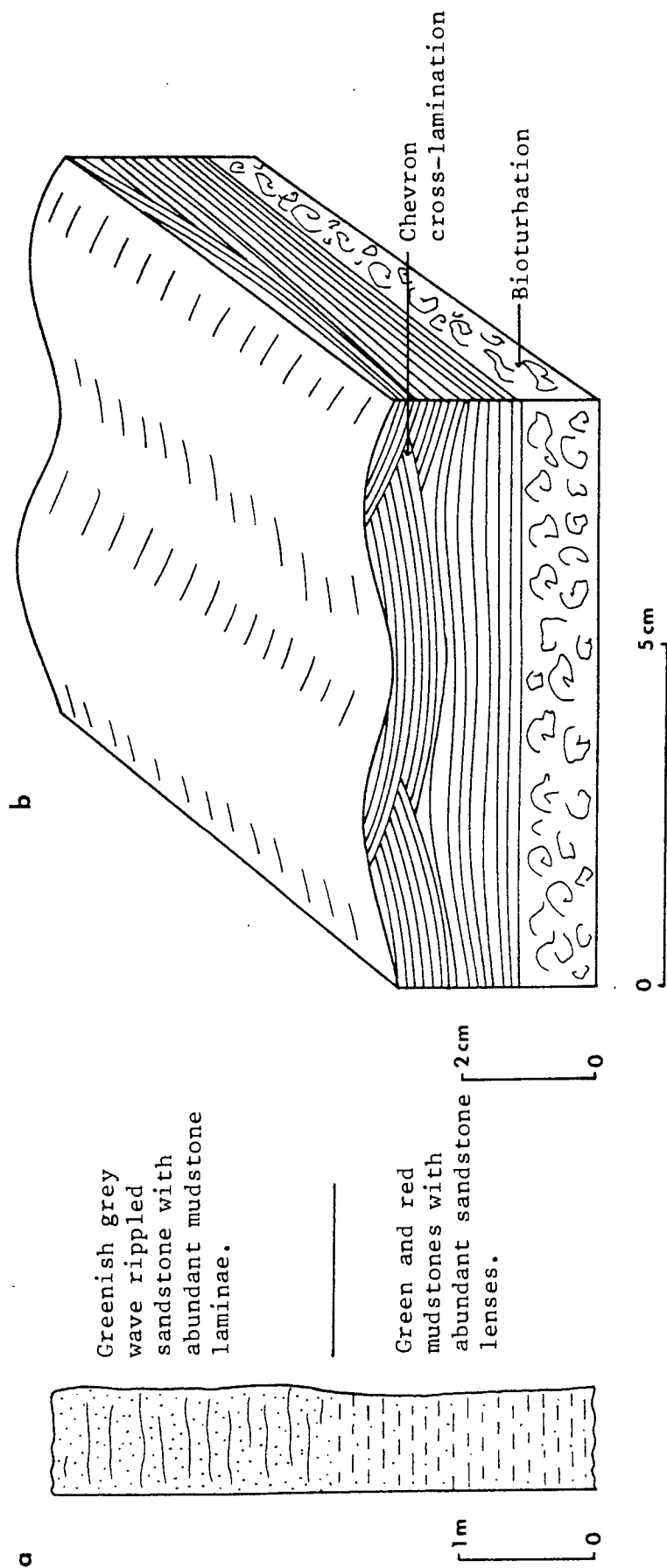


Fig. 2.38 a. Section in the Arden Sandstone Member. Henly in Arden (SP 167 654).
 b. Ripple cross-lamination.

was produced by oscillatory wave movement where the straight even lamination graded into high angle cross-lamination causing chevron upbuilding (Fig. 2.38b) by interfingering of both lee and stoss side laminae of the wave ripples. About 2 cm below the sandstones shows bioturbation filled with clay. This ripple cross-lamination structure is caused by persistent oscillatory wave action (Reineck and Singh, 1973, after Boersma, 1970) and indicates a shallow marine environment.

2.8 CONCLUSIONS

The different Formations comprising the Triassic sequence in Central England were deposited in a variety of environments ranging from pebbly braided rivers to shallow marine. At the beginning of Triassic time the conglomeratic Kidderminster, Cannock Chase, and Polesworth Formations were deposited in a fault bounded basin by marginal alluvial fans and a fast moving braided river system flowing from the south-southwest through the Worcester Graben. These rivers carried huge amounts of sediments from the highlands to the south and southeast represented by the London Brabant Massif and the Armorican Heights in Northern France. The deposition of the Wild-moor Sandstone Formation followed and this represents the deposits of sandy, low-sinuosity rivers. Later the relief became lower and during Bromsgrove Sandstone Formation times a northward sloping plain with meandering rivers were established. The deposition of the Mercia

Mudstone Group represents quiet water conditions probably of marginal playa type which were subjected to occasional marine flooding when the local halite and evaporite deposits were formed. A major marine transgression is represented by the deposition of the Arden Sandstone Member.

CHAPTER 3

PETROLOGY AND PROVENANCE

3.1 MINERALOGY OF THE TRIASSIC SANDSTONES

More than a hundred sandstone samples representing different parts of the Sherwood Sandstone Group and the Mercia Mudstone Group were studied in thin sections, grain mounts, and polished grain mounts. Point counting using the ribbon method (Carver, 1967), with 500 counts per thin section was carried out on most of the specimens.

Quartz constitutes the major component in the Triassic sandstones ranging from 73% to 96%. Feldspars comprise up to 25%, and rock fragments (including chert) a maximum of 20%. According to Folk's (1968) classification the Triassic sandstones are mainly subarkoses; a few are considered to be sublitharenites, and occasionally quartz arenite and lithic arkose (Fig. 3.1).

3.2 QUARTZ

Quartz grains in the Triassic sandstones include many varieties which reflect the type of rocks in the source area. The grains are rounded to subrounded displaying a slight elongation parallel to the c-axis and orientation parallel to the bedding. This elongation is due to preferred abrasion and the weak tendency of quartz to fracture parallel to the c-axis rather than perpendicular to it (Folk, 1968). Attempts to study the quartz surface textures using the SEM were unsuccessful

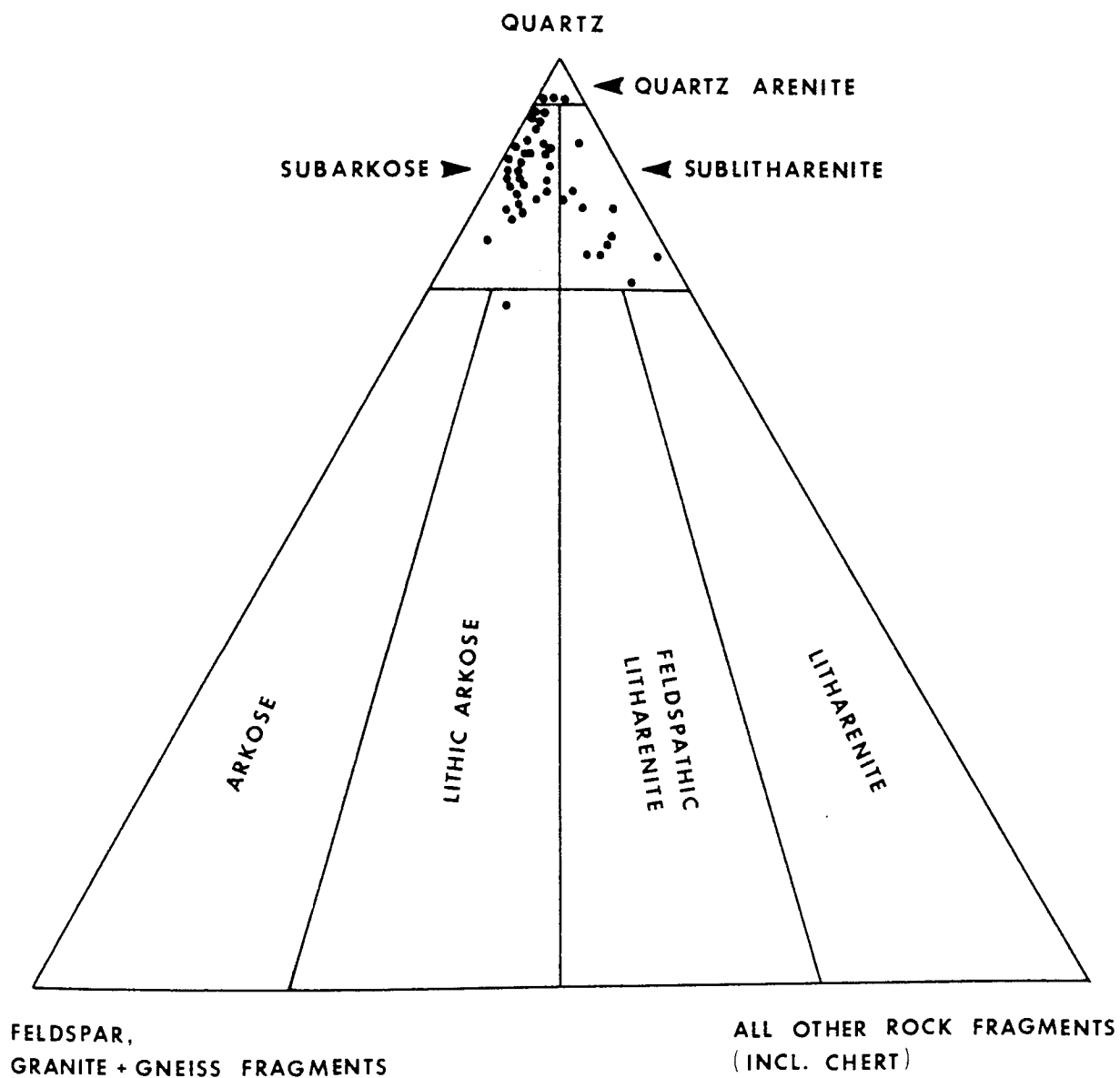


Fig.3.1 Classification of the Triassic sandstones (after Folk, 1968).

due to the fact that the grain surfaces are covered with small authigenic quartz overgrowths which mask the original surface textures.

Monocrystalline quartz makes up the bulk of the fine size fraction in the Triassic sandstones. It usually has straight to slightly undulose extinction, and a few grains have inclusions or vacuoles. The medium and coarse size fractions consist of up to 65% polycrystalline quartz and have a higher percentage of undulose quartz. It seems likely therefore that the fine size fraction contains a large amount of disaggregated polycrystalline quartz grains and broken undulose grains. Undulose quartz is thermodynamically less stable than nonundulose quartz and tends to break into small grains (Blatt et al. 1980). The origin of undulose quartz is a matter of debate. Undulosity may increase when the sediments have subsequently been folded and faulted in tectonically active area (Conolly, 1965, Füchtbauer, 1974, Basu et al. 1975). Deep burial may produce undulose extinction but lithostatic pressure alone has only a minor effect on the percentage of undulose quartz grains (Füchtbauer, 1974). Metamorphic quartz shows a marked undulosity but large plutonic quartz was also found to have a high degree of undulosity (Pettijohn, 1975). As a result the presence of undulose quartz cannot be considered a reliable indicator of provenance (Blatt and Christie, 1963).

3.2.1 Igneous Quartz

A high proportion of the quartz in the Triassic sand-

stones is monocrystalline and subsequent with straight to slightly undulose extinction with no inclusions and few vacuoles. This type of quartz may represent a plutonic source area, but it can be produced from other source areas (Blatt, 1967, Folk, 1968). Polycrystalline quartz composed of two crystals with straight to slightly curved intercrystal boundaries may be from a plutonic source. A plutonic source may also be represented by undulous quartz where the undulosity was produced due to different c-axis orientations when the different zones are separated by lines of vacuoles or bubbles which indicate traces of healed fractures (Blatt, 1967, Folk, 1968). This type of quartz (PL.3.1A) is common in the Triassic sandstones. It is also common to find quartz with different types of mineral inclusions. Oriented acicular rutile inclusions (PL.3.1B) may indicate a granitic source; other types of inclusions such as needle-shaped tourmaline (PL.3.1C) and zircon (PL.3.1D) may originate in either igneous or metamorphic rocks (Blatt et al. 1980).

Quartz from hydrothermal rocks is represented by monocrystalline or polycrystalline grains with abundant water filled vacuoles giving the grain a milky colour (PL.3.1E). Vermicular chlorite inclusions (PL.3.1F) also indicate a hydrothermal source (Fuchtbauer, 1974, Blatt et al. 1980). The abundance of the above mentioned types of quartz in the Triassic sandstones indicate that a substantial amount of the detrital quartz is of hydrothermal origin.

3.2.2 Metamorphic Quartz

Polycrystalline quartz of metamorphic origin is most abundant in the Sherwood Sandstone Group whereas the sandstone units in the upper part of the Triassic sequence (The Mercia Mudstone Group) contain less polycrystalline quartz. This may be due to the disaggregation of polycrystalline quartz by more intensive mechanical abrasion as the depositional areas became more distal in later Triassic times.

Polycrystalline quartz with ten or more individual crystals is an excellent indicator of metamorphic source (Sholle, 1979). According to Blatt et al. (1980) sand size polycrystalline quartz with five or more crystals is usually derived from gneisses. This type of gneissic quartz is abundant in the Sherwood Sandstone Group and represented by polycrystalline grains with elongated individual crystals and crenulated (PL.3.2A) or sutured (PL.3.2B) crystal boundaries. This includes stretched metamorphic quartz, formed when quartz bearing rocks such as sandstones, granites, schists, or vein quartz are sheared or strained in the absence of recrystallization (Folk, 1968). Polycrystalline quartz from a gneissic source displaying a bimodal size distribution of the individual crystals (PL.3.2C) is also abundant and reflects an arrested stage in the recrystallization of the source rocks (Blatt, 1967, Blatt et al. 1980).

Other types of metamorphic quartz were recognized in the Triassic sandstones. These include, polycrystalline quartz with elongate individual crystals having straight inter-crystalline boundaries with slightly undulose extinction, and oriented mica inclusions (PL.3.2D) indicating a schistose origin (Folk, 1968), and polycrystalline quartz with silt size individual crystals (PL.3.2E) derived from fine schists (Folk, 1968, Blatt et al. 1980).

3.2.3 Sedimentary Quartz

Quartz grains with rounded overgrowths (PL.3.2F) indicate reworked sandstones. This type of quartz is abundant in the Bromsgrove Sandstone Formation and the sandstone units of the Mercia Mudstone Group especially the Arden Sandstone Member. This may suggest derivation from earlier Triassic sandstones such as the Kidderminster, Cannock Chase, and Polesworth Formations. It is also found occasionally in the Kidderminster Formation indicating a sedimentary source probably from pre-Triassic sediments.

3.3 UNDULATORY EXTINCTION AND POLYCRYSTALLINITY AS PROVENANCE INDICATORS

Basu et al. (1975) used undulatory extinction and polycrystallinity for provenance interpretation. The variables used in this study were: the amount of monocrystalline quartz, the amount of undulose quartz, and the amount of polycrystalline quartz which was divided into the ones with 2-3 crystals per grain and the type with more than three crystals per grain.

These divisions were based on the fact that low rank metamorphic rocks contain a larger amount of quartz with more than three crystals per grain and contain both undulose and nonundulose quartz, whereas plutonic quartz is predominantly nonundulose. Large populations of undulose quartz (apparent undulosity $> 5^{\circ}$) are more diagnostic than a large population of nonundulose quartz. Also high rank metamorphic rocks give rise to polycrystalline quartz with a number of crystals similar to that of plutonic rocks.

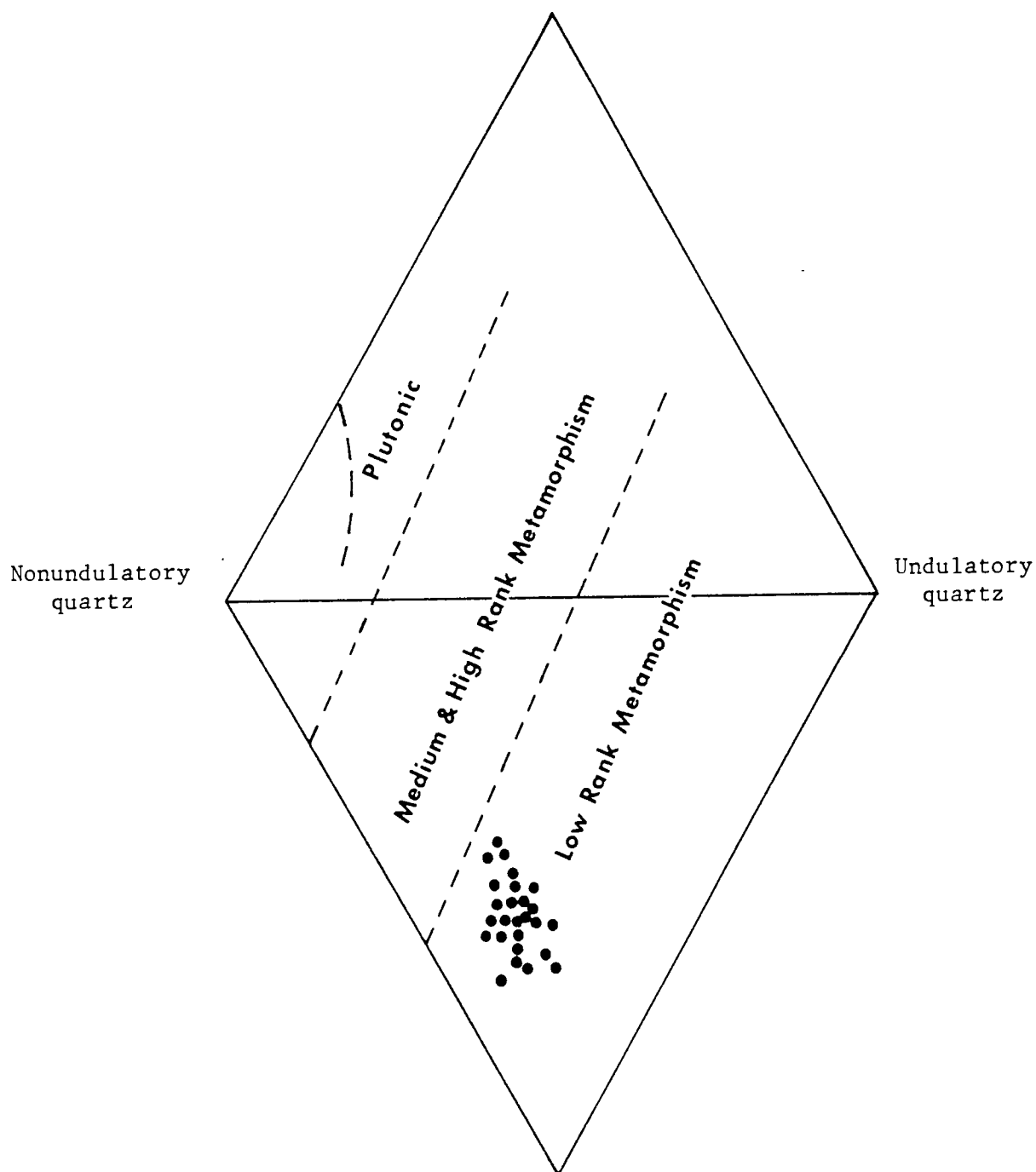
The limitations of this technique are:

1. Sandstones deposited in tectonically active areas may have a higher proportion of undulosity induced by folding and faulting.
2. Texturally immature sandstones show a higher proportion of polycrystalline grains whereas in more mature sandstones polycrystalline quartz breakage produces more monocrystalline quartz.

In order to minimize these effects Basu et al. (1975) restricted their studies to the medium sand fraction.

In the present study point counting for the above mentioned variables was carried out on thin sections of the medium size fraction of selected sandstone samples from different formations in the Sherwood Sandstone Group. Plotting the results on the four variable diagram (Fig. 3.2) suggests that the source area of the Triassic sandstones in the West Midlands was predominantly composed of low rank metamorphic rocks.

Polycrystalline 2-3 crystals/grain $\geq 75\%$ of
the total polycrystalline quartz



Polycrystalline > 3 crystals/grain $> 25\%$ of
the total polycrystalline quartz

Fig.3.2 Four variable plot of detrital quartz in the Triassic sandstones. Dashed lined boundaries between source rock areas are taken from Basu et al. (1976, Fig.6).

3.4 CATHODOLUMINESCENCE

Different types of quartz were also distinguished using cathodoluminescence. Carbon coated polished thin sections of selected sandstone samples were studied using the electron probe microanalyser. Cathodoluminescence was observed by defocussing the electron beam on a spot and using a 40 kV voltage. Photographs with an exposure time between 15 and 20 seconds were taken using a 400 ASA Kodak colour transparency film from which colour prints were made.

The most abundant type of quartz in the Triassic sandstones is the one with light to dark brown luminescence (PL.3.3A), and this is a characteristic of metamorphic quartz, whereas blue-violet to blue luminescent quartz (PL.3.3B) is less abundant and indicates rapidly cooled rocks of volcanic origin (Zinkernagel, 1978). Some of the quartz from the Kidderminster and Cannock Chase Formations shows a heterogenous blue luminescence (PL.3.3C) which indicates a source from contact metamorphic rocks (Zinkernagel, 1978) but studies by Sprunt et al. (1978) suggested that metamorphic quartz may also show homogeneous blue luminescence. Traces of healed fractures were also revealed by cathodoluminescence in this type of quartz. These features have been described by Sippel (1968).

Quartz with red-violet luminescence (PL.3.3D) was occasionally found in the Triassic sandstones. Red luminescence may be due to the presence of radioactive impurities (Smith and Stenstrom, 1965), and probably

indicates an igneous source (Zinkernagel, 1978). Red luminescence may also be a characteristic of quartz subjected to low temperature deformation or low temperature secondary quartz (Sprunt et al. 1978).

Recrystallized quartz in which recrystallized brown quartz heals original areas which show blue luminescence (PL.3.3E) was occasionally found in the sandstones of the Cannock Chase Formation. This type of quartz may indicate source rocks within zones of contact metamorphism (Zinkernagel, 1978).

Sedimentary quartz with rounded overgrowth which is abundant in the Bromsgrove Sandstone Formation and the sandstone units of the Mercia Mudstone Group, and was difficult to recognize due to the lack of a clear dust line, is easily recognized by the non-luminescence of the overgrowths (PL.3.3F). This type of quartz represents only a minor percentage of the total quartz content of the studied samples.

Cathodoluminescence studies show that the most predominant quartz type in the Triassic sandstones is of metamorphic origin with subordinate igneous and sedimentary quartz. This is consistent with the provenance studies based on the polycrystallinity and undulatory extinction, and petrographic evidence which indicates an abundance of metamorphic rock fragments.

3.5 FELDSPARS

The feldspar content of the Triassic sandstones range from 3% to 25% of which orthoclase and sanidine constitute

the main bulk. Microclines and plagioclase do not exceed 1%. Most of the detrital K-feldspar grains are surrounded by authigenic overgrowths. They are subangular to subrounded and show a varying degree of alteration which is mainly by vacuolization (PL.3.4A). Microclines constitute only a minor percentage with a typical polysynthetic twinning and usually surrounded by authigenic K-feldspar overgrowths (PL.3.4B). Microcline perthites are occasionally found (PL.3.4C).

The microclines may have been derived from granites, gneisses, or pegmatites (Kerr, 1959, Pettijohn, 1975). Perthite (PL.3.4D) and drop perthite (PL.3.4E) are also found occasionally and represent a high grade metamorphic or plutonic source (Folk, 1968, Barth, 1969, Füchtbauer, 1974). Plagioclase is rarely found and usually shows alteration by sericitization (PL.3.4F).

Since orthoclase and sanidine indicate an acid igneous or high grade metamorphic source; then the upward increase in the amount of feldspar in the Bromsgrove Sandstone Formation (Fig. 3.3) may indicate that more sediments were supplied from igneous and high grade metamorphic rocks at this time. This might be attributed to an uplift during the time of the Bromsgrove Sandstone deposition. As a result of this uplift, rapid erosion enriched the upper sandstone units with feldspars from igneous and high grade metamorphic origin. The abundance of igneous rock fragments and the upward increase of biotite (Fig. 3.3) and apatite (Fig. 3.4) support this conclusion.

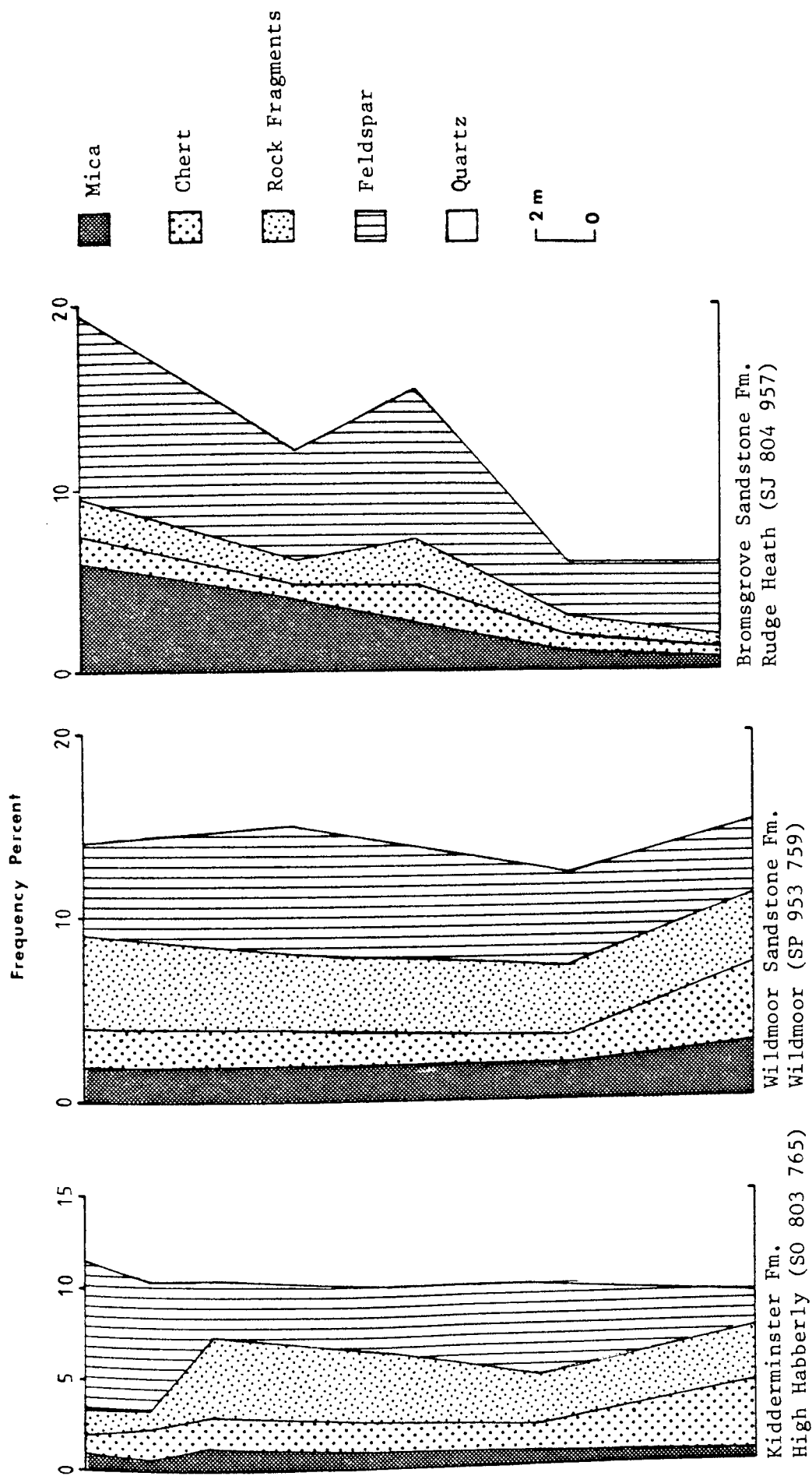


Fig.3.3 Vertical variations in the mineralogical composition of the Triassic sandstones.

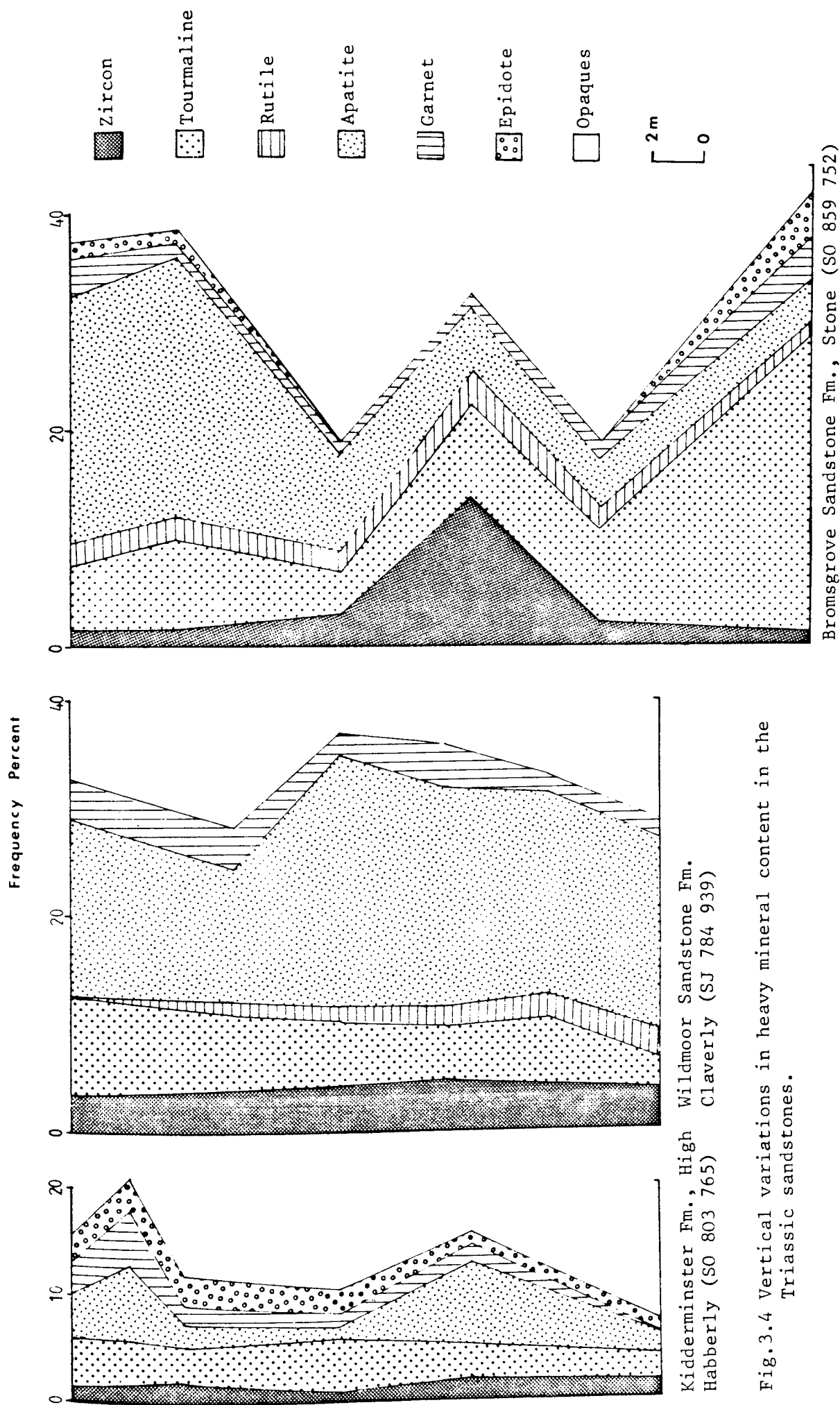


Fig.3.4 Vertical variations in heavy mineral content in the Triassic sandstones.

3.6 ROCK FRAGMENTS

Rock fragments constitute up to 20% in the Triassic sandstones specially in the Sherwood Sandstone Group. In the sandstone units of the Mercia Mudstone Group rock fragments are less abundant and represented largely by carbonate rock fragments, which are probably of intraformational origin or derived from the Bromsgrove Sandstone Formation.

Igneous rock fragments are mainly volcanic fragments consisting of very fine crystalline matrix and small lath-like plagioclase crystals (PL.3.5A). Plutonic rock fragments are less common and usually represented by fragments of graphic granite showing quartz and feldspar intergrowth (PL.3.5B). These types of rock fragments are more abundant in the Bromsgrove Sandstone Formation.

Extrusive rock fragments are expected to be more abundant in sediments than intrusive rock fragments due to the size control and the fact that weathering quickly weakens the bonds between the feldspar grains in granites causing the disintegration of the intrusive rock fragments (Blatt et al. 1980).

Metamorphic rock fragments are more abundant than igneous and sedimentary rock fragments especially in the Kidderminster, Cannock Chase, Polesworth, and Wildmoor Sandstone Formations. They are characterized by their distinctive texture, and usually consist mainly of mica with lens-like elongate quartz crystals and probably represent mica schists (PL.3.5C). Fragments of sheared metaquartzites are represented by large grains consisting

of many elongate quartz crystals (PL.3.5D).

Sedimentary rock fragments include sandstone, siltstone, and carbonate rock fragments. Sandstone and siltstone rock fragments are more abundant in the Bromsgrove Sandstones. They are subangular to subrounded (PL.3.5E), and may indicate an intraformational origin since they do not have the durability to survive long transportation. Another type of sandstone rock fragments which are well-rounded and cemented by iron oxide (PL.3.5F) are common in the Kidderminster Formation and may have been derived from pre-Triassic sandstones.

Carbonate fragments are also found in the early Triassic conglomeratic sandstones of the Kidderminster and Cannock Chase Formations. They include foraminiferal limestones (PL.3.6A) which have been derived from the Carboniferous Limestone. Dolomite fragments (PL.3.6B) are abundant in the Arden Sandstone Member and are probably of intraformational origin.

Chert is present either as a microcrystalline quartz (PL.3.6C) or with chalcedony (PL.3.6D) and constitutes up to 4%. Chalcedony is found occasionally and usually shows a zebraic texture (PL.3.6E). Chert and chalcedony may originate from bedded chert, chert nodules, or cavity fillings by fibrous quartz. In this particular case it may have originated from chert nodules in the Carboniferous Limestone.

3.7 PHYLLOSILICATES

These are mainly biotite, muscovite, and occasionally

chlorite. They are abundant in the Bromsgrove sandstones where they reach up to 5% and increase upward in a trend similar to that of the feldspars (Fig. 3.3). They represent only a small proportion of the other Triassic sandstones. Biotite is the main constituent and shows indications of intensive alteration by oxidation. The biotite flakes are usually angular to subrounded, sometimes well-rounded and show step-like fractures (PL.3.6F).

In general the abundance of mica suggests a metamorphic source (Pettijohn et al. 1972), but since muscovite is more stable than biotite, then the abundance of biotite may suggest rapid erosion or an abundance of volcanic rocks in the source area (Folk, 1968). This is consistent with the conclusion that the uplift at the time of the Bromsgrove sandstones deposition caused rapid erosion and more supplies from igneous sources as indicated also by the upward increase in the amount of feldspar in the Bromsgrove Sandstone Formation.

3.8 HEAVY MINERALS

The heavy mineral fraction in the Triassic sandstones does not exceed 1%. Heavy mineral analysis of 80 sandstone samples representing different parts of the Sherwood Sandstone and the Mercia Mudstone Groups was carried out using heavy liquid (Bromoform, S.G.=2.9). Grain mounts and polished grain mounts were prepared and studied using standard petrographic procedures (transmitted and reflected light) and the SEM with EDAX. Point counting (500 counts

per slide) was carried out and the results show that opaque minerals constitute the major part of the heavy mineral fraction especially in the early Triassic sandstones. They reach a maximum in the Kidderminster and Cannock Chase Formations where they constitute up to 93% of the total heavy mineral fraction. The Wildmoor and Bromsgrove Sandstone Formations contain less opaque minerals with a maximum of 72% and 81% respectively (Fig. 3.4).

The mica was not counted with the heavy mineral fraction because it does not always sink in bromoform, hence gives an unreliable percentage.

3.8.1 Non-opaque Minerals

Seven non-opaque heavy minerals were identified in the studied samples. These are divided into ultra and metastable minerals. Ultrastable minerals include zircon, tourmaline, and rutile. Metastable minerals include apatite, garnet, epidote, and sphene.

Zircon: The zircon content ranges from 1% to 14% of the heavy mineral fraction. In the Triassic sandstones; zircon appear as colourless grains, globular or oval in shape, sometimes zoned (PL. 3.7A), and sometimes as euhedral crystals with doubly terminated prisms (PL. 3.7B). Fine needle-shaped zircons are also common (PL. 3.7C). Inclusions in zircons are found occasionally and represented by vacuoles or bubbles (PL. 3.7C). Previous studies showed that zircon is highly resistant to mechanical abrasion (Dietz, 1973), and to weathering (Grimm, 1973) and

therefore studies of grain surface textures show a smooth surface (PL. 3.7D).

Euhedral zircon may have been of first cycle origin whereas rounded zircons are derived from sedimentary rocks or paraschists (Blatt et al. 1980). Idiomorphic zircon is an indicator of volcanisms (Callender in Folk, 1968) and elongated zircon crystals occur in rapidly cooled dykes (Claus, 1936 in Füchtbauer, 1974). Zircon with bipyramidal habit indicates extremely alkaline source rocks whereas prismatic forms come from granites (Pettijohn et al. 1972).

Tourmaline: Tourmaline is an abundant heavy mineral throughout the Triassic and constitutes up to 23% of the heavy mineral fraction in some of the Bromsgrove Sandstone horizons (Fig. 3.4). They are subrounded to well rounded grains, strongly pleochroic, and mainly yellowish brown and brown in colour. Green tourmaline is also common whereas blue tourmaline is only occasionally found.

Different types of tourmaline were recognized in the Triassic sandstones. They include, medium sized grains of brown or green tourmaline full of bubbles and cavities (PL. 3.7E) indicating a granitic source (Krynine, 1946). Tourmaline with mineral inclusions is also abundant and includes grains with rutile and zircon microlites (PL. 3.7F PL. 3.8A). Blue tourmaline may indicate a pegmatitic source (Krynine, 1946, Pettijohn, 1975). Tourmaline is less resistant to mechanical abrasion than zircon, so it

is usually better rounded, but it has a high weathering resistance (Grimm, 1973).

Rutile: Rutile constitutes up to 3% of the heavy mineral fraction in the Triassic sandstones. It is represented by subrounded reddish brown to opaque grains with slight pleochroism and twinning (PL. 3.8B). It may represent a pegmatitic, crystalline schists, or contact metamorphic source rocks (Füchtbauer, 1974). Rutile has an extremely high weathering resistance (Grimm, 1973) but like tourmaline it is moderately rounded during transportation (Dietz, 1973).

Apatite: Apatite is the most abundant non-opaque mineral in the Triassic sandstones especially in the Wildmoor and Bromsgrove Sandstone Formations, where it constitutes up to 24% of the heavy mineral fraction (Fig. 3.4). It occurs as colourless, well rounded grains, oval in shape and sometimes with liquid and gas inclusions (PL. 3.8C), and occasionally found as elongate grains (PL. 3.8D). The abundance of apatite may indicate a plutonic source (Folk, 1968), but it is ubiquitous in both igneous and metamorphic rocks (Füchtbauer, 1974).

Previous studies have shown that apatite is sensitive to weathering (Grimm, 1973, Nickel, 1973, Füchtbauer, 1974), but it is relatively stable in the field of intrastratal solution (Nickel, 1973). In view of the above the abundance of apatite in the Triassic sandstones indicates an arid to semi-arid climate where the effect of chemical weathering was insignificant. The upward increase of apatite in the

Bromsgrove Sandstone Formation (Fig.3.4) may indicate a rapid erosion which might have been caused by uplift in the source area. This is consistent with the upward increase in the feldspar and biotite.

Garnet: The proportion of garnet reaches a maximum of 4% of the heavy mineral fraction in the Wildmoor Sandstone Formation and parts of the Bromsgrove Sandstone Formation. Garnet indicates an igneous or metamorphic source area. In the Triassic sandstones it is represented by relatively large irregular, isotropic grains with high refractive index and different types of etching marks. These include knobs and pits (PL. 3.8E), V-shaped marks (PL. 3.8F), and step-like etching marks (PL. 3.9A and B) which is the most abundant type.

Like apatite garnet is very sensitive to weathering (Grimm, 1973, Nickel, 1973) but relatively stable in the field of intrastratal solution (Nickel, 1973). As a result the intensive etching of the garnet grains in the Triassic sandstones is an indication of the intensity of intrastratal dissolution.

Epidote: Epidote is present as yellowish brown faintly pleochroic grains which make up to 4% of the heavy mineral fraction in some of the horizons of the Bromsgrove Sandstone Formation. It is less abundant in the Kidderminster, Cannock Chase, and Polesworth Formations, and rarely found in the Wildmoor Sandstone Formation. The grains usually show hacksaw terminations (PL. 3.9C)

which indicate an intensive dissolution. SEM examination revealed the presence of dissolution pits and marks all over the grain surface in addition to the usual hacksaw terminations (PL.3.9D). Epidote may have originated from a hydrothermal or metamorphic source (Folk, 1968, Pettijohn, 1975).

Sphene: Sphene is found only occasionally in the Triassic sandstones. It is present as light brownish grains with metallic iridescence due to the strong dispersion of the axes. Sphene may represent either igneous or metamorphic source rock (Füchtbauer, 1974).

3.8.2 Opaque Minerals

Opaque heavy minerals in the Triassic sandstones are mainly haematites, martites, leucoxene, and occasionally ilmenite. Haematite is the most common and shows a variety of textures. Botryoidal (PL. 3.9E) and rhythmically banded haematite with silica (PL.3.9F) are common types. These may have been derived from a low temperature hydrothermal source or may represent oxidised, rhythmically precipitated pyrite. Haematite with exsolution discs of ilmenite or titanomagnetite and lamellae of rutile (PL.3.10A) are the most common types of opaque grains. Such haematites may have an igneous or metamorphic source. Haematite with exsolution discs of rutile (PL.3.10B) probably represent grains in which the ilmenite has been oxidized into rutile and may have been derived from older sediments.

Polycrystalline haematite (PL. 3.10C) in which haematite was formed after magnetite or maghemite at different points simultaneously may also indicate an older sedimentary source.

Martite is most abundant in the Kidderminster, Cannock Chase, Polesworth and Bromsgrove Sandstone Formations. It represents haematite formation after magnetite, usually along the (111) planes producing a triangular pattern (PL. 3.10D). It may indicate a volcanic origin where magnetite was heated in an oxidizing atmosphere, e.g. the surface of lava flows, and in this case the lamellae are relatively broad (Rhamdohr, 1980). Martite may also occur at low temperature in the post-depositional oxidizing environment, and this is probably the origin of the martite in the Kidderminster, Cannock Chase, and Polesworth Formations, where the martite grains are mainly subangular, sometimes angular, and thought to be originally deposited as magnetite or maghemite octahedra. The martites of the Bromsgrove Sandstone Formation are well-rounded, and some of them may have been derived from earlier Triassic sandstones.

Leucoxenes are also abundant in the Triassic sandstones and show typical milky white internal reflection in reflected light, sometimes with colour banding (PL. 3.10E). They are fine intergrowths of amorphous titanium oxide produced by oxidation of ilmenite and may indicate a source from older red beds. Haematite with rounded overgrowths

(PL. 3.10F) is common in the Bromsgrove sandstones and also indicates a sedimentary source, probably from the Old Red Sandstone.

3.9 PROVENANCE

The mineralogy of the Triassic sandstones indicates that the source rocks were predominantly metamorphic. Igneous and sedimentary rocks seem to have been less abundant in the source area, and the detrital grains of sedimentary origin are predominantly intraformational. This was reflected by the abundance of metamorphic quartz, metamorphic rock fragments, and rounded zircons. The study of undulatory extinction and polycrystallinity indicated that the detrital quartz is largely of low rank metamorphic source. This was confirmed by the abundance of brown luminescent quartz. Detrital grains of igneous origin are less abundant in the Triassic sandstones. They are represented by quartz of hydrothermal origin, volcanic and plutonic rock fragments, euhedral and prismatic zircons, tourmaline with bubbles and cavities, and blue tourmaline. Further supply from an igneous source to the Bromsgrove sandstones is indicated by the upward increase of feldspar, biotite, and apatite. This might be attributed to an uplift in the source area at the time of the Bromsgrove sandstone deposition. Sedimentary source is represented by quartz and haematite with reworked overgrowths, and sedimentary rock fragments. They represent only a minor constituent and are more common in the

Bromsgrove Sandstone Formation and the sandstones of the Mercia Mudstone Group, and in this case they are thought to be of intraformational origin, especially the carbonate rock fragments.

3.10 SIZE-COMPOSITION TRENDS

Size-composition trends were used by Young et al. (1975) for palaeoclimatic interpretation. Distinction between semi-arid and humid palaeoclimates was made by comparing plots of the proportions of various framework grains in different size classes in the range - 1 ϕ to 4 ϕ . Mack and Suttner (1977) also used this method for palaeoclimatic interpretation of the Fountain Formation (Carboniferous) in the Colorado Front Range by comparing the size-composition trends with those of Holocene sands from the same source rocks.

The rationale behind these studies is the belief that intensive chemical weathering in a humid climate rapidly destroys the labile minerals in rock fragments, thus reducing the amount of rock fragments in all size fractions and consequently increasing the amount of polycrystalline and monocrystalline quartz.

A major objection to the validity of the size-composition concept has been made by Walker (1978) who has argued that diagenetic destruction of polycrystalline quartz and rock fragments, especially by clay replacement, causes the relative increase in the amount of monocrystalline quartz, hence limiting the reliability of this method for

pal climatic interpretation (Walker, 1974, Walker et al. 1978, Walker, 1978).

Thirty two sandstone samples representing different parts of the Kidderminster, Cannock Chase, Polesworth, Wildmoor Sandstone, and Bromsgrove Sandstone Formations were sieved into coarse(- 1Ø to - Ø), medium (1Ø to 2Ø), and fine (2Ø to 4Ø) fractions. Thin sections were prepared for each size fraction and point counting of 500 counts per thin section was carried out. Modal percents of polycrystalline quartz, monocrystalline quartz, and rock fragments have been recalculated to 100 percent, and size-composition plots for each of the three stratigraphic divisions of the Sherwood Sandstone Group were constructed (Fig. 3.5).

In all the size fractions rock fragments are more abundant in the Kidderminster, Cannock Chase, and Polesworth Formations than the Wildmoor Sandstone Formation, and more abundant in the Wildmoor Sandstone Formation than the Bromsgrove Sandstone Formation (Fig. 3.5). If the size-composition trend concept is valid then this could suggest that during the deposition of the Kidderminster, Cannock Chase, and Polesworth Formations the source area climate was semi-arid and became more humid during the deposition of the Wildmoor and Bromsgrove Sandstone Formations.

Monocrystalline quartz shows a trend opposite to that of the rock fragments (Fig. 3.5). Greater abundance of monocrystalline quartz in the Bromsgrove Sandstones supports

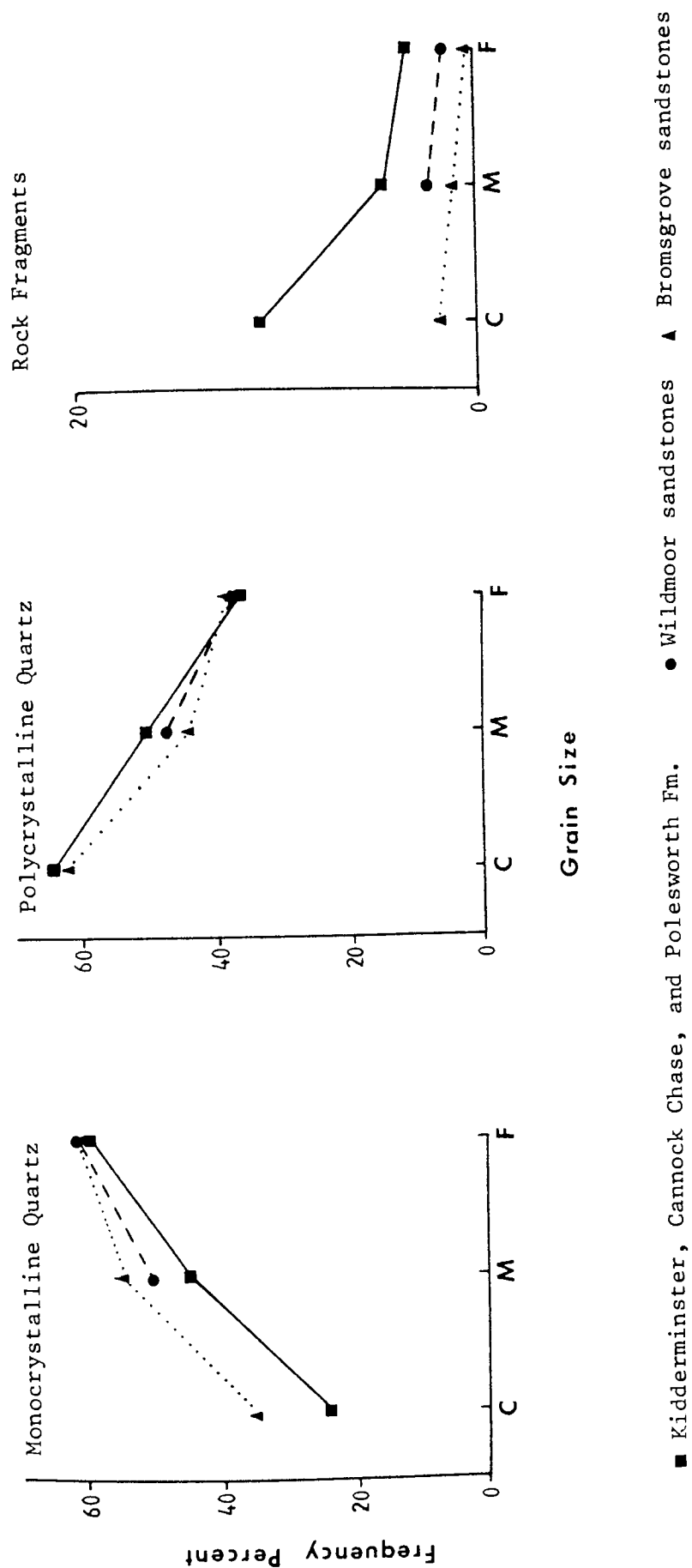


Fig.3.5 Variations in composition with size in the Triassic sandstones.

the interpretation that the climate became more humid than it was during early Triassic time.

In the coarse and medium size fraction, polycrystalline quartz shows a similar trend to that of the rock fragments whereas in the fine size fraction the opposite trend is seen, although there is only slight overall variation. This is contrary to the observation of Mack and Suttner (1977), who suggested that the destruction of rock fragments results in larger amounts of polycrystalline quartz. This upward decrease in the amount of polycrystalline quartz (Fig. 3.6), may be due to the effect of transportation. In early Triassic times the relief was high and the rivers were braided. Although this transporting agent is not a significant modifier of detrital mineralogy (Mack, 1978), the drainage system later became more sinuous and source areas more distant, and this could readily result in breakage of polycrystalline quartz leading to a general increase in the proportion of monocrystalline quartz.

3.11 CONCLUSIONS

The main source for the Triassic sandstones seems to be from medium to low rank metamorphic rocks, with additional supplies from igneous and sedimentary sources. This was reflected by the abundance of metamorphic quartz and rock fragments and supported by the study of undulatory extinction and polycrystallinity which have indicated that the detrital quartz is mainly from a low rank metamorphic source. Cathodoluminescence studies also showed that most

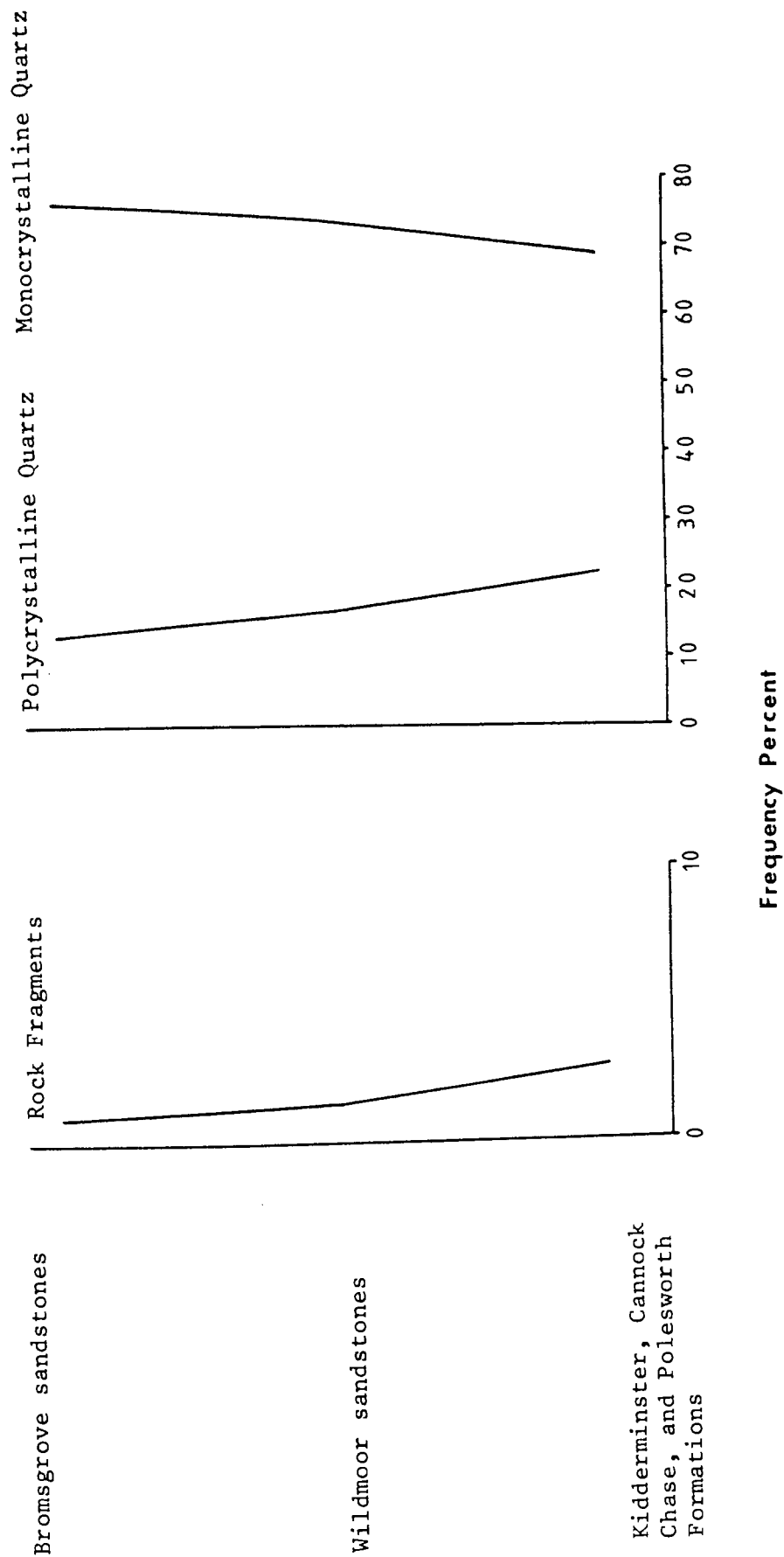


Fig.3.6 Variations in composition as a function of stratigraphic position in the Sherwood Sandstone Group.

of the quartz is of metamorphic origin. Sedimentary rock fragments and reworked detrital grains are more abundant in the Bromsgrove sandstones and the sandstones of the Mercia Mudstone Group, and these are more likely of intraformational origin, especially the carbonate rock fragments. Further supplies from an igneous source was indicated by the upward increase of feldspar and biotite in the Bromsgrove Sandstone Formation indicating a period of further uplift which had caused high relief and rapid erosion at that time. This was also supported by the upward increase in apatite, which is most sensitive to weathering.

The principal source area of the Triassic rocks of Central England is considered to have been to the south-southeast in the Variscan Mountains of Northern Europe (see 2.3, Fig. 2.17), where the sediments were deposited from rivers flowing to the north and northwest, as indicated by the palaeocurrent studies.

High relief, rapid erosion, and arid climate at the beginning of the Triassic is reflected by the relative abundance of rock fragments in the Kidderminster, Cannock Chase, and Polesworth Formations as indicated by the size-composition trends. The abundance of apatite and garnet in some horizons, also indicates an arid climate, since they are most sensitive to weathering. Later the climate became more humid and consequently chemical weathering destroyed the labile minerals in the rock fragments

resulting in an upward decrease in their amount which have caused the relative increase in the amount of monocrystalline quartz. The polycrystalline quartz on the other hand showed an upward decrease which is attributed to the effect of transportation. At the beginning of the Triassic the rivers were braided and did not significantly modify the detrital mineralogy. Later in the Triassic times the drainage system became more sinuous and the source area more distant, causing the breakage of polycrystalline quartz which led to the general increase in the proportion of monocrystalline quartz in the sandstones.

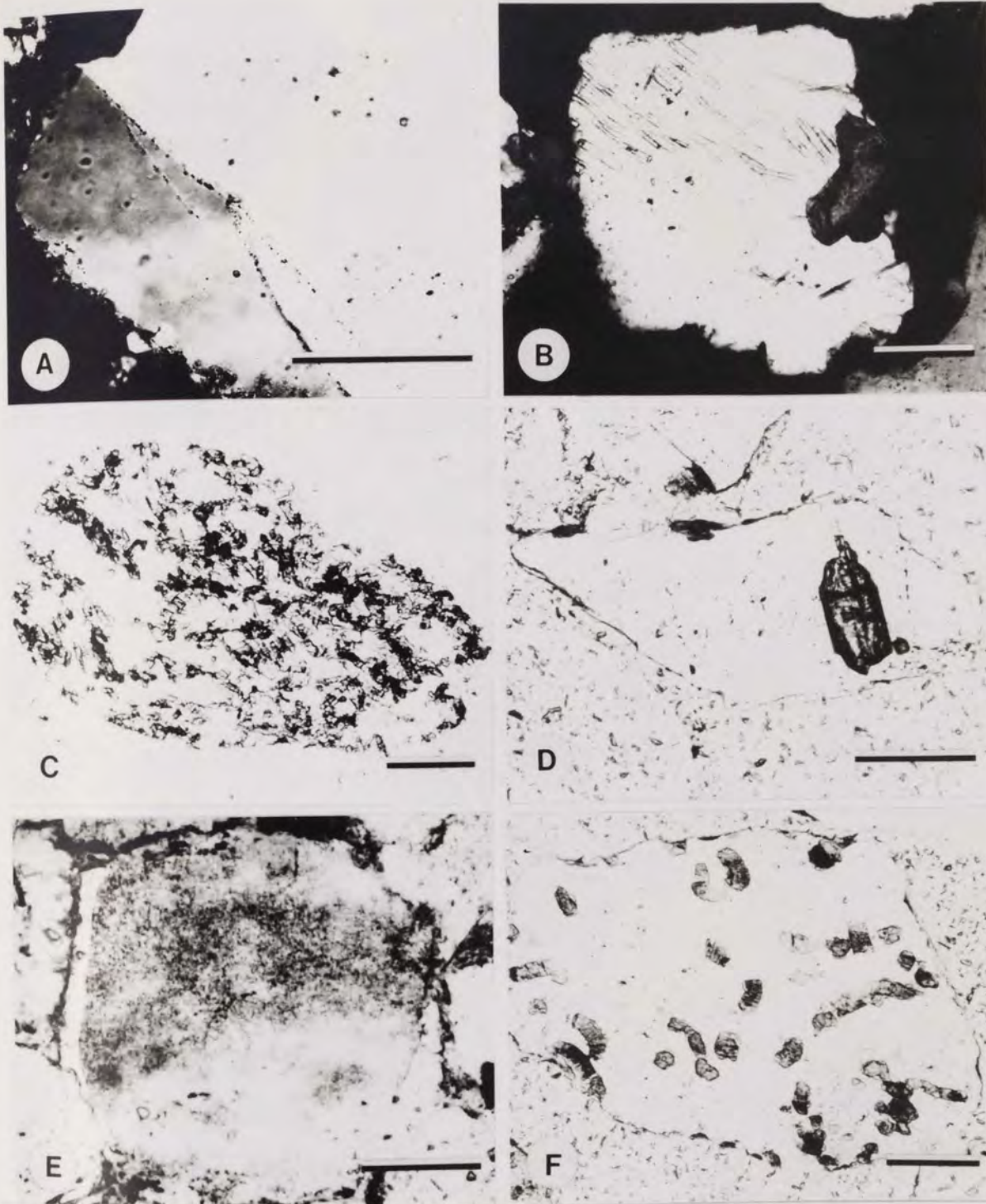


PLATE 3.1

- A. Different zones of undulose quartz separated by lines of vacuoles or bubbles indicating traces of healed fractures, XN, Kidderminster Fm.
- B. Quartz with acicular rutile inclusions. Tourmaline inclusion is also present, XN, Bromsgrove Sandstone Fm.
- C. Quartz with needle-shaped tourmaline inclusions, PPL, Bromsgrove Sandstone Fm.
- D. Quartz with zircon inclusion, PPL, Wildmoor Sandstone Fm.
- E. Quartz with abundant vacuoles, probably liquid filled, PPL, Wildmoor Sandstone Fm.
- F. Quartz with vermicular chlorite inclusions, PPL, Wildmoor Sandstone Fm.

Scale bar = 100 μ m

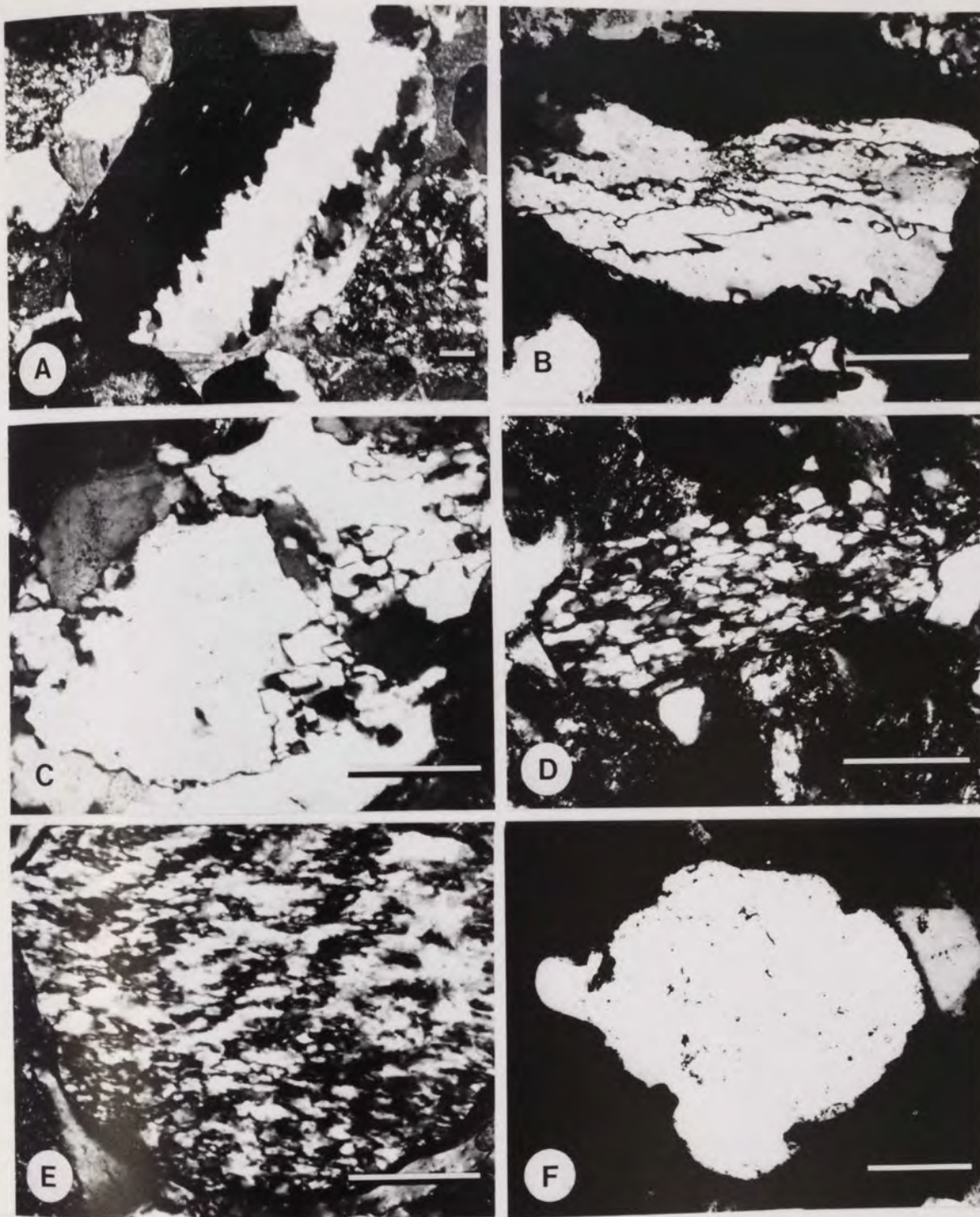


PLATE 3.2

- A. Polycrystalline quartz with elongated individual crystals and crenulated crystal boundaries, XN, Bromsgrove Sandstone Fm.
- B. Polycrystalline quartz with elongated individual crystals and sutured crystal boundaries, XN, Kidderminster Fm.
- C. Polycrystalline quartz displaying bimodal size distribution of the individual crystals, XN, Cannock Chase Fm.
- D. Polycrystalline quartz with elongated crystals having straight crystal boundaries and oriented mica inclusions, XN, Kidderminster Fm.
- E. Polycrystalline quartz with silt size individual crystals, XN, Cannock Chase Fm.
- F. Quartz of sedimentary origin indicated by reworked overgrowth, XN, Bromsgrove Sandstone Fm.

Scale bar = 150 μ m

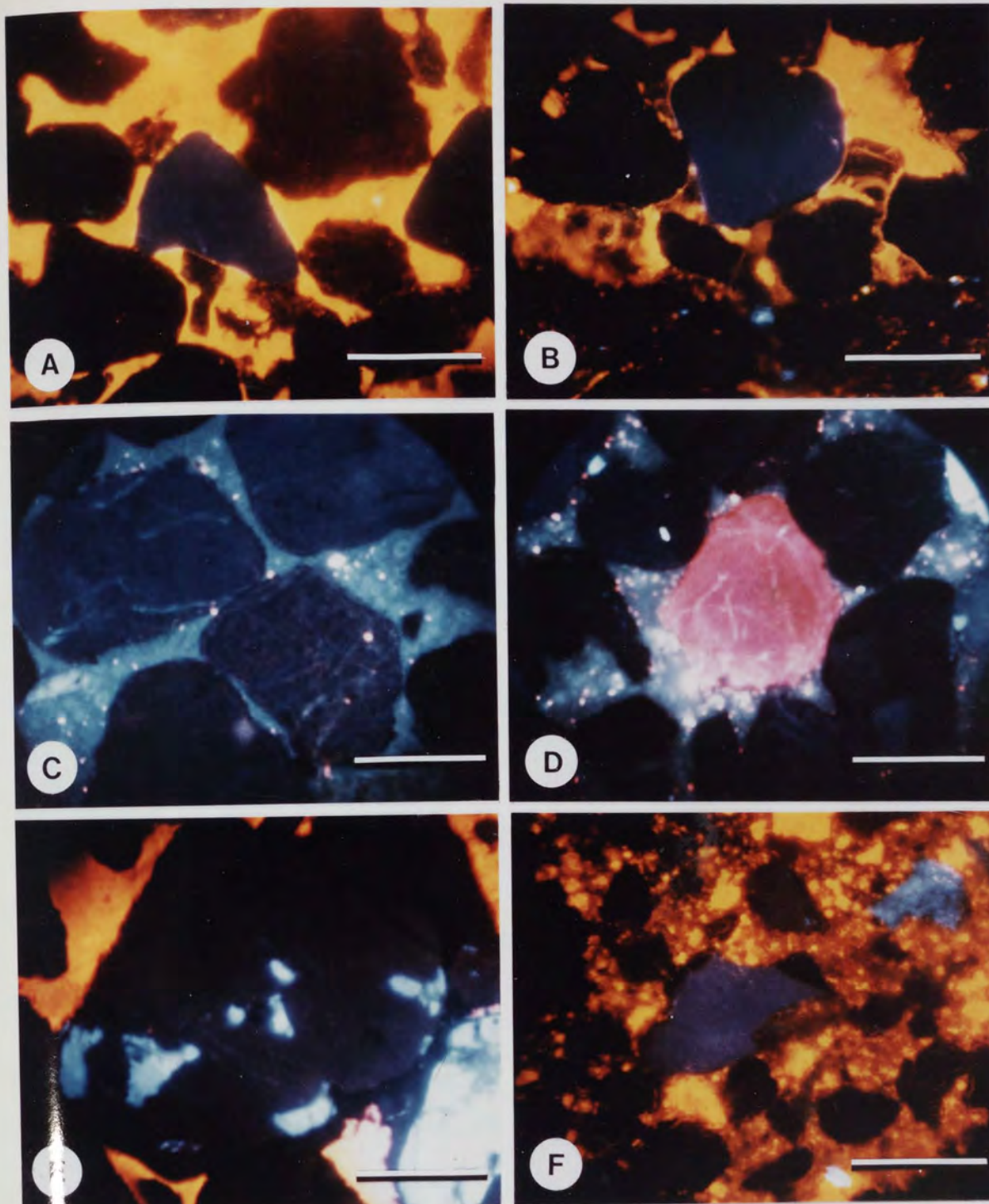


PLATE 3.3

- A. Sandstone with predominantly brown luminescent quartz. Blue-violet quartz is also present. Calcite cement display bright yellow luminescence, Bromsgrove Sandstone Fm.
- B. Quartz with blue-violet to dark blue luminescence, Bromsgrove Sandstone Fm.
- C. Quartz with heterogeneous blue luminescence showing traces of healed fractures, Wildmoor Sandstone Fm.
- D. Quartz with red-violet luminescence, Wildmoor Sandstone Fm.
- E. Crystallized brown luminescent quartz with initial blue luminescent portions, Cannock Chase Fm.
- F. Blue-violet luminescent quartz with non-luminescent rounded overgrowth. Dolomite cement display an orange yellow luminescence, Arden Sandstone Member.

Scale bar = 200 μ m

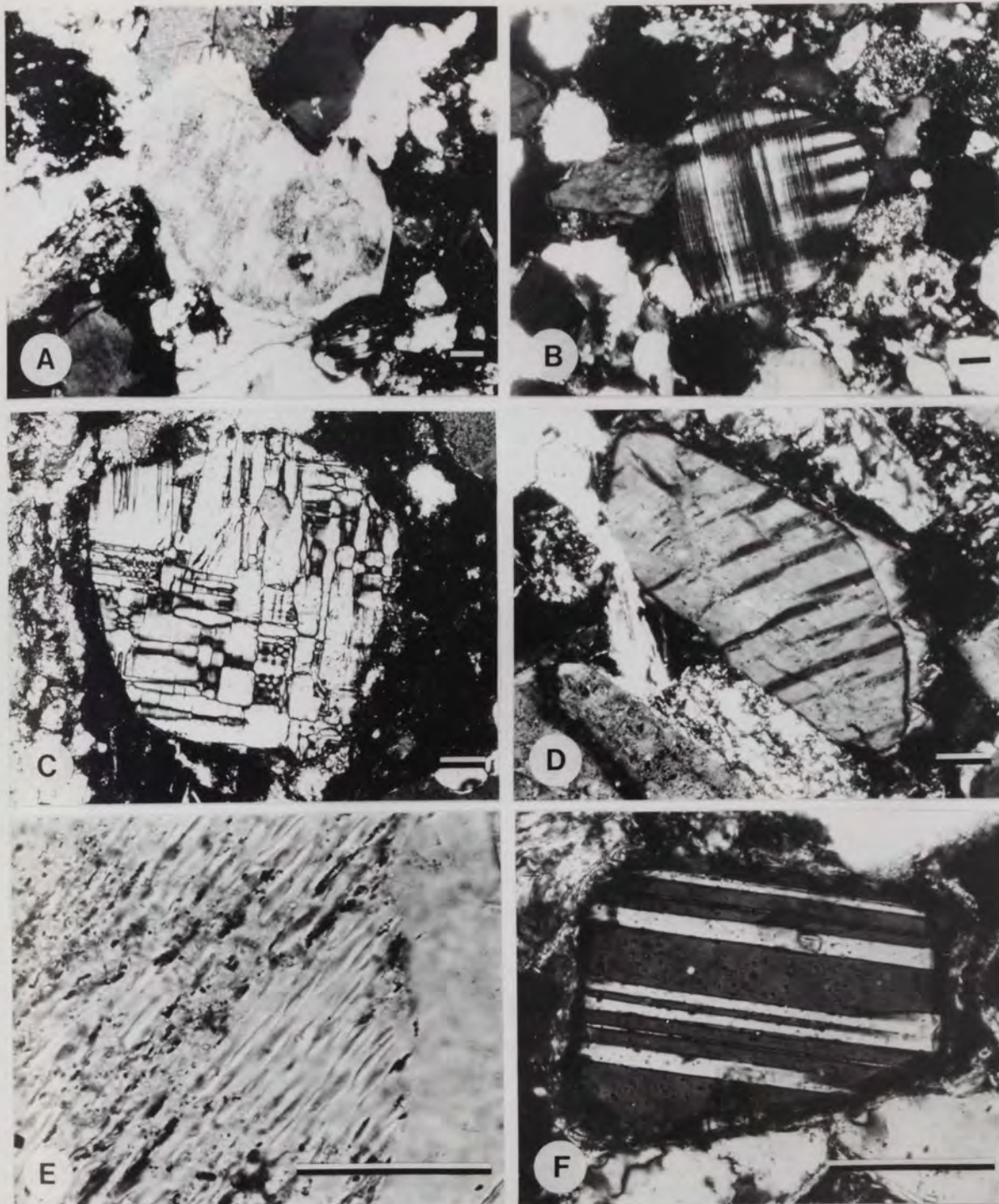


PLATE 3.4

- A. Detrital K-feldspar altered by vacuolization and surrounded by authigenic overgrowth, XN, Bromsgrove Sandstone Fm.
 - B. Detrital microcline with polysynthetic twinning, XN, Cannock Chase Fm.
 - C. Detrital perthitic microcline, XN, Bromsgrove Sandstone Fm.
 - D. Perthite with rhombic authigenic K-feldspar overgrowth, XN, Bromsgrove Sandstone Fm.
 - E. Drop perthite surrounded by authigenic K-feldspar overgrowth, XN, Cannock Chase Fm.
 - F. Detrital plagioclase altered by sericitization, XN, Wildmoor Sandstone Fm.
- Scale bar = 60 μm

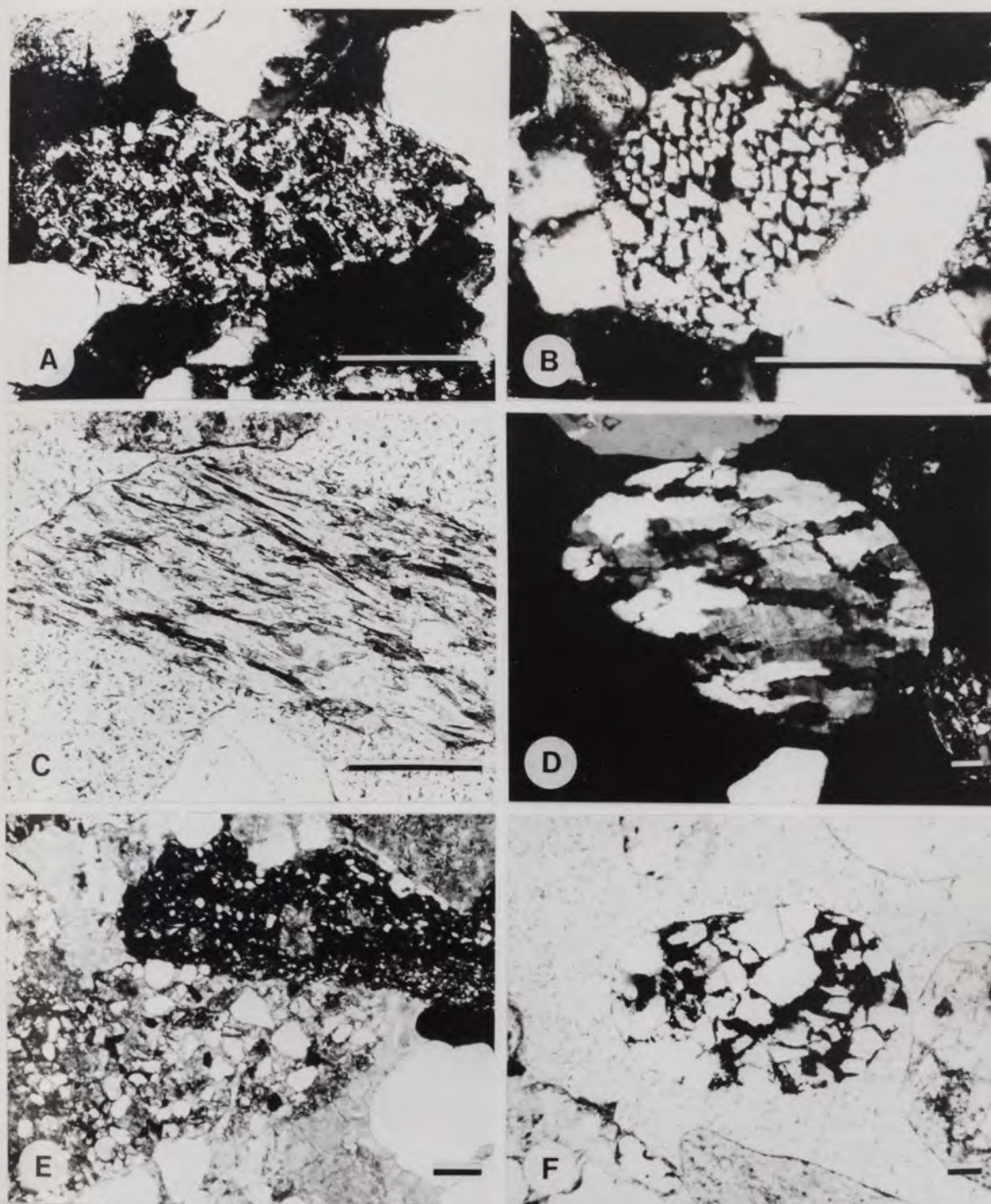


PLATE 3.5

- A. Volcanic rock fragment consisting of fine crystalline matrix and small lath-like plagioclase crystals, XN, Wildmoor Sandstone Fm.
- B. Fragment of graphic granite showing quartz and feldspar intergrowth, XN, Arden Sandstone Member.
- C. Metamorphic rock fragment consisting of mica with lens-like elongated quartz crystals, PPL, Wildmoor Sandstone Fm.
- D. Fragment of sheared metaquartzite consisting of elongate quartz crystals, XN, Bromsgrove Sandstone Fm.
- E. Sandstone and siltstone rock fragments, XN, Bromsgrove Sandstone Fm.
- F. Sandstone rock fragment of haematite cemented sandstone, PPL, Cannock Chase Fm.

Scale bar = 200 μ m

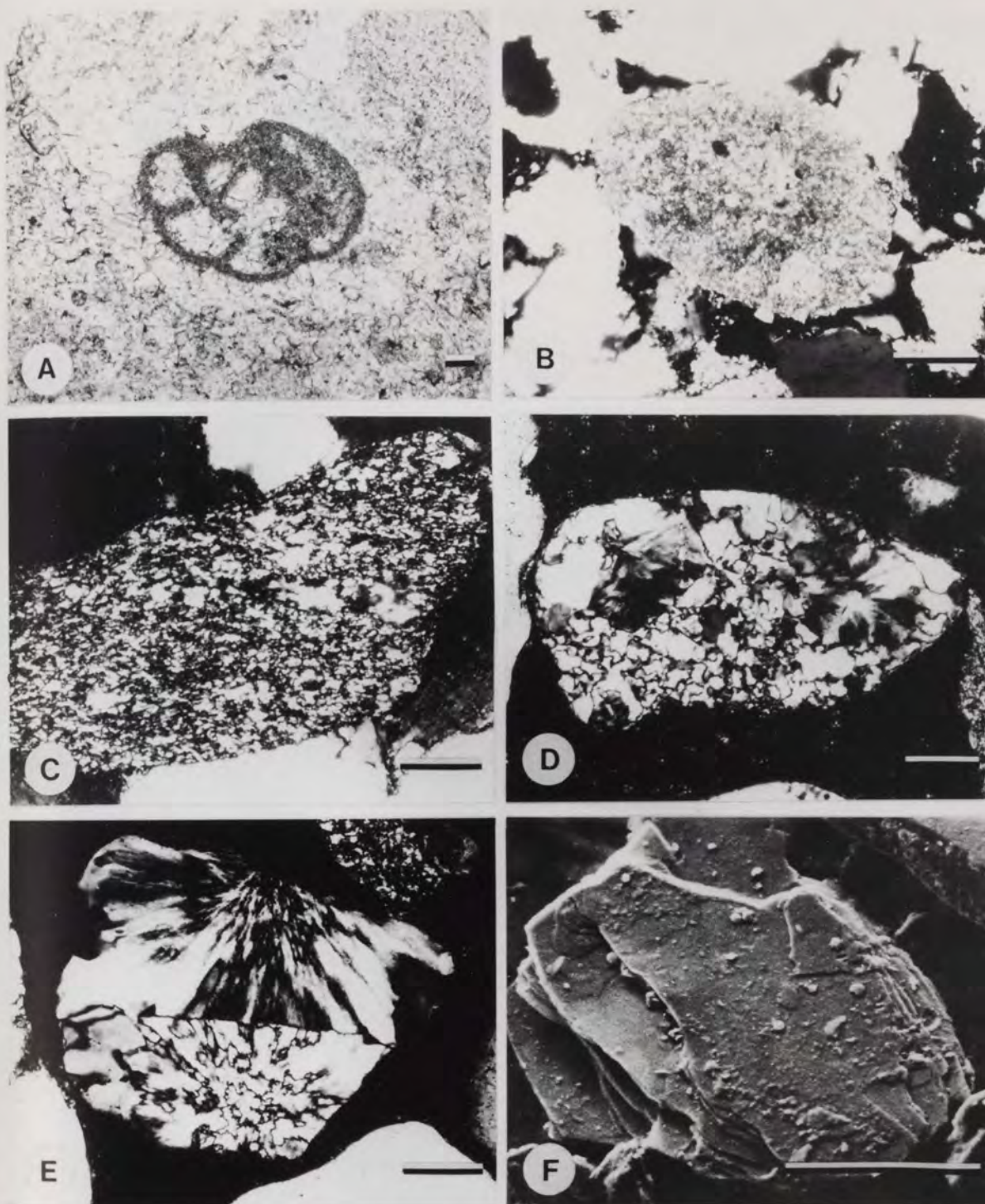


PLATE 3.6

- A. Carbonate rock fragment represented by a fragment of foraminiferal limestone, PPL, Cannock Chase Fm.
- B. Well rounded detrital dolomite fragment, XN, Arden Sandstone Member.
- C. Detrital chert with a combination of microcrystalline and macrocrystalline quartz, XN, Kidderminster Fm.
- D. Chalcedonic macrocrystalline chert fragment, XN, Bromsgrove Sandstone Fm.
- E. Zebraic chalcedony in which the fibres are alternately light and dark, XN, Bromsgrove Sandstone Fm.
- F. Detrital biotite with step-like fractures. Pseudo-hexagonal haematite flakes are also present on the grain surface, SEM photomicrograph, Bromsgrove Sandstone Fm.

Scale bar = 100 μ m

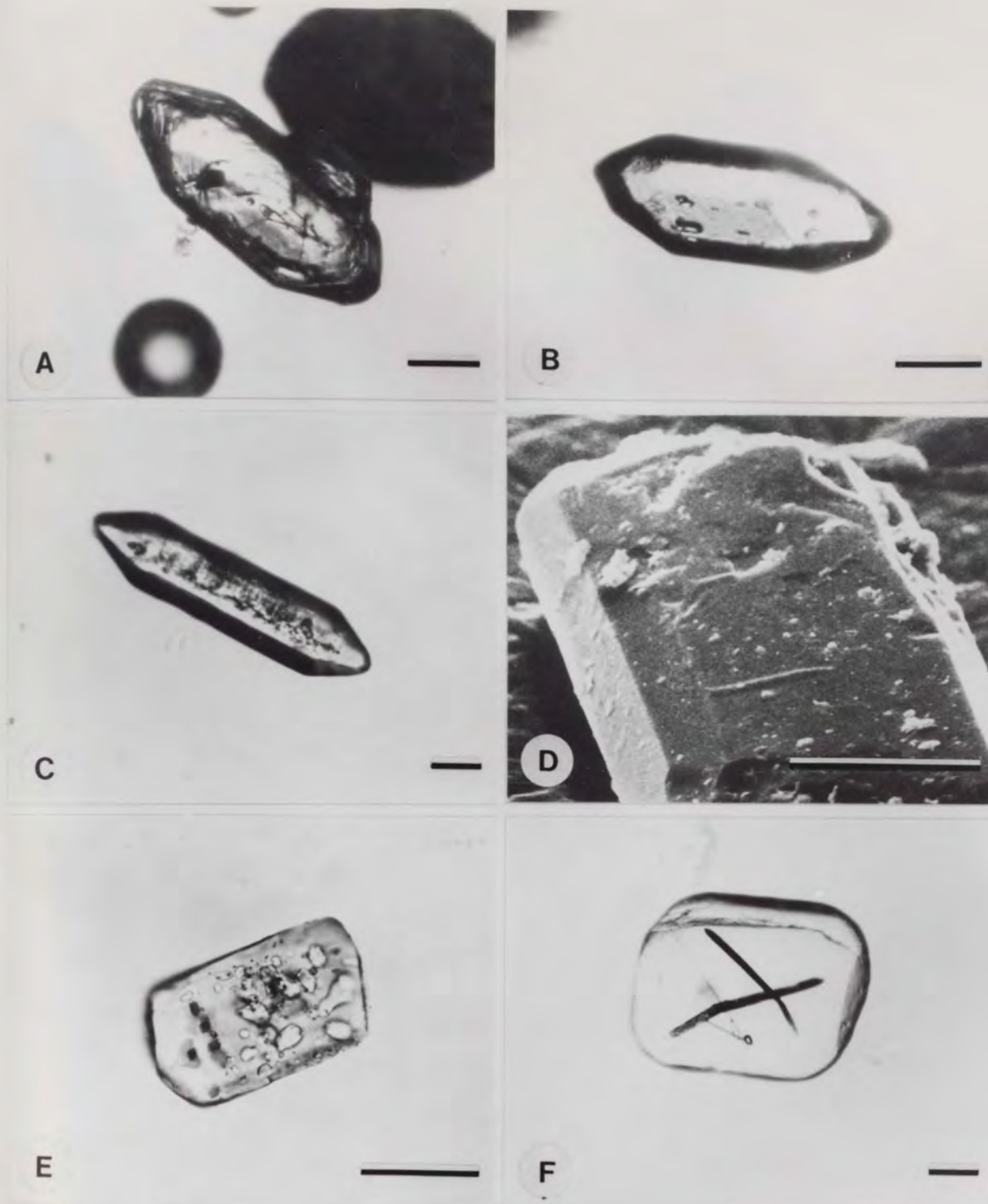


PLATE 3.7

- A. Zoned zircon showing abraded bipyramidal prismatic form, PPL, Bromsgrove Sandstone Fm.
- B. Euhedral zircon crystal with bipyramidal terminations and liquid inclusions, PPL, Bromsgrove Sandstone Fm.
- C. Needle-shaped bipyramidal zircon with abundant inclusions, PPL, Bromsgrove Sandstone Fm.
- D. Detrital zircon with a smooth surface texture except for some angular fractures probably caused during sample disaggregation, SEM photomicrograph, Bromsgrove Sandstone Fm.
- E. Subrounded tourmaline filled with bubbles and cavities, PPL, Bromsgrove Sandstone Fm.
- F. Tourmaline with rutile microlite inclusions, PPL, Wildmoor Sandstone Fm.

Scale bar = 50 μm

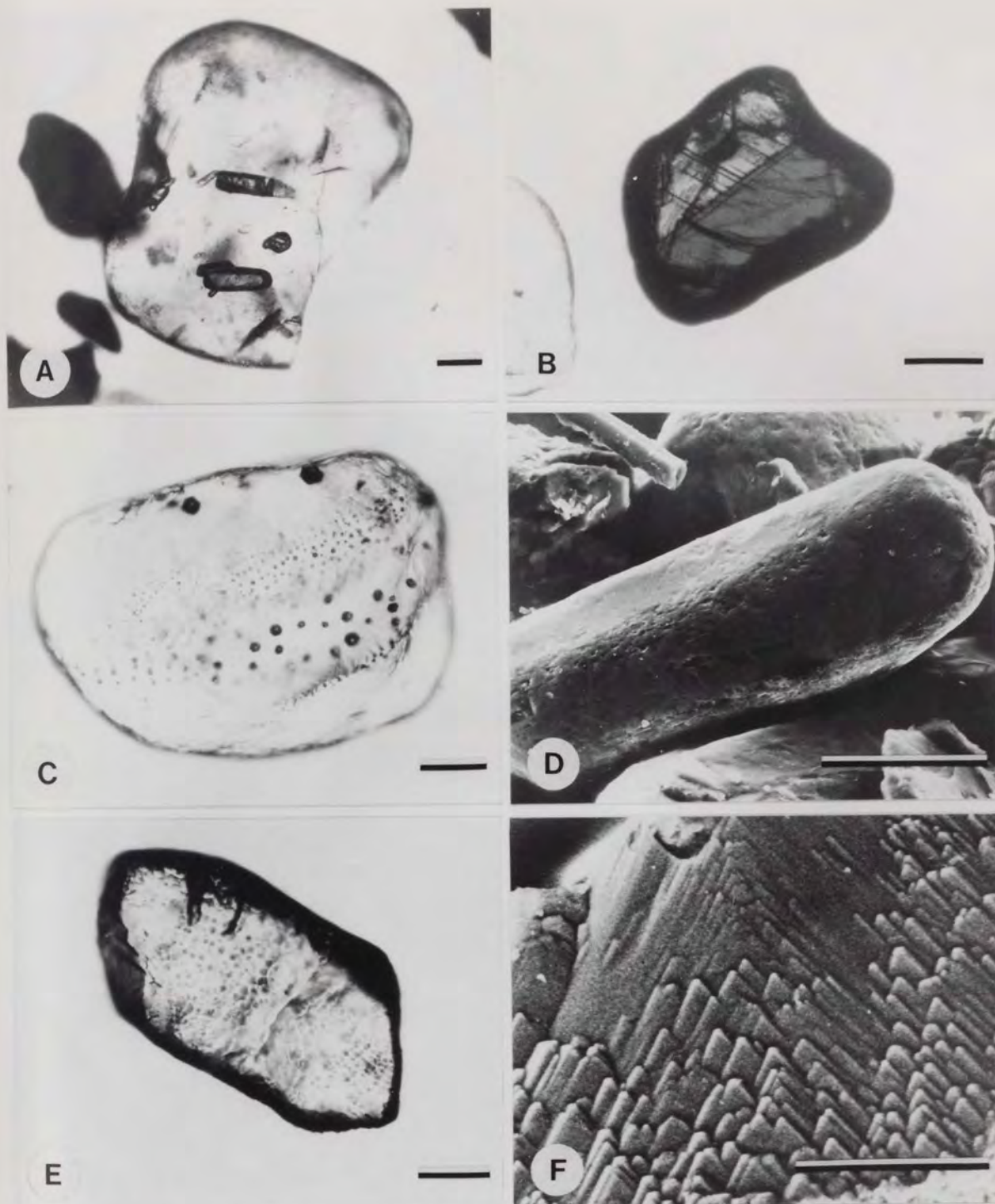


PLATE 3.8

- A. Well rounded detrital tourmaline with zircon inclusions, PPL, Wildmoor Sandstone Fm.
 - B. Detrital rutile showing twinning and striations, PPL, Wildmoor Sandstone Fm.
 - C. Well rounded apatite with abundant mineral and gas inclusions, PPL, Cannock Chase Fm.
 - D. Elongated apatite grain with pitted surface probably resulted during transportation, SEM photomicrograph, Wildmoor Sandstone Fm.
 - E. Subrounded garnet with knobs and pits caused by dissolution, PPL, Arden Sandstone Fm.
 - F. Garnet with v-shaped dissolution marks on the surface, PPL, Cannock Chase Fm.
- Scale bar = 50 μ m

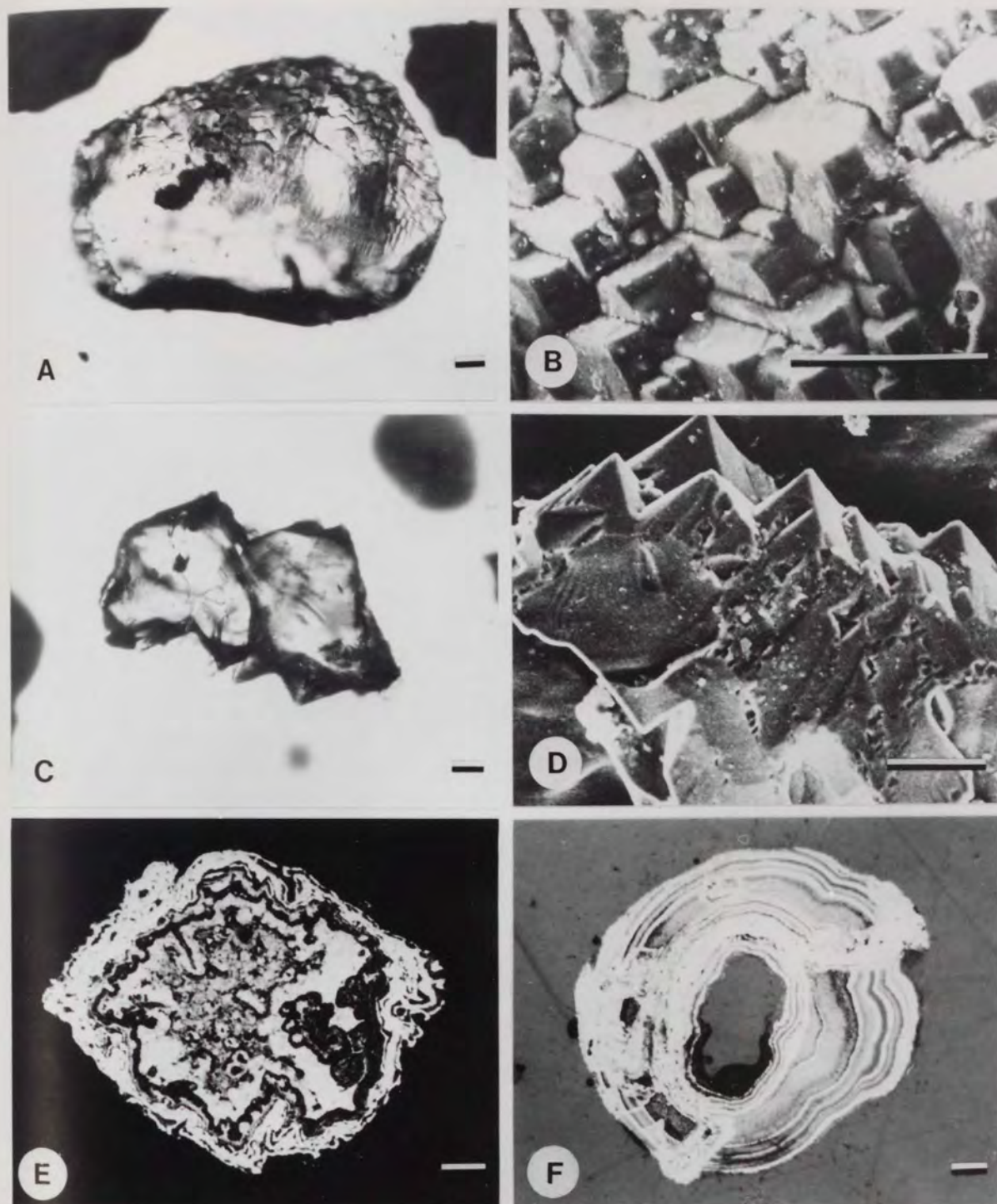


PLATE 3.9

- A. Step-like dissolution marks on the surface of detrital garnet, PPL, Bromsgrove Sandstone Fm.
 - B. Enlargement of A, SEM photomicrograph.
 - C. Detrital epidote with hacksaw terminations caused by dissolution, PPL, Kidderminster Fm.
 - D. V-shaped dissolution marks and hacksaw terminations of detrital epidote, SEM photomicrograph, Cannock Chase Fm.
 - E. Detrital grain of botryoidal haematite, reflected light, oil, PPL, Cannock Chase Fm.
 - F. Detrital grain of rhythmically banded haematite and silicate, reflected light, oil, PPL, Wildmoor Sandstone Fm.
- Scale bar = 30 μ m

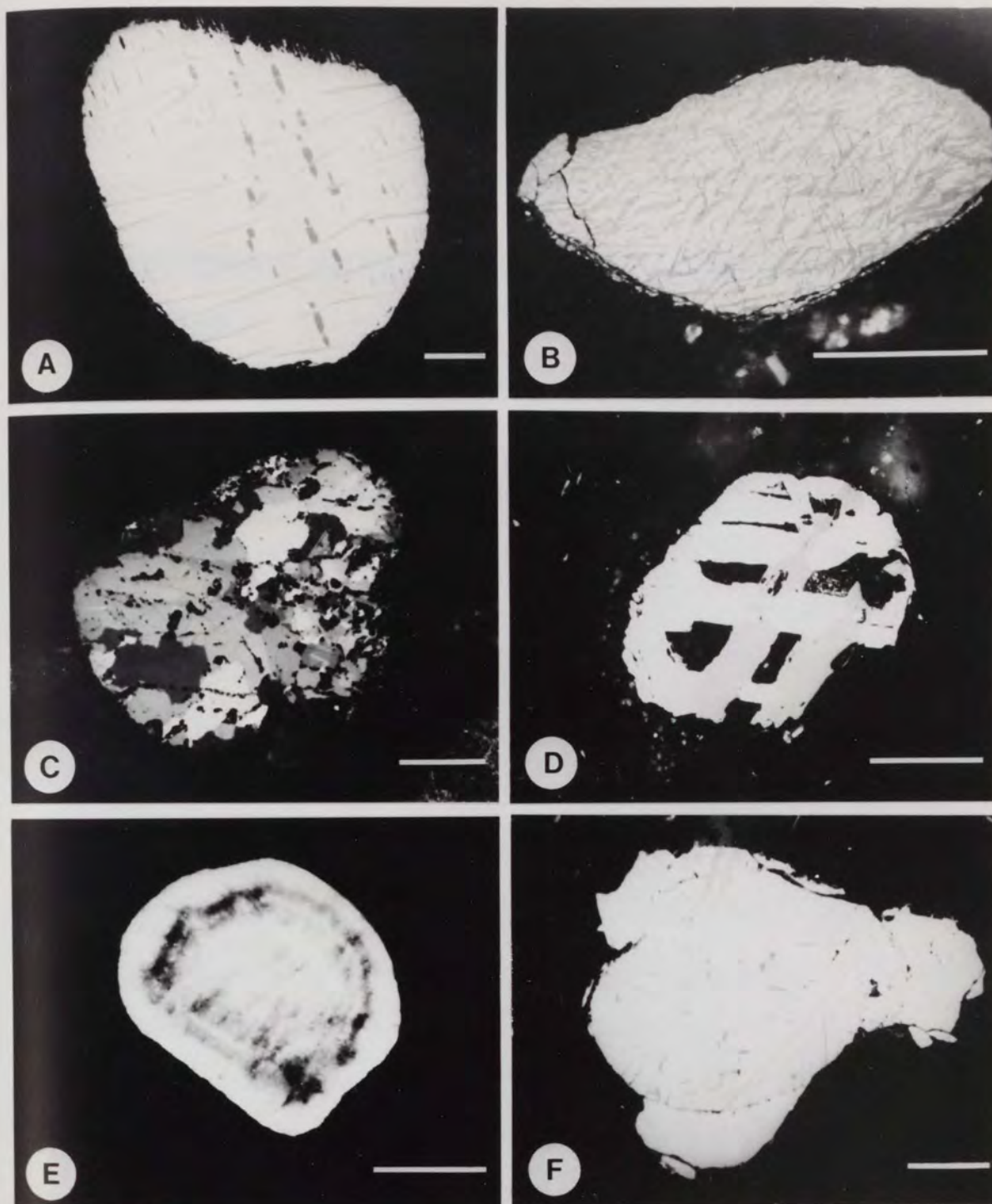


PLATE 3.10

- A. Detrital haematite with exsolution discs of ilmenite (darker grey) along the (0001) plane, and lamellae of rutile (lighter grey) along the (0111) and (0112) planes, reflected light, oil, PPL, Bromsgrove Sandstone Fm.
 - B. Detrital haematite with exsolution discs of rutile along the (0111) and (0112) planes, reflected light, oil, PPL, Cannock Chase Fm.
 - C. Detrital polycrystalline haematite representing points of simultaneous oxidation of magnetite into haematite, reflected light, oil, PCP, Cannock Chase Fm.
 - D. Well rounded detrital martite grain showing the triangular pattern produced by the formation of haematite after magnetite along the (111) planes, reflected light, oil, PCP, Bromsgrove Sandstone Fm.
 - E. Detrital leucoxene with colour banding, reflected light, oil, CP, Wildmoor Sandstone Fm.
 - F. Detrital haematite with exsolution discs of ilmenite and lamellae of rutile surrounded by reworked haematite overgrowth, reflected light, oil, PPL, Bromsgrove Sandstone Fm.
- Scale bar = 50 μm

CHAPTER 4

DIAGENESIS

4.1 DIAGENESIS OF THE TRIASSIC SANDSTONES IN CENTRAL ENGLAND

Diagenesis is the process involving all physical and chemical changes which take place in sediments after deposition and before the onset of metamorphism. These include compaction, authigenesis, replacement, dissolution, cementation, and all the chemical changes which take place in the interstitial fluids.

The Triassic sandstones in Central England show different diagenetic features. These include:

- (a) Mechanical infiltration of clay.
- (b) The intrastratal dissolution of detrital grains, particularly feldspars and other metastable silicate minerals such as epidote and garnet.
- (c) Dissolution of unstable ferromagnesian silicates such as hornblende. The scarcity of hornblende and absence of pyroxene in the Triassic sandstones may also be explained by their scarcity in the source area.
- (d) Clay replacement of detrital grains.
- (e) Pseudomorphism of biotite by haematite.
- (f) The formation of a suite of authigenic minerals including quartz, K-feldspar, illite, kaolinite, mixed-layer illite-montmorillinite, haematite, anatase, and later carbonate cement.

These diagenetic features are typical of continental red beds (Walker, 1976, Walker et al. 1978, Turner, 1980).

Since early diagenetic processes take place in an aqueous setting near the depositional interface the depositional environment exersices considerable influence on diagenetic reactions including the resultant authigenic mineral assemblages (Turner, 1980). In the case of continental red beds calcium and silicon are readily available since they are more abundant in river waters than marine waters due to their removal by calcareous shelled organisms, diatoms, and radiolaria in the marine environment. In addition, the dissolution of framework silicates and the clay replacement of detrital grains affects the composition of the interstitial waters and consequently the type of authigenic minerals.

Dissolution of authigenic K-feldspar and the replacement of detrital grains by carbonate cement are common features of the later stages of diagenesis in the Triassic sandstones.

4.2 MECHANICAL INFILTRATION OF CLAY

Mechanically infiltrated clay in the form of grain coatings is a common feature in ancient red beds. The studies of Walker (1976) and Walker et al. (1978) showed that desert alluvium, when initially deposited, is free of interstitial matrix. In arid climates the water table is low, particularly in alluvial fans at the basin margins,

and as a result the drainage is influent causing the infiltration of clay (Turner, 1980). The process of mechanical infiltration of clay decreases the textural maturity of sediments and changes the mineralogy by adding clay minerals that were not present in the original sediments and hence changes the bulk chemical composition (Walker et al. 1978).

Mechanically infiltrated clay represents the earliest diagenetic process in the Triassic sandstones. It is present sporadically and is absent from many sandstone horizons. This may be due to dissolution. Alternatively the sediments may have been washed later by meteoric water, or perhaps more likely, the clay may have not penetrated into many of these relatively fine grained Triassic sandstones. The SEM examination of the studied samples with the aid of EDAX revealed the presence of two textural varieties of mechanically infiltrated clay in the Triassic sandstones. These include a texture where thin clay flakes are arranged parallel to the surface of the framework grains (PL. 4.1A). It may indicate an early stage of accumulation representing a process which may have happened later in the diagenetic history. This type of infiltrated clay is common in the Bromsgrove Sandstone Formation. The other type, which is the most common, and was previously described by Walker (1976) and Walker et al. (1978) is represented by a clay skin (PL. 4.1B) composed of mixed sizes of clay patelets parallel to the grain surface (PL. 4.1C and D). This type of texture indicates an advanced stage

of accumulation (Walker et al, 1978).

4.3 DISSOLUTION OF FRAMEWORK SILICATES

Dissolution of unstable ferromagnesian minerals such as pyroxene and hornblende is a common diagenetic process in continental red beds. Walker (1967, 1976) and Walker et al. (1978) showed that the relicts of these minerals are common in Cenozoic first-cycle desert alluvium. In ancient red beds they are scarcely found. The destruction of unstable ferromagnesian minerals by intrastratal solution affects the porosity, mineralogical and textural maturity of the sediments, and most important, represents a significant source of ions such as K, Na, Al, Si, Mg, Fe, and Mn for the interstitial environment. These ions are thought to be the main source for the formation and type of different authigenic minerals including the pigmentary haematite which is responsible for the characteristic colour of continental red beds (Walker, 1976, Walker et al. 1978), Turner, 1980).

In the present study the Triassic sandstones are characterized by the absence of pyroxene (presumed dissolved) and the scarcity of hornblende which in most cases is reduced into needle-like relicts (PL. 4.1E). Pyroxene and hornblende may have been originally scarce in the source area and the few hornblende grains present may have been derived from a secondary nearby source. In view of the fact that the source area consisted mainly of low-rank metamorphic rocks (see Chapter 3) it is unlikely that hornblende or pyroxene would be abundant as detrital minerals. Detrital plagioclase grains also suffered from dissolution (PL. 4.1F).

Other metastable silicate minerals such as epidote and garnet were also affected by the same process. According to Waugh (1978) intrastratal dissolution in the Triassic sandstones is sufficiently advanced to affect minerals higher in the stability series such as the detrital K-feldspars, but in the studied samples no evidence of dissolution of the detrital K-feldspar grains has been found.

4.4 CLAY REPLACEMENT

This process is closely associated with dissolution and causes the release of different elements into the interstitial environment. It is a common diagenetic feature in the Sherwood Sandstone Group where it affected polycrystalline quartz and rock fragments in particular.

Chlorite was found to replace polycrystalline quartz grains along the intercrystalline boundaries (PL. 4.2A). Igneous and metamorphic rock fragments were also replaced by chlorite, the replacement taking place peripherally and along the crystal boundaries (PL. 4.2B). The composition of the replacement clay was found to be chlorite in all the studied samples and that is different from the composition of the mechanically infiltrated clay which was mainly illite and occasionally chlorite.

4.5 AUTHIGENIC MINERALS

Dissolution of framework silicates and clay replacement of the detrital grains have released different elements into

the interstitial environment. The authigenic mineral suite of the Triassic sandstones includes quartz, K-feldspar, illite kaolinite, mixed layer illite-montmorillinite, haematite and anatase. Such an authigenic mineral suite is a characteristic feature of continental red beds (Turner, 1980).

4.5.1 Clay Minerals

Authigenic clay minerals are more common in the Sherwood Sandstone Group than the sandstones of the Mercia Mudstone Group. These include illite, kaolinite, and occasionally mixed-layer illite-montmorillinite. The SEM with EDAX was used to distinguish between authigenic and detrital clay minerals. Clay composition was determined by x-ray diffraction analysis. The selected sandstone samples were gently crushed and then immersed in a high intensity ultrasonic bath for a few hours. Decantation and the use of a suction pump provided oriented samples on ceramic tiles. Diffraction patterns of untreated glycolated, and heated (550°C) samples were produced (Fig.4.1). These diffraction patterns indicate the abundance of illite, kaolinite, and mixed-layer illite-montmorillinite. The presence of a small amount of chlorite is thought to have resulted from contamination by sedimentary rock fragments and allogenic clay which is present as thin lenses.

Authigenic illite is the most abundant clay, and occurs mainly as pore linings covering detrital grain surfaces and is absent only at the grain contacts (PL. 4.2C). It consists of irregular flakes arranged perpendicular to

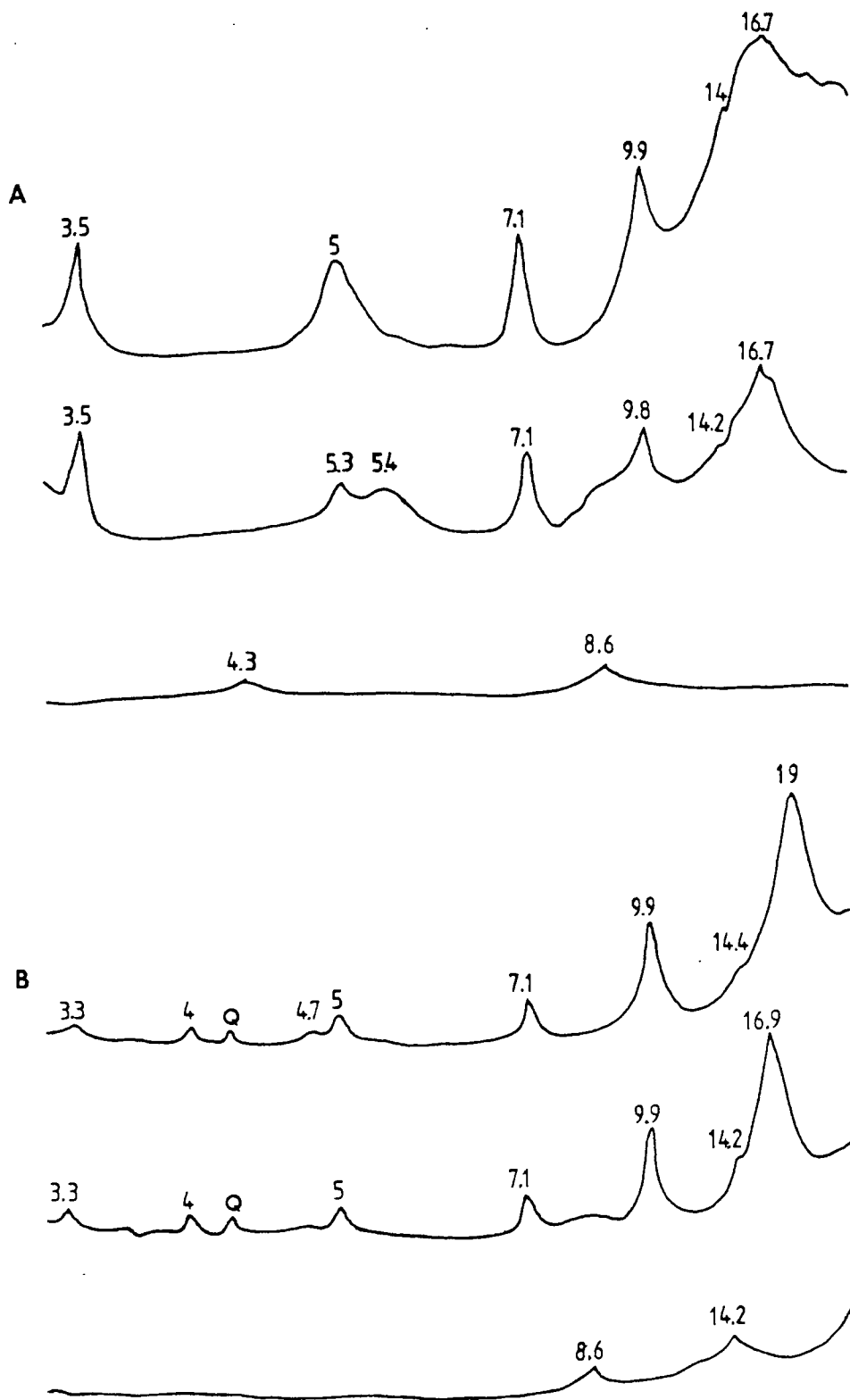


Fig.4.1 X-ray diffraction patterns of the clay fraction in the Triassic sandstones showing the presence of illite, kaolinite, mixed-layer illite-montmorillonite, and a small amount of chlorite. Each one represents diffraction patterns of untreated, glycolated, and heated (550°C) samples.

the grain surface forming a boxwork texture (PL. 4.2D). This type of authigenic illite represents the earliest authigenic mineral to form, and is most abundant in the Kidderminster Formation. The other type of authigenic illite was formed at later stages of diagenesis. It is present as spherical aggregates and clusters and textural relationship shows that it was formed after the dissolution of the authigenic K-feldspar (PL. 4.2 E F, 4.3A). This type of illite is common in the Bromsgrove Sandstone Formation.

Authigenic kaolinite is less abundant and found more commonly in the Wildmoor sandstones and the sandstones of the Mercia Mudstone Group. It occurs as pore fillings and displays the typical vermicular habit consisting of stacked pseudo-hexagonal plates (PL. 4.3 B & C).

Authigenic mixed-layer illite-montmorillonite was occasionally found and usually occurs as grain coatings in which the individual flakes curl away from the grain surface showing a highly crenulated texture which may have resulted from dehydration (PL. 4.3D, E, F). X-ray diffraction pattern of ethylene glycol treated samples (Fig. 4.1a) indicates a mixed-layer illite-montmorillonite with about 30% montmorillonite similar to the type described by Reynolds and Hower (1970).

4.5.2 Quartz

Quartz is an abundant authigenic mineral in the Triassic sandstones and shows a number of different stages

of development. Large well-developed overgrowths are abundant in the Bromsgrove and Arden sandstones, but in the rest of the Triassic sandstones they are less common and usually show only the initial stages of development. Many of the features described by Waugh (1970a,b) are present.

These overgrowths start as small crystallographic projections on the grain surfaces and when the grain surface was coated with authigenic illite the quartz crystals have grown over it indicating that the authigenic quartz post-dates the formation of authigenic illite (PL. 4.4A). These crystal projections are governed by the structure and crystallographic orientation of the host detrital grains. The development of quartz overgrowths on the individual crystal units of a polycrystalline quartz is the same with only one difference and that is the orientation of the crystalline projections differ from one crystal unit to another (PL. 4.4B & C). Sometimes these crystalline projections merge and show poorly defined crystal faces, forming an interconnected anastomosing network on the detrital grain surface (PL. 4.4D). This is similar to the type described by Pittman (1972).

Merging and overlapping of these crystalline projections forms a concentration of larger oriented crystal projections (PL. 4.4E). Finally with further growth a large complete simple crystalline projection is formed (PL. 4.4F). In strained quartz grains, the same intensity of undulose

extinction is transmitted into the overgrowths. The formation of complete quartz overgrowths in this way is exactly the same as that described by Waugh (1970 a,b) in the Penrith Sandstone of NW England. The quartz overgrowths are characterized by their non-luminescence (PL. 4.16A) which is typical of low temperature authigenic quartz.

4.5.3 K-feldspar

The authigenic K-feldspar in British Triassic sandstones was first mentioned by Reynolds (1929). Williams (1973) described the authigenic K-feldspar in the Early Triassic sandstones of NE Scotland. Waugh (1978) made the first detailed description of the development of pure K-feldspar in the British Permo-Triassic sandstones. It is the most common authigenic mineral in the Sherwood Sandstone Group, but is less commonly found in the sandstones of the Mercia Mudstone Group. It occurs as overgrowths around the detrital feldspar grains (PL. 4.5A), or as clusters of whole crystals, with adularia habit (PL. 4.5B) ranging in size from 5-15 μm and lacking any detrital core (c.f. Walker et al. 1978). These crystals were found to be elongated along the c-axis (PL. 4.5C) in the sandstones of the Kidderminster Formation.

Virtually all the detrital K-feldspar grains are partially or entirely enveloped by these euhedral rhombic overgrowths. They are fresh and unaltered showing no twinning or perthitic texture and their boundary is sharply

defined by the boundary between the highly altered core and the fresh unaltered overgrowth or by a prominent difference in optical orientation. Although many overgrowths are in optical continuity it is also common to see overgrowths which are optically discontinuous with the host detrital grain. Optical discontinuity has been attributed to differences in composition and/or in the degree of Al/Si disorder between the detrital core and overgrowth (Pettijohn, 1975, Kastner and Siever, 1979).

Electron probe microanalysis for K_2O , Na_2O , BaO , CaO , Al_2O_3 , and SiO_2 was carried out on selected samples from the Kidderminster, Cannock Chase, Wildmoor Sandstone, and Bromsgrove Sandstone Formations. The analyses were carried out with a Cambridge Microscan Electron Probe using 0.25×10^{-7} Amp. current and 15 KV voltage. Spot analyses were usually performed on an overgrowth and its host detrital grain to allow comparison between the two. The results (Table 4.1) show that the overgrowths are virtually pure end member $KAlSi_3O_8$ ranging from 96.5 - 100 mole % Or except for the Cannock Chase Formation (grain No. 1-4), where values down to 92.2 mole % Or are present, with up to 7.7 mole % An and 2.5 mole % Cn. Albite, on the other hand, ranges from 0.1 - 1.8 mole % and celsian and anorthite do not exceed 0.3 and 2.9 mole % respectively (Table 4.1). An important feature in this analysis is the detection of Ba which is not usually observed in authigenic K-feldspars which are noted for their chemical purity (Kastner and Siever, 1979).

TABLE 4.1 Composition of cores and corresponding overgrowths of K-feldspar grains in the Triassic sandstones. The molecular compositions are calculated by normalizing the oxide totals. (1 - 4 Cannock Chase Formation, 5 - 8 Wildmoor Sandstone Formation, 9 - 21 Bromsgrove Sandstone Formation).

Grain No.	Oxides (Wt. %)					Molecular Composition				
	K ₂ O	Na ₂ O	BaO	CaO	Al ₂ O ₃	SiO ₂	Or	Ab	Cn	An
1 Overgrowth	16.25	0.050	0.069	0.086	16.42	66.46	96.3	0.4	2.5	0.7
1 Core	15.83	0.665	0.377	—	16.96	66.34	92.7	5.9	1.4	—
2 Overgrowth	16.99	0.032	0.069	0.027	16.54	66.38	97.0	0.3	2.4	0.3
2 Core	14.88	1.385	0.597	0.018	17.23	65.75	85.6	12.1	2.1	0.2
3 Overgrowth	17.00	0.015	—	0.850	16.80	64.81	92.2	0.1	—	7.7
3 Core	16.00	0.570	—	0.021	16.80	66.00	94.7	5.1	—	0.2
4 Overgrowth	17.03	0.076	—	0.150	16.43	66.10	97.9	0.7	—	1.4
4 Core	16.17	0.300	0.660	—	16.80	66.30	95.0	2.6	2.4	—
5 Overgrowth	17.60	0.070	0.052	—	16.30	65.10	99.2	0.6	0.2	—
5 Core	16.50	0.412	0.086	—	16.60	65.40	96.2	3.6	0.2	—
6 Overgrowth	17.87	0.059	0.032	—	16.10	65.17	99.4	0.5	0.1	—
6 Core	17.30	0.436	0.046	—	16.10	65.30	96.2	3.6	0.2	—
7 Overgrowth	17.50	0.012	0.076	—	16.00	65.10	99.7	0.1	0.2	—
7 Core	15.80	0.816	0.310	—	16.20	65.40	92.6	7.3	0.1	—
8 Overgrowth	17.40	0.059	0.022	—	16.10	66.90	99.3	0.5	0.2	—
8 Core	16.42	0.841	0.165	0.294	16.20	65.70	89.8	7.0	0.5	2.7
9 Overgrowth	16.82	0.035	—	0.064	16.30	65.90	99.2	0.2	—	0.6
9 Core	16.50	0.031	0.656	0.021	16.48	65.85	97.2	0.3	2.3	0.2
10 Overgrowth	17.05	0.023	0.046	0.188	16.35	66.23	98.1	0.1	0.1	1.7
10 Core	16.10	0.740	0.276	0.021	16.40	67.00	92.4	6.4	1.0	0.2
11 Overgrowth	17.40	0.065	0.041	0.307	16.10	65.50	96.5	0.5	0.1	2.9
11 Core	15.30	1.120	1.150	0.012	16.60	66.40	86.4	9.5	4.0	0.1
12 Overgrowth	16.58	0.198	—	0.015	17.00	66.30	98.1	1.8	—	0.1
12 Core	14.68	1.336	0.116	0.068	18.10	65.80	86.9	12.0	0.4	0.7
13 Overgrowth	16.10	0.023	0.086	0.136	16.20	67.20	98.0	0.2	0.3	1.4
13 Core	15.00	0.528	0.256	0.023	16.50	68.00	93.8	5.0	1.0	0.2
14 Overgrowth	17.38	0.053	—	0.020	17.65	64.70	99.4	0.4	—	0.2
14 Core	16.80	0.354	0.179	0.045	17.30	65.50	95.9	3.1	0.6	0.4

Table 4.1 Cont....

Oxides (Wt. %)						Molecular Composition					
Grain No.	K ₂ O	Na ₂ O	BaO	CaO	Al ₂ O ₃	SiO ₂	Or	Ab	Cn	An	
15	Overgrowth	17.50	0.053	----	----	16.80	65.00	99.6	0.4	---	---
	Core	15.00	1.020	----	----	17.40	66.00	90.6	9.4	---	---
16	Overgrowth	16.96	0.097	----	----	16.70	66.30	99.0	1.0	---	---
	Core	15.68	0.637	0.555	----	16.80	66.40	92.0	6.0	2.0	---
17	Overgrowth	17.70	0.035	-----	----	16.20	66.15	99.7	0.3	---	---
	Core	16.40	0.876	0.265	----	16.50	65.50	91.5	7.5	1.0	---
18	Overgrowth	17.80	-----	-----	----	16.00	66.20	100.0	---	---	---
	Core	16.80	0.540	0.350	0.044	16.00	66.60	94.0	4.6	1.0	0.4
19	Overgrowth	17.27	-----	0.149	-----	16.00	66.60	99.5	-----	0.5	---
	Core	16.33	0.448	0.160	-----	15.90	67.20	95.5	4.0	0.5	---
20	Overgrowth	17.20	0.029	0.062	-----	16.24	66.60	99.5	0.3	0.2	---
	Core	16.82	0.606	0.124	0.027	16.00	66.00	94.4	5.0	0.4	0.2
21	Overgrowth	17.46	-----	0.046	-----	15.90	66.56	99.8	---	0.2	---
	Core	15.40	1.023	0.934	-----	16.60	66.30	87.9	8.9	3.2	---

The chemical purity of the overgrowths is reflected by their nonluminescence (PL. 4.16B) which is a characteristic of low temperature authigenic feldspars. The detrital cores on the other hand, display a bright blue luminescence typical of high temperature feldspars (Smith and Stenstrom, 1965). This blue luminescence was found to be lighter in colour when the detrital core had a relatively higher Ba content (PL. 4.16C). Stablein and Dapples (1977) also described this phenomena.

Smith (1974) proposed a scheme of nomenclature for the K-feldspars by plotting the mole % Or against the optic axial angle - $2V$. Measurements of the optic axial angles of the overgrowths gave values ranging from - 45° to - 50° . Therefore, according to Smith (1974, Fig. 9.12), the overgrowths may be described as potassian low sanidines. The detrital cores on the other hand, may be either orthoclase or sanidine.

It was found that overgrowths around detrital sanidines are in optical continuity with the host grain, but when the host grain is orthoclase or microcline the overgrowths are optically discontinuous. Furthermore, there is no evidence of any compositional difference between the overgrowth and host grain in many feldspars and the difference in the degree of optical continuity thus appears to be due to differences in structure or Al/Si ordering, rather than differences in composition.

Zoned K-feldspar overgrowths are particularly abundant

in the Bromsgrove Sandstone Formation. They range in size from 30-85 μm , and are usually not in optical continuity with the host detrital grain (PL. 4.5 D & E). Electron beam traverses across zoned overgrowths (Fig. 4.2) show a variation in weight percentage of K_2O corresponding to small fluctuation in the amount of BaO and Na_2O . These slight compositional variations are consistent with the observed optical zonation.

Different stages of development of the authigenic K-feldspar were recognised in the Sherwood sandstones. The sequence of development is basically the same as that described by Waugh (1978).

The initial stage is represented by the formation of small oriented rhombohedral crystals ranging in size from 1 - 5 μm (PL. 4.5F). The term "adularia habit" was given to such crystals by Baskin (1956) and is used here as a morphological term only. These crystals usually show a preferred orientation determined by the crystallographic structure of the host detrital grain, but the presence of whole authigenic crystals in pore spaces, and the formation of adularia on the surfaces of detrital quartz grains (PL. 4.6A) indicates that the overgrowths are not always governed by the detrital feldspar grains. When the surfaces of detrital feldspar grains are coated with authigenic illite these adularia crystals have grown over it (PL. 4.6B) indicating that the authigenic K-feldspar precipitation post-dates the formation of authigenic illite.

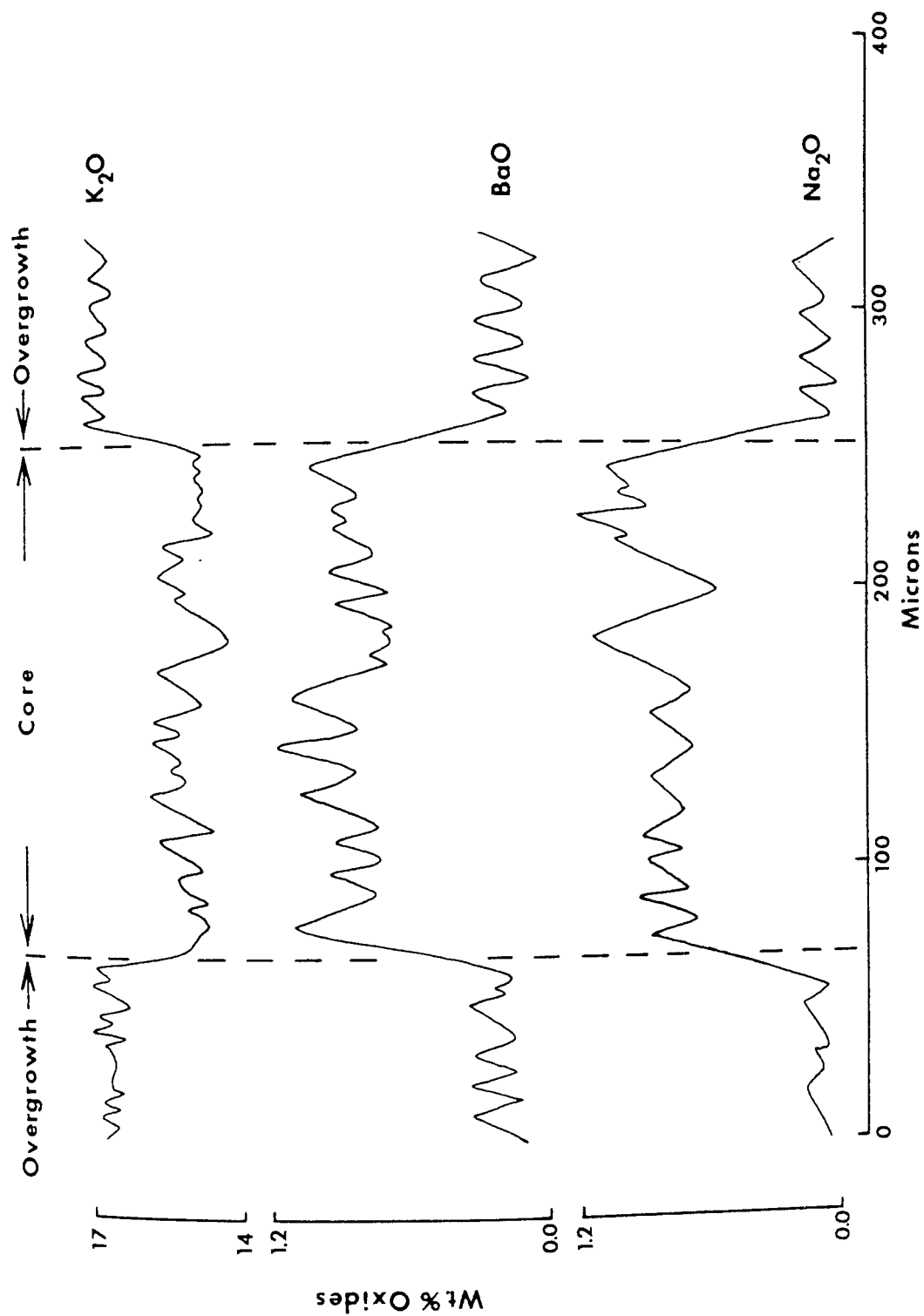


Fig.4.2 Electron probe traverse across a zoned K-feldspar overgrowth and the host detrital grain showing fluctuations in K₂O, BaO, and Na₂O.

Merging, stacking, and growing of these rhombic crystals results in the formation of larger crystal faces (PL. 4.6C). Further merging may produce an almost complete smooth crystal face (PL. 4.6D).

The final stage of development is represented by the detrital feldspar grain being entirely enveloped by the overgrowth forming an almost complete crystal with hack-saw terminations (PL. 4.6E).

The overgrowths show a structure intermediate between orthoclase and adularia in which the (100) and (001) forms are well developed and the (101) is absent or poorly developed and recognized as a ridged irregular surface (PL. 4.6F). Sometimes the (100) and (001) forms are equally developed and become indistinguishable giving the crystal a diamond shaped appearance (PL. 4.7A). It is common to see some irregularities on the crystal faces due to the incomplete stacking of the rhombic units (PL. 4.7B). At later stages of diagenesis the authigenic K-feldspar overgrowths were affected by illite replacement (PL. 4.7C).

Authigenic K-feldspar overgrowths were affected by dissolution at later stages of diagenesis. This dissolution has taken place preferentially along the cleavage traces (PL. 4.7D), and in many cases only the relicts of the overgrowth remain attached to the detrital grain (PL. 4.7E&F).

4.5.4 Haematite

Authigenic haematite is present in a variety of textures in the Triassic sandstones. Ultrafine haematite pigment present as grain coatings is the main colouring agent in the Triassic sandstones, and sometimes more than one generation was recognized (PL. 4.8A), especially in the sandstones of the Kidderminster Formation. Acicular and large euhedral haematite overgrowths are most abundant in the Bromsgrove sandstones; they are less commonly found in the Wildmoor sandstones, and rarely found in the rest of the Triassic Formations. Micro-crystalline haematite is present as hexagonal platelets through the interstitial matrix (PL. 4.8B). The large euhedral overgrowths surrounding the detrital haematites and ilmenohaematites are well developed in the Bromsgrove sandstones, where different stages of development are recognized. The earliest stages are represented by flat rhombohedral crystals ranging in size from 1 to 5 μm and arranged perpendicular to the grain surface (PL. 4.8C). The orientation of these crystals is controlled by the crystallographic structure of the host detrital grain. In polycrystalline detrital haematite grains the different crystallographic orientations of the individual crystals is reflected in the orientation of the authigenic crystals (PL. 4.8D). This is also true in the case of authigenic overgrowths developing on the surface of martite grains (PL. 4.8E). Merging and growth produces larger rhombohedral

crystals (PL.4.8F). Sometimes these authigenic crystals, as they are formed along the (111) plane (PL.4.9A), may merge together forming long parallel ridges on the surface of the detrital grain (PL. 4.9B). Finally, with further growth a large euhedral overgrowth is formed (PL. 4.9C). Authigenic haematite overgrowth was also found to fill the fractures of detrital ilmenohaematite grains (PL.4.9D).

An earlier stage of oxidation, i.e. the transformation of magnetite into haematite is common in the Triassic sandstones and represented by haematite grains with relict maghemite in the middle (PL.4.9E). In the Wildmoor sandstones where the haematite overgrowths are less well developed it is common to see rhombohedral haematite crystals with unaltered maghemite centres (PL.4.9F), where the formation of haematite after maghemite along the (111) planes has taken place.

EPMA of the haematite overgrowths and their host detrital grains showed that the authigenic overgrowths contain from 0.52 to 11.15 wt. % titanium and up to 0.5 wt. % vanadium, whereas the detrital haematite grains generally have less titanium and vanadium (Table 4.2). This indicates that the interstitial solution was enriched with titanium and vanadium. In the case of the host detrital grain being an ilmenohaematite, the authigenic haematite overgrowths have less titanium than the host grain, which originally had high titanium.

4.5.5 Titanium Oxides

Authigenic titanium oxides are abundant in the Triassic

TABLE 4.2 Electron probe microanalysis of detrital and authigenic haematites in the Triassic sandstones. (1-4 Wildmoor Sandstone Formation, 5-13 Bromsgrove Sandstone Formation.

Grain No.	Textural phase	Oxides (Wt. %)					
		TiO ₂	Fe ₂ O ₃	V ₂ O ₅	MnO	Cr ₂ O ₃	CuO
1	Authigenic	0.42	99.60	----	0.11	----	0.14
2	Detrital	0.13	99.42	0.18	0.29	0.14	0.08
2	Maghemite core	0.07	98.40	0.30	0.59	1.35	0.05
3	Authigenic	0.05	99.20	0.05	0.07	----	0.08
3	Maghemite core	0.06	99.88	0.03	0.09	----	0.10
4	Authigenic	11.38	87.65	0.46	0.32	0.15	0.04
4	Detrital	13.50	86.00	0.40	0.35	0.14	0.11
5	Authigenic	4.36	95.12	0.44	0.05	0.05	0.13
5	Detrital	12.93	85.82	0.64	0.32	0.16	0.13
5	Ilmenite exsolution	48.50	49.62	0.34	0.58	0.06	0.05
6	Euhedral overgrowth	5.40	92.90	0.40	----	0.08	0.09
6	Cement	4.50	94.26	0.38	----	----	0.08
7	Authigenic	5.40	94.20	0.46	----	0.06	----
7	Detrital	2.20	96.76	0.08	0.11	----	0.10
8	Authigenic	3.30	95.30	0.42	0.05	0.06	0.07
8	Detrital	0.25	98.80	0.27	0.09	0.05	0.07
9	Authigenic	2.90	95.66	0.27	0.15	0.10	0.08
9	Detrital ilmenohaematite	56.20	43.15	0.14	0.87	----	0.05
10	Authigenic	0.52	99.34	0.09	----	----	----
10	Detrital	0.06	99.85	0.14	0.06	0.07	0.08
11	Authigenic	3.20	96.36	0.51	----	----	0.06
11	Detrital	7.70	91.55	0.28	0.33	0.06	0.12
11	Exsolution Discs	61.30	38.17	0.26	0.18	0.07	0.12
12	Authigenic	11.15	87.58	0.37	0.36	0.10	----
13	Detrital Polycrystalline	0.05	99.61	----	0.28	----	0.13

sandstones and present either as euhedral overgrowths around the detrital titanium oxide grains (PL. 4.10 A & B), ilmenohaematite grains (PL. 4.10C) where peripheral alteration has taken place (PL. 4.10D), or as discrete crystals. These discrete crystals are present either as clusters of crystals filling pore spaces (PL. 4.10E) or as single crystals among the authigenic illite matrix (PL. 4.10F). Authigenic titanium oxide crystals were also found filling the dissolution voids of detrital ilmenites, which usually show indications of intensive alteration to titanium oxide (PL. 4.11A).

EPMA of the authigenic titanium oxides shows a higher percentage of iron (up to 0.83 wt. %) and vanadium (up to 0.96 wt. %), whereas the detrital grains contain less iron and vanadium (Table 4.3).

Ixer et al (1979) described the authigenic titanium oxide in the St. Bees Sandstone (Triassic) of Cumbria and suggested that titanium ions may have been released to the interstitial environment during the martitization of detrital titanomagnetites. The abundance of martites in the Triassic sandstones may support the above suggestion.

4.6 PSEUDOMORPHISM OF BIOTITE BY HAEMATITE

Replacement of phyllosilicates by haematite is a common diagenetic feature in continental red beds. Haematite aureoles around detrital biotite grains caused by the distribution of iron by oxygenated pore water were

TABLE 4.3 Electron probe microanalyses of authigenic and detrital titanium oxides in the Bromsgrove Sandstone Formation

Grain No.	Textural phase	Oxides (Wt. %)					
		TiO ₂	Fe ₂ O ₃	V ₂ O ₅	MnO	Cr ₂ O ₃	CuO
1	Authigenic	98.66	0.77	0.96	0.07	----	0.12
2	Authigenic	98.80	0.63	0.58	----	----	0.07
3	Authigenic	98.85	0.68	0.41	0.11	----	0.05
4	Authigenic	98.47	0.57	0.65	----	----	0.05
4	Detrital	98.38	0.12	0.59	0.15	0.05	----
5	Authigenic	97.89	0.76	0.88	0.07	0.23	0.09
6	Authigenic	98.30	0.76	0.49	0.05	----	0.10
7	Authigenic	98.37	0.63	----	----	----	0.10
7	Detrital	98.55	0.55	----	----	----	0.06
8	Authigenic	98.18	0.83	0.59	0.07	----	0.10
8	Detrital	98.54	0.50	0.15	----	----	0.13

described by Walker (1967, 1976) and Walker et al. (1978). Turner and Archer (1977) described in detail the sequence of biotite alteration to haematite and its contribution to the colour of the Old Red Sandstone of Northern Scotland.

In the present study the different stages of alteration from fresh biotite grains to those almost completely replaced by haematite were recognized in the Sherwood Sandstone Group especially the Bromsgrove Sandstone Formation.

The initial stages of development are represented by the formation of translucent hexagonal haematite flakes along the cleavage planes (PL. 4.11 B & C). Some of these haematite crystals are twinned (PL. 4.11D). With progressive oxidation these hexagonal haematite flakes begin to coalesce, forming large discontinuous pseudo-hexagonal sheets (PL. 4.11E). Finally, stacking of these haematite sheets forms nearly complete pseudomorphs parallel to the cleavage planes (PL. 4.11F).

Compacted parts of the detrital biotite grains are not affected by oxidation whereas parts accessible to interstitial solutions are altered (PL. 4.12A). This may indicate that haematization took place well after compaction.

EDAX spot analysis of the hexagonal flakes and the surface of the biotite (Fig. 4.3) shows the high iron content of these flakes relative to the background.

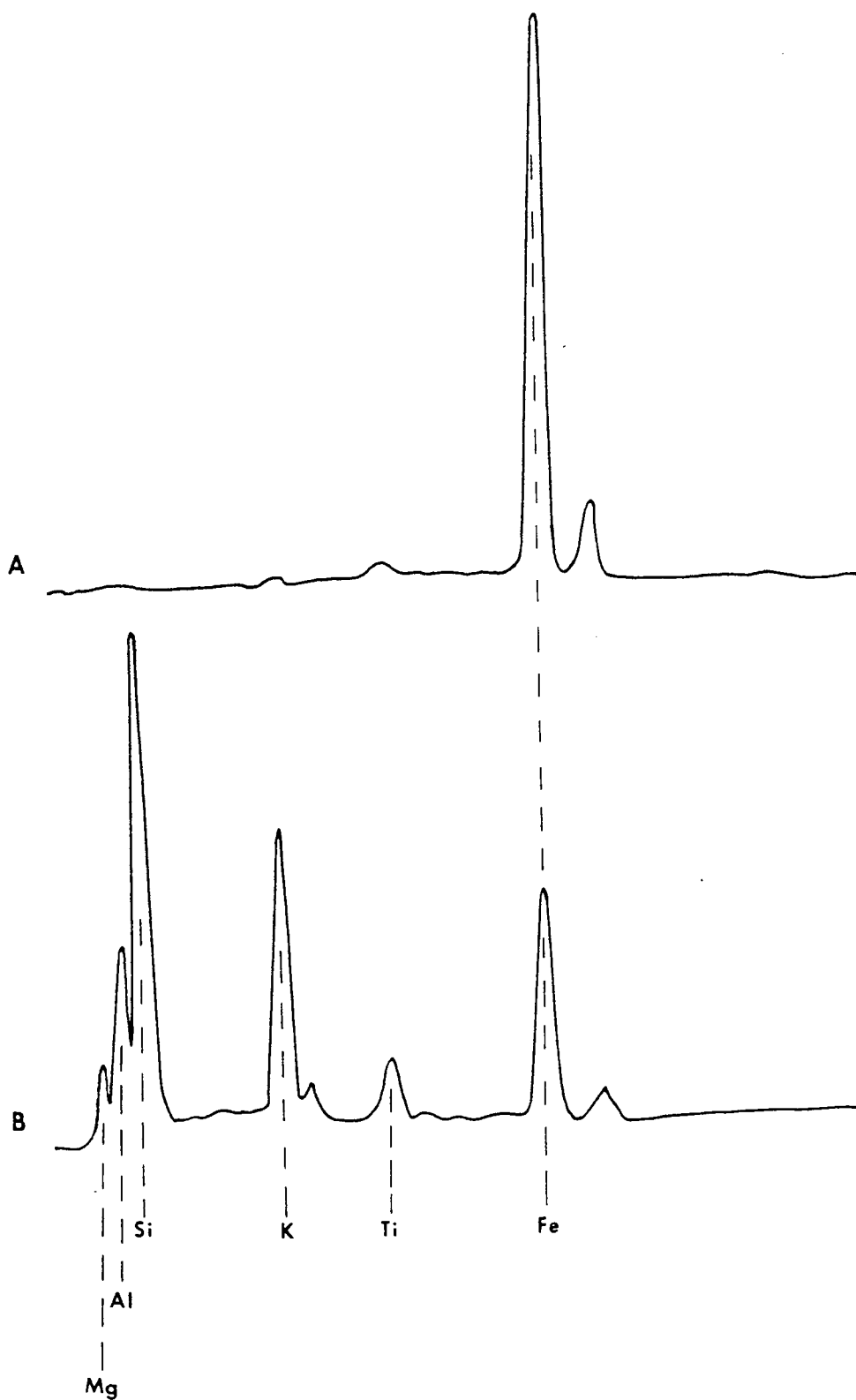


Fig.4.3 EDAX spot analysis of A.hexagonal haematite flake, and B.the surface of a biotite grain in the background.

4.7 MARTITIZATION

The formation of haematite after magnetite is referred to as martitization (Rhamdohr, 1980). In the present study the sandstones of the Kidderminster, Cannock Chase, and Polesworth Formations were found to contain a high proportion of martites, whilst the Wildmoor and Bromsgrove sandstones contain a lesser proportion and they are only occasionally found in the sandstones of the Mercia Mudstone Group. This distribution may reflect different sources.

Many martites are subrounded to rounded showing a triangular pattern resulting from the formation of haematite along the octahedral (111) planes of magnetite (PL. 4.12B & C). Subangular octahedral martite grains are also common (PL. 4.12D). Under reflected light many martites show clear polycrystallinity (PL. 4.12E).

Martitization may result from post-depositional oxidation of magnetite or titanomagnetite into haematite. It is not clear whether haematite ($\alpha\text{-Fe}_2\text{O}_3$) forms directly after magnetite or whether an intermediate phase of maghemite ($\gamma\text{-Fe}_2\text{O}_3$) is involved (Turner, 1980). The presence of an intermediate phase of maghemite may be indicated by the presence of martites with relict maghemite (PL. 4.12F) in sandstones with green reduction spots from the Mercia Mudstone Group. These sandstones may not have been completely oxidized in the first place.

4.8 CEMENTATION

In general the Triassic sandstones are friable and loosely consolidated. Calcite and oxidised clay pellicles + iron oxide are the most common cementing materials in the Sherwood Sandstone Group, whereas dolomite is the main cementing material in the sandstones of the Mercia Mudstone Group.

Calcite cement is present either as uniformly or patchily distributed pore fillings (PL. 4.13A). Staining by the combined Potassium ferricyanide plus Alizarin Red S (Dickson, 1966), revealed the presence of two zones of ferroan calcite, alternating with two non-ferroan calcite zones (PL. 4.13B). The ferroan calcite zones are characterized by their bright yellow luminescence (PL.4.16D). This calcite cement zonation is common in the Bromsgrove Sandstone Formation and absent from the rest of the Triassic sandstones. Ferrous iron in pore water must be at least 200 ppm Fe^{++} for a stain reaction with the Potassium ferricyanide (Oldershaw and Scoffin, 1967). The presence of these compositional zones in the calcite cement probably reflects multiple, local sources for the cement.

Calcite cement replacement of the detrital grains is a common feature in the Cannock Chase and Bromsgrove Sandstone Formations. Calcite cement has replaced the detrital quartz grains (PL. 4.13C), and corroded both

the authigenic and ^{detrital} K-feldspar (PL. 4.13D). In most cases only the relict structure of the detrital grain was preserved (PL. 4.13E & F).

Calcite cement replacement of the detrital grains may indicate that the pore waters were supersaturated with calcium carbonate (Pettijohn et al. 1972), and that calcite cementation is of the late diagenetic stage (Füchtbauer, 1974). This is clearly demonstrated in the present study where the calcite cements have replaced the authigenic K-feldspar.

Dolomite is the main cementing material in the sandstones of the Mercia Mudstone Group and usually shows evidence of recrystallization (PL. 4.14A) and zoned dolomite crystals are abundant (PL. 4.14B). Cathodoluminescence study showed the dolomite cement to give a reddish to orange yellow luminescence (PL. 4.16E) and revealed the zonation of some dolomite crystals surrounding detrital dolomite grains (PL. 4.16F).

Dolomite cement was also found to replace the detrital grains; detrital plagioclase being affected and also authigenic K-feldspar overgrowths (PL. 4.14C). In most cases only the relict structure of the detrital grains remains inside the dolomite crystal (PL. 4.14D).

Calcite cement in the form of large crystals preceded the dolomite cement in the Arden sandstones (PL. 4.14E & F). Later dissolution seems to have affected these calcite crystals as indicated by the V-shaped etching marks on the

crystal faces (PL. 4.15A) and the needle-shaped relicts on the corners (PL. 4.15B & C).

Oxidised clay pellicles (PL. 4.15D) are the main cementing materials in the Wildmoor Sandstone Formation and some of the sandstone horizons of the Kidderminster and Bromsgrove Sandstone Formations. Haematite cement is also present as a local cement in small patches (PL. 4.15E & F).

4.9 DISCUSSION

Dissolution of framework silicates is the earliest diagenetic process in the Triassic sandstones after the mechanical infiltration of clay. It is represented by the occurrence of relict hornblende grains with well-developed dissolution needles. The general scarcity of ferromagnesian silicates may also be due to their removal by intrastratal dissolution. Plagioclase, epidote and garnet have also been partially dissolved. Waugh (1978) in his study of the authigenic K-feldspar in the British Permo-Triassic sandstones suggested that the hydrolysis of silicates might proceed with age to include minerals higher in the stability series like the detrital K-feldspar. In the present study no evidence of dissolution of the detrital K-feldspars have been found so far.

In these Triassic sandstones the process of intrastratal dissolution of framework silicates together with clay replacement of the detrital grains provided the interstitial environment with the necessary Al, K, Fe, Mg, Na, Ca, and Si ions which are required for the

precipitation of authigenic minerals. The thermodynamic and kinetic factors which govern the formation of authigenic minerals in the $K_2O - Na_2O - Al_2O_3 - SiO_2 - H_2O$ system were described by Hess (1966), Helgeson et al. (1969, 1978), and Kastner and Siever (1979). These thermodynamic relations are presented in a combination diagram (Fig. 4.4) which shows the aqueous solution in equilibrium with solid phases and activity of H_4SiO_4 and K^+ at $0^\circ C$ and 1 Atm. Aluminium is assumed to be present as $Al(OH)_4^-$ or some form of stable complex (Hem et al. 1973). The diagenetic sequence of (1) illite, (2) quartz, (3) K-feldspar, (4) illite, (5) mixed-layer illite-montmorillonite, (6) kaolinite is consistent with an initial increase in K^+ or H_4SiO_4 as dissolution and authigenesis progressed causing the precipitation of illite, which is mainly in the form of grain coatings, then quartz, followed by K-feldspar, and then later illite and mixed-layer illite-montmorillonite. Finally, kaolinite precipitated as pore fillings. In samples with no authigenic illite quartz is the first to form and in this case the quartz overgrowths are well-developed forming large prisms and bipyramids.

The precipitation of illite would naturally deplete the interstitial environment of K^+ ions. As a result, in specimens rich in authigenic illite, only the early stages of development of K-feldspar overgrowths are present. This contrasts with previous observations in the Triassic sandstones and suggests a delicate balance between K^+/H^+

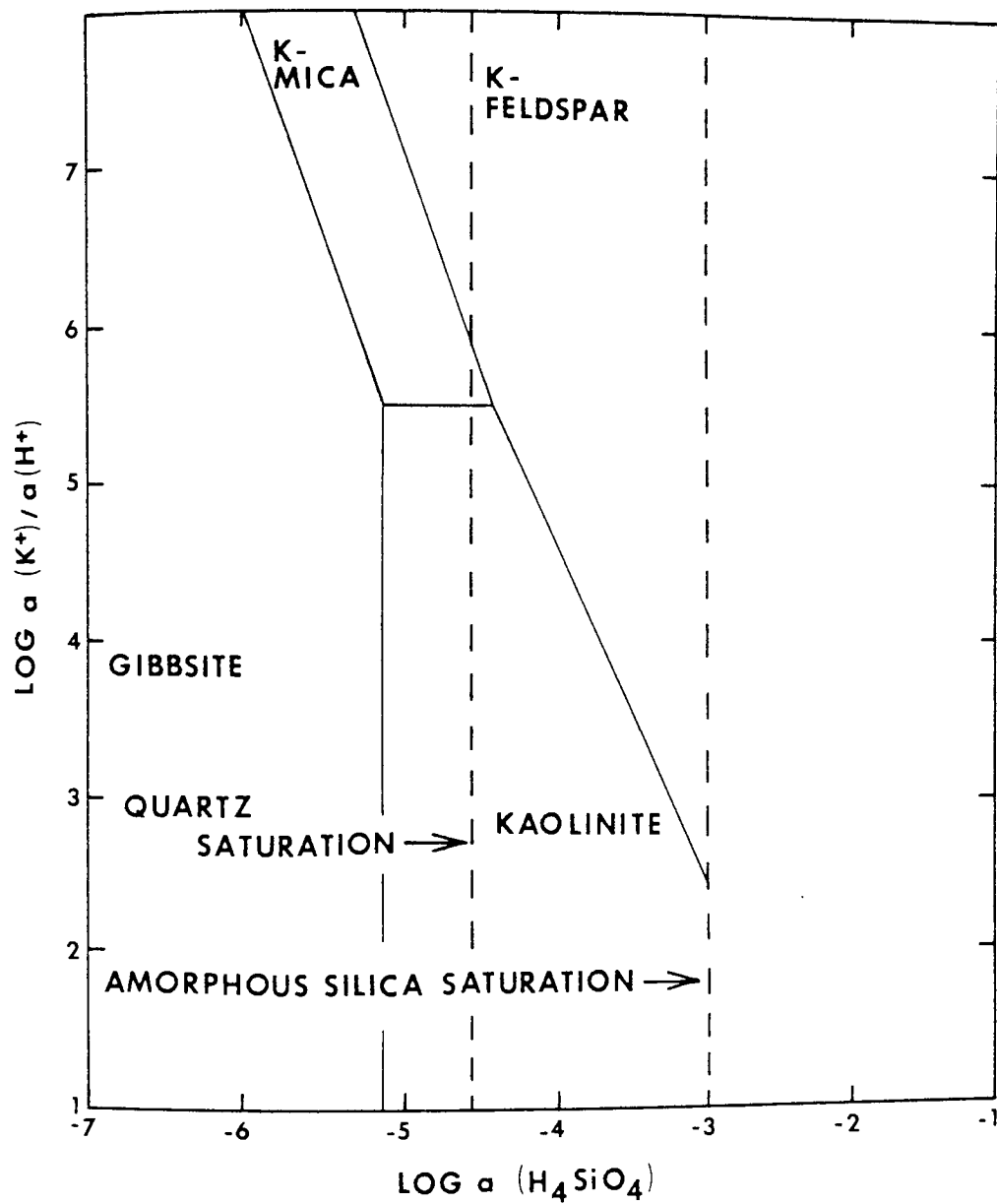


Fig.4.4 Combination diagram showing the relationships between K-mica, K-feldspar, and kaolinite in terms of K^+/H^+ ratio and H_4SiO_4 activity (after Helgeson et al. 1969).

ratio and H_4SiO_4 activity; higher K^+/H^+ ratio and/or H_4SiO_4 activity would favour authigenic K-feldspar precipitation. Zoned overgrowths are due to local concentration of Na^+ and Ba^{++} ions. Dissolution of the K-feldspar overgrowths and subsequent replacement by illite resulted from lowering of the K^+/H^+ ratio and must have brought the interstitial solution into equilibrium with illite. As a result the second generation of illite was precipitated. Mixed-layer illite-montmorillinite may have formed with or after the illite by local chemical changes, or it may represent an alteration product of illite. Kaolinite precipitated later as pore filling during later stages of diagenesis where K^+/H^+ was still low.

The formation of authigenic haematite seems to have happened simultaneously over a long period of time. The ultrafine pigmentary haematite resulted from the precipitation of ferric oxyhydroxides is the main colouring agent in the Triassic sandstones. The behaviour of precipitated ferric oxyhydroxides is best described in terms of Eh and pH (Whittemore and Langmuir, 1975). This is best represented by the Eh-pH diagram for the system $\text{Fe} - \text{H}_2\text{O} - \text{O}_2 - \text{CO}_2$ (Fig. 4.5) which shows the stability fields of solids and predominant ionic species. In an oxidizing interstitial environment high Eh and/or high pH favours the precipitation of ferric oxyhydroxides. The haematite pigment is present as clay and grain coatings, in the latter case two generations of pigment were recognized in the Kidderminster Formation, one of

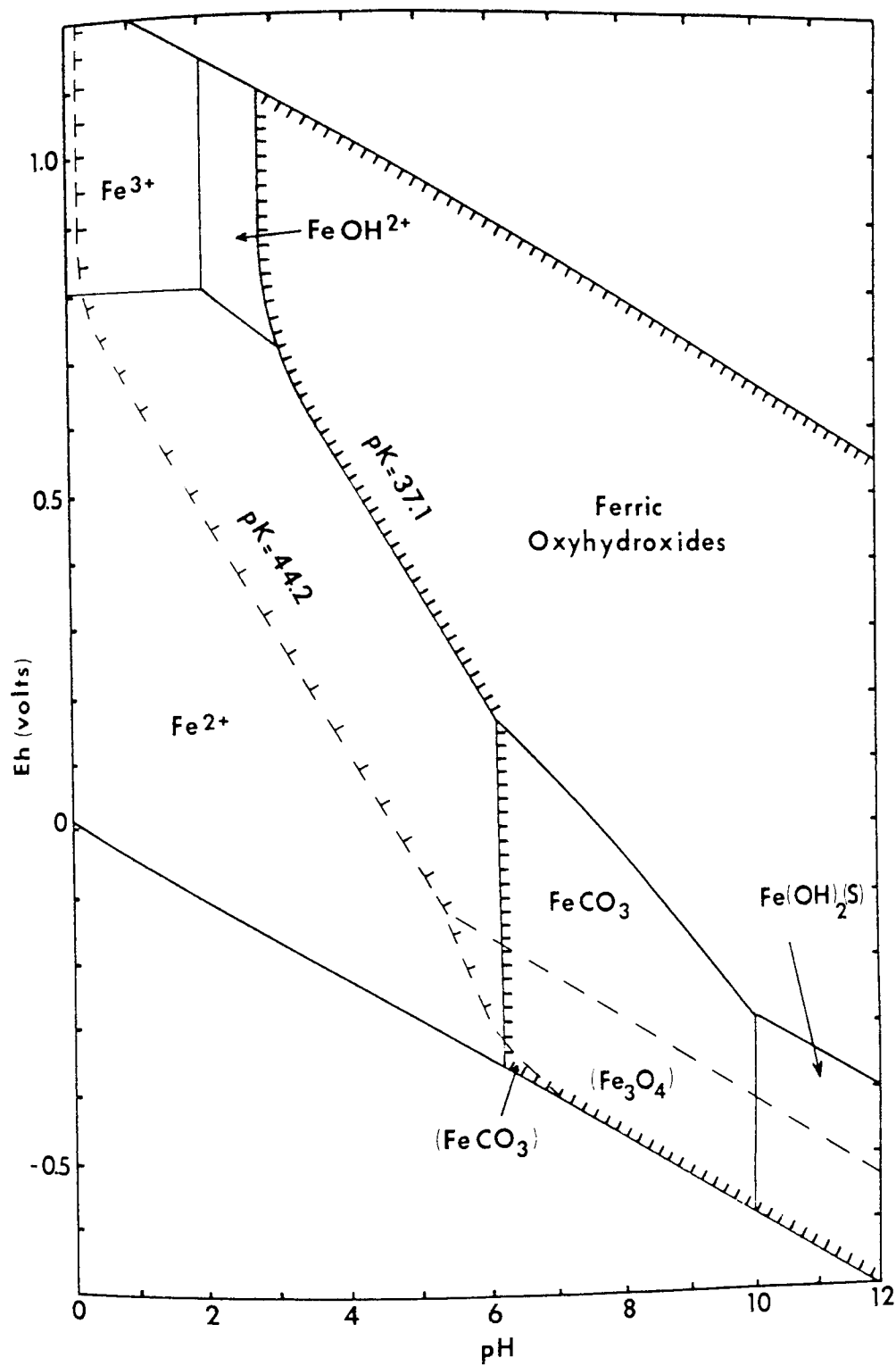


Fig.4.5 Eh-pH diagram for the system Fe-H₂O-O₂-CO₂ (after Whittemore and Langmuir, 1975).

early diagenetic origin coating the detrital grains, the other of late diagenetic origin coating the authigenic K-feldspar overgrowths. Microcrystalline haematite platelets have formed after the second generation of authigenic illite. Microcrystalline haematite and large euhedral haematite overgrowths are abundant in the Bromsgrove Sandstone Formation and scarcely found in the rest of the Triassic sandstones. No textural relationship was found between the large euhedral haematite overgrowths and the other authigenic minerals except that it was formed after the haematite cement which is found localized in small patches. Pseudomorphism of biotite by haematite seems to have occurred at later stages of diagenesis, well after compaction.

Secondary reduction zones are abundant in the Bromsgrove Sandstone Formation and the Mercia Mudstone Group. In the Bromsgrove sandstones they are represented by more or less continuous green horizons and attributed to chlorite which was formed under reducing conditions. In the Mercia Mudstone Group reduction spots or mottling are abundant in some of the sandstone horizons. It is generally attributed to an early post-depositional reduction of ferric oxyhydroxide by residual organic material (Sherlock, 1949, Trotter, 1953), but the presence of martites with relict maghemite in these sandstones may indicate that they have not been completely oxidized in the first place, or subjected to reducing

conditions at early stages of diagenesis before being completely oxidized (see also Durrance et al. 1978).

Authigenic titanium oxides in the form of overgrowths around the detrital titanium oxide and ilmenohaematite grains or as discrete crystals filling the pore space are probably precipitated from titanium ions released into the intrastratal solution as a result of titanomagnetite martitization.

Carbonate cement was the last phase to precipitate and compositional changes in the interstitial solution are indicated by the presence of ferroan calcite zones in the calcite cement of the Bromsgrove Sandstone and Cannock Chase Formations. This may reflect fluctuation in the abundance of Fe^{++} ions in the interstitial solution and also fluctuating redox conditions.

Calcite and dolomite cements have partially to completely replaced many of the detrital grains. This might be attributed to supersaturation of the interstitial solution with Ca^{++} , Mg^{++} and carbonate ions. In the Arden sandstones the dolomite cement was followed by calcite cement in the form of localized patches of large crystals of calcite. These calcite crystals show evidence of dissolution, indicating further changes in the chemistry of the interstitial solution, probably representing the latest diagenetic changes and possibly having taken place in recent times.

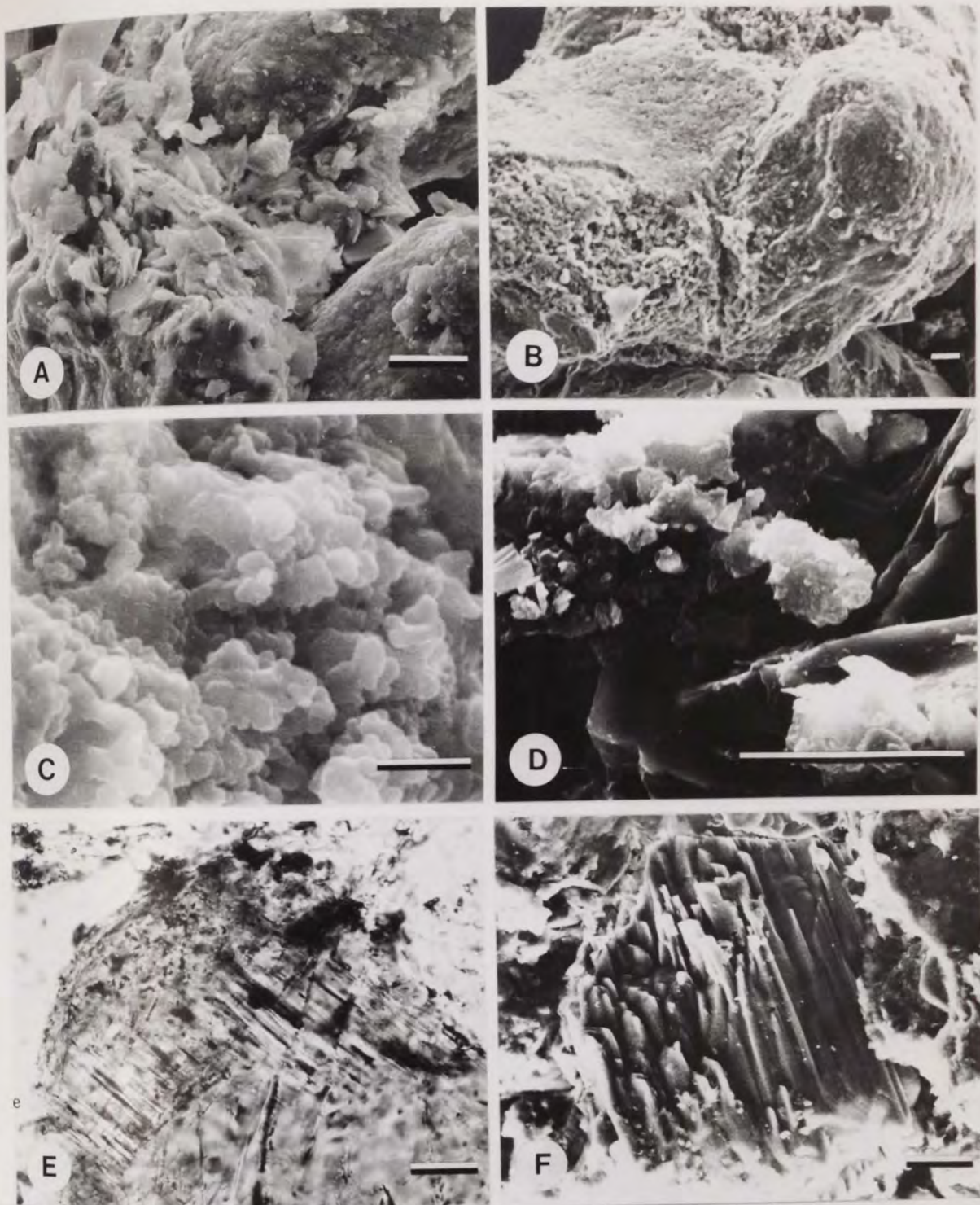


PLATE 4.1

- A. Thin flakes of mechanically infiltrated clay oriented parallel to grain surface, SEM photomicrograph, Bromsgrove Sandstone Fm.
 - B. Broken clay skin coating framework grain, SEM photomicrograph, Bromsgrove Sandstone Fm.
 - C. Mechanically infiltrated clay platelets oriented parallel to grain surface, SEM photomicrograph, Bromsgrove Sandstone Fm.
 - D. Clay platelets of different sizes oriented parallel to grain surface, SEM photomicrograph, Bromsgrove Sandstone Fm.
 - E. Detrital hornblende with needle-shaped relicts as a result of dissolution, PPL, Kidderminster Fm.
 - F. Partially dissolved plagioclase grain, SEM photomicrograph, Bromsgrove Sandstone Fm.
- Scale bar = 20 μ m

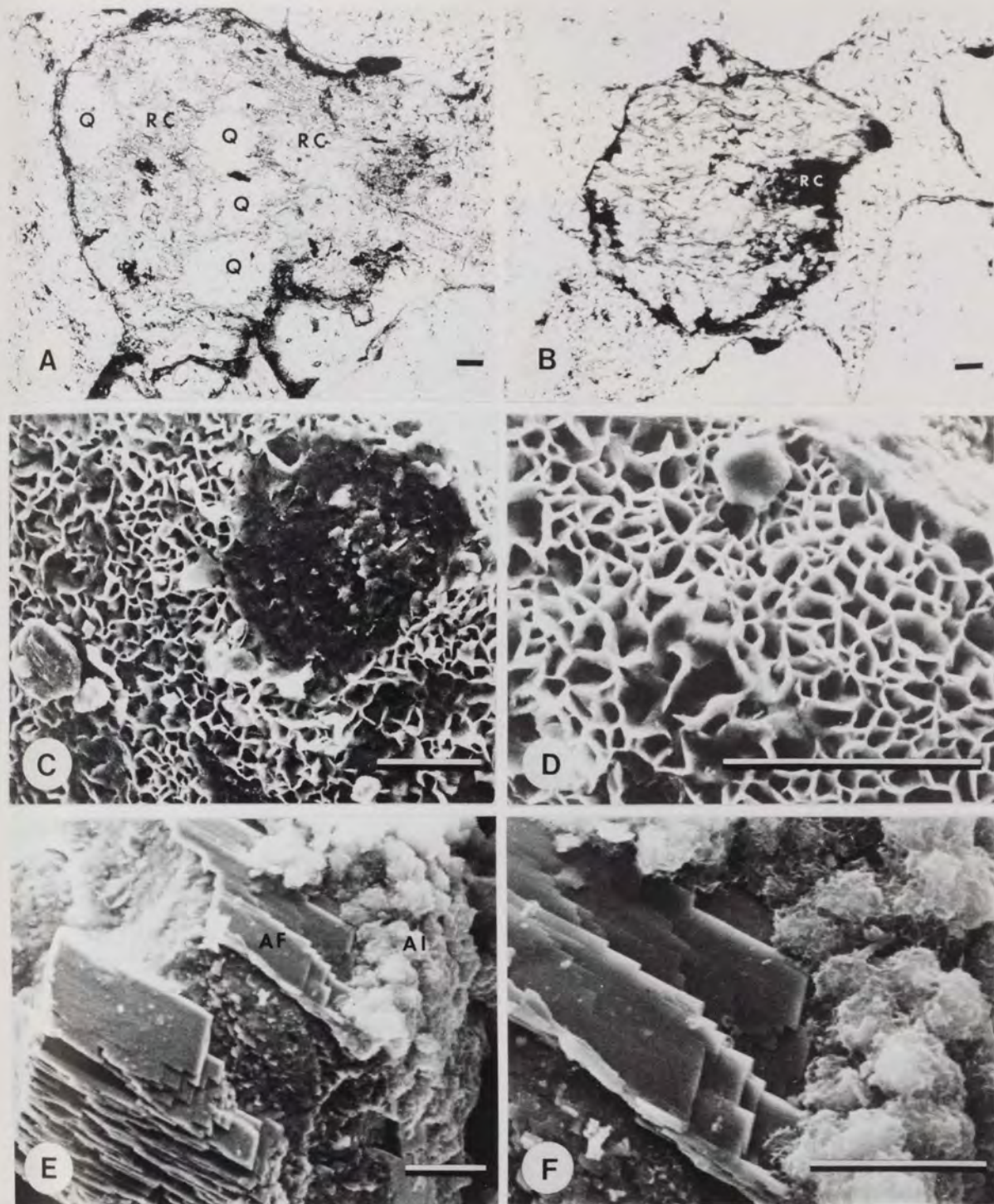


PLATE 4.2

- A. Polycrystalline quartz (Q) partially replaced by clay (RC) along intercrystalline boundaries, PPL, Kidderminster Fm.
- B. Metamorphic rock fragment peripherally replaced by clay (RC), PPL, Kidderminster Fm.
- C. Authigenic illite coating detrital grain surface and absent from areas of grain contacts, SEM photomicrograph, Kidderminster Fm.
- D. Authigenic illite as grain coating showing irregular flakes oriented perpendicular to grain surface forming boxwork texture, SEM photomicrograph, Wildmoor Sandstone Fm.
- E. Authigenic illite (AI) as an interstitial matrix superimposed on authigenic K-feldspar (AF) which has been previously dissolved, SEM photomicrograph, Bromsgrove Sandstone Fm.
- F. Enlargement of E showing the spherical aggregates of authigenic illite.

Scale bar = 30 μm

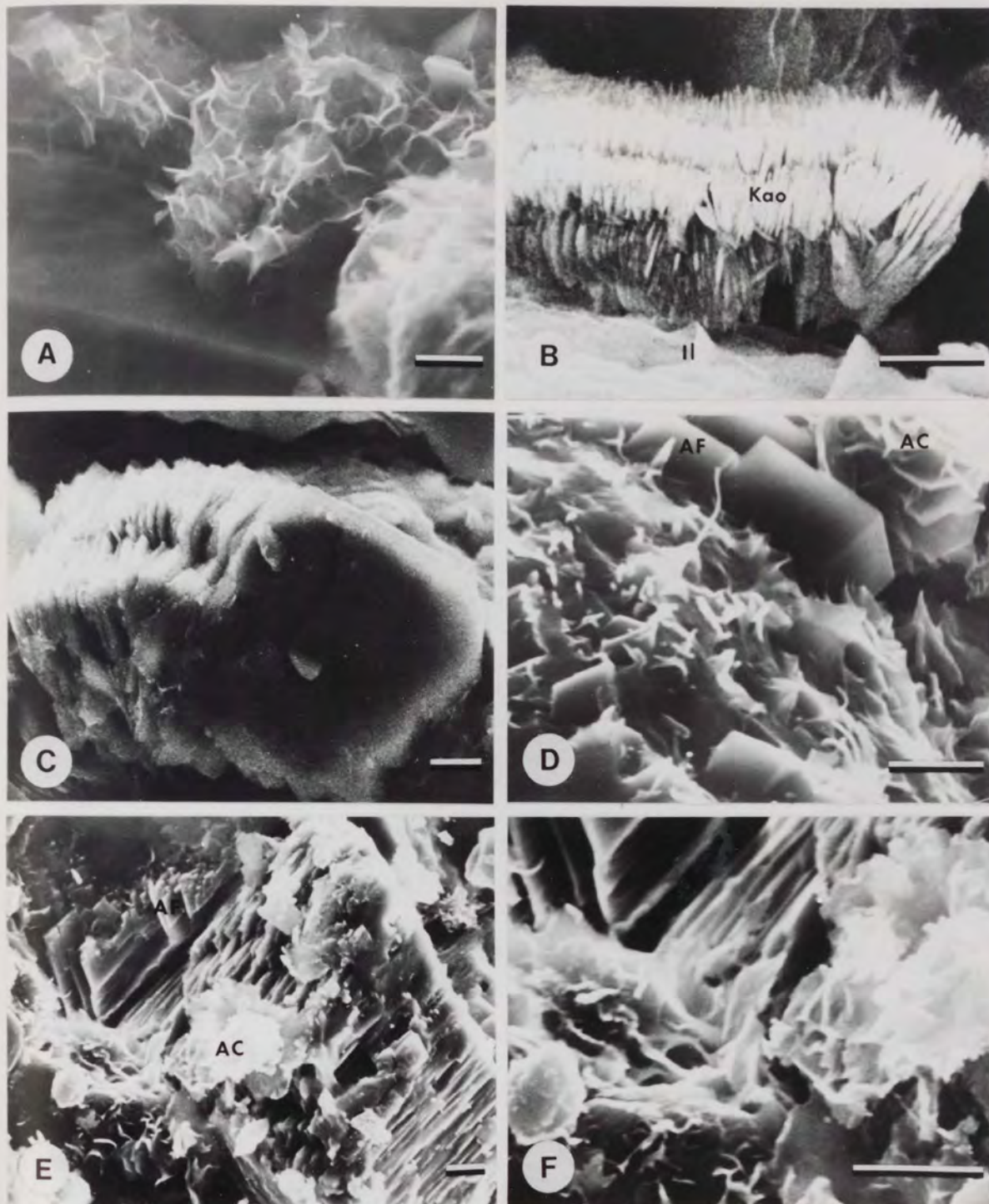


PLATE 4.3 - All SEM photomicrographs

- A. Spherical aggregates of authigenic illite filling pore space, Bromsgrove Sandstone Fm.
- B. Vermicular authigenic kaolinite (Kao) filling pore space, framework grain surface is coated with illite (Il), Wildmoor Sandstone Fm.
- C. Stacked pseudo-hexagonal plates of authigenic kaolinite displaying a vermicular habit, Wildmoor Sandstone Fm.
- D. Authigenic mixed-layer illite-montmorillonite (AC) superimposed on authigenic K-feldspar (AF), Bromsgrove Sandstone Fm.
- E. Authigenic mixed-layer illite-montmorillonite (AC) superimposed on dissolved authigenic K-feldspar (AF), Bromsgrove Sandstone Fm.
- F. Enlargement of E showing clay flakes curling away from grain surface due to dehydration.

Scale bar = 5 μ m.

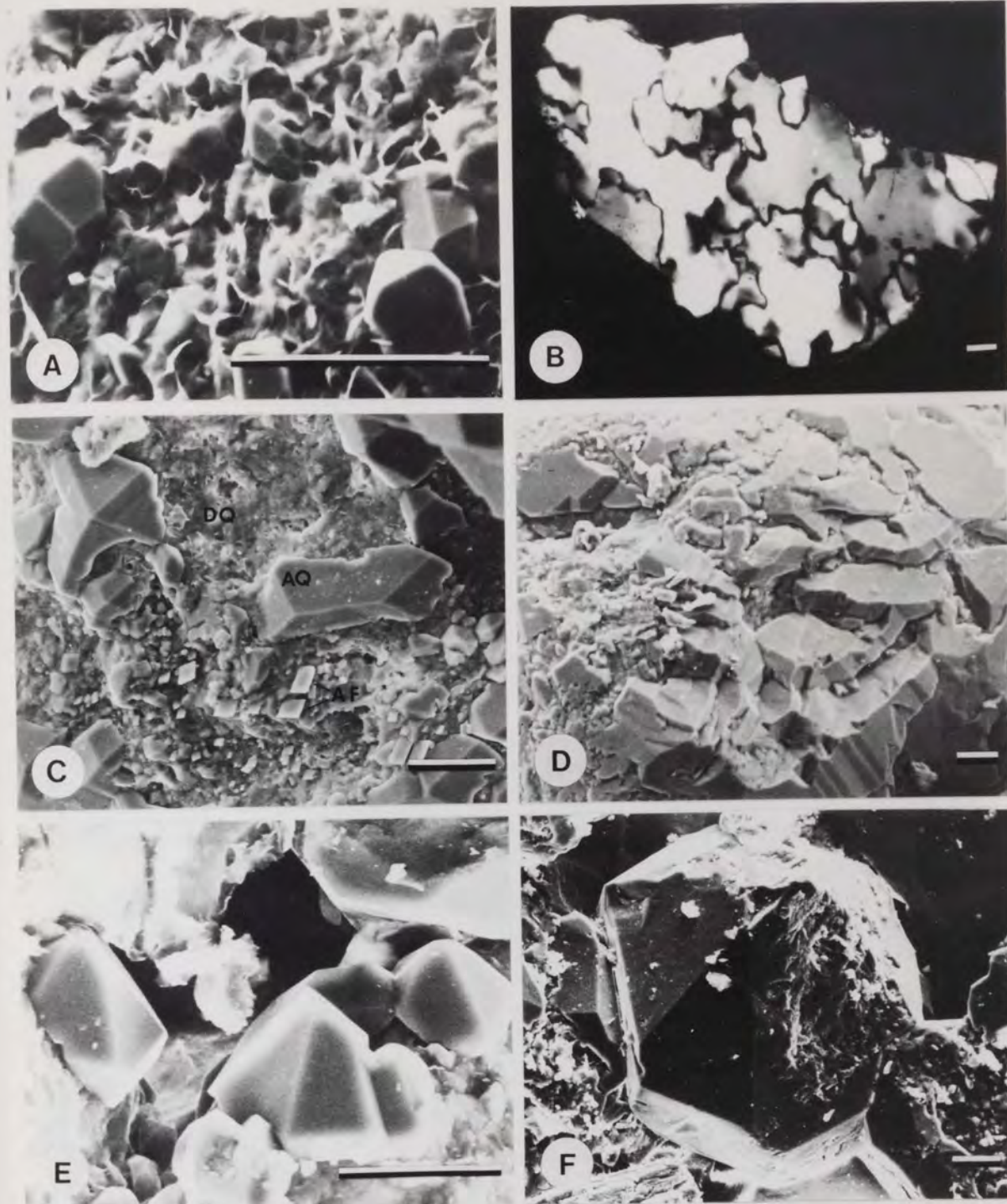


PLATE 4.4

- A. Crystalline projections of authigenic quartz developed on the surface of a detrital quartz grain coated with authigenic illite, SEM photomicrograph, Bromsgrove Sandstone Fm.
 - B. The orientation of the authigenic crystalline projections corresponds to the different orientations of the individual crystals of a detrital polycrystalline quartz, XN, Cannock Chase Fm.
 - C. Different orientations of authigenic quartz (AQ) on the surface of a polycrystalline detrital quartz (DQ). Authigenic K-feldspar (AF) is also present, SEM photomicrograph, Bromsgrove Sandstone Fm.
 - D. Anastomosing interconnected network of authigenic quartz overgrowth, SEM photomicrograph, Bromsgrove Sandstone Fm.
 - E. Concentration of large oriented crystalline projections of authigenic quartz, SEM photomicrograph, Bromsgrove Sandstone Fm.
 - F. Simple complete crystalline projection of authigenic quartz, SEM photomicrograph, Arden Sandstone Member.
- Scale bar = 20 μm

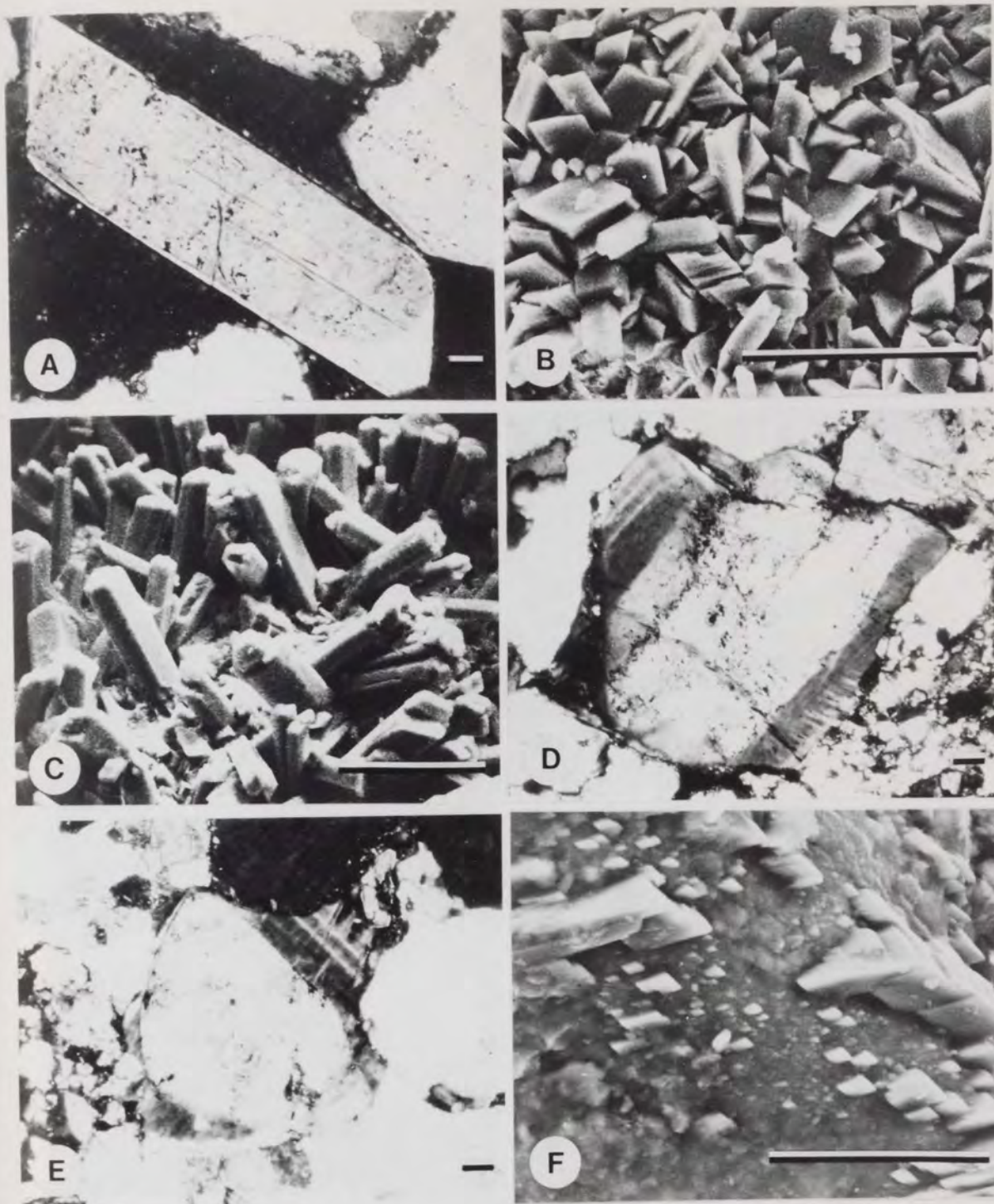


PLATE 4.5

- A. Euhedral authigenic K-feldspar overgrowth surrounding detrital feldspar grain, XN, Bromsgrove Sandstone Fm.
 - B. Cluster of whole authigenic K-feldspar crystals filling pore space, SEM photomicrograph, Bromsgrove Sandstone Fm.
 - C. Authigenic K-feldspar crystals elongated along the c-axis, SEM photomicrograph, Kidderminster Fm.
 - D. Zoned euhedral K-feldspar overgrowth, XN, Bromsgrove Sandstone Fm.
 - E. Zoned K-feldspar overgrowth with hacksaw terminations, XN, Bromsgrove Sandstone Fm.
 - F. Small oriented rhombohedral crystals of authigenic K-feldspar with adularia habit developed on the surface of a detrital feldspar grain, SEM photomicrograph, Bromsgrove Sandstone Fm.
- Scale bar = 30 μ m

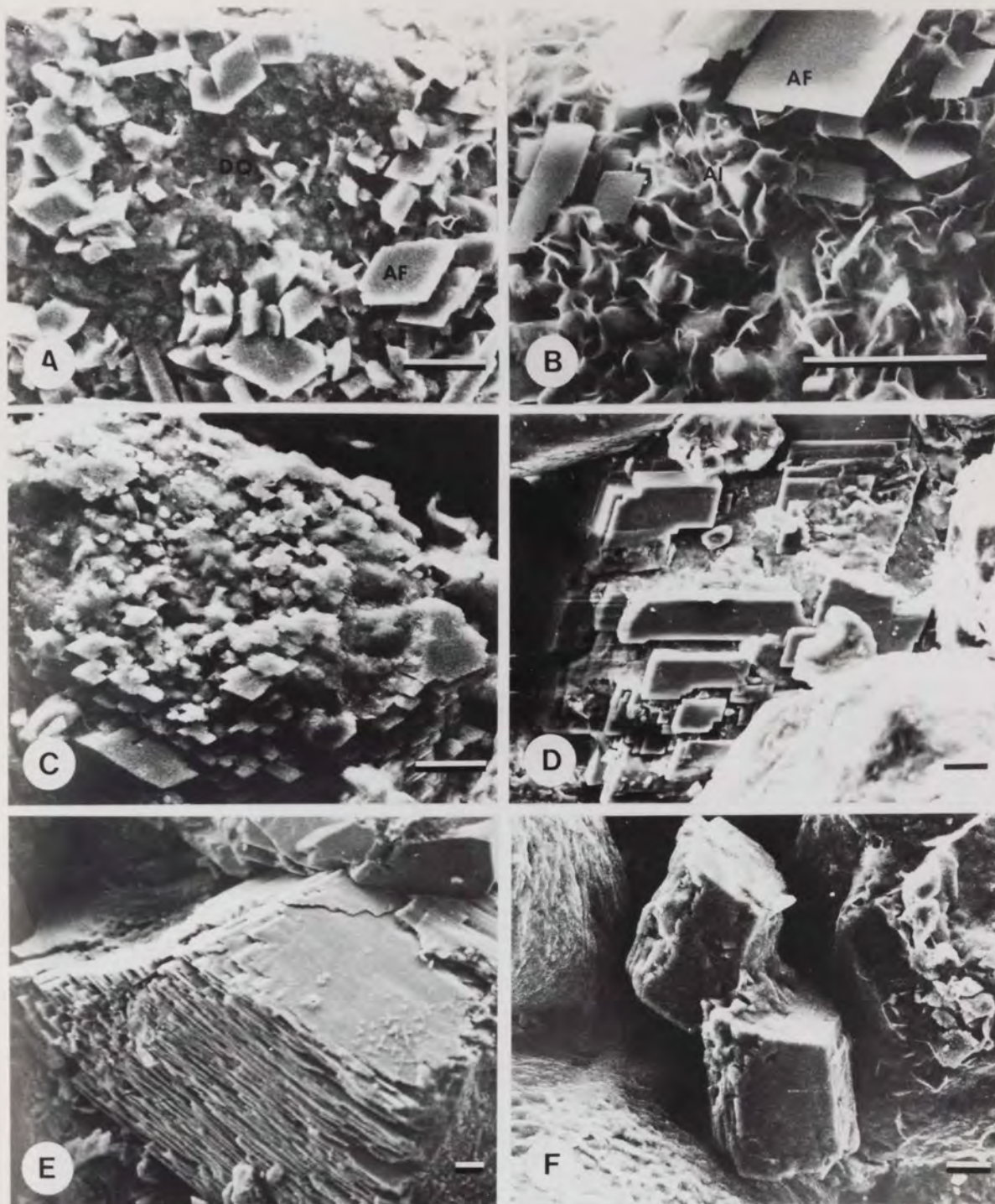


PLATE 4.6- All SEM photomicrographs.

- A. Rhombohedral crystals of authigenic K-feldspar (AF) developed on the surface of a detrital quartz grain (DQ), Kidderminster Fm.
 - B. Authigenic K-feldspar (AF) developed on a grain surface coated with authigenic illite (AI), Bromsgrove Sandstone Fm.
 - C. Merging and stacking of authigenic K-feldspar crystals forming larger crystal faces, Cannock Chase Fm.
 - D. Further development of authigenic K-feldspar producing large crystal faces, Bromsgrove Sandstone Fm.
 - E. Large euhedral authigenic K-feldspar overgrowth completely surrounding the detrital grain, Bromsgrove Sandstone Fm.
 - F. Rhombic crystals of authigenic K-feldspar in which the (101) form is absent, Bromsgrove Sandstone Fm.
- Scale bar = 15 μ m

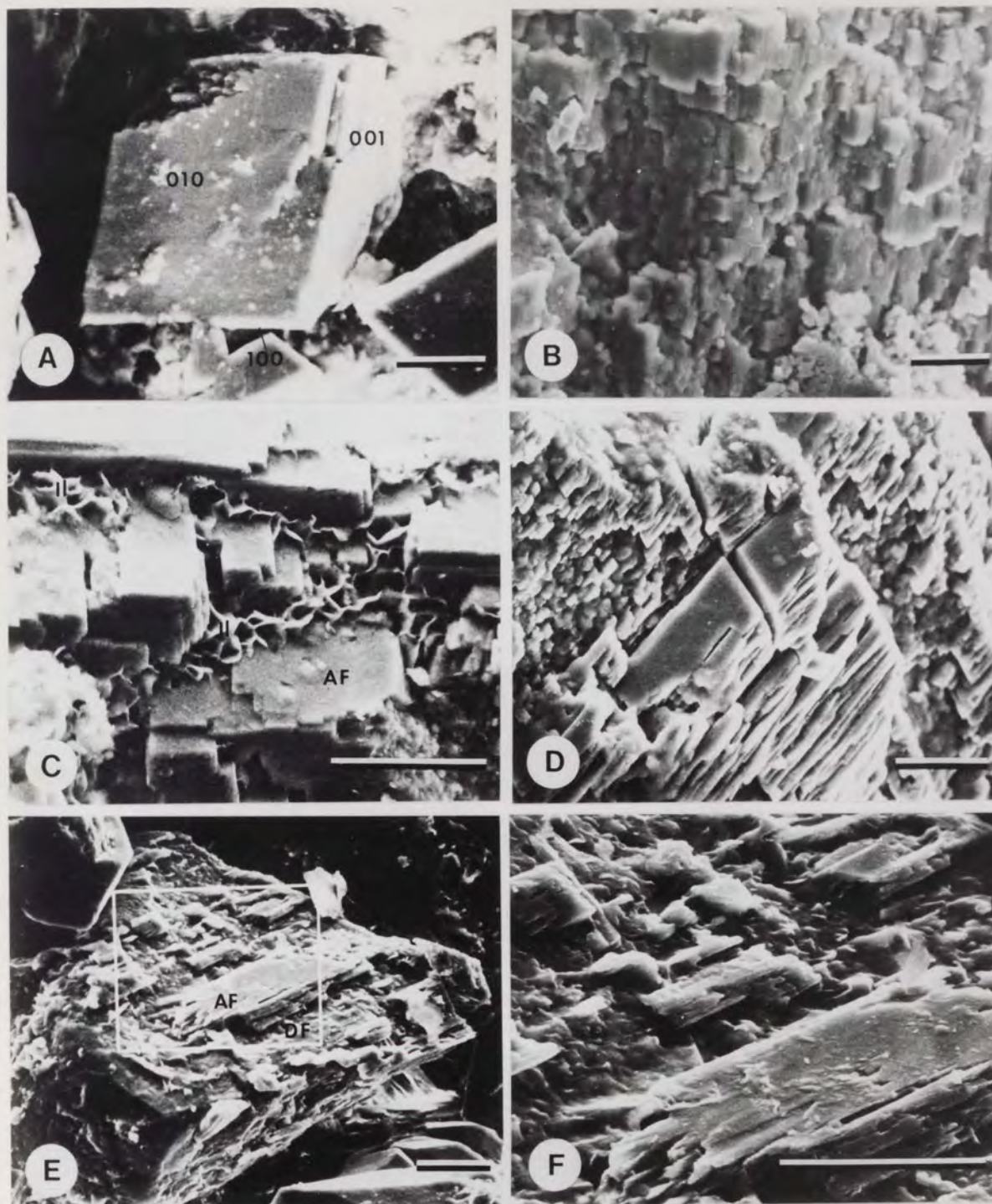


PLATE 4.7- All SEM photomicrographs

- A. Equally developed (100) and (001) forms giving the authigenic crystal a diamond shape, Bromsgrove Sandstone Fm.
 - B. Irregular crystal faces formed as a result of incomplete stacking of the rhombic units, Bromsgrove Sandstone Fm.
 - C. Illite (Il) replacing authigenic K-feldspar (AF), Polesworth Fm.
 - D. Preferential dissolution of authigenic K-feldspar along the cleavage traces, Bromsgrove Sandstone Fm.
 - E. Advanced stage of dissolution in which only relicts of authigenic K-feldspar (AF) remain attached to the detrital grain (DF), Arden Sandstone Member.
 - F. Enlargement of E showing relicts of dissolved authigenic K-feldspar.
- Scale bar = 20 μ m

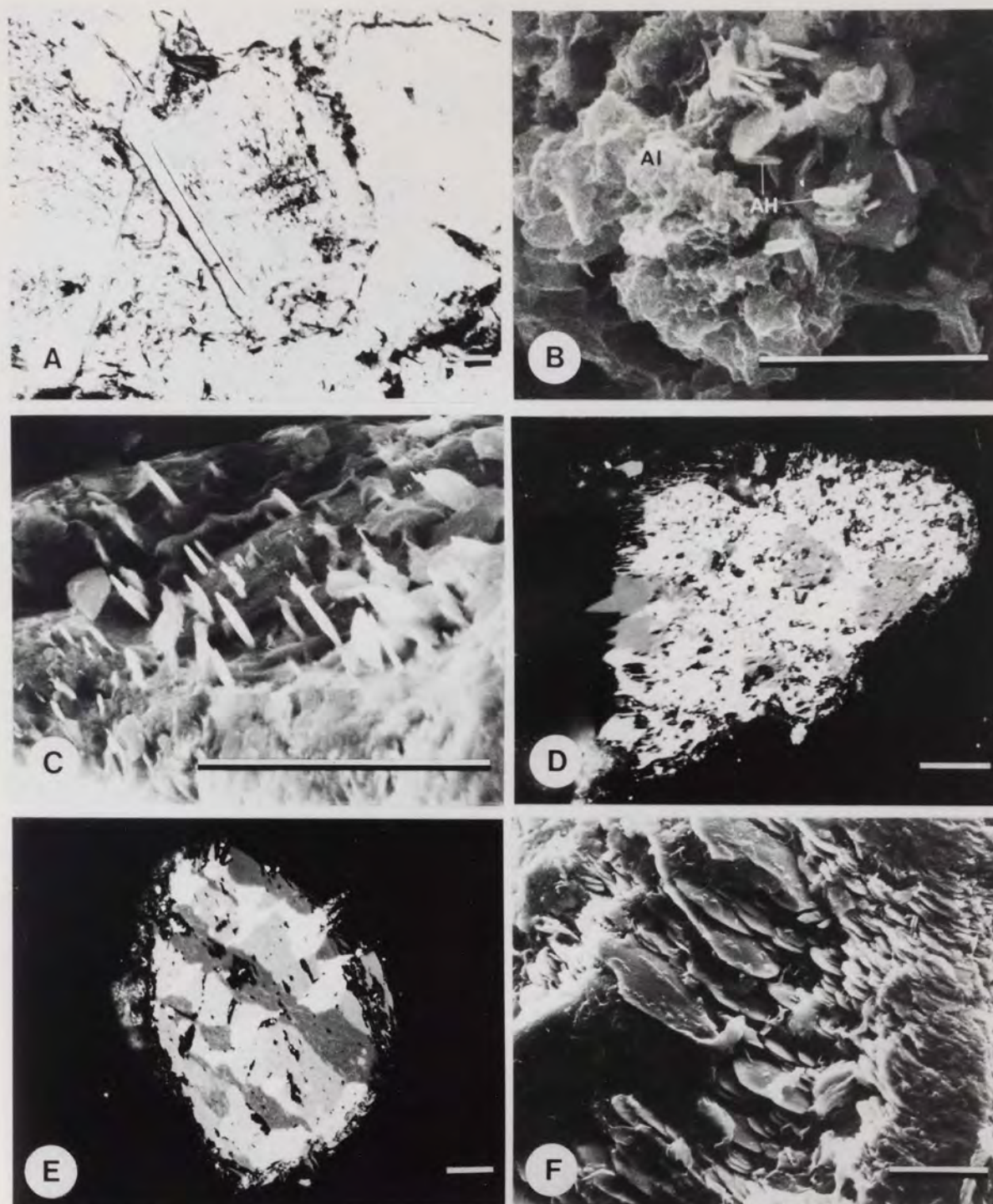


PLATE 4.8

- A. Haematite pigment coating both the detrital and authigenic K-feldspar, PPL, Kidderminster Fm.
 - B. Hexagonal platelets of authigenic haematite (AH) superimposed on authigenic illite (AI), SEM photomicrograph, Bromsgrove Sandstone Fm.
 - C. Flat rhombohedral crystals of authigenic haematite arranged perpendicular to the detrital grain surface, SEM photomicrograph, Bromsgrove Sandstone Fm.
 - D. Authigenic haematite overgrowth with different orientations reflecting different crystallographic orientations of a polycrystalline detrital haematite, reflected light, oil, PCP, Bromsgrove Sandstone Fm.
 - E. Authigenic haematite overgrowth on a martite grain reflecting the different crystallographic orientations of the host grain, reflected light, oil, PCP, Bromsgrove Sandstone Fm.
 - F. Merging and growth producing larger rhombohedral haematite crystals, SEM photomicrograph, Bromsgrove Sandstone Fm.
- Scale bar = 15 μm

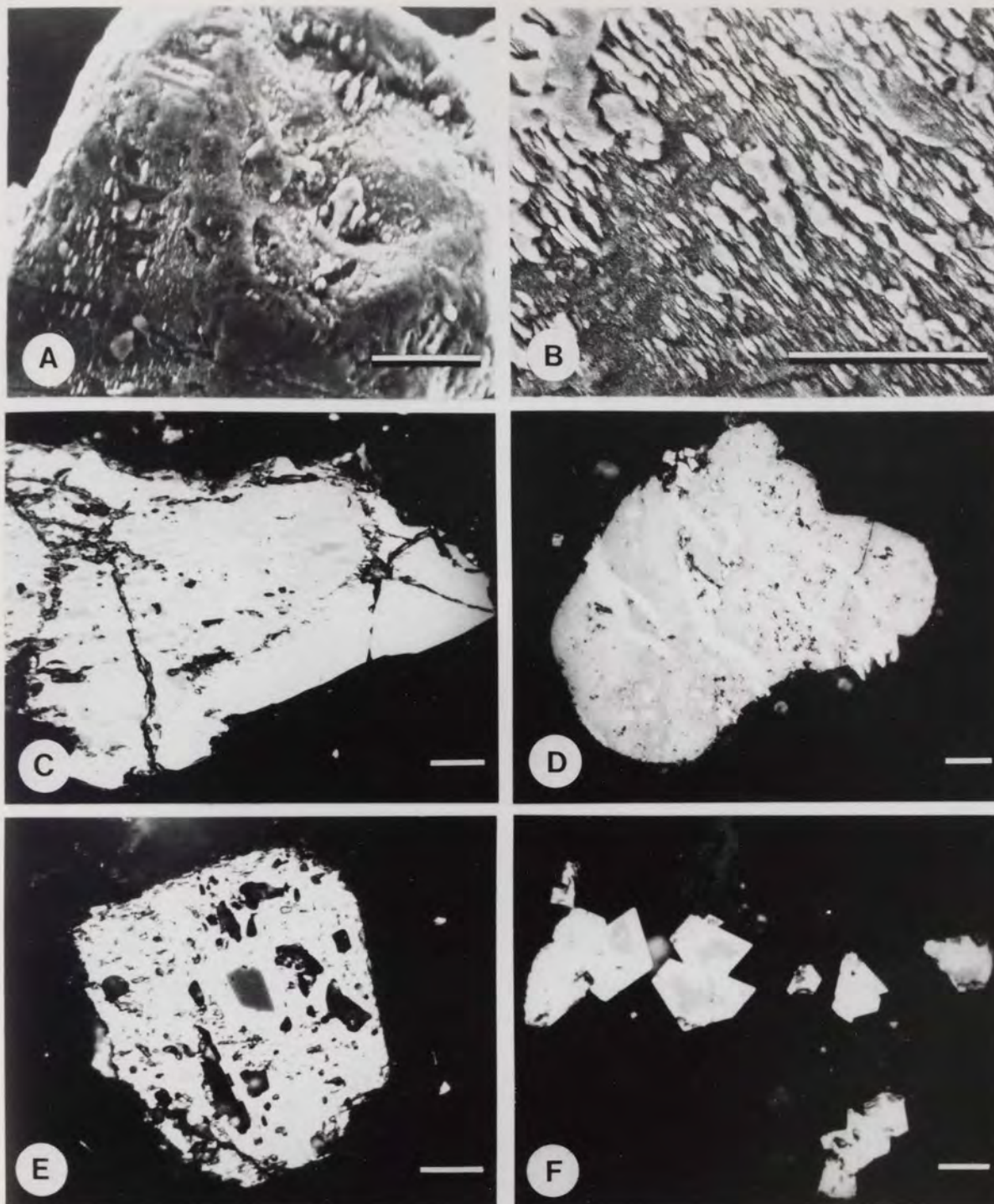


PLATE 4.9

- A. Authigenic haematite crystals arranged in parallel lines along the (111) planes, SEM photomicrograph, Bromsgrove Sandstone Fm.
 - B. Parallel ridge-like haematite overgrowth resulted from merging along the (111) planes, SEM photomicrograph, Bromsgrove Sandstone Fm.
 - C. Large euhedral haematite overgrowth surrounding a detrital haematite with exsolution discs of ilmenite, reflected light, oil, PPL, Bromsgrove Sandstone Fm.
 - D. Authigenic haematite filling fractures of a detrital ilmenohaematite, reflected light, oil, PPL, Bromsgrove Sandstone Fm.
 - E. Haematite with relict maghemite in the middle and the margin, reflected light, oil, PPL, Bromsgrove Sandstone Fm.
 - F. Haematite crystals formed after maghemite along the (111) planes, reflected light, oil, PPL, Wildmoor Sandstone Fm.
- Scale bar = 15 μ m

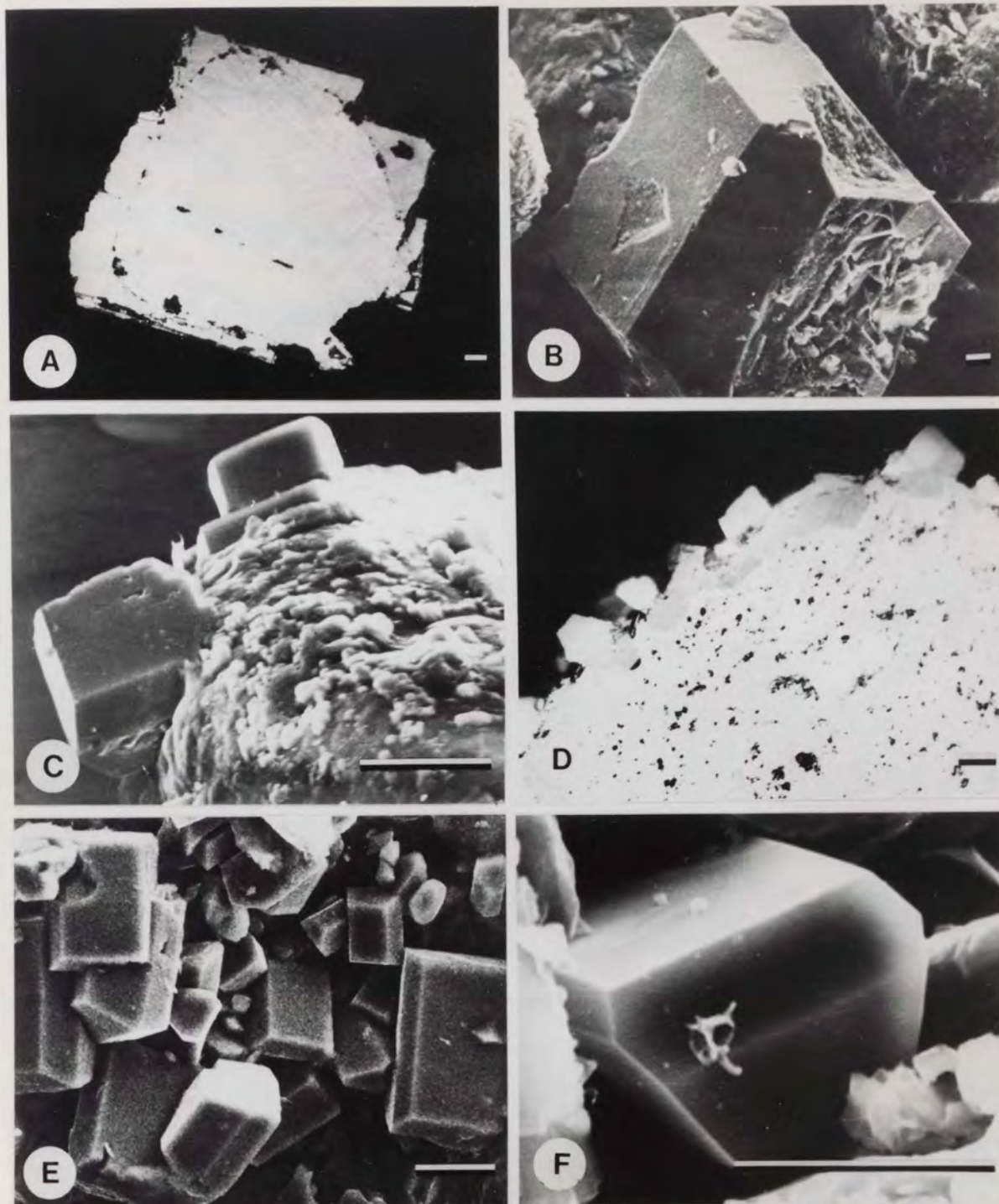


PLATE 4.10

- A. Detrital titanium oxide grain surrounded by authigenic overgrowth, reflected light, oil, PCP, Bromsgrove Sandstone Fm.
- B. Authigenic titanium oxide surrounding the detrital grain, SEM photomicrograph, Bromsgrove Sandstone Fm.
- C. Authigenic titanium oxide grown over a detrital ilmenohaematite, SEM photomicrograph, Bromsgrove Sandstone Fm.
- D. Detrital ilmenohaematite peripherally altered into titanium oxide which is also present as euhedral overgrowth, reflected light, oil, PCP, Bromsgrove Sandstone Fm.
- E. A cluster of authigenic titanium oxide crystals filling pore space, SEM photomicrograph, Wildmoor Sandstone Fm.
- F. Single crystal of authigenic titanium oxide within illite, SEM photomicrograph, Wildmoor Sandstone Fm.

Scale bar = 10 μ m

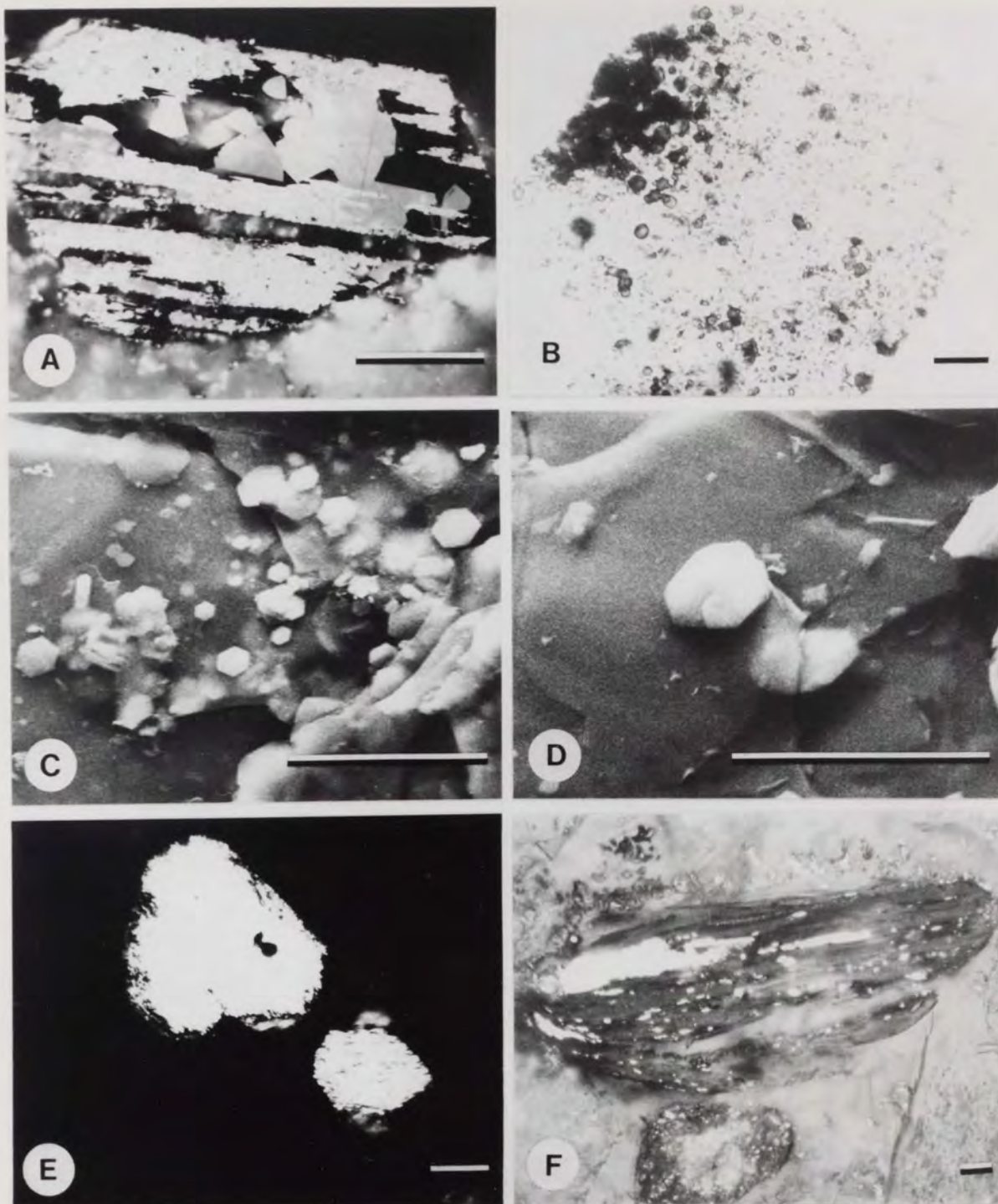


PLATE 4.11

- A. Authigenic titanium oxide crystals filling dissolution void in ilmenite which also shows signs of alteration into titanium oxide, reflected light, oil, PCP, Bromsgrove Sandstone Fm.
 - B. Translucent hexagonal haematite flakes developed along biotite cleavage plane, PPL, Bromsgrove Sandstone Fm.
 - C. Hexagonal haematite flakes on the surface of a biotite grain, SEM photomicrograph, Bromsgrove Sandstone Fm.
 - D. Enlargement of the hexagonal haematite flakes showing twinning, SEM photomicrograph, Bromsgrove Sandstone Fm.
 - E. Development of large pseudo-hexagonal sheets of haematite parallel to the biotite cleavage planes, reflected light, oil, PCP, Bromsgrove Sandstone Fm.
 - F. Complete haematite pseudomorph parallel to the cleavage planes, reflected light, oil, PCP, Bromsgrove Sandstone Fm.
- Scale bar = 15 μ m

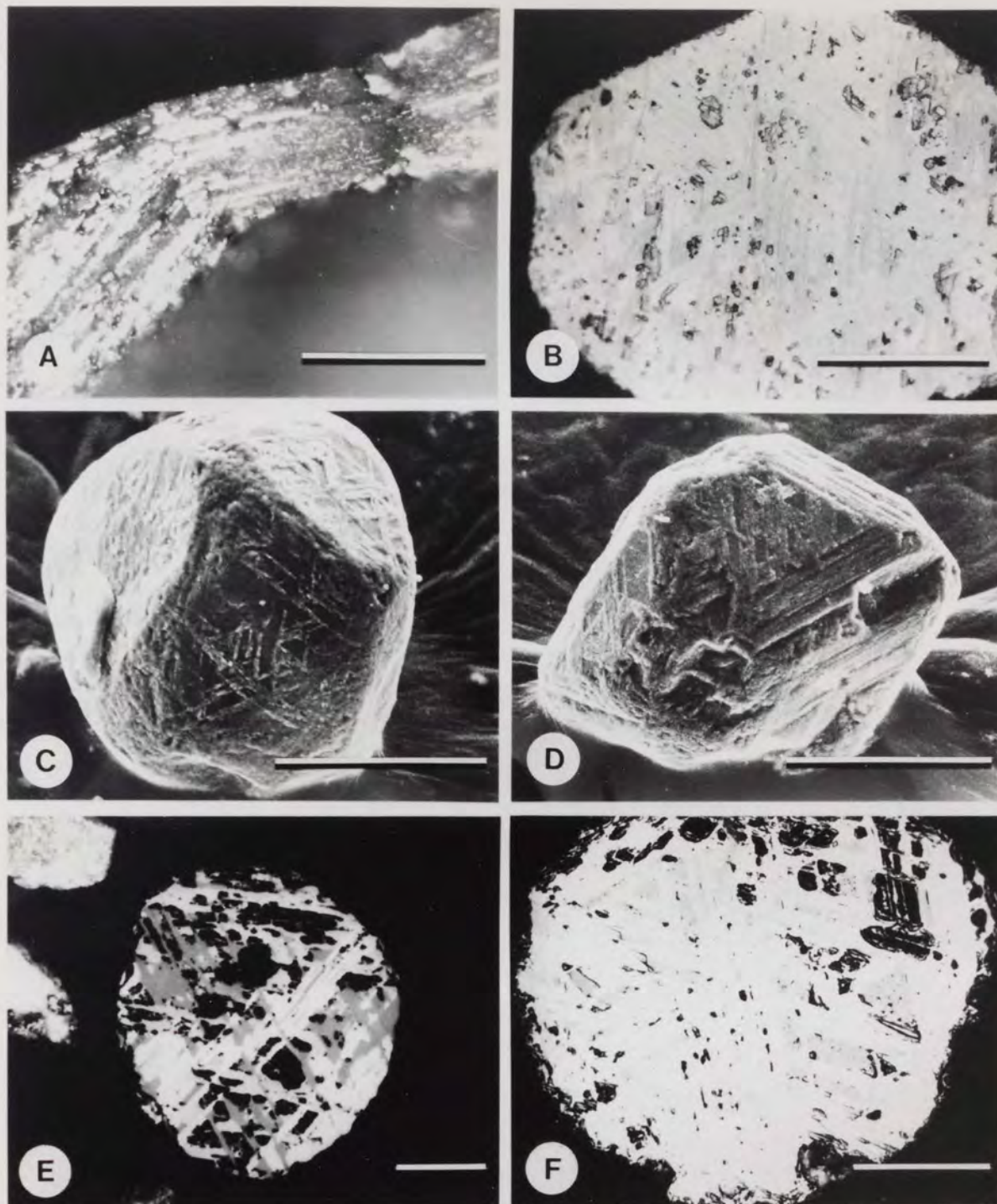


PLATE 4.12

- A. Partially pseudomorphosed haematite after biotite with the compacted part of the grain being less altered, reflected light, oil, PCP, Bromsgrove Sandstone Fm.
 - B. Martite showing triangular pattern of the octahedral (111) planes, reflected light, oil, PPL, Cannock Chase Fm.
 - C. Martite showing triangular pattern of alteration on the grain surface, SEM photomicrograph, Wildmoor Sandstone Fm.
 - D. Subangular martite grain also showing the triangular pattern of alteration, SEM photomicrograph, Poleworth Fm.
 - E. Well rounded martite showing clear polycrystallinity, reflected light, oil, PCP, Bromsgrove Sandstone Fm.
 - F. Martite with relicts of maghemite showing an earlier stage of martitization, reflected light, oil, PPL, Mercia Mudstone Group.
- Scale bar = 50 μ m

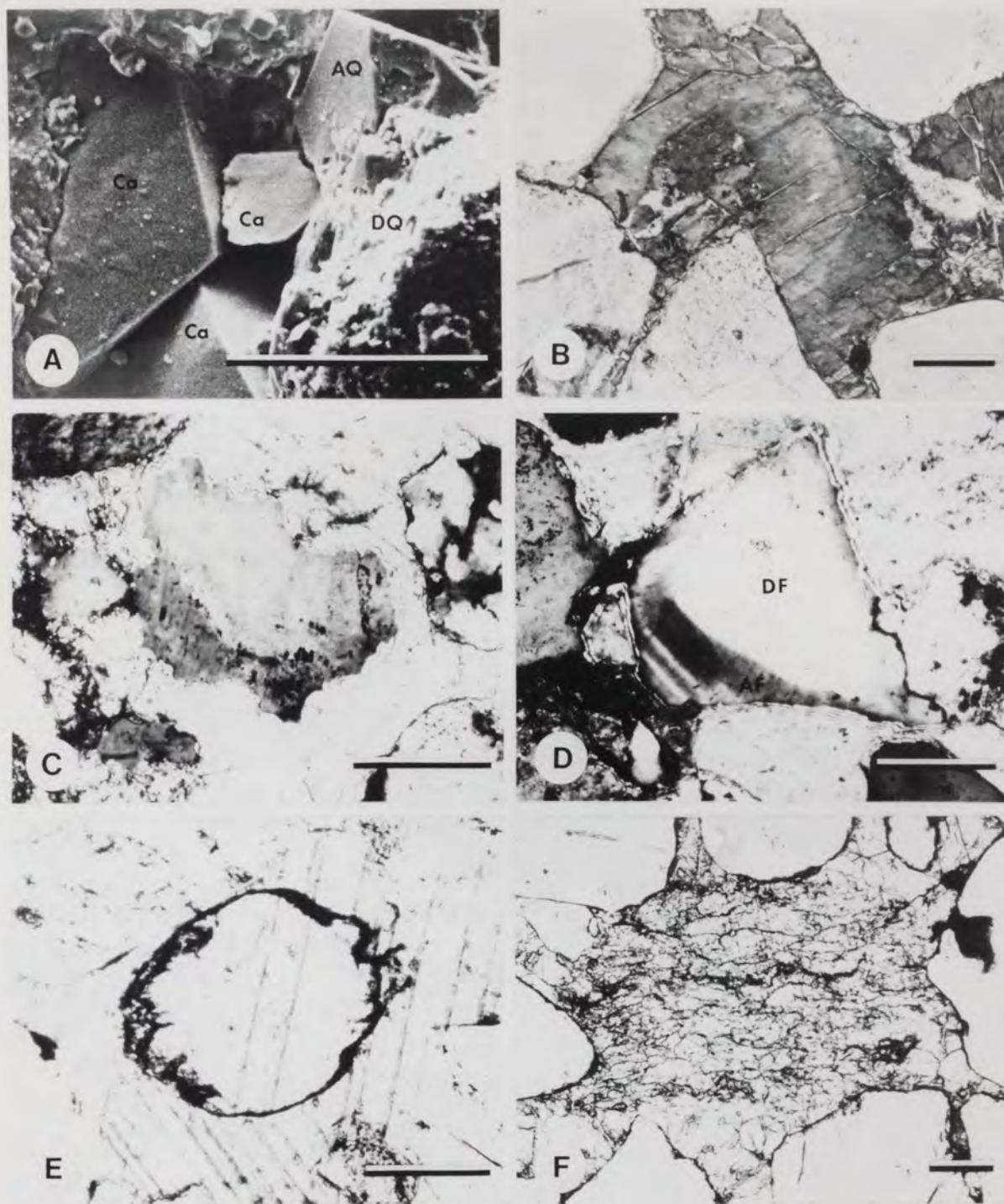


PLATE 4.13

- A. Calcite cement (Ca) as patchly distributed pore filling. Authigenic quartz (AQ) overgrowth on the detrital quartz (DQ) is also present, SEM photomicrograph, Arden Sandstone Member.
 - B. Stained calcite cement shows two zones of ferroan calcite, PPL, Bromsgrove Sandstone Fm.
 - C. Detrital quartz grain replaced by calcite cement, XN, Bromsgrove Sandstone Fm.
 - D. Detrital (DF) and authigenic (AF) K-feldspar corroded by calcite cement, XN, Bromsgrove Sandstone Fm.
 - E. Relict structure of a detrital grain preserved in the calcite cement, XN, Bromsgrove Sandstone Fm.
 - F. Relict structure of a metamorphic rock fragment preserved in calcite cement, PPL, Bromsgrove Sandstone Fm.
- Scale bar = 100 μ m

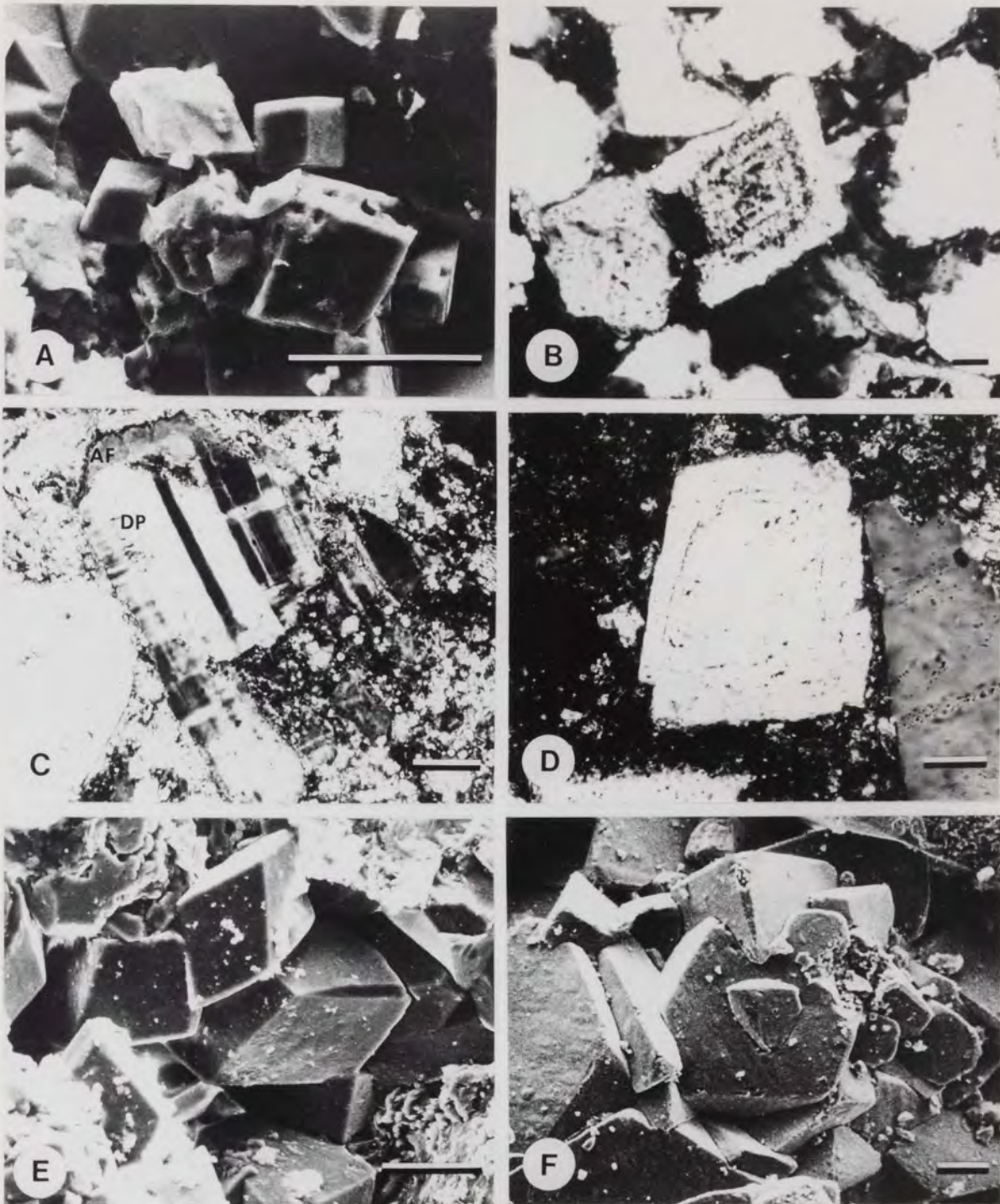


PLATE 4.14

- A. Recrystallized dolomite cement filling pore space, SEM photomicrograph, Arden Sandstone Member.
 - B. Zoned dolomite crystals in the cement, XN, Arden Sandstone Member.
 - C. Dolomite cement replacing the detrital plagioclase (DP) and corroding the authigenic K-feldspar (AF), XN, Arden Sandstone Member.
 - D. Dolomite replacing a detrital grain and leaving the relict structure preserved within the crystal, XN, Arden Sandstone Member.
 - E. Large rhombic calcite crystals filling pore space and succeeding the dolomite cement, SEM photomicrograph, Arden Sandstone Member.
 - F. Large twinned calcite crystals filling pore space as isolated patches of calcite within the dolomite cement, SEM photomicrograph, Arden Sandstone Member.
- Scale bar = 30 μm

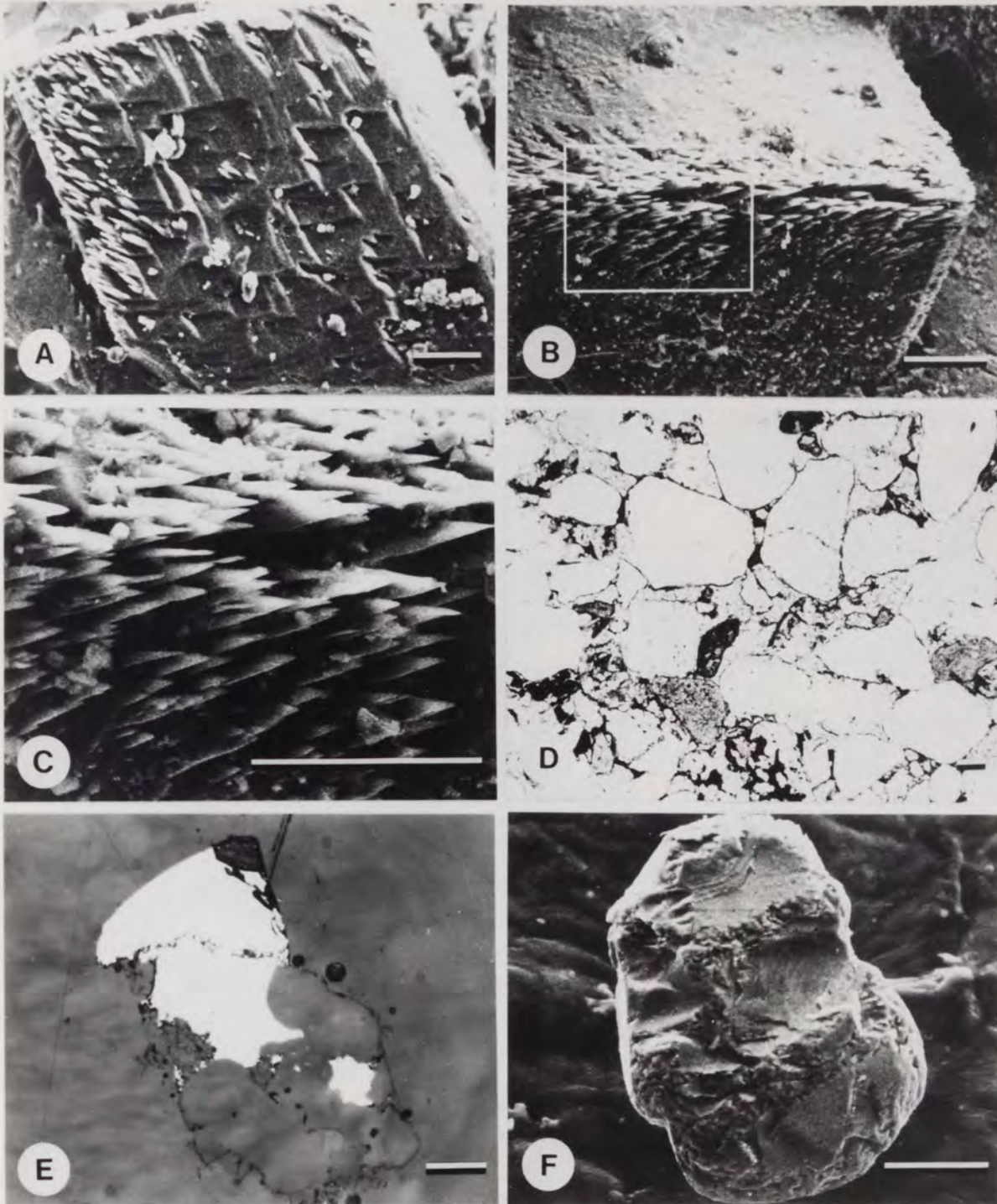


PLATE 4.15

- A. Calcite crystals with V-shaped etch marks and needle-shaped remnants on the corner, SEM photomicrograph, Arden Sandstone Member.
 - B. Calcite crystals with needle-shaped remnants at the corners, SEM photomicrograph, Arden Sandstone Member.
 - C. Enlargement of B showing the needle-shaped remnants resulting from dissolution.
 - D. Oxidized clay pellicles as a cement, PPL, Wildmoor Sandstone Fm.
 - E. Haematite cement and overgrowth, reflected light, oil, Bromsgrove Sandstone Fm.
 - F. Haematite cement as a local patch showing impressions of the different detrital grains attached to it, SEM photomicrograph, Bromsgrove Sandstone Fm.
- Scale bar = 30 μ m

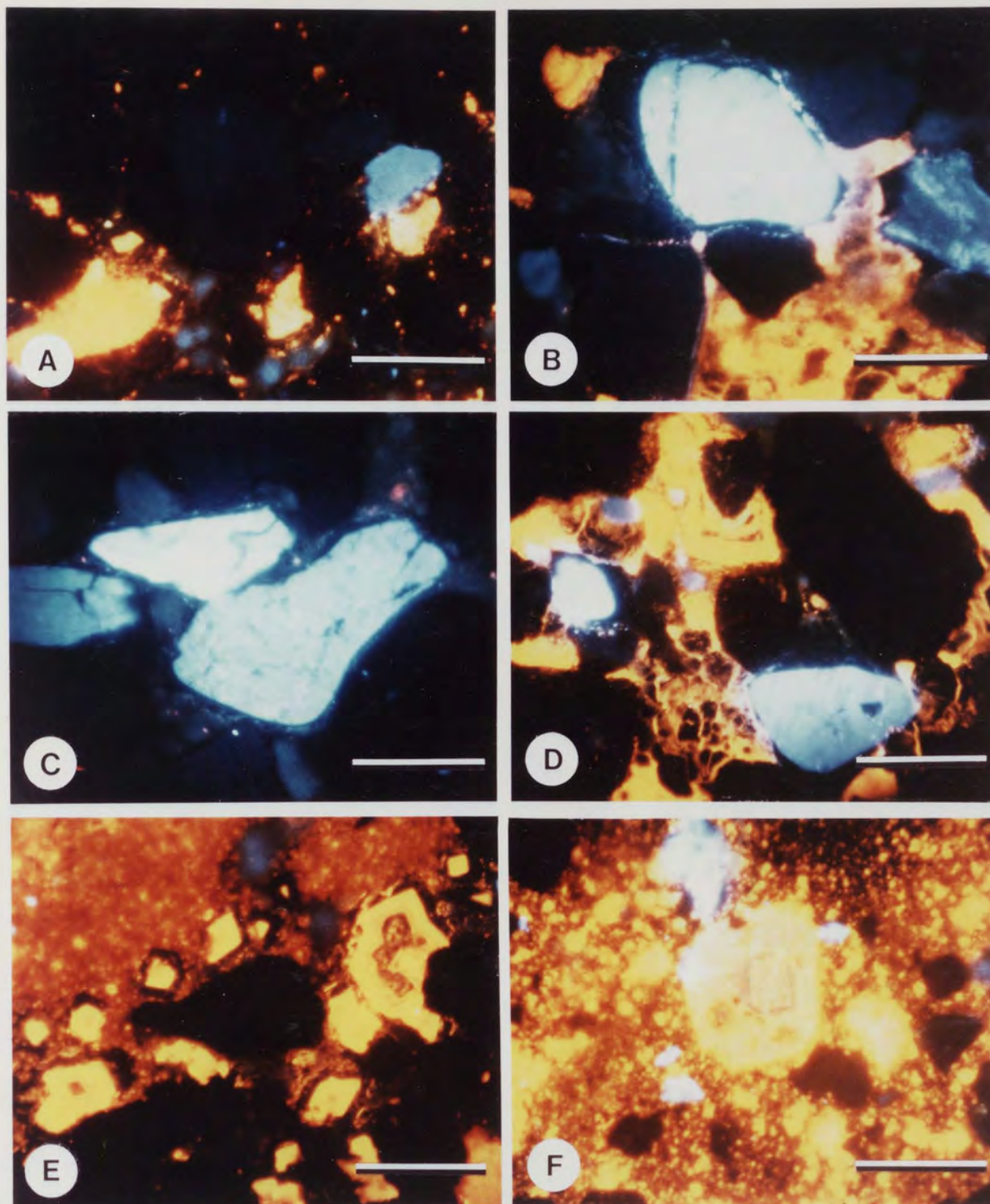


PLATE 4.16

- A. Blue-violet detrital quartz with non-luminescent authigenic overgrowth, Arden Sandstone Member.
 - B. Detrital feldspar with bright blue luminescence surrounded by non-luminescent authigenic K-feldspar. Blue luminescent detrital quartz is also present, Bromsgrove Sandstone Fm.
 - C. Detrital K-feldspar with bright blue luminescence with the middle grain having lighter blue colour due to higher Ba content. All grains are surrounded by non-luminescent overgrowth, Kidderminster Fm.
 - D. Zones of ferroan calcite cement shows bright yellow luminescence, brown quartz and feldspar with bright blue luminescence are also present, Bromsgrove Sandstone Fm.
 - E. Zoned dolomite crystals with bright yellow luminescence in orange yellow luminescent microcrystalline dolomite cement, Arden Sandstone Member.
 - F. Detrital dolomite grain surrounded by zones of dolomite with brighter yellow luminescence, Arden Sandstone Member.
- Scale bar = 200 μ m

CHAPTER 5

PALAEOMAGNETISM OF THE TRIASSIC RED BEDS

5.1 ROCK MAGNETISM

The study of the bulk magnetic properties of iron bearing rock forming minerals with specific investigation of the total magnetic properties is referred to as rock magnetism (Turner, 1980). The most important remanence carrying minerals are the magnetites, titanomagnetites, and their oxidized equivalent the titanomaghemites. Haematite is responsible for part of the remanence in some highly oxidized igneous rocks and carries the bulk of the remanence in many types of sediments, particularly red beds.

The fossil magnetism of a rock is termed the natural remanent magnetism (NRM). There are several specific types of NRM; the magnetization acquired by the cooling of magnetic minerals through their Curie point is referred to as thermoremanent magnetism (TRM). The alignment of magnetic particles during deposition or by rotation in unconsolidated sediments produces a detrital remanent magnetism (DRM). It is usual to distinguish between DRM and PDRM (post-depositional remanent magnetism). In the former, which is probably rare in nature, particles are aligned during suspension deposition and this alignment is retained during consolidation (King, 1955, Griffiths et al. 1960). In PDRM the alignment into the ambient

magnetic field occurs in wet sediments after deposition and is subsequently fixed or "locked in" during consolidation. PDRM appears to be the common process of magnetization in recent fine grained sediments (Verosub, 1977, Suttill, 1980).

Different factors affect the formation and preservation of DRM. These include:

1. Inclination error which arises when an aligned particle touches the bottom and rolls into the nearest depression (Griffiths et al. 1960).
2. The direction of magnetization is affected by the angle of the bedding plane (King, 1955).

The magnetization of sediments or rocks by the chemical growth of magnetic minerals is referred to as chemical remanent magnetism (CRM). CRM is the process through which the majority of red bed formations were magnetized (Collinson, 1965). There are a variety of diagenetic processes which produce CRM in red beds (Turner, 1980). These include:

1. The ageing of ferric oxyhydroxide.
2. The precipitation and growth from solution of ferric oxyhydroxide.
3. The intrastratal formation of ferric oxyhydroxide from silicate alteration.
4. The pseudomorphism of silicates by ferric oxyhydroxide.

5. Formation of authigenic iron oxide overgrowths.
6. In situ oxidation of magnetite.

These processes produce pigmentary fine particles of haematite as well as black specularite grains.

5.2 RED BED MAGNETISM

The age of magnetization of red beds is a direct result of the role of acquisition of remanence, and the complexity of such magnetization arises from the variable rate of remanence acquisition processes attributed to different discrete diagenetic changes (Turner, 1980). Three types of magnetization, A, B, and C were recognized in continental red beds by Turner (1979). Type A red beds retain features of magnetization acquired at the time or shortly after deposition, and usually contain a single non-viscous component of magnetization in individual specimens. Some formations may have discrete normal and reversed polarity zones and secular variations may be preserved. The age of this type of red beds is primarily Mesozoic, and particularly Triassic. The Moenkopi Formation (Triassic) of the Colorado Plateau and the St. Bees Sandstone (Triassic) of northern England are typical examples of type A red beds.

Type B red beds on the other hand, show more complicated magnetizations in which the individual specimens have composite magnetization. The individual components are often antiparallel, and intermediate directions result

from two or more components which are not antipodally opposed. Discrete zones of normal and reversed polarity are not usually found in this type of red beds. The Cenozoic red beds studied by Larson and Walker (1975) are examples of type B red beds.

Type C red beds are characterized by a magnetization consisting of a single well grouped directions. In this case a complete replacement of the original magnetization has occurred and it bears no relationship to the depositional age. Type C magnetization often formed after folding and in some cases the direction is so close to the present Earth's field that the NRM can be inferred to have formed in relatively recent times. The Late Precambrian red beds of the Longmyndian (Lomax and Briden, 1977) and the Navajo Sandstone (Jurassic) of the USA (Johnson, 1976) are good examples of type C red beds.

5.3 PALEOMAGNETISM OF THE BRITISH TRIASSIC RED BEDS

The magnetism of British Triassic red beds has been studied by many workers. They include: Clegg et al (1954), Creer (1957, 1959), Chamalaun (1963), Turner and Ixer (1977), Eustance (1981), and Turner (1981). Most of the early work was on the Mercia Mudstone Group. Turner and Ixer (1977) and Turner (1981) studied the St. Bees Sandstone of northern England and discussed the effect of different diagenetic processes on the development of magnetization.

In the USA there have been many detailed studies of

Triassic red beds and particularly the Moenkopi Formation. Baag and Helsley (1974) and Parucker et al. (1980), have stressed the importance of depositional processes in the remanence acquisition whereas Walker et al. (1981) have concluded that diagenetic processes are more important.

In addition to remanence components associated with changes in detrital or early diagenetic processes, the magnetic components carried by specularite must be interpreted bearing in mind the post-depositional changes which affect the specularite grains. As a result of these diagenetic changes specularites may carry secondary CRM components acquired during the transformation of titanomagnetite into haematite and the formation of authigenic haematite overgrowths (Turner and Ixer, 1977, Turner, 1981).

In the present study five textural groups of haematite were recognized in the Triassic sandstones of Central England. These include:

1. Finely crystalline haematite pigment which occurs mainly as grain coatings and in the matrix.
2. Clay-oxide pellicles and pellets.
3. Partially pseudomorphosed biotite by haematite.
4. Specularite grains with different textural varieties. These include mon and polycrystalline haematites, martites, and haematites with exsolution discs of ilmenite or rutile. All except for the haematite with exsolution discs of ilmenite may have formed

post-depositionally by replacement of detrital magnetites (Walker et al. 1981).

5. Authigenic haematite overgrowths and haematite cement.

5.4 INITIAL MEASUREMENTS

Fifteen field oriented samples representing different parts of the Sherwood Sandstone and Mercia Mudstone Groups were collected. Six cores the size of 2.5 x 2.5 cm cylinders were obtained from each sample. The NRM of these samples was initially measured using a "Digico" spinner magnetometer, and the directions were corrected for the local tectonic dip. The results show a steep inclination and grouping of the data in the NE and SW quadrants (Table 5.1, Fig. 5.1).

5.5 THERMAL DEMAGNETIZATION-PILOT SPECIMENS

Thermal demagnetization was used to separate the different magnetic components and to determine the role of pigment and specularite as NRM carriers. Experimental work shows that specularite is more stable than pigment during thermal demagnetization (Collinson, 1974, Tauxe et al. 1980). In continental red beds where the magnetization is carried by different textural phases of haematite of different grain sizes, magnetic components carried by the finest grain size i.e. the pigmentary haematite are removed lower in the blocking temperature spectrum, whereas coarser specularite grains became unblocked at higher

TABLE 5.1 SITE MEAN DIRECTIONS - INITIAL MEASUREMENTS AT 20°C

Sample No.	Stratigraphic unit	Grid Reference	Declination (Degrees)	Inclination (Degrees)	Intensity (μ G)	α_{95} (Degrees)	K	N
T ₁	Mercia Mudstone Group	SP 205829	238	62	0.675	56	2.8	5
T ₂	Mercia Mudstone Group	SP 205829	333	67	0.680	60	2.2	6
T ₃	Arden Sandstone Member	SP 167654	34	64	0.400	11	35.8	6
T ₄	Arden Sandstone Member	SP 167654	10	63	0.265	14	24.0	6
T ₅	Arden Sandstone Member	SP 167654	260	57	0.450	51	4.2	4
T ₆	Mercia Mudstone Group	SP 164757	226	73	0.520	16	19.0	6
T ₇	Mercia Mudstone Group	SP 164757	186	51	0.615	60	5.2	3
T ₈	Kidderminster Fm.	SO 807768	354	69	2.470	16	18.7	6
T ₉	Kidderminster Fm.	SO 807768	13	62	2.508	30	5.8	6
T ₁₀	Bromsgrove Sandstone Fm.	SO 858752	252	86	1.540	21	10.8	6
T ₁₁	Bromsgrove Sandstone Fm.	SO 858752	15	53	1.810	34	4.8	6
T ₁₂	Bromsgrove Sandstone Fm.	SO 858752	8	58	1.613	15	21.9	6
T ₁₃	Wildmoor Sandstone Fm.	SO 952759	24	56	1.010	16	18.6	6
T ₁₄	Wildmoor Sandstone Fm.	SO 952759	326	62	0.935	28	6.7	6
T ₁₅	Wildmoor Sandstone Fm.	SO 952759	29	67	2.146	29	6.1	6

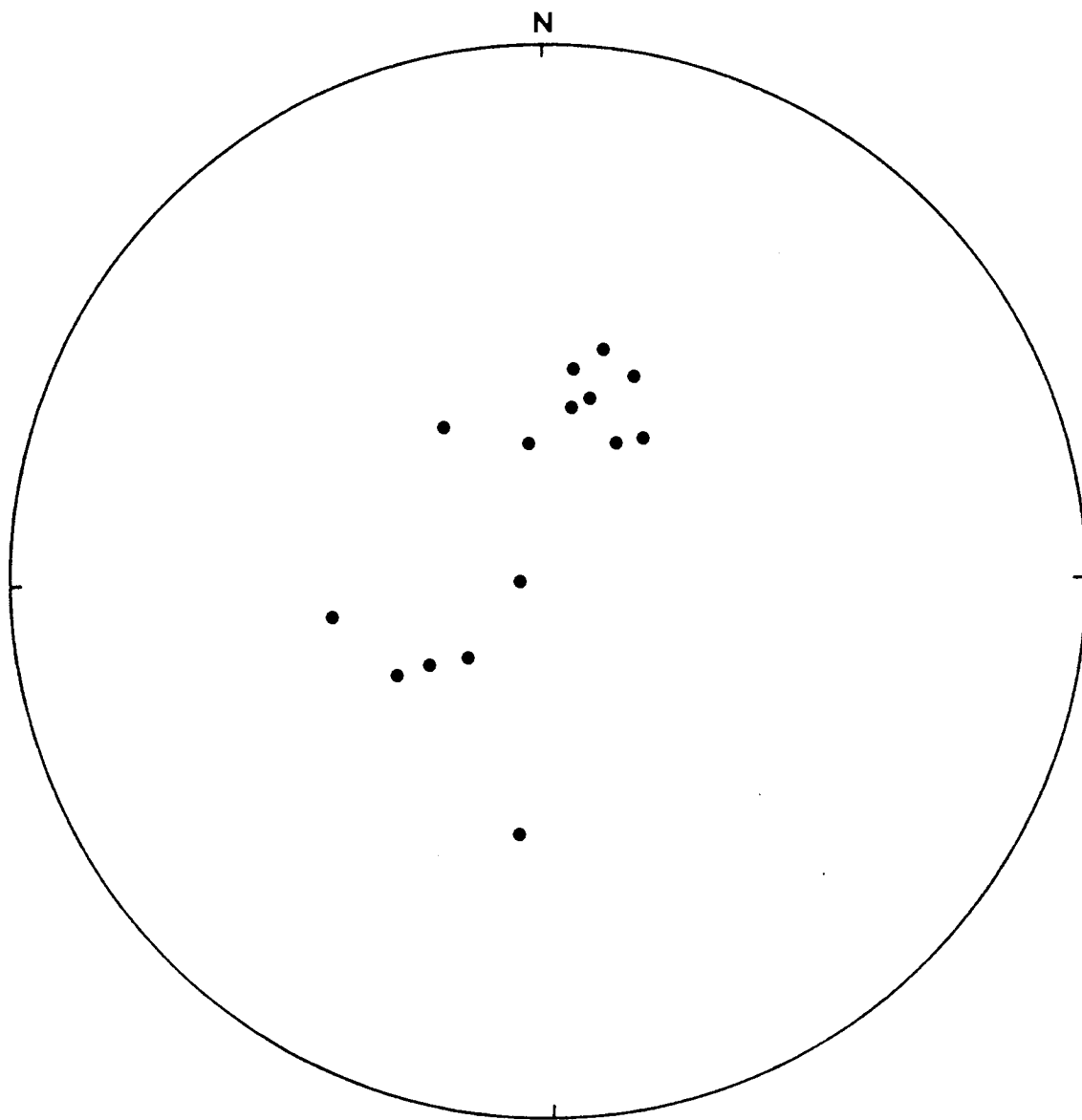


Fig.5.1 Stereographic projection showing site mean directions of the Triassic sandstones. Initial measurements at 20°C.

temperatures often close to the Curie temperature of haematite (Turner, 1981).

One core from each of the fifteen samples was selected and heated at 100°C intervals up to 500°C then at 50°C intervals up to 680°C. After each temperature increment, the specimens were allowed to cool in a field free space ($< 10\alpha$) and then remeasured.

Two types of magnetization were recognised in the Triassic sandstones in Central England: specularite dominant and mixed specularite-pigment magnetizations.

5.5.1 Specularite Dominant Magnetization

It is the most common type of magnetization in the Triassic sandstones. A typical example is sample T₉ from the Kidderminster Formation. In this sample coarse specularite grains constitute up to 1% and consists mainly of martites with other textural phases of haematite. No haematite overgrowths are present. The fine pigmentary haematite is present as grain coatings and in this case two generations of haematite pigment were recognized in the Kidderminster Formation. The first one is of an early diagenetic origin coating the detrital grains, the second is of late diagenetic origin coating the authigenic K-feldspar overgrowths.

During partial thermal magnetization a pronounced initial intensity increase at 100°C (Fig. 5.2a) may be due to the removal of antiparallel components. The

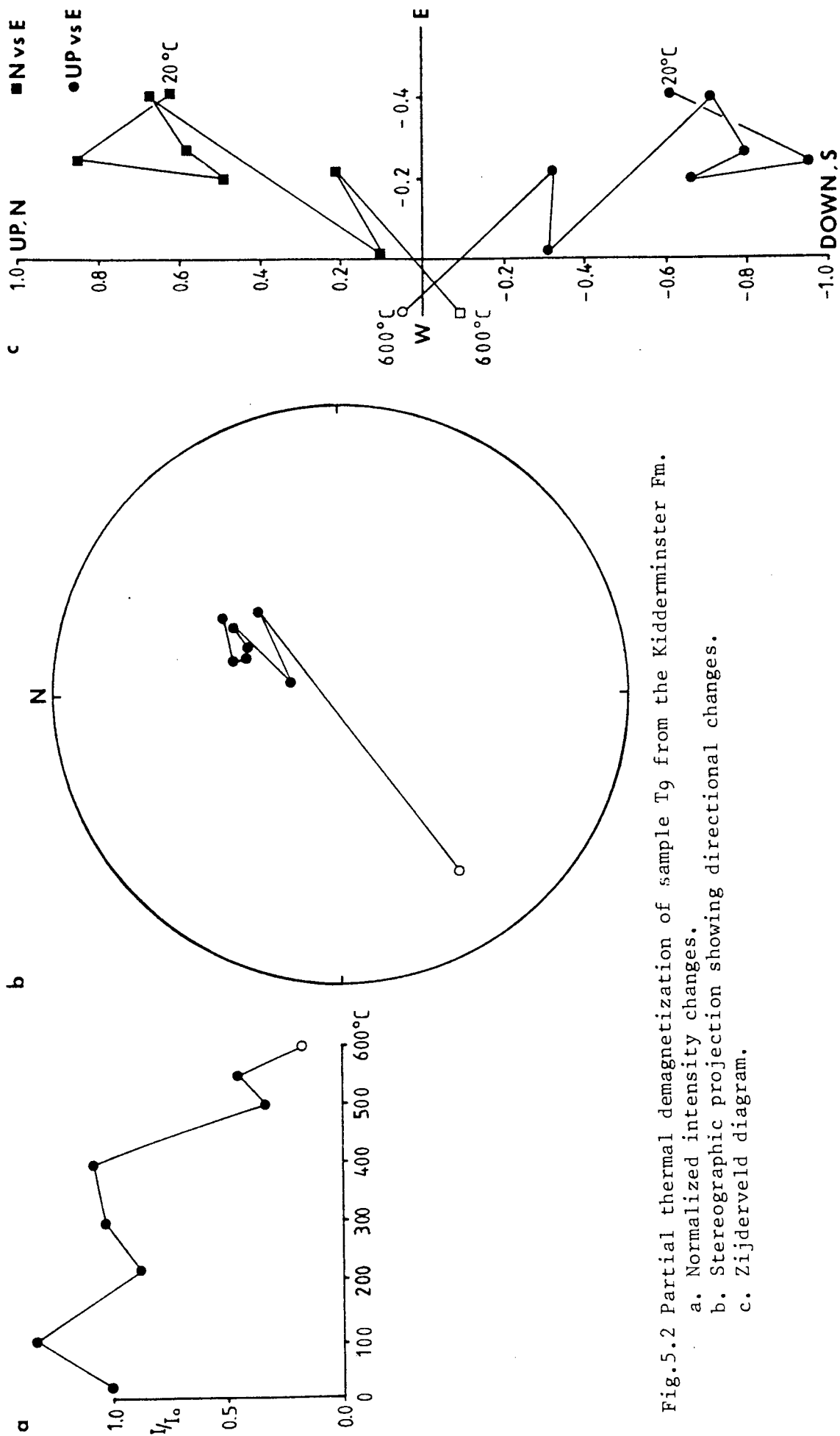


Fig.5.2 Partial thermal demagnetization of sample T9 from the Kidderminster Fm.

a. Normalized intensity changes.

b. Stereographic projection showing directional changes.

c. Zijderveld diagram.

components with low blocking temperature (220°C) are carried by the fine pigmentary haematite and account for 20% of the NRM intensity. Components with higher blocking temperature (at 500°C and 600°C) are carried by the coarse specularite grains and constitute the remaining 80% of the NRM intensity.

The stereographic projection (Fig. 5.2b) shows an initial direction of magnetization with a moderately steep positive inclination towards the northeast. During partial thermal demagnetization the direction becomes a little steeper at first but remains in the NE quadrant, then it becomes shallower and negatively inclined towards the southwest.

The Zijderveld diagram (Fig. 5.2c) is complicated and does not show straight line segments representing the different magnetic components, but a break point between the components of low and high blocking temperatures can be recognized. It is difficult to isolate the magnetic components which have low blocking temperature probably because they were unblocked at the same time and represent CRM carried by the two generations of fine pigmentary haematite. A magnetic component with high blocking temperature can be isolated. The declination (D) of the magnetic component being demagnetized is the angle measured in the horizontal plane eastward from north. I_{app} is the angle measured in the vertical plane (UP vs E), the

inclination (I) of the component then will be $\tan I = \tan I_{app} |\sin D|$ (Dunlop 1979). In this case the magnetic component with high blocking temperature is represented by the line (400 - 600°C in Fig. 5.2c) and has $D = 35^\circ$, $I = 50^\circ$. This magnetic component may represent a PDRM or early diagenetic CRM carried by the coarse specularite grains. It may include a superimposed component representing a CRM carried by the martites. This superimposed component may have been acquired long after deposition during the transformation of magnetite into haematite through the process of martitization.

The green sandstone horizons of the Mercia Mudstone Group are good examples of specularite dominant magnetization. Sample T_2 taken from the lower part of the Mercia Mudstone Group is a light red, medium grained sandstone with abundant green reduction spots and bands. The opaque heavy mineral fraction consists mainly of haematites, both mono and polycrystalline, martites some of which are not completely transformed into haematite, and a few titanium oxide grains.

During partial thermal demagnetization of T_2 , the NRM intensity shows an initial increase until 220°C (Fig. 5.3a), then after a slight decrease it increases again until 500°C and then decreases progressively until it reaches its minimum at 650°C. This high blocking temperature is a characteristic of specularite dominant magnetization (Turner, 1981).

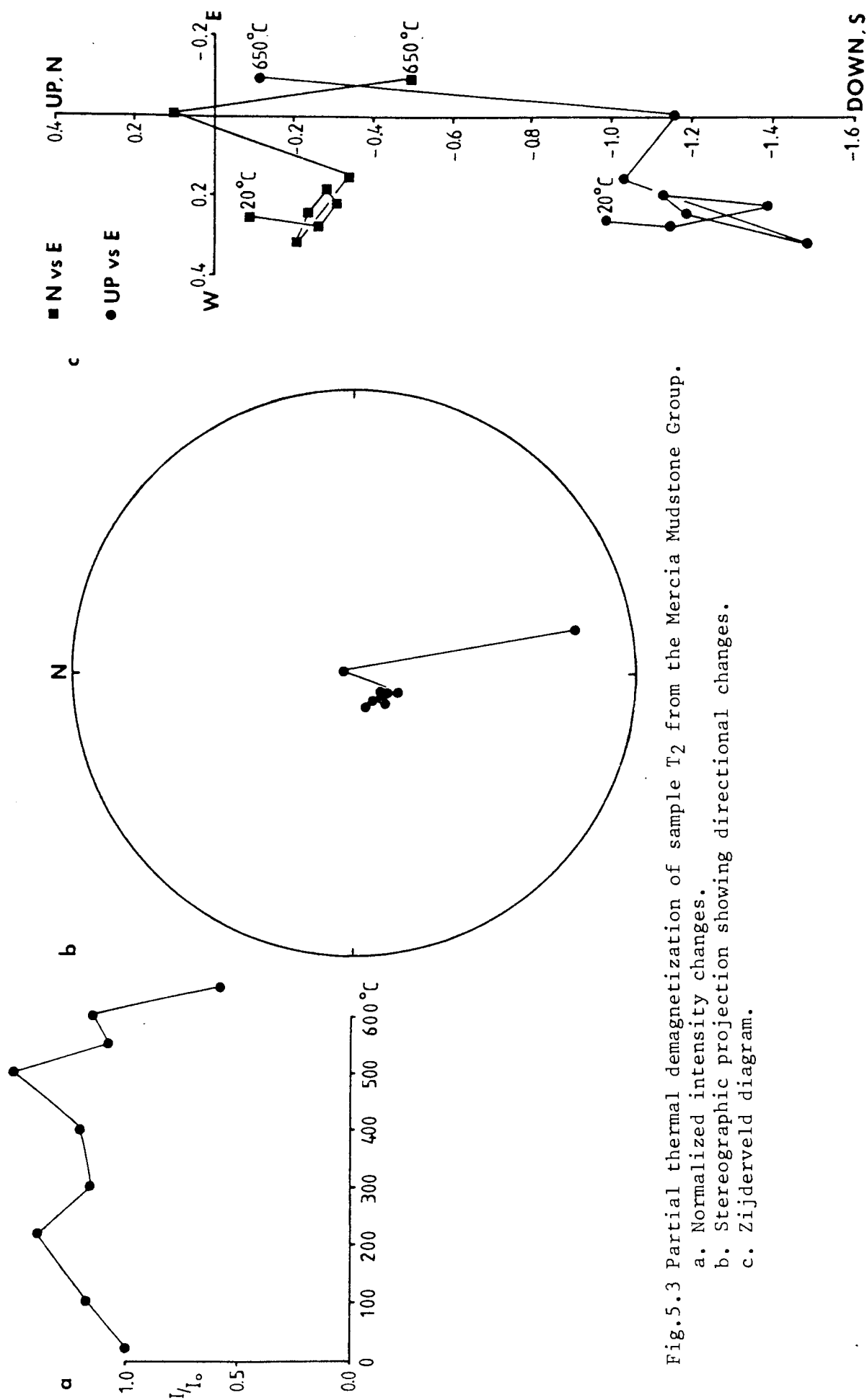


Fig.5.3 Partial thermal demagnetization of sample T2 from the Mercia Mudstone Group.

- a. Normalized intensity changes.
- b. Stereographic projection showing directional changes.
- c. Zijderveld diagram.

The stereographic projection (Fig. 5.2b) shows an initial direction with a steep positive inclination towards the southeast. No prominent change in the direction occurs throughout the heating process until 600°C, where it becomes steeper towards the north, then finally shallower and inclined towards the S-SE.

The Zijderveld diagram (Fig. 5.3c) is also complicated with no straight line segments, but a magnetic component with high blocking temperature can tentatively be isolated. It is represented by the line (500 - 650°C in Fig. 5.3c) and has $D = 305^\circ$ measured on the horizontal plane (N vs E in Fig. 5.3c) and $I = 19^\circ$ measured on the vertical plane (UP vs E in Fig. 5.3c). It represents a magnetic component carried by the coarse specularite grains.

In specularite dominant magnetization the pigment plays only a minor role as remanence carrier. The magnetization is multicomponent as indicated by the lack of a stable endpoint (Turner, 1981). The fine pigmentary haematite carries the low blocking temperature components which represent a CRM. The high blocking temperature components are carried by the coarse specularite grains. The haematite grains may carry a PDRM whereas the martites may carry a CRM. There is very little difference in the coercivity spectrum of the different components carried by the specularite, hence the rather irregular Zijderveld diagrams. This highlights the fact that thermal demagnetization will not necessarily separate the various components.

5.5.2 Mixed Specularite-pigment Magnetization

The Wildmoor sandstones are good examples of rocks with mixed specularite-pigment magnetization. They are medium to fine grained bright red sandstones characterized by the presence of very fine and fine-grained laminae. The heavy mineral fraction contain < 0.5% specularite grains. These specularite grains consist mainly of haematites with few martite grains.

During partial thermal demagnetization of sample T₁₃ from the Wildmoor Sandstone Formation, an initial linear decrease of intensity until 300°C (Fig. 5.4a) indicates the presence of a magnetic component with low blocking temperature probably carried by the pigment. This component accounts for 50% of the NRM intensity. Then after a slight increase at 400°C and 500°C the intensity reaches its minimum at 600°C. The component with such a high blocking temperature is carried by the specularite grains and constitutes the remaining 50% of the NRM.

The stereographic projection show an initial direction with steep positive inclination towards the southeast (Fig. 5.4b). During partial thermal demagnetization the direction becomes shallower inclining towards the south and then steep again. Finally, it changes towards the northwest with a shallow inclination.

The Zijderveld diagram (Fig. 5.4c) is irregular and complicated with no straight line segments. This is due

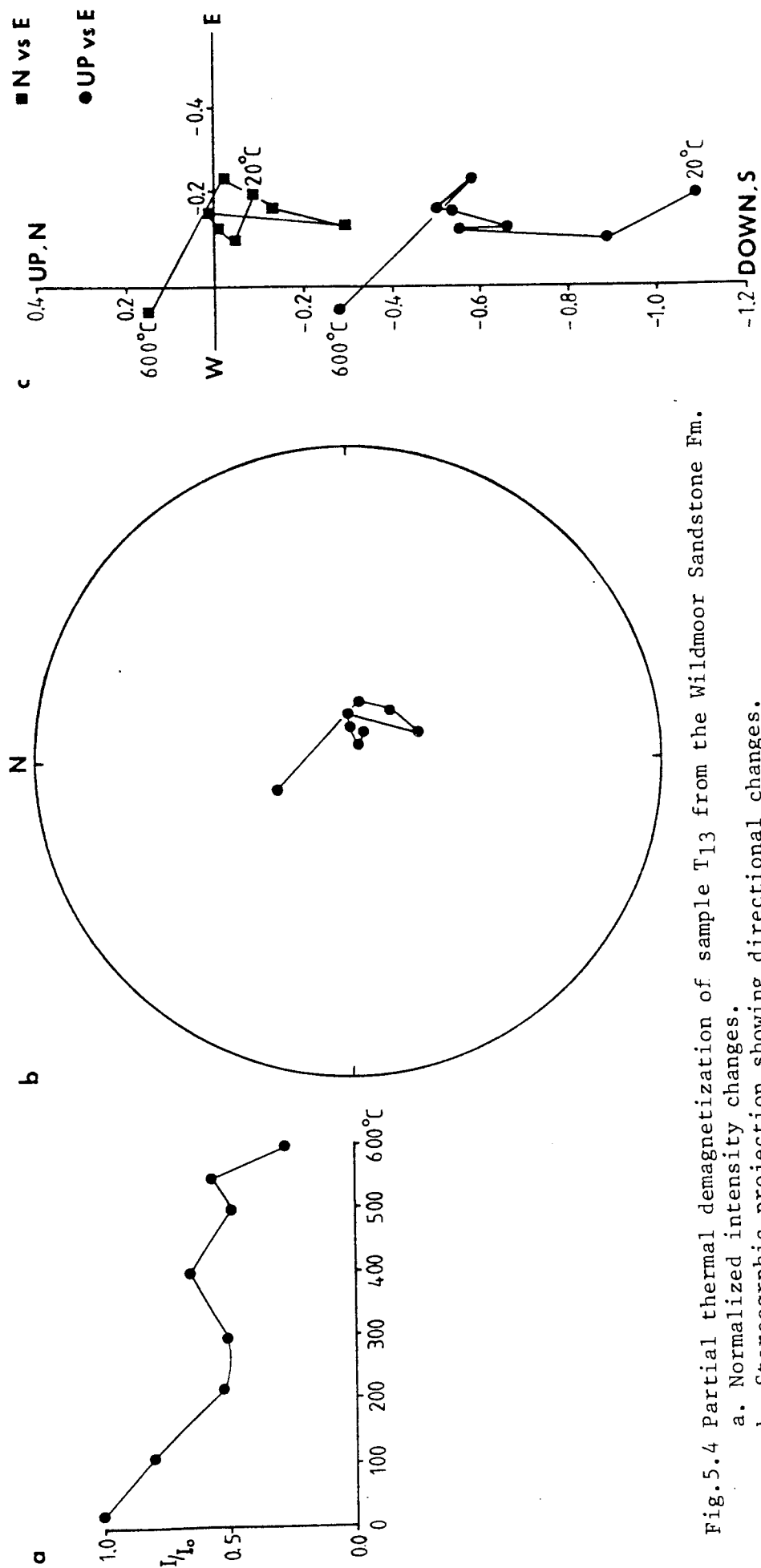


Fig. 5.4 Partial thermal demagnetization of sample T₁₃ from the Wildmoor Sandstone Fm.
a. Normalized intensity changes.
b. Stereographic projection showing directional changes.
c. Zijderveld diagram.

to the presence of different magnetic components with very little difference in their coercivity spectra. As a result more than one component becomes unblocked at the same time. Hence the little change in the direction throughout the thermal demagnetization process. This is the case of nearly all the studied samples whether they represent a specularite dominant or mixed specularite-pigment magnetization.

Sample T₁₀ from the Bromsgrove Sandstone Formation is another example of mixed specularite-pigment magnetization. It is a medium grained dark red sandstone with abundant clay lenses which account for the higher percentage of fine material, hence the higher percentage of fine pigmentary haematite. The heavy mineral fraction consists mainly of partially haematized biotites, haematites, and a few martites. Many of the haematite grains are surrounded by large euhedral overgrowths.

During partial thermal demagnetization of sample T₁₀ there is an initial linear intensity decrease until 300°C (Fig. 5.5a), indicating the presence of a low blocking temperature component carried by the fine pigmentary haematite which is present both as grain coating and in partially haematized biotites. This component accounts for about 50% of the NRM intensity. After a slight decrease at 400°C and 500°C the intensity reaches its minimum at 550°C. This higher blocking temperature component accounts for the remaining 50% of the NRM intensity and is

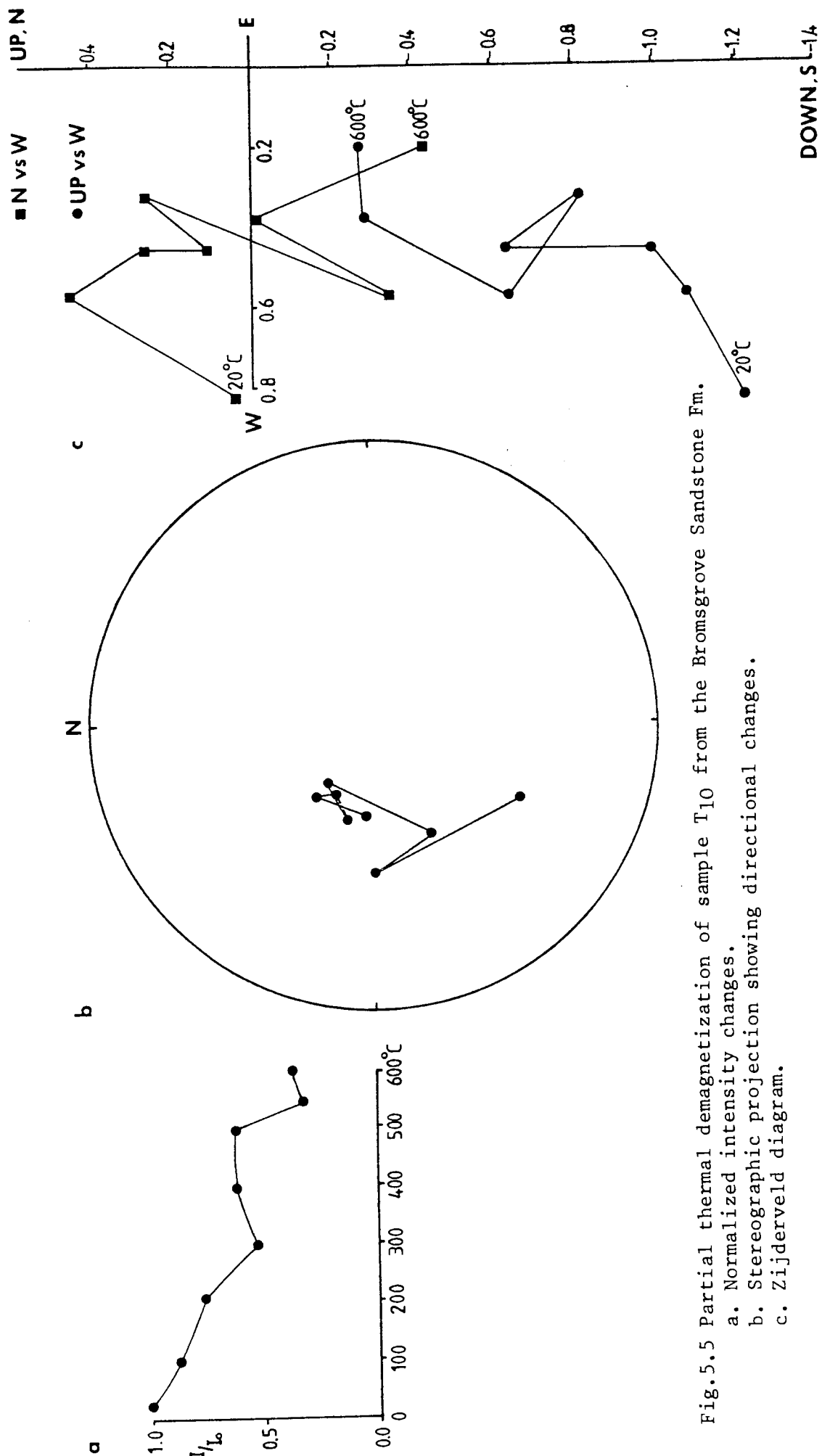


Fig. 5.5 Partial thermal demagnetization of sample T10 from the Bromsgrove Sandstone Fm.

a. Normalized intensity changes.

b. Stereographic projection showing directional changes.

c. Zijderveld diagram.

carried by the specularite grains.

The stereographic projection shows an initial direction with steep positive inclination towards the northwest (Fig. 5.5b). During partial thermal demagnetization the direction does not change much until 400°C after which it becomes shallower and inclined towards the south.

The points on the Zijderveld diagram (Fig. 5.5c) are scattered and none of the different magnetic components can be isolated. In this particular case the fine pigmentary haematite and the partially haematized biotite carry low blocking temperature components. They represent CRM acquired post-depositionally over a long period of time. Magnetic components with high blocking temperature are carried by the coarse specularite grains. The large euhedral haematite overgrowths which in many cases are as large as the host detrital grains carries a high blocking temperature component representing a CRM superimposed on a possible PDRM carried by the specularite grains.

Mixed specularite-pigment magnetization is multi-component and the fine pigmentary haematite plays an important role as a remanence carrier. Sandstones with higher percentage of the fine size fraction and abundant clay lenses are good examples of mixed specularite-pigment magnetization.

5.6 BULK DEMAGNETIZATION

All the specimens were thermally cleaned at 300°C.

In doing so all components, including viscous and others with low blocking temperatures and mainly residing in the pigmentary haematite were removed. As a result the magnetic directions become shallower and spread along a N-NE and S-SW axis (Table 5.2, Fig. 5.6). This axis represents approximately the Triassic geomagnetic axis and the thermally cleaned directions are clearly intermediate between the Triassic normal and reversed positions. They are thus multicomponent and reflect the complex nature of coarse particle oxide diagenesis in the Triassic sandstones. They are similar to type B magnetization as described by Turner (1979) where the individual components are often antiparallel and intermediate directions result from two or more components which are not antipodally opposed. In this case no discrete zones of normal and reversed polarity can be found.

5.7 CONCLUSIONS

Two types of magnetization were recognized in the Triassic sandstones of Central England. These are, specularite dominant magnetization, and mixed specularite-pigment magnetization. The magnetization in each case is multicomponent and each component is carried by a different haematite textural phase. These are, the fine pigmentary haematite, clay-oxide pellicles, pseudomorphosed biotite by haematite, specularite grains, and authigenic haematite overgrowths and cement. All but the haematite with exsolution discs of ilmenite can carry a CRM component

TABLE 5.2 SITE MEAN DIRECTIONS AFTER THERMAL CLEANING AT 300° C

Site No.	Stratigraphic Unit	Grid Reference	Declination (Degrees)	Inclination (Degrees)	Intensity (μ G)	95 (Degrees)	K	N
T ₁	Mercia Mudstone Group	SP 205829	186	32	0.662	>90	1.7	4
T ₂	Mercia Mudstone Group	SP 205829	288	54	0.897	73	2.0	5
T ₃	Arden Sandstone Member	SP 167654	132	60	0.284	>90	1.3	5
T ₄	Arden Sandstone Member	SP 167654	311	79	0.128	27	8.8	5
T ₅	Arden Sandstone Member	SP 167654	357	34	0.156	>90	2.1	3
T ₆	Mercia Mudstone Group	SP 164757	200	48	0.370	58	2.6	5
T ₇	Mercia Mudstone Group	SP 164757	210	50	0.155	>90	2.1	2
T ₈	Kidderminster Fm.	SO 807768	339	70	1.373	31	7.1	5
T ₉	Kidderminster Fm.	SO 807768	5	63	2.562	21	14.7	5
T ₁₀	Bromsgrove Sandstone Fm.	SO 858752	155	79	1.156	35	5.6	5
T ₁₁	Bromsgrove Sandstone Fm.	SO 858752	14	52	2.150	28	8.2	5
T ₁₂	Bromsgrove Sandstone Fm.	SO 858752	8	37	0.794	22	12.8	5
T ₁₃	Wildmoor Sandstone Fm.	SO 952759	8	50	0.547	19	16.9	5
T ₁₄	Wildmoor Sandstone Fm.	SO 952759	317	63	0.636	54	2.9	5
T ₁₅	Wildmoor Sandstone Fm.	SO 952759	39	59	0.771	49	3.4	5

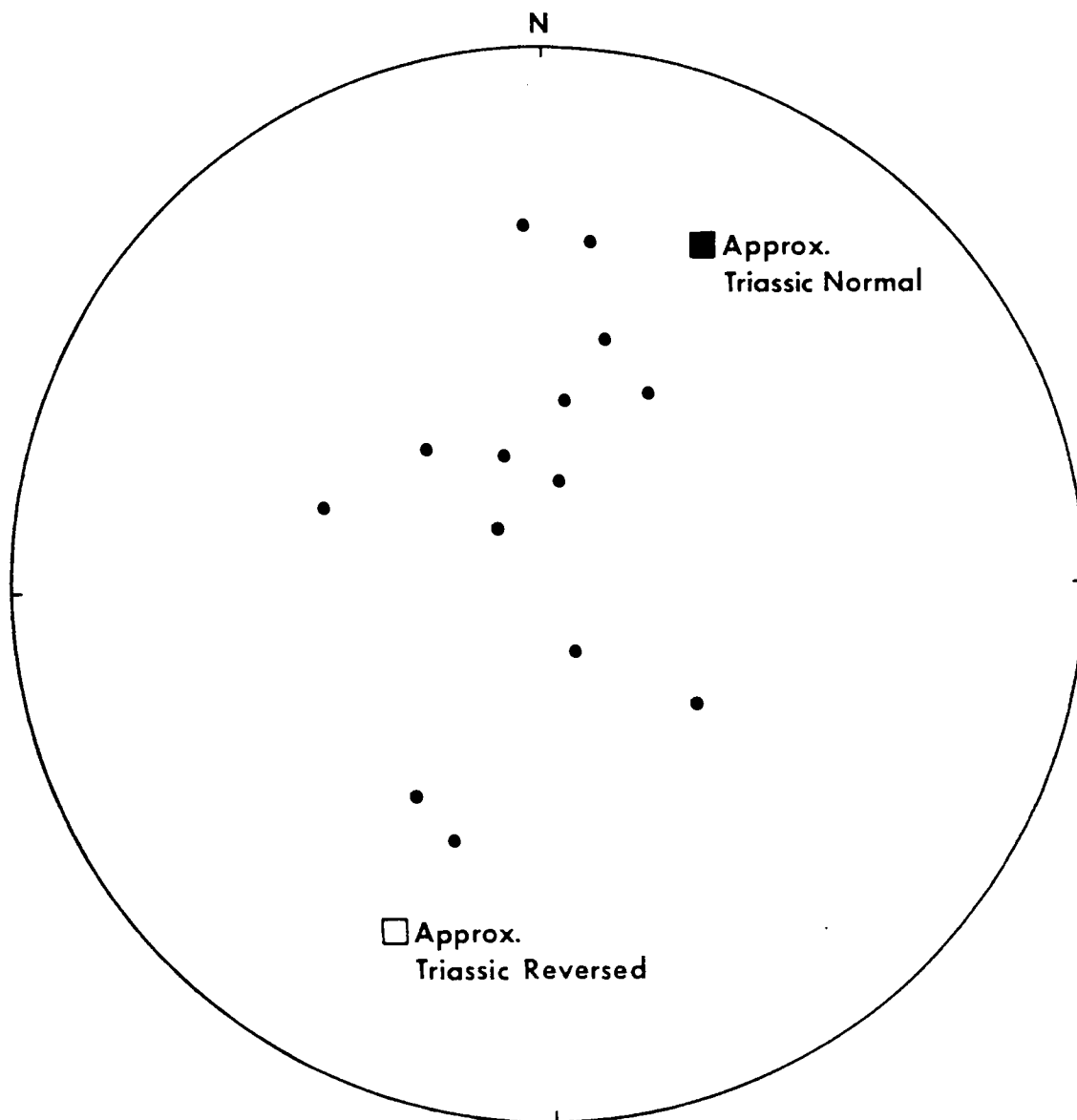


Fig.5.6 Stereographic projection showing site mean directions of the Triassic sandstones after thermal cleaning at 300°C.

acquired post-depositionally throughout the different diagenetic processes including the formation of haematite pigment, pseudomorphism of biotite, the formation of authigenic haematite overgrowths, and martitization. The mono and polycrystalline haematites may or may not be of a detrital origin and only the haematite with exsolution discs of ilmenite could carry a DRM or PDRM components.

Magnetic components carried by the pigment are characterized by their low blocking temperature whereas high blocking temperature components are carried by the coarse specularite grains. In each case there is a little difference between the coercivity spectrum of the different components. As a result more than one component becomes unblocked at nearly the same time, causing little change in the direction and the resulting Zijdeveld diagram is complex and irregular.

The individual specimens have composite magnetization and the individual components are intermediate between the Triassic normal and reversed directions. Therefore the Triassic sandstones of Central England are typical examples of type B red beds.

The overall paleomagnetic properties of the Triassic sandstones depend on the relative abundance of the different textural phases of haematite, and the different magnetic components were acquired during different post-depositional

intervals. In coarse to medium sandstones where the specularite are abundant the magnetization is specularite dominant and the pigment plays only a minor role as a remanence carrier. In fine grained sandstones, especially those with abundant clay lenses, the pigment plays a major role as a remanence carrier, and the magnetization can be described as mixed specularite-pigment.

REFERENCES

- Arthurton, R.S., 1980. Rhythmic sedimentary sequences in the Triassic Keuper Marl (Mercia Mudstone Group) of Cheshire, Northwest England. *Geol. J.*, 15, 43-58.
- Allen, J.R.L., 1965. Fining upwards cycles in alluvial successions. *Geol. J.*, 4, 229-246.
- Allen, J.R.L., 1970. Studies in fluvial sedimentation: A comparison of fining-upwards cyclothems with special reference to coarse-member composition and interpretation. *J. Sedim. Petrol.*, 40, 298-323.
- Audley-Charles, M.G., 1970a. Stratigraphic correlation of the Triassic rocks of the British Isles. *Q. Jl. geol. Soc. Lond.*, 126, 19-47.
- Audley-Charles, M.G., 1970b. Triassic palaeogeography of the British Isles. *Q. Jl. geol. Soc., Lond.*, 126, 49-89.
- Baag, Czung-Go. and Helsley, C.E., 1974. Evidence for penecontemporaneous magnetization of the Moenkopi Formation. *J. Geophys. Res.*, 79, 3308 - 3320.
- Barth, T.F.W., 1969. Feldspars. Wiley, New York, 261 pp.
- Baskin, Y., 1956. A study of authigenic feldspars. *J. Geol.*, 64, 132-155.
- Basu, A., Young, S.W., and Suttner, L.D., 1975. Re-evaluation of the use of undulatory extinction and polycrystallinity in detrital quartz for provenance interpretation. *J. Sedim. Petrol.*, 45, 873-882.
- Benton, M.J., and Tucker, M.E., 1980. Red beds and dinosaur evolution: A study of climatic influence. British Ass., The University, Newcastle upon Tyne, 3pp.
- Blatt, H., 1967. Original characteristics of clastic quartz grains. *J. Sedim. Petrol.*, 37, 401-424.
- Blatt, H., and Christic, J.M., 1963. Undulatory extinction in quartz of igneous and metamorphic rocks and its significance in provenance studies of sedimentary rocks. *J. Sedim. Petrol.*, 33, 1326-1339.
- Blatt, H., Middleton, G., and Murray, R., 1980. Origin of sedimentary rocks. 2nd Ed., Prentice-Hall, New Jersey, 782 pp.

- Bluck, B.J., 1967. Deposition of some Upper Old Red Sandstone conglomerates in the Clyde area. A study in the significance of bedding. *Scott J. Geol.*, 3, 139-167.
- Bluck, B.J., 1974. Structure and directional properties of some valley sandur deposits in Southern Iceland. *Sedimentology*, 21, 533-554.
- Bonney, T.D., 1900. The Bunter Pebble Beds of the Midlands and the source of their materials. *Q. Jl. geol. Soc. Lond.*, 56, 287-306.
- Bosworth, T.O., 1912. The Keuper Marls around Charnwood. *Q. Jl. geol. Soc., Lond.*, 68, 281-294.
- Brennand, T.P., 1975. The Triassic of the North Sea. In: A.W. Woodland (Ed.): Petroleum and the continental shelf of North West Europe. Vol. 1, Geology, Applied Science Pub., 295-310.
- Cant, D.J., and Walker, R.G., 1976. Development of a braided fluvial facies model for the Devonian Battery Point Sandstone, Quebec. *Can. J. Earth Sci.*, 13, 102-119.
- Carver, R.E., 1967. Procedures in sedimentary petrology. Wiley. Interscience, New York.
- Clegg, J.A., Almond, M., and Stubbs, P.H.S., 1954. The remanent magnetization of some sedimentary rocks in Britain. *Phil. Mag.*, 45, 583-598.
- Chamalaun, F.H., 1963. Thermal demagnetization of red sediments. Ph.D. Thesis, Unpub., University of Durham.
- Collinson, D.W., 1965. The remanent magnetism and magnetic properties of red sediments. *Geophys. J.R. astro. Soc.*, 10, 105-126.
- Collinson, D.W., 1974. The role of pigment and specularite in the remanent magnetism of red sandstones. *Geophys. J.R. astro. Soc.*, 38, 253-264.
- Collinson, J.D., 1970. Bedforms of the Tana River, Norway. *Geogr. Annalr.*, 52-A, 31-56.
- Colter, V.S., and Barr, K.W., 1975. Recent development in the geology of the Irish Sea and Cheshire Basin. In: A.W. Woodland (Ed.): Petroleum and the continental shelf of North West Europe. Vol. 1, Geology, Applied Science Publ., 61-73.

- Colter, V.S., and Ebbern, J., 1978. The petrography and reservoir properties of some Triassic sandstones of the Northern Irish Sea Basin. *J. geol. Soc., Lond.*, 135, 57-62.
- Connolly, J.R., 1965. The occurrence of polycrystallinity and undulatory extinction in quartz in sandstone. *J. Sedim. Petrol*, 35, 116-135.
- Craig, G.V., 1965. Permian and Triassic. In: G.V. Craig (Ed.): *The geology of Scotland*, Oliver and Boyd, 384-416.
- Creer, K.M., 1957. The natural remanent magnetization of certain stable rocks from Great Britain. *Phil. Trans. R. Soc. Lond.*, A250, 111-129.
- Creer, K.M., 1959. A.C. demagnetization of unstable Keuper Marls from South West England. *Geophys. J.R. astro. Soc.*, 4, 261-275.
- Dickson, J.A.D., 1966. Carbonate identification and genesis as revealed by staining. *J. Sedim. Petrol.*, 36, 491-545.
- Dietz, V., 1979. Experiments on the influence of transport on shape and roundness of heavy minerals. *Contributions to Sedimentology.*, 1, 69-102.
- Dunlop, D.J., 1979. On the use of Zijderveld diagrams in multicomponent palaeomagnetic studies. *Phys. Earth Planet. Int.*, 20, 12-24.
- Dumbleton, D.T., and West, G., 1966. Studies of the Keuper Marl mineralogy. *Road. Res. Lab. Rep.*, 40, 1-25.
- Eastwood, T., Whitehead, T.H. and Robertson, T., 1925. *Geology of the country round Birmingham. Mem. Geol. Surv. No. 168.*
- Elliot, R.E., 1961. The stratigraphy of the Keuper series in Southern Nottinghamshire. *Proc. Yorks. Geol. Soc.*, 33, 197-234.
- Eustance, N.B., 1981. Palaeomagnetism and diagenesis in sedimentary rocks. Ph.D. Thesis, Unpub. The University of Newcastle upon Tyne.
- Eynon, G., and Walker, R.D., 1974. Facies relationships in Pliocene outwash gravels, Southern Ontario : A model for bar growth in braided rivers. *Sedimentology*, 21, 43-70.
- Fitch, F.J., Miller, J.A., and Thompson, D.B., 1966. The paleogeographic significance of isotopic age determination on detrital mica from the Triassic of Stockport - Macclesfield district, Cheshire, England. *Paleogeogr. Paleocol.*, 2, 281-312.

- Fleet, W.F., 1923. Notes on the Triassic sands near Birmingham, with special reference to their heavy detrital minerals. *Proc. geol. Ass.*, 34, 114-119.
- Fleet, W.F., 1925. The chief heavy detrital minerals in the rocks of the English Midlands. *Geol. Mag.*, 62, 98-128.
- Folk, R.L., 1968. Petrology of sedimentary rocks. Hamphills, Austin, Texas, 170 pp.
- Friedman, G.M., 1967. Dynamic processes and statistical parameters compared for size frequency distribution of beach and river sands. *J. Sedim. Petrol.*, V.37, 327-354.
- Füchtbauer, H., 1974. Sediments and sedimentary rocks 1. 2nd Ed., Schweizerbart, Stuttgart, 464 pp.
- Griffith, D.H., King, R.F., Rees, A.I., and Wright, A.E., 1960. Remanent magnetism of some recent varved sediments. *Proc. R. Soc. Lond.*, A 256, 359-383.
- Grimm, W.D., 1973. Stepwise heavy mineral weathering in the residual quartz gravel. Bavarian Molasse (Germany). *Contributions to Sedimentology*, 1, 103-125.
- Hains, B.A., and Horton, A., 1969. Central England, 3rd Ed., British Regional Geology. *Instit. Geol. Sci.*, 142 pp.
- Helgeson, H.C., Garrels, R.M., and Mac Kenzie, F.T., 1969. Evaluation of irreversible reactions in geochemical processes involving minerals and aqueous solutions II, Applications - *Geochim. et Cosmochim. Acta.*, 33, 455-481.
- Helgeson, H.C., Delany, J.M., Nesbitt, H.W., and Bird, D.K., 1978. Summary and critique of the thermodynamic properties of rock forming minerals. *Am. J. Sci.*, 278A, 229 pp.
- Hem, J.D., Robertson, C.E., Lind, C.J., and Polizer, W.L., 1973. Chemical interactions of aluminium with aqueous silica at 25°C. *U.S. Geol. Surv. Water Supply paper*, 1827E, 55 pp.
- Hess, P.C., 1966. Phase equilibria of some minerals in the $K_2O-Na_2O-Al_2O_3-SiO_2-H_2O$ system at 250°C and 1 atmosphere. *Am. J. Sci.*, 264, 280-309.
- Heward, A.P., 1978. Alluvial fan and lacustrine sediments from the Stephanian A and B (La Magdalena, Cinera-Matallana and Sabero) coalfields, Northern Spain. *Sedimentology*, 25, 45-486.

- Ireland, R.J., Pollard, J.E., Steel, R.J., and Thompson, D.B., 1978. Intertidal sediment, and trace fossils from the Waterstones (Scythian-Anisian) at Daresbury, Cheshire. *Proc. York. geol. Soc.*, 41, Part 4, 399-486.
- Ixer, R.A., Turner, P., and Waugh, R., 1979. Authigenic iron and titanium oxides in Triassic red beds; St. Bees Sandstone, Cumbria, Northern England. *Geol. J.*, 14, 179-192.
- Jeans, C.V., 1978. The origin of the Triassic clay assemblages of Europe with special reference to the Keuper Marl and Rhaetic of parts of England. *Phil. Trans. Roy. Soc.*, 549-636.
- Jeavons, W., 1947. On the origin of the Bunter Pebble Beds of the West Midlands area with reference to other deposits. M.Sc. Thesis, Unpubl. University of Birmingham.
- Johnson, A.H., 1976. Paleomagnetism of the Jurassic Navajo Sandstones from southwestern Utah. *Geophys. J., astro. Soc.*, 44, 161-175.
- Kastner, M., and Siever, R., 1979. Low temperature feldspace in sedimentary rocks. *Am. J. Sci.*, 279, 435-479.
- King, R.F., 1955. Remanent magnetism of artificially deposited sediments. *Mon. Notic. R. astro. Geophys. Supp.* 7, 115-134.
- Klien, G. De V., 1962. Triassic sedimentation, Maritime Provinces, Canada, *Geol. Soc. Am. Bull.*, 73, 1127-1146.
- Krynine, P.D., 1946. The tourmaline group in sediments, *J. Geol.*, 54, 65-87.
- Laming, D.J.C., 1966. Imbrication paleocurrents and other sedimentary features in the lower New Red Sandstones, Devonshire, England. *J. Sedim. Petrol.*, 36, 940-959.
- Larson, E.E., and Walker, T.R., 1975. Development of chemical remanent magnetization during early stages of red-bed formation in Late Cenozoic sediments, Baja, California. *Bull. geol. Soc. Am.*, 86, 639-650.
- Lomas, J., 1907. Desert conditions and the origin of the British Triassic. *Proc. Liverpool geol. Soc.*, 10, 172-197.

- Lomax, K., and Briden, J.C., 1977. Palaeomagnetic studies of the Longmyndian and other British late Pre-cambrian/early Palaeozoic rocks, and their regional tectonic implications. J. geol. Soc., London., 133, 5-21.
- Mack, G.H., 1978. The survivability of labile light-mineral grains in fluvial aeolian and littoral marine environments: The Permian Cutler and Ceda Mesa Formations, Moab, Utah. J. Sedim., Petrol., 25, 587-604.
- Mack, G.H. and Suttner, L.J., 1988. Paleoclimatic interpretation from a petrographic comparison of Holocene sands and the Fountain Formation (Pennsylvanian) in the Colorado Front Range. J. Sedim., Petrol., 47, 89-100.
- Matly, C.A., 1912. The Upper Keuper (or Arden) Sandstone Group and associated rocks of Warwickshire. Q. Jl. geol. Soc., Lond., 68, 252-280.
- Mc Donald, B.C., and Banerjee, I., 1971. Sediments and bedforms on a braided outwash plain. Can. J. Earth Sci., 8, 1282-1301.
- Mitchel, G.H., Pocock, R.W., and Taylor, J.H., 1961. Geology of the country around Droitwich, Abberley and Kidderminster. Mem. Geol. Surv. No. 182.
- Moiola, R.J., and Weister, D., 1969. Textural parameters: An evaluation. J. Sedim. Petrol., 38, 45-53.
- Moody-Stuart, M., 1966. High-and low-sinuosity stream deposits with examples from the Devonian of Spitsbergen. J. Sedim. Petrol., 36, 1102-1117.
- Nickel, E., 1973. Experimental dissolution of light and heavy minerals in comparison with weathering and interstitial solution. Contributions to Sedimentology. 1, 1-68.
- Oldershaw, A.E., and Scoffin, T.P., 1967. The source of ferroan and nonferroan calcite cements in the Halkin and Wenlock Limestones. Geol. J., 5, 309-320.
- Passega, R., 1957. Texture as characteristic of clastic deposition. Bull. Am. Ass. Petrol. Geol., 41, 1952-1984.
- Pettijohn, F.J., 1975. Sedimentary Rocks. 3rd Ed., Harper and Row, New York, 628 pp.

- Pettijohn, F.J., Potter, P.E., and Siever, R., 1972.
Sand and Sandstone. Springer, Heidelberg, 618 pp.
- Pittman, E.D., 1972. Diagenesis of quartz in sandstones
as revealed by scanning electron microscopy.
J. Sedim. Petrol., 42, 507-519.
- Parucker, M.E., Elston, D.P., and Shoemaker, E.M., 1980.
Early acquisition of characteristic magnetization
in red beds of the Moenkopi Formation (Triassic),
Gray Mountain, Arizona, J. geophys. Res., 85,
997-1012.
- Reading, H.G. 1972. Sedimentary environments and facies.
Blackwell Sci. Pub., Oxford, 557 p.
- Reineck, H.E., and Singh, I.B., 1973. Depositional
sedimentary environments. Springer-Verlag, Berlin.
439 pp.
- Reynolds, 1929. Some new occurrences of authigenic
potash feldspar. Geol. Mag., 66, 390-399.
- Reynolds, R.C., and Hower, J., 1970. The nature of
interlayering in mixed-layer illite-montmorillonite.
Clays and Clay Minerals, 18, 25-36.
- Richardson, L., 1905. On the occurrence of Rhaetic
rocks at Berrow Hill, near Tewkesbury. Q. Jl.
Geol. Soc., Lond., 61, 425-430.
- Richardson, L., and Fleet, W.F., 1926. On sandstones
and breccias below the Trias of Stratford on Avon
and elsewhere in Warwickshire. Proc. Geol. Ass.,
37, 283-305.
- Rust, B.R., 1972. Pebble orientation in fluvial
sediments. J. Sedim. Petrol., 42, 384-388.
- Sholle, P.A., 1979. A color illustrated guide to
constituents, textures, cements, and porosities
of sandstones and associated rocks. Am. Ass.
Petrol. Geol., Mem. No.28, 201 pp.
- Sherlock, R.L., 1926. A correlation of the British
Permo-Triassic rocks, I, North England, Scotland
and Ireland. Proc. Geol. Ass., 39, 49-95.
- Sherlock, R.L., 1947. The Permo-Triassic Formations:
A World Review. Hutchinson, London, 367 pp.
- Sipple, R.F., 1968. Sandstone Petrology, evidence from
luminescence petrography. J. Sedim. Petrol., 38,
530-554.

- Smith, J.V., 1974. Feldspar Minerals, 2, chemical and textural properties. Springer-Verlag, 690 pp.
- Smith J.V., and Stenstrom, R.C., 1965. Electron-excited luminescence as a petrologic tool. J. Geol., 73, 627-635.
- Smith, N.D., 1970. The braided stream depositional environment: comparison of the Platte River with some Silurian elastic rocks, North-Central Appalachians. Bull. Geol. Soc., Am., 81, 2993-3014.
- Smith, N.D., 1974. Sedimentology and bar formation in the Upper Kicking Horse River, a braided outwash stream. J. Geol., 82, 205-224.
- Sprunt, E.S., Dengler, L.A., and Sloan, D., 1978. Effects of metamorphism on quartz cathodoluminescence. Geology, 6, 305-308.
- Stablein, N.K., and Dapples, E.C., 1977. Feldspars of the Tunnel City Group (Cambrian), Western Wisconsin, J. Sedim. Petrol., 47, 1512-1538.
- Steel, R.J., 1976. Devonian basins of Western Norway: Sedimentary response to tectonism and to varying tectonic context. Tectone physics, 36, 207-224.
- Steel, R.J., Maehle, S., Nelsen, H., Røe, S.L., and Spinnager, A., 1977. Coarsening-upwards cycles in the alluvium of Homelen Basin (Devonian) Norway: Sedimentary response to tectonic events. Bull. geol. Soc., Sm., 88, 1124-1134.
- Sengupta, S., 1966. Studies on orientation and imbrication of pebbles with respect to cross-stratification. J. Sedim. Petrol., 36, 362-369.
- Stewart, H.B., 1958. Sedimentary reflections of depositional environment in San Miguel Lagoon, Baja, California, Mexico. Bull. Am. Ass. Petrol. Geol., 42, 2567-2618.
- Suttill, R.J., 1980. Post-depositional remanent magnetization in recent tidal flat sediments. Earth Planet. Sci. Lett., 39, 132-140.
- Taux, L., Kent, D.V., and Opdyke, N.D., 1980. Magnetic components contributing to the NRM of Middle Siwalik red beds. Earth Planet. Sci. Lett., 49, 279-284.

- Thompson, D.B., 1970a. Sedimentation of the Triassic (Scythian) red pebbly sandstones in the Cheshire Basin and its margins. *Geol. J.*, 7, 183-216.
- Thompson, D.B., 1970b. The stratigraphy of the so-called Keuper Sandstone Formation (Scythian-Anisian) in the Permo-Triassic Cheshire Basin. *Q. Jl. geol. Soc., Lond.*, 126, 151-181.
- Trotter, F.M., 1953. Reddened beds of Carboniferous age in North-West England and their origin. *Proc. Yorks. geol. Soc.*, 29, 12-20.
- Turner, P., 1979. The palaeomagnetic evolution of continental red beds. *Geol. Mag.*, 116, 289-301.
- Turner, P., 1980. Continental red beds. Development in sedimentology, No. 29, Elsevier, Amsterdam, 562 pp.
- Turner, P., 1981. Relationship between magnetic components and diagenetic features in reddened Triassic alluvium (St. Bees Sandstone, Cumbria, UK). *Geophys. J. R. astro. Soc.*, 67, 395-413.
- Turner, P., and Archer, R., 1977. The role of hematite in the diagenesis of red beds from the Devonian of Northern Scotland. *Sedim. Geol.*, 19, 241-251.
- Turner, P., and Ixer, R.A., 1977. Diagenetic development of unstable and stable magnetization in the St. Bees Sandstone (Triassic) of northern England. *Earth Planet. Sci. Lett.*, 34, 113-124.
- Verosub, K.L., 1977. Depositional and post-depositional processes in the magnetization of sediments. *Rev. Geophys. Spac. Phys.*, 15, 129-143.
- Walker, T.R., 1967. Formation of red beds in modern and ancient deserts. *Bull. geol. Soc. Am.*, 72, 353-368.
- Walker, T.R., 1974. Formation of red beds in moist tropical climates: A hypothesis. *Bull. geol. Soc. Am.*, 85, 633-638.
- Walker, T.R., 1976. Diagenetic origin of continental red beds. In: H. Flake (Ed). *The continental Permian in Central, West and South Europe*. D. Radel, Dordrecht- Holland, 240-282.
- Walker, T.R., 1978. Paleoclimate interpretation from a petrographic comparison of Holocene sands and the Fountain Formation (Pennsylvanian) in the Colorado Front Range: A discussion. *J. Sedim. Petrol.*, 48, 1011-1013.

- Walker, T.R., Larson, E.E., and Hoblitt, R.P., 1980.
The nature and origin of haematite in the Moenkopi
Formation (Triassic), Colorado Plateau: A
contribution to the origin of magnetism in red
beds. *J. geophys. Res.*, 86, 317-333.
- Walker, T.R., Waugh, B., and Crone, A.J., 1978.
Diagenesis in first-cycle desert alluvium of Cenozoic
age, southwestern United States and northwestern
Mexico. *Bull. geol. Soc. Am.*, 89, 19-32.
- Warrington, G., 1967. Correlation of the Keuper Series
of the Triassic by Miospores. *Nature*, 214,
1327-1324.
- Warrington, G., 1970. The stratigraphy and palaeon-
tology of the Keuper Series of the Central Midlands
of England. *Q. Jl. geol. Soc., Lond.*, 126,
187-223.
- Warrington, G., 1974. Palynology of the Triassic. In:
B.J. Williams and A. Whittaker (Ed)., q-2, 19-21.
- Warrington, G., Audley-Clarke, M.G., Elliott, R.E.,
Evans, W.B., Ivimey-Cook, H.C., Kent, P.E.,
Robinson, P.L., Shotton, F.W., and Taylor, F.M.,
1980. Triassic. *Geol. Soc. Spec. Rep.*, No.13,
78 pp.
- Waugh, B., 1970a. Formation of quartz overgrowths in
the Penrith Sandstone (Lower Permian) of north-
west England as revealed by scanning electron
microscopy. *Sedimentology*, 14, 309-320.
- Waugh, B., 1970b. Petrology, provenance and silica
diagenesis of the Penrith Sandstone (Lower
Permian) of northwest England. *J. Sedim. Petrol.*,
40. 1226-1240.
- Waugh, B., 1978. Authigenic K-feldspar in British
Permo-Triassic sandstones. *J. geol. Soc., Lond.*,
135, 51-56.
- Wills, L.J., 1948. The palaeogeography of the Midlands.
University Press of Liverpool, 144 pp.
- Wills, L.J., 1970. The Triassic succession in the
Central Midlands and its regional setting. *Q. Jl.
geol. Soc., Lond.*, 126, 225-285.
- Wills, L.J., 1976. The Trias of Worcestershire and
Warwickshire. *Inst. Geol. Sci. Rep.*, 76/2, 211 pp.
- Whithead, T.H., and Pocock, R.W., 1947. Dudley and
Bridgnorth. *Mem. Geol. Surv.*, No. 167.

- Whittemore, D.O., and Langmuir, D., 1975. The solubility of ferric oxyhydroxides in natural waters. *Ground Water*, 13, 6 pp.
- Williams, D., 1973. The sedimentology and petrology of the New Red Sandstone of the Elgin Basin, northwest Scotland. Ph.D. Thesis, Unpubl., University of Hull, 212 pp.
- Williams, P.F., and Rust, B.R., 1969. The sedimentology of a braided river. *J. Sedim. Petrol.*, 39, 649-679.
- Young, S.W., Baru, A., Suttner, L.J., Mack, G.H., and Darnell, N.A., 1975. Use of size composition trends in Helocene soil and fluvial sand for paleoclimate interpretation. *Proc. IX Sedim. Cong.*, Nice, France, Theme 1, 201-209.
- Ziegler, P.A., 1975. North Sea Basin history in the tectonic framework of North-Western Europe. In: A.W. Woodland (Ed).: *Petroleum and the continental shelf of North West Europe*. Vol. 1. Geology, Applied Science Pub., 131-150.
- Ziegler, P.A., 1978. North-Western Europe: Tectonic and basin development. *Geol. Mij.*, 57, 589-626.
- Zinkernagel, U., 1978. Cathodoluminescence of quartz and its application to sandstone petrology. *Contributions to Sedimentology*, 8, 69 pp.